Neurological - Molecular Interface in Food Intake and Metabolism in Birds and Mammals

Wei Zhang

Dissertation submitted to the faculty of the Virginia Polytechnic Institute and State University in partial fulfillment of the requirements for the degree of

Doctor of Philosophy

In

Animal and Poultry Sciences

Elizabeth R. Gilbert, Chair

Mark A. Cline

Paul B. Siegel

Honglin Jiang

Dongmin Liu

Leif Andersson

July 1st, 2014

Blacksburg, VA

Keywords: NPY, adipogenesis, body weight lines, appetite regulation, energy homeostasis, serotonin, 3T3L1 cell line, ZBED6, cytokines, inflammation, obesity

Neurological - Molecular Interface in Food Intake and Metabolism in Birds and Mammals

Wei Zhang

ABSTRACT

Obesity is a physiological consequence of dysregulated energy homeostasis. Energy homeostasis depends on energy intake and energy expenditure. Factors controlling the development of different adipose tissue deposits in the body and their distinct metabolic phenotypes are of considerable interest from both an agricultural and biomedical perspective. Following the literature review, the first chapter was devoted to studies designed to bridge the neural-adipose interface in understanding the relationship between appetite regulation and adipose tissue deposition in chickens, using chickens selected for low or high juvenile body weight as a model. Appetite regulation in the brain, particularly the hypothalamus, is the main factor governing food intake. Neuropeptide Y (NPY), known as a potent orexigenic factor, also promotes energy storage in fat in mammals and thus has a dual role in promoting energy intake via appetite regulation in the brain and energy storage/expenditure via direct effects on adipose tissue function. There have been no reports of the effects of NPY on adipose tissue function in any avian species. By exposing chicken preadipocytes to different concentration of NPY, we found that NPY enhances both proliferation and differentiation and thus appears to play a major role in chicken adipogenesis, an effect that has not yet been reported, to our knowledge. In the body weight selected chicken lines, we found that NPY and receptor sub-type expression was elevated in the abdominal fat of chickens from the high body weight chicken line and expression of these genes displayed heterosis in the reciprocal crosses of the parental

lines as compared to both the high and low body weight selected lines. Intriguingly, expression of those same genes was greater in the low weight than high weight chickens in the hypothalamus. Hypothalamic transcriptomic profiling revealed that genes involved in serotonergic and dopaminergic systems may also play an important role in both appetite regulation and insulin-regulated energy homeostasis in the body weight chicken lines. Intracerebroventricular injection of serotonin in broiler chicks was associated with a dose and time dependent reduction in food intake that was coupled with the activation of the ventromedial hypothalamus and arcuate nucleus, as determined by c-fos immunoreactivity. The remainder of this dissertation project describes the effects of knocking down expression of a recently discovered transcription factor, ZBED6, on mouse preadipocyte proliferation and differentiation. The dissertation ends with a study using diet-induced porcine prepubertal obesity as a model to examine differences in adipokine gene expression between different fat depots from pigs that consumed diets that differed in carbohydrate composition. Overall, we conclude that both NPY and monoamines such as serotonin and dopamine are of importance in the regulation of energy balance in chickens. Moreover, we propose that NPY is a factor that mediates hypothalamus and adipose tissue crosstalk in chickens. An understanding of this system may provide a new avenue for the treatment of obesity and associated disease complications by re-orchestrating the neuronal outputs or adiposity inputs. This information may also be of value in developing strategies to improve feed conversion and meat yield in commercial broiler.

Acknowledgements

Dr. Gilbert: I am very lucky to have you as my advisor. All of the words are blank for me to express my appreciation to you. I still remember the first day we met at the airport. From that moment, I knew that we were going to rock. Thank you for your patience in teaching me the lab techniques and always keeping your door open for me. Also, thank you for all your encouragement, professional guidance and endless inspirational discussions. Thank you for providing me opportunities to attend various conferences even during the "economic crisis period". Your efficiency at editing my papers and lab work always made me want to write more. You are more than a teacher to me in many ways. The time we spent hiking, traveling, and talking about life philosophy will always be the best part of my memories. You have made my Ph.D. study enjoyable and rewarding. I could not have made it this far without you.

Dr. Cline: Although only be able to work with you for 2 years, you have had a tremendous influence on me. I admire you as a teacher and a scientist. Thank you for helping me with my experiments at 5 in the morning, for always being straight with me about my weakness and helping me to improve in many aspects. You are one of the best teachers, and I thoroughly enjoy your classes. Also, thank you for giving me the chance to teach the lab. It was a great experience. You have ignited my desire for pursuing neuroscience.

Dr. Siegel: It is very hard for me to convey my gratitude for everything that you have done for me. Your enthusiasm for science deeply inspired me 5 years ago when you help revised my manuscript in China. Everything feels like it happened yesterday. You have given me every reason for continuing my study abroad, however, I had never imagined

that I would be able to work with you again someday. Thank you so much for your constructional suggestions to my dissertation. The questions you asked were always thought-provoking, which help me to envision the whole picture. Your presence on the farm, in the office and our lab always motivated me to work harder. I could not have made it all the way to where I am today without your encouragement, support and help. I have learned a lot from you and am going to carry that over to the next journey of my research. I will miss all of your life stories. They always led up to meaningful afterthoughts.

Dr. Jiang: Your insightful suggestions and criticisms at different stages of my research have made a big difference in my dissertation. Your strict requirements have held me to a high research standard. Your warm smiles in the hallway always reminded me that nothing is impossible. Thank you for being such a good role model for me to believe that language and culture is not a hindrance for pursuing science.

Dr. Liu: I may not be able to achieve my dream for studying abroad without you. Thank you for taking the chance to bring me here 4 years ago and for always keeping me and my career development in your mind. You always kindly helped me before I even asked and reached your hand out at the most critical times. I appreciate all of your suggestions to my work and the intellectual inputs into my dissertation. Thank you for always being there for me and letting me know that there is someone I can come to when I needed advice.

Dr. Andersson: You have proved to me that there is a way to balance research and other parts of life. Thank you for taking advantage of every opportunity you can get to advise me and provide suggestions to my projects.

Dr. Susan Hutson: Thank you for the warm welcoming party, for having me over for the Christmas festival many times and for letting me spend the most wonderful time with your family. You are as dear as my family and as close as a dear friend. I admire you for being an outstanding female role model. I just want to let you know that I appreciate everything that you have done for me.

Dr. Sally Johnson: You don't how much you have helped me during my experiments. Thank you for generously showing Yue and me the primary cell culture, for patiently explaining to us how it works and details that we needed to pay attention to. You are so knowledgeable and kind. I also appreciate your help in many other things. You always helped me to cool down and to feel like there is some one that I can count on when things don't work.

Dr. Sungwon Kim: What can I do without you? You are one of the most wonderful friends to have. I wish that I knew you earlier. Through these past three years, you have taught me so much in many aspects. I enjoy the criticism from you because I know you want the best out of me. Thanks for always challenging me in many things. They help to shape my mind and force me to really think hard. You have seen me grow, and I want you to know that I will always do my best. Best of luck in your research and life at the Roslin Institute.

Thanks to all the department faculty members, staff, and colleagues, especially to Dr. Jason and Tracy Scheffler, Dr. Rami Dalloul, Dr. Samer EI-Kadi, Dr. Eric Wong, Dr. Michael Denbow, Dr. Ben Dorshorst, Dr. Hao Shi, Dr. Ed Smith, Dr. Rob and Shelly Rhoads, Dr. Jeffery Escobar, Dr. Mike McGilliard, Ellie Stephens, Lee Johnson, Pat Williams, Barbara Self, David Linker, Jennifer Sottosanti Bradley, Melissa Cromer,

Mary Jane Thompson, Christa Honaker, Mike Graham, Brad Reinholt, Eric England, Sarah McCoski, Tiffany Potter, Myeongseon Park, Alamanda Calvert, Victoria McCracken, and Jason Smith. I am so grateful that our paths have crossed. I appreciate each and every one of you for your kind help along my Ph.D. journey. I will cherish all of our experiences together and I want to thank you from the bottom of my heart.

Thanks all my lab mates and friends: Lindsay Sumners, Jiaqing Yi, Guoqing Wang, Shuai Zhang, Laura Nelson, Brittany Rice, Grace Parker, Douglas Gantt, Steven Shipp, Miranda Gerrard, Betty McConn, Dillon Didehvar, Kelsey Marshall, Mary Davis, Catherine Farnan, Xiaoling Zhao, Shiping Bai, Yue Lu, Ting Lu, Ying Jiang, Xing Fen, Jingyi Li, Shengchen Su, Lidan Zhao, Xiaomei Ge, Xiaofei Cong, Haibo Zhu, Guohao Xie, Ming Xie, Zhenhe Zhang, Deng Lei, Delight Yokley, Kristen Clermont, Tere Williams, Craig and Jillian Shillaber, Dustin Sechrest, Josh Abelard, Robert and Karen Howe. You have ended my lonely lab life and turned it into a cheerful journey. I deeply appreciate all of your help during these three years. I couldn't have gotten my dissertation done smoothly without any of you. I will miss you all.

"Dr. Morris", thank you for your companionship and for everything that you have done for me. You make me happy. Good luck with the next step of your career.

Lastly, I want to thank my family. Your support and love have made me go so far. But, no matter where I am or where I will be, we are always together.

Table of Contents

List of Tables

List of Figures

Chapter 1

Introduction

Energy homeostasis plays a pivotal function for normal physiological activities. To maintain energy balance, energy intake needs to match energy expenditure over time. Interruption of this balance can cause various conditions in both humans and animals. Persistent positive energy storage leads to obesity that is characterized by excess fat deposition in the body. The growing obesity epidemic has been in the spotlight for decades. Various pharmacological and surgical methods have been applied for the treatment of obesity. However, due to the complexity of the pathology and the obesogenic environment of modern society, there is still a lack of effective and desirable therapies for obesity in the long term. The detrimental effects of obesity were unappreciated for years and are still being identified. Studies in recent years have indicated that obesity is associated with metabolic syndrome and predisposes individuals to many other diseases such as diabetes, cardiovascular disease and cancer [1-3]. Therefore, understanding the etiology and pathogenesis of obesity is critical in order to find long-term solutions for combatting metabolic disorders and related diseases.

The treatment of obesity is more than just simply to move excess fat, but to understand and control the energy homeostasis. Food intake is the main contributor to energy intake and is governed by the brain. However, energy expenditure is controlled by many internal and external activities. Therefore, identifying strategies for appetite control is a major target nowadays for the control of excess energy deposition, especially as our technology and knowledge in neuroscience has advanced in recent years. Food intake is a complicated process controlled by both the hunger and reward systems in the central

nervous system. Fasting is a strong stimulator of the hunger system that activates the orexigenic modulators in the central nervous system. The hypothalamus is a major area in the brain regulating appetite. It comprises various nuclei such as the arcuate (ARC), Lateral hypothalamus (LH), ventromedial hypothalamus (VMH), dorsomedial hypothalamus (DMH), paraventricular (PVN) that act in concert to activate pathways that regulate meal size and meal number. In the ARC nucleus, there are two distinct groups of neurons. One group is known as neuropeptide Y (NPY)/agouti-related peptide (AgRP) neurons that stimulate food intake when the hunger system is activated. Whereas, the other group of neurons known as the pro-opiomelanocortin (POMC)/cocaine amphetamine regulated transcript (CART) neurons play an opposite role to suppress food intake when the reward system is turned on. Apart from the major appetite regulatory factors, many other neurotransmitters such as various biogenic amines are also critical in mediating appetite and in controlling food intake. Monoamine signaling pathways are common targets of anti-obesity drugs [4].

One of the main consequences of positive energy storage is excess fat deposition. Proper control of fat accumulation is beneficial for our body in terms of energy storage, ameliorating physical trauma, maintaining temperature, and providing structural support for organs. However, too much fat accumulation has various detrimental effects. For human and rodents, there are two types of fat: brown and white adipose tissue serving different functions. White adipose tissue is a site for the storage of excess of energy with a great capacity for expansion. It is associated with inflammation and metabolic disorders during obesity. Brown adipose tissue is mainly used to dissipate energy for heat production, and therefore plays a role in maintaining body temperature and counteracting

weight gain. Brown fat is predominant in infants. It was reported that brown fat in human newborns is about 1% of their body weight [5] and decreases with aging. The adipose tissue is distributed all over the body and is mainly divided into subcutaneous and intro-abdominal fat. Most concerning for health outcomes is the intro-abdominal fat such as visceral fat, which releases metabolites that drain directly into the portal vein in the circulation, which may have negative health outcomes especially in obese individuals. This is closely associated with the other function of adipose tissue as an endocrine organ. Adipose tissue is heterogeneous and comprises adipocytes, adipose progenitors, fibroblasts, macrophages, monocytes, and endothelial cells. Various hormones, adipokines, pro- and anti-inflammatory factors are secreted by adipose tissue that play a major role in whole body energy homeostasis. Dysregulation of this system can cause or exacerbate obesity. About one third of the volume of adipose tissue is mature adipocytes [6]. Adipocytes are derived from mesenchymal stem cells, which can be induced to become preadipocytes and mature through adipogenesis during steps including preadipocyte proliferation and adipocyte terminal differentiation. Adipogenesis is a multi-step highly controlled process involving a cascade of transcription factors, cofactors and signaling intermediates [6]. Understanding these processes is important for therapeutic intervention of fat accumulation and resetting energy homeostasis.

Neuropeptide Y (NPY) is one of the most potent orexigenic signals in the arcuate of the hypothalamus [7]. Most recent studies have focused on central effects of NPY on peripheral energy regulation and fat metabolism [8, 9] and found that it plays an important role in positive energy storage. Given the sequence and functional conservation of NPY between different species, we hypothesize that NPY plays a similar role in

energy regulation in birds as in mammals to promote energy storage. Chicken is a versatile model for study of energy homeostasis because it has the same de novo fatty acid synthesis pathways and anatomical sites as humans. Also, it is small with a short reproduction period and is easy to handle. The two body-weight chicken lines selected for low or high juvenile body weight by Dr. Siegel are a precious research model for eating disorders and obesity due to their distinct appetite and body fat mass differences. My project aims to 1) understand the role in NPY in chicken food intake and fat deposition, 2) identify other major factors resulting in differences in appetite regulation and body composition between the two chicken lines, 3) explore other factors affecting adipose tissue function in mammalian models including a mouse preadipocyte cell line and prepubertal obese pigs.

With these projects, I seek to benefit animal production from an agricultural point of view and to also provide some insight for basic research in understanding mechanisms associated with food intake and fat deposition from a comparative biology and biomedical point of view. The complex interplay between brain and fat turnover involving appetite regulation, energy storage is critical to have a more complete understanding of whole body energy balance.

Reference

1. Aggoun Y: **Obesity, metabolic syndrome, and cardiovascular disease**. *Pediatric research* 2007, **61**(6):653-659.
2. Bae HS, Kim HJ, Hong JH, Lee JK, Lee NW, Song JY: **Obesity and epithelial ovarian cancer survival: a systematic review and meta-analysis**. *Journal of ovarian research* 2014, **7**:41.
3. Zhang Y, Liu H, Yang S, Zhang J, Qian L, Chen X: **Overweight, obesity and endometrial cancer risk: results from a systematic review and meta-analysis**. *The International journal of biological markers* 2014, **29**(1):e21-29.
4. Schwartz MW, Woods SC, Porte D, Jr., Seeley RJ, Baskin DG: **Central nervous system control of food intake**. *Nature* 2000, **404**(6778):661-671.

5. Cypess AM, Kahn CR: **The role and importance of brown adipose tissue in energy homeostasis**. *Current opinion in pediatrics* 2010, **22**(4):478-484.
6. Moreno-Navarrete JM, Fernandez-Real JM: **Adipose tissue biology**: Springer; 2012.
7. Williams G, Harrold JA, Cutler DJ: **The hypothalamus and the regulation of energy homeostasis: lifting the lid on a black box**. *The Proceedings of the Nutrition Society* 2000, **59**(3):385-396.
8. Shi YC, Lau J, Lin Z, Zhang H, Zhai L, Sperk G, Heilbronn R, Mietzsch M, Weger S, Huang XF *et al*: **Arcuate NPY controls sympathetic output and BAT function via a relay of tyrosine hydroxylase neurons in the PVN**. *Cell metabolism* 2013, **17**(2):236-248.
9. Chao PT, Yang L, Aja S, Moran TH, Bi S: **Knockdown of NPY expression in the dorsomedial hypothalamus promotes development of brown adipocytes and prevents diet-induced obesity**. *Cell metabolism* 2011, **13**(5):573-583.

Chapter 2

Hypothalamus-adipose tissue crosstalk: neuropeptide Y and the regulation of energy metabolism

Abstract: Neuropeptide Y (NPY) is an orexigenic neuropeptide that plays a role in regulating adiposity by promoting energy storage in white adipose tissue and inhibiting brown adipose tissue activation in mammals. This review describes mechanisms underlying NPY's effects on adipose tissue energy metabolism, with an emphasis on cellular proliferation, adipogenesis, lipid deposition, and lipolysis in white adipose tissue, and brown fat activation and thermogenesis. In general, NPY promotes adipocyte differentiation and lipid accumulation, leading to energy storage in adipose tissue, with effects mediated mainly through NPY receptor sub-types 1 and 2. This review highlights hypothalamus-sympathetic nervous system-adipose tissue innervation and adipose tissue-hypothalamus feedback loops as pathways underlying these effects. Potential sources of NPY that mediate adipose effects include the bloodstream, sympathetic nerve terminals that innervate the adipose tissue, as well as adipose tissue-derived cells. Understanding the role of central vs. peripherally-derived NPY in whole-body energy balance could shed light on mechanisms underlying the pathogenesis of obesity. This information may provide some insight into searching for alternative therapeutic strategies for the treatment of obesity and associated diseases.

Introduction

Obesity is defined as a state of increased adiposity resulting from chronic nutrient excess, where energy intake significantly exceeds energy expenditure [1]. Energy intake is reflected by food intake and energy expenditure can be affected by basal metabolism,

physical activity, and thermogenesis [2]. Dysregulation of either central or peripheral signals may lead to a state of anorexia or obesity. According to the Center for Disease Control in 2011-2012, more than one third of all U.S. adults are considered to be overweight or obese and these numbers are expected to continue to rise. The rise in obesity, a predisposing factor for developing diabetes, hypertension, hyperlipidemia, cancer and other disorders, has driven a major interest in the regulation of appetite, food intake and fat accumulation [3]. Energy homeostasis is governed by a complex neuroendocrine system including appetite regulatory hypothalamic peptides, as well as adipocyte-derived peripheral signals such as leptin. These signals act in a reciprocal manner to integrate information about energy status, a system referred to as the hypothalamus-adipose tissue axis. The recognition of the importance of the hypothalamus-adipose tissue axis in energy balance has propelled studies aimed at understanding the roles of adipose- and hypothalamic-derived peptides on energy intake, storage and expenditure.

One of the major regulators of energy intake, neuropeptide Y (NPY), has emerged as an important player in the hypothalamus-adipose tissue axis. Neuropeptide Y, a 36 amino acid peptide, is one of the most potent orexigenic hypothalamic neuropeptides identified to date. [4]. Depending on the anatomical location and the receptor sub-type, NPY is also involved in other physiological processes such as locomotion, learning and memory, anxiety, epilepsy, circadian rhythm, and cardiovascular function [3]. The goal of this review is to provide a more in-depth and holistic understanding of the role of NPY in energy homeostasis, bridge the gap between appetite/central nervous system and adipose tissue/peripheral studies, as well as define current challenges and possible future

study directions. To emphasize the potential dual roles of NPY in energy intake and energy storage/expenditure, we highlight the idea of hypothalamus and adipose tissue crosstalk and the connection to the sympathetic nervous system. Numerous studies demonstrate that NPY is a major mediator in promoting energy storage, positing that it could serve as a potential biomarker for obesity. Consistent with this hypothesis, the NPY receptor sub-type 5 (NPYR5) antagonist, velneperit, has been recently explored in clinical testing as a potential anti-obesity drug [5]. Therefore, a better understanding of the mechanisms of how NPY influences body adiposity may facilitate therapeutic interventions for obesity.

NPY and receptor sub-type tissue distribution

In the central nervous system (CNS), NPY is found in highest concentration within the hypothalamus, brain stem, and anterior pituitary. In the arcuate nucleus (ARC) of the hypothalamus, NPY is highly expressed with another orexigenic neuropeptide, agouti-related peptide (AgRP), an endogenous melanocortin receptor 3 and 4 (MC3R and MC4R, respectively) antagonist [6]. The ARC NPY neurons serve as a feeding center that senses and integrates peripheral energy signals, such as blood glucose concentration, ghrelin, leptin and insulin, due to the unique anatomic structure of the ARC in lacking a blood brain barrier [7]. The synthesis and secretion of ARC NPY is induced in response to energy deficiency and greater metabolic demand such as increased exercise, cold and pregnancy [8].

The NPY affects food intake by innervating with other appetite regulatory factors in the CNS and regulates energy utilization via modulation of fat deposition and metabolism. These functions are achieved by binding to various NPY receptors (NPYRs)

that are distributed across the body, the most well-known being NPYR1, NPYR2, and NPYR5, all of which are G protein coupled receptors [9]. In situ hybridization assays on adult mouse brain sections revealed widespread distribution of NPYR1, while NPYR2 and 5 displayed a more restricted pattern of expression [10]. The NPYR1 is considered to be most directly involved in food intake and energy expenditure, whereas the NPYR2 receptor is an autoreceptor that is mainly expressed in the ARC, and can regulate food intake and energy balance through modulation of endogenous NPY release [11, 12]. The NPYR1 has a high affinity for the NPY analog [Leucine^{31}, Proline^{34}] and requires a complete N terminus for binding. It has lower affinity for NPY C-terminal fragments such as NPY_{13-36} and NPY_{3-36} [13]. The NPYR2 requires intact carboxyl-terminal fragments for binding [14]. The preferred binding ligands, distribution of NPYRs, and NPY function in the CNS and adipose tissue are summarized in **Table 2.1**.

In the periphery, NPY is widely distributed in the sympathetic nerves, the adrenal medulla, platelets, and various cell types within white adipose tissue [15]. The expression of NPY and NPYR2 can be induced in macrophages [16], platelets, nerves, and adipocytes by stress or genetically- or high fat diet-induced obesity in mice [16, 17]. In human adipose tissue, NPY was detected in mature adipocytes but not in preadipocytes [18]. Others detected NPY mRNA in human subcutaneous and visceral fat [19] and murine adipocytes as well as various cell types from adipose tissue stromal vascular fractions (SVF) [16]. Increased expression of NPY in adipose tissue appears to be a common feature of obesity in different species. Abundance of NPY mRNA and protein was greater in visceral fat (pooled mesenteric, omental and retroperitoneal) of 21 day-old obese rats born from dams that were fed a low-protein diet during gestation and lactation,

compared to controls [20]. There was also greater NPY mRNA in visceral fat of obese Zucker rats compared to their lean counterparts, and both an insulin analogue and dexamethasone augmented NPY expression in lean but not obese rats [20]. We reported greater expression of NPY and NPYR1 and NPYR5 mRNA in the abdominal fat of obese chickens compared to lean chickens [21].

The NPYR1, NPYR2 and NPYR5 have all been detected in various cell types from different fat depots in rodent models [16, 22, 23], although in one report NPYR5 was not detected by real time PCR in either adipocytes or the SVF of adipose tissue from either lean or obese mice [16] and in another only NPYR5 was detected in sympathetic neuron/3T3-L1 co-cultures [24]. Human and mouse preadipocytes, adipocytes and endothelial cells express NPYR2 [17] and mouse NPYR1 expression was detected in mouse preadipocytes and adipocytes [24]. Others reported that NPYR1 mRNA was abundant in both rat and mouse preadipocytes, whereas NPYR2 and NPYR5 were undetectable [20]. We demonstrated that NPY, NPYR1, NPYR2 and NPYR5 mRNA were expressed in chicken abdominal fat, albeit at lower quantities than in the hypothalamus, with differential expression between chickens selected for low or high body weight, and highly negative heterosis, suggesting a role for the NPY system in energy balance in chickens [21]. Thus, in a variety of vertebrates, NPY and NPYR1, 2 and 5 are expressed in various cell types in white adipose tissue.

Adipose tissue function and sympathetic nervous system innervation

As the primary energy storage reservoir, adipose tissue plays an important role in energy balance. It contains two distinct types of fat tissue: white adipose tissue (WAT) and brown adipose tissue (BAT). White adipose tissue is specialized for the storage of

chemical energy in the form of triacylglycerol (TAG), while BAT dissipates chemical energy in the form of heat through non-shivering thermogenesis. As will be discussed in this review, major mechanisms for WAT expansion and turnover are changes in rates of adipocyte precursor cell proliferation, differentiation of precursor cells into adipocytes (adipogenesis), as well as changes in synthesis of fatty acids (lipogenesis), TAGs, and hydrolysis of stored lipids (lipolysis) to liberate glycerol and free fatty acids in the adipocyte [25]. Unlike WAT, BAT dissipates chemical energy in the form of heat generation by means of uncoupling protein 1 (UCP1) expression to uncouple respiration in the mitochondria [2]. Increased BAT in animals was associated with a lean and healthy phenotype [26], whereas loss of BAT was correlated with obesity and metabolic diseases [27]. BAT is predominantly distributed in the interscapular region of mammals. Although brown fat was once considered only necessary in early neonates, recent positron emission tomography scanning studies demonstrated that this tissue is present and plays a pivotal role in energy balance in adult humans [28, 29]. Therefore, induction of BAT in humans offers the possibility of increasing energy expenditure without necessarily causing dysfunction in other tissues, and is hence an obvious therapeutic target for treating obesity.

White adipose tissue is a heterogeneous organ comprised of mature adipocytes, preadipocytes, mesenchymal stem cells, immune cells, and a matrix of collagen fibers that house numerous nerve endings and vascular networks [30]. Thus, NPY can potentially affect WAT metabolism through the neuroendocrine route, where it is co-stored with norepinephrine (NE) and can be secreted via sympathetic nervous system (SNS) innervation, autocrine mechanisms by mature adipocytes, paracrine pathways by

immune cells [16], as well as endocrine routes by platelets from the blood vessels, or across the blood brain barrier [31]. Neuropeptide Y coexists within the nerve terminal with NE and adenosine triphosphate in postganglionic sympathetic nerve fibers throughout the body, and can be co-released from the axon terminals in different quantities depending on the stimulation intensity and the pattern of sympathetic nerve activation [32, 33]. Retrograde and anterograde fluorescence tract tracers were used to reveal sympathetic innervation of adipose tissue and that different fat depots were differentially innervated (reviewed by [34]). As will be described later in this review, the hypothalamus-SNS-WAT pathway provides a plausible mechanism for how NPY exerts reciprocal functions on energy intake via the hypothalamus and energy storage and expenditure via WAT.

NPY promotes adipogenesis and inhibits lipolysis in adipose tissue

NPY was shown to have hyperplasic, adipogenic and antilipolytic effects in adipose tissue cells, and angiogenic effects in the vasculature surrounding adipose cells (a major contributor to adipose expansion) both in vitro and in vivo [17, 35], although in one study there was no effect of NPY treatment on lipid accumulation in 3T3-L1 cells at 8 days post-differentiation [20]. Effects of NPY on adipose tissue function were thought to occur mainly via NPYR1- and NPYR2-mediated pathways, although NPYR5 has also been implicated in the cellular responses [14, 17, 31, 36, 37]. Two weeks of cold exposure, combined with consumption of a high-fat and high-sugar diet, was associated with increased expression of NPY and NPYR2 in subcutaneous fat depots of mice, with expression localized to blood vessels, nerves and adipocytes [17]. Conditional knockdown of NPYR2 in only the peripheral tissues (including adipose) of adult mice

prevented high fat diet-induced obesity [38]. In normal chow-fed mice, the knockdown had no effect on food intake or body weight, suggesting that NPYR2 plays an important role in energy oxidation in peripheral tissues [38]. The NPYR2 germline knock-out mice were not susceptible to cold stress-induced augmentation of diet-induced obesity and treatment of wild-type mice with a NPYR2 antagonist for 2 weeks via slow-release pellets delivered to the adipose tissue reduced visceral fat depot mass by 40%. Similarly, conditional knockdown of NPYR2 by an adenoviral vector injected into the subcutaneous abdominal fat of mice led to a 50% reduction in stress-induced fat expansion after 2 weeks [17]. These results collectively suggest that those NPY-mediated effects on adipose tissue were occurring mainly through NPYR2 [17]. Similarly, in immune-deficient mice or rhesus monkeys that received subcutaneous injections of a 14-day slow-release NPY pellet, a ring of new fat tissue appeared around the pellet, and was sustained for at least 3 months, demonstrating the ability of NPY to locally promote de novo fat formation [39]. Neuropeptide Y-mediated effects on fat were also demonstrated with a translational application to reconstructive surgery [39]. Freshly collected human adipose tissue was transplanted into immune-deficient mice and effects of NPY on fat graft survival and vascularity were assessed [39]. Treatment with NPY enhanced long-term (3 month) human fat graft survival and vascularity in the athymic mice, whereas in mice that did not receive NPY pellet injection, there was greater than 70% resorption of the xenograft, a major concern with such transplantation surgeries in humans [39]. Researchers showed that the effects on fat pad mass were due to enhanced survival of the human graft and not synthesis of new adipose tissue by the host animal, illustrating a potential clinical application of NPY.

In genetically obese (B6.V-Lep$^{ob/J}$) mice, plasma concentrations of NPY were more than 200% greater than wild-type mice, and the obese mice also displayed greater expression of NPY and NPYR2 mRNA in subcutaneous fat, suggesting that the elevated circulating NPY originated from adipose tissue [17]. Interestingly, in both obese and lean wild-type mice, there was substantial adipose tissue expansion as a result of treatment with NPY pellets (1 μg per 14-day release pellet) delivered locally to the subcutaneous abdominal fat [17]. These effects were blunted when mice were injected with a pellet containing BIIE0246, an NPYR2 antagonist (1 umol/day for 14 d), with a decrease in fat mass accompanied by reduced vascularity and increased apoptosis in the abdominal fat pads [17]. Results from these studies implied that NPY's actions on adipose tissue include promotion of both adipogenesis and angiogenesis, both mediated primarily through NPYR2 [17].

Function through NPYR2 could be mediated through enzymatic cleavage of the NPY peptide in adipose tissue [35]. In one study, NPY and dipeptidyl peptidase –IV (DPPIV) mRNA were detected in both 3T3-L1 preadipocytes and terminally differentiated adipocytes, and treatment of preadipocytes with recombinant DPPIV promoted differentiation of cells into adipocytes [35]. The DPPIV is known to cleave NPY into the NPYR2 agonist NPY_{3-36}. Immunoneutralization of NPY or treatment with a NPYR2 antagonist, but not NPYR1 or NPYR5 antagonists, blunted DPPIV's adipogenic effects [35]. Treatment with NPY alone also promoted preadipocyte differentiation and combined treatment of NPY with a DPP-IV inhibitor , vildagliptin, blocked NPY's adipogenic effects, lending further support to the idea that DPP-IV cleaves NPY in

adipose tissue and thereby promotes adipogenesis via NPYR2-mediated cell signaling [35].

Effects of NPY on TAG hydrolysis, on the other hand, were shown to occur mainly through NPYR1, with effects on lipolysis influenced by the nutritional state, other cellular factors, and genetic background of the animal. For example, in cultured rat adipocytes, NPY dose-dependently inhibited lipolysis, an effect that was blunted when the animals were fasted for 48 hours prior to treatment [14]. Receptor-specific NPY fragments were used to show that inhibition of lipolysis was mediated through NPYR1. In visceral fat cells (but not subcutaneous) from rats that were injected with 6-hydroxydopamine (OHDA) (a neurotoxin for sympathetic neurons that is used to chemically ablate sympathetic nerves), lipolysis was increased and the effects were shown to occur via NPYR2-mediated signaling mechanisms [14]. Using receptor-specific peptide fragments, it was shown that inhibition of lipolysis in adipose tissue occurred through NPYR1 but not NPYR2, and that the increase in lipolysis observed after sympathectomy and treatment with a NPYR2-specific peptide could be due to a switching of the receptor from G_i to G_s coupling [14].

Metabolic differences observed between subcutaneous and visceral fat depots may be partly explained by differences in SNS innervation. In general, visceral fat in humans is associated with adverse health outcomes, whereas subcutaneous adipose tissue is considered to be an energy storage reservoir that is relatively benign [25]. Recently, Nguyen et al. demonstrated that while there was some overlap in central sympathetic neural circuits between inguinal (subcutaneous) and mesenteric (visceral) fat in Siberian hamsters, there were more neurons involved in innervating the inguinal fat pads, and

interestingly, food withdrawal induced a stronger sympathetic drive to inguinal adipose tissue [40]. Thus, research on NPY's role in adipose tissue function should take into consideration the differences in physiology between fat depots in different anatomical locations under different nutritional conditions.

The effects of NPY on lipolysis appear to be highly dependent on other cellular factors influencing β-adrenergic stimulation in the adipocyte. In one study, NPY was shown to have no effect on lipolysis in differentiated 3T3-L1 cells under basal conditions, but augmented β-adrenergic-mediated stimulation of lipolysis [41]. When cells were pretreated with isoproterenol (10 nM; β-adrenergic agonist) and/or forskolin (activates adenylyl cyclase to raise intracellular cAMP), NPY treatment had no effect on forskolin-induced lipolysis, but increased isoproterenol-induced lipolysis by 30%, suggesting that NPY's effect occurred upstream of adenylyl cyclase activation [41]. To explain why results differed from previous reports of NPY's inhibitory effects on lipolysis in cultured adipocytes [14, 42, 43], it was suggested that NPY's effect on lipolysis depends on the magnitude of β-adrenergic and lipolytic stimulation by other factors. For example, when concentrations of isoproterenol increased, NPY blunted rather than augmented the stimulation of lipolysis, thus suggesting that perhaps under conditions of strong and weak stimulation of lipolysis, NPY has an inhibitory and stimulatory effect, respectively [41]. Consistent with other studies, the effects of NPY on lipolysis were shown to occur through NPYR1, and it was suggested that differential effects of NPY on lipolysis occurring through the same receptor are due to differences in receptor coupling to different secondary messengers, with inhibitory and stimulatory effects on lipolysis occurring through decreases in cAMP and increases in calcium, respectively [41]. That

NPY and NE are co-stored and secreted by postsympathetic nerve terminals in adipose tissue provides an additional layer of complexity to the understanding of how the different systems interact to regulate energy metabolism in adipose tissue [41]. Thus, NPY's effects on lipolysis can be modulated by nutritional status, adrenergic activity, and changes in receptor activity to achieve tight regulation of energy balance based on energy demand, with differences between visceral and subcutaneous fat.

Thus, NPY's effects on adipose tissue appear to be related to SNS output and as described above, NPY may influence angiogenesis, adipogenesis, lipolysis, and hypertrophy in WAT. Obesity is characterized by WAT hypercellularity and hypertrophy, particularly in visceral fat, and changes in SNS activity, consistent with enhanced lipid storage and reduced oxidation [44, 45]. The decreased SNS outflow observed in some obesity models may stimulate WAT hyperplasia, based on experiments showing that sympathetic nerve denervation induces cellular proliferation in adipose tissue and NE treatment in cell culture reduced preadipocyte proliferation, an effect that was blunted by the β-adrenoceptor antagonist propranolol [46, 47]. Although mechanisms of NPY's role in hyperplasia are not as well studied, it was shown that through NPYR1, NPY stimulated mouse and rat preadipocyte proliferation via activation of the extracellular signal-regulated kinase (ERK) 1/2 signaling pathway [20]. In high-fat diet-fed mice that were exposed to cold stress for 2 weeks, there was an increase in the number of small adipocytes (< 10 μM) that were immunoreactive for both NPYR2 and cell proliferation markers, suggesting that NPY plays a role in inducing hyperplasia via NPYR2. Similarly, co-culture of 3T3-L1 preadipocytes or endothelial cells with sympathetic neuron-derived tumor cells (tyrosine hydroxylase-positive) up-regulated expression of NPYR2 and

induced proliferation in both the endothelial cells and preadipocytes, and enhanced differentiation of preadipocytes into adipocytes [17]. Enhanced differentiation was associated with increased lipid accumulation and secretion of leptin and resistin. These effects were blocked by treatment with a NPYR2 receptor antagonist, suggesting that in adipose tissue, SNS-derived NPY modulates proliferation, adipogenesis and angiogenesis via up-regulation of NPYR2 [17].

The SNS innervation to WAT is known to play three major functions including the regulation of lipolysis, cellular proliferation and protein/peptide secretion [34]. Catecholamines (especially NE) are potent lipolytic factors acting through β-adrenergic receptors, which then activate the cyclic adenosine monophosphate (cAMP) – protein kinase A (PKA) signaling cascades. Sympathetic neuron and adipocyte co-culture studies indicated that NPY secreted from sympathetic neurons inhibited β-adrenergic-mediated lipolysis [31], although as discussed above, NPY treatment could elicit different effects on lipolysis depending on the combination of other factors present in the cell culture model [41]. Cross-talk between adipocytes and SNS neurons are thus mediated by multiple signals and NPY may modulate β-adrenoceptor-mediated lipolysis and adipokine secretion. Surgical sympathetic nerve denervation increased the numbers of bromodeoxyuridine-labeled cells that were also immunoreactive for a preadipocyte-specific membrane protein 3 (AD-3), indicating a specific increase in preadipocyte proliferation [48, 49]. Decreased sympathetic drive to WAT resulted in WAT expansion that was associated with decreases and increases in β-adrenergic and α_2-adrenergic receptor numbers, respectively [50].

An in vitro study demonstrated that epinephrine (EPI) enhanced the expression of

NPY and its receptors in murine embryonic stem cells (mESCs), and that accelerated differentiation of mESCs into adipocytes was associated with increased expression of preadipocyte factor 1 (PREF-1), fatty acid-binding protein 4 (FABP4) and peroxisome proliferator-activated receptor γ **(**PPARγ) [51]. These effects were blocked by treatment with NPYR1, 2 and 5 antagonists [51]. The effect of EPI-mediated NPY up-regulation was believed to be associated with greater DNA methylation at the nerve growth factor responsive element and calmodulin-responsive element sites of the NPY gene promoter region [51]. While cell culture-based studies have shown a strong effect of EPI on lipolysis, it has been demonstrated in-vivo that adrenal medullary-derived EPI likely is a minor contributor to whole-body adipose lipolysis, with the majority controlled by SNS-derived NE, as reviewed by [52].

NPY reduces brown adipose tissue deposition and activation

Brown adipose tissue is almost exclusively under SNS innervation. The release of norepinephrine (NE) from SNS terminals stimulates β_3-adrenergic receptor-activated BAT thermogenesis [53]. Central administration of NPY in rats inhibited BAT thermogenesis through guanosine diphosphate binding reduction (an indicator of brown fat thermogenic activity) to BAT mitochondria, and stimulated WAT lipid storage by enhancing lipoprotein lipase (LPL) activity, which is a rate-limiting step in catalyzing hydrolysis of plasma lipoproteins into free fatty acids for uptake into peripheral tissues [54]. Despite ample evidence that NPY reduces BAT-associated thermogenesis, it was not until recently that our understanding of the involvement of various CNS-specific nuclei/subnuclei was revealed. Chao et al. demonstrated the role of hypothalamic dorsomedial NPY in adipose tissue function [55]. Knockdown of NPY expression using

adeno-associated virus-mediated RNAi in the dorsomedial nucleus (DMN) of rat hypothalamus promoted development of brown adipocytes in inguinal white adipose tissue or transformation from WAT to BAT (also known as brown-in-white, beige or brite cells) characterized by increases in mitochondrial UCP1 and peroxisome proliferator activated receptor-γ coactivator -1 α (PGC1α) expression, when measured at 16 weeks post treatment. This led to increased BAT activity and thereby enhanced energy expenditure and cold-induced thermogenesis [55]. The inducible nature of brown adipocytes in white adipose tissue is intriguing as a possible anti-obesity target and these data show that effects of hypothalamic NPY on brown fat include both inhibition of brown fat thermogenesis and effects on recruitment of brown adipocytes within white adipose depots. These studies are also fascinating because they provide more insight into the physiological function of specific hypothalamic nuclei, such as the DMN.

Other studies using mouse models in which NPY was either overproduced in the ARC of wild type mice or selectively reintroduced into the ARC of otherwise NPY-deficient mice, together with NPY receptor knockout mice, indicated that overexpression of ARC NPY reduced sympathetic outflow via NPYR1 receptor-mediated reduction in tyrosine hydroxylase (TH; an indicator of SNS outflow) expression in the PVN and various regions in the brainstem. Reduced SNS innervation was associated with the down-regulation of UCP1 expression in BAT, which could be reversed after surgical sympathetic denervation to BAT [56]. The ICV injection of NPY suppressed SNS activity in a dose-dependent manner, which was followed by a gradual recovery. Unilaterally microinjecting NPY into the paraventricular nucleus (PVN) suppressed the SNS, and the opposite was observed after medial preoptic area microinjection. No effect

was observed with injection into the anterior hypothalamic area, ventromedial nucleus (VMN), or lateral hypothalamus (LH) [57]. Reduced SNS outflow decreases release of NE from sympathetic nerve endings and inhibits the thermogenic function of brown adipose tissue (BAT) by deactivating the cAMP-dependent PKA pathway, which further down-regulates UCP1-associated thermogenesis.

Taken together, these data indicate that NPY promotes positive energy balance by stimulating adipogenesis and inhibiting lipolysis in WAT. Increased thermogenesis in brown fat and recruitment of brown adipocytes in white adipose tissue after NPY suppression suggests that the NPY system also has an inhibitory effect on BAT activity. These effects appear to be mediated through the regulation of the hypothalamus-SNS-adipose tissue axis. The possible mechanisms described above are summarized in **Figure 2.1 and Figure 2.2**.

Hypothalamus-adipose tissue crosstalk

The NPY system represents a form of communication between the hypothalamus and adipose tissue, and is linked to positive energy balance through increases in energy intake and storage and reduced energy expenditure. This is achieved indirectly through bidirectional neuronal and hormonal communication, and possibly via direct circulation through the blood brain barrier. The hypothalamus is the energy sensory center for signals produced by peripheral tissues such as the gastrointestinal tract and adipose tissue. Hypothalamus-mediated white and brown adipose tissue turnover is mainly regulated through SNS outflow, as summarized above. The study of the role of specific hypothalamic nuclei in the regulation of peripheral adiposity did not receive much attention until recently, partly due to advents in molecular technology as well as a better

understanding of brain neural circuits. A body of evidence has shown that NPY in the ARC, PVN, and DMN neurons is involved in adiposity and BAT thermogenesis through regulation of the SNS outflow [55, 56]. Whether other hypothalamic nuclei play the same role remains elusive.

While early studies revealed that adipose tissue was innervated by the sympathetic nervous system, they did not reveal the specific brain nuclei from which the SNS outflow to WAT originated. A transneuronal tract tracer, a pseudorabies virus (PRV), was used for this purpose, because it is a neurotropic virus that binds to the presynaptic neural membrane, fuses with the axon membrane, and then delivers uncoated capsids in the axon (described in an excellent review by [34]). The capsids are then transported to the cell body where they replicate and can exit the infected cell via the dendrites, thereby only infecting neurons that are synaptically connected to those PRV-containing cells [34]. Immunostaining after PRV injection into fat revealed that in hamsters, regions of the hypothalamus including the ARC, dorsal, lateral, suprachiasmatic, PVN, and nuclei and medial preoptic area, were identified as sites that modulated SNS outflow to the WAT. [34]. Hypothalamus-SNS-BAT circuitries were demonstrated to be hyperactive in the PVN, DMN, LH, anterior hypothalamic nucleus, and posterior hypothalamic nucleus [58]. Whether adipose tissue is also under the control of the parasympathetic nervous system is still controversial [59, 60]. Identification of hypothalamic nuclei associated with adiposity and brown fat thermogenesis may provide better targets toward the control of overweight and obesity through the manipulation of the hypothalamus-adipose tissue axis, and allow for development of more pathway-specific therapeutic strategies.

Adipose tissue not only dynamically accumulates and releases lipids, but also serves as an endocrine organ that produces adipokines, hormones, and appetite-regulating factors as the sensory input reflecting the amount of lipid and adipocyte turnover. Sensory information is transported via dorsal root ganglion to the spinal cord and then on to the brain to interact with the SNS outflow to the adipose tissue [34, 58, 61]. The sensory innervation of adipose tissue may serve as a feedback loop to regulate the level of its sympathetic drive and also regulate adipocyte turnover [62]. Sensory information includes adipokines such as adiponectin, apelin, resistin and leptin, that all target various regions in the hypothalamus and regulate body energy homeostasis [63]. Leptin is one of the best studied adipokines that informs the brain of body fat levels. Treatment of human abdominal subcutaneous adipocytes with recombinant human NPY reduced leptin secretion but did not affect release of adiponectin and tumor necrosis factor α [18]. Interestingly, high fat diet-induced diabetic mice subjected to intra-abdominal UCP1 overexpression using an adenoviral vector had significantly reduced food intake characterized by reduced NPY mRNA in the hypothalamus, and improved insulin and leptin sensitivity. Local nerve dissection showed that these actions were achieved by afferent-nerve signals from intra-abdominal fat tissue to the hypothalamus that modulated hypothalamic leptin sensitivity, illustrating the importance of the hypothalamus-adipose tissue feedback loop [64]. This may suggest that brown adipocytes in WAT play an important role in whole-body energy metabolism and ectopic UCP1 expression could be a promising future research direction. In summary, an adiposity negative-feedback model indicates that adiposity signals can inform the brain of changes in body fat mass so that the brain can mount adaptive adjustments in energy intake to stabilize fat stores in the

long term. Understanding the neural signaling pathways and endocrine regulation associated with the adiposity negative feedback may provide a new avenue for treatment of obesity and associated diseases.

Central vs. peripheral circulating NPY

NPY is expressed in both the hypothalamus and periphery and is detected in the circulation. Understanding the cellular sources, routes of delivery to various tissues and the rate of decay are critical for understanding the physiological roles of NPY. The majority of NPY is secreted by the neurons in the CNS with lower concentrations in the peripheral system. In the SVF fraction of adipose tissue from mice, secreted NPY was reported to be in the picomolar range, consistent with physiological concentrations in humans [16]. Recent studies showed that the concentration of cerebrospinal fluid (CSF) NPY (cNPY; 792.1 pg/mL) was 3 fold greater than plasma NPY (pNPY; 220.0 pg/mL) in humans [65]. Therefore, whether hypothalamus-derived NPY can enter the blood stream is critical in understanding the regulation of food intake and fat deposition. A clinical study demonstrated that circulating NPY in obese women was elevated as compared to women from the control group [66]. However, no statistically significant cross-correlations have been identified between CSF and plasma NPY in healthy males. Circulating NPY was also elevated in genetically obese mice [17]. The cNPY/pNPY ratio depends on the rates of NPY production, degradation, reabsorbtion in both compartments and potential transport across the blood brain barrier. Although NPY was shown to cross the blood-brain barrier intact via a non-saturatable transporter in rats, which is still unidentified in humans [67], the absence of cross-correlation between CSF and plasma may be due to local protease degradation as indicated by Baker et al [39]. As a peptide,

the active window of time for NPY is short as compared to a steroid neurotransmitter. Ahlborg et al showed that in adult men the half-life for NPY is up to 39 min [68]. The concentration of NPY in both central and peripheral compartments has a higher heritability than other neuropeptides [69, 70], which makes it an attractive candidate for research on genetic aspects of metabolic diseases. Thus, a further understanding of factors governing NPY concentrations and transport in the circulation and between central and peripheral systems, especially in humans, will rely on more research together with advanced techniques that are sensitive to lower concentrations of NPY.

Conclusions and implications

Neuropeptide Y stimulates food intake and white fat deposition and at the same time reduces brown fat activation and consequently thermogenesis, yielding a net accumulation of energy via enhanced energy intake and storage (**Figure 2.3**). The function of NPY is determined by site-specific NPY and NPY receptor-subtype expression, NPY release, degradation, and concentrations in the circulation, all of which are regulated by numerous energy balance strategies. This provides tight regulation of an essential system to ensure that the NPY signals can respond rapidly and for prolonged durations during short and long-term control of energy homeostasis in various food-accessible conditions. Understanding the role of NPY in energy homeostasis has critical implications for biomedical applications, the most common pharmacological therapies nowadays for obesity involving gastrointestinal surgery and pharmacological interventions. Drugs that are intended for weight loss affect either metabolism by reducing absorption of nutrients from food or through the CNS by decreasing appetite and increasing energy expenditure. In light of the purported systemic role of NPY, it

becomes a promising candidate for controlling the development and treatment of obesity. Whether NPY can be used as a biomarker for obesity awaits further determination. A body of studies aimed to manipulate NPY and NPY receptor-subtype function highlight the feasibility of targeting the NPY system for therapeutic strategies. However, the mechanisms underlying the effects of NPY are complicated, especially in view of brain-adipose cross talk.

References

1. Morton GJ, Cummings DE, Baskin DG, Barsh GS, Schwartz MW: **Central nervous system control of food intake and body weight**. *Nature* 2006, **443**(7109):289-295.
2. Rosen ED, Spiegelman BM: **Adipocytes as regulators of energy balance and glucose homeostasis**. *Nature* 2006, **444**(7121):847-853.
3. Mercer RE, Chee MJ, Colmers WF: **The role of NPY in hypothalamic mediated food intake**. *Frontiers in neuroendocrinology* 2011, **32**(4):398-415.
4. Carlquist M, Jornvall H, Tatemoto K, Mutt V: **A porcine brain polypeptide is identical to the vasoactive intestinal polypeptide**. *Gastroenterology* 1982, **83**(1 Pt 2):245-249.
5. George M, Rajaram M, Shanmugam E: **New and emerging drug molecules against obesity**. *Journal of cardiovascular pharmacology and therapeutics* 2014, **19**(1):65-76.
6. Broberger C, Johansen J, Johansson C, Schalling M, Hokfelt T: **The neuropeptide Y/agouti gene-related protein (AGRP) brain circuitry in normal, anorectic, and monosodium glutamate-treated mice**. *Proceedings of the National Academy of Sciences of the United States of America* 1998, **95**(25):15043-15048.
7. Kohno D, Yada T: **Arcuate NPY neurons sense and integrate peripheral metabolic signals to control feeding**. *Neuropeptides* 2012, **46**(6):315-319.
8. Leibowitz SF, Wortley KE: **Hypothalamic control of energy balance: different peptides, different functions**. *Peptides* 2004, **25**(3):473-504.
9. Larhammar D, Blomqvist AG, Soderberg C: **Evolution of neuropeptide Y and its related peptides**. *Comparative biochemistry and physiology C, Comparative pharmacology and toxicology* 1993, **106**(3):743-752.
10. Naveilhan P, Neveu I, Arenas E, Ernfors P: **Complementary and overlapping expression of Y1, Y2 and Y5 receptors in the developing and adult mouse nervous system**. *Neuroscience* 1998, **87**(1):289-302.
11. Gehlert DR: **Role of hypothalamic neuropeptide Y in feeding and obesity**. *Neuropeptides* 1999, **33**(5):329-338.

12. Batterham RL, Cowley MA, Small CJ, Herzog H, Cohen MA, Dakin CL, Wren AM, Brynes AE, Low MJ, Ghatei MA *et al*: **Gut hormone PYY(3-36) physiologically inhibits food intake**. *Nature* 2002, **418**(6898):650-654.
13. Kamiji MM, Inui A: **Neuropeptide y receptor selective ligands in the treatment of obesity**. *Endocrine reviews* 2007, **28**(6):664-684.
14. Labelle M, Boulanger Y, Fournier A, St Pierre S, Savard R: **Tissue-specific regulation of fat cell lipolysis by NPY in 6-OHDA-treated rats**. *Peptides* 1997, **18**(6):801-808.
15. Hirsch D, Zukowska Z: **NPY and stress 30 years later: the peripheral view**. *Cellular and molecular neurobiology* 2012, **32**(5):645-659.
16. Singer K, Morris DL, Oatmen KE, Wang T, DelProposto J, Mergian T, Cho KW, Lumeng CN: **Neuropeptide Y is produced by adipose tissue macrophages and regulates obesity-induced inflammation**. *PloS one* 2013, **8**(3):e57929.
17. Kuo LE, Kitlinska JB, Tilan JU, Li L, Baker SB, Johnson MD, Lee EW, Burnett MS, Fricke ST, Kvetnansky R *et al*: **Neuropeptide Y acts directly in the periphery on fat tissue and mediates stress-induced obesity and metabolic syndrome**. *Nature medicine* 2007, **13**(7):803-811.
18. Kos K, Harte AL, James S, Snead DR, O'Hare JP, McTernan PG, Kumar S: **Secretion of neuropeptide Y in human adipose tissue and its role in maintenance of adipose tissue mass**. *American journal of physiology Endocrinology and metabolism* 2007, **293**(5):E1335-1340.
19. Sitticharoon C, Chatree S, Churintaraphan M: **Expressions of neuropeptide Y and Y1 receptor in subcutaneous and visceral fat tissues in normal weight and obese humans and their correlations with clinical parameters and peripheral metabolic factors**. *Regulatory peptides* 2013, **185**:65-72.
20. Yang K, Guan H, Arany E, Hill DJ, Cao X: **Neuropeptide Y is produced in visceral adipose tissue and promotes proliferation of adipocyte precursor cells via the Y1 receptor**. *FASEB journal : official publication of the Federation of American Societies for Experimental Biology* 2008, **22**(7):2452-2464.
21. Zhang W, Sumners LH, Siegel PB, Cline MA, Gilbert ER: **Quantity of glucose transporter and appetite-associated factor mRNA in various tissues after insulin injection in chickens selected for low or high body weight**. *Physiol Genomics* 2013, **45**(22):1084-1094.
22. Gong HX, Guo XR, Fei L, Guo M, Liu QQ, Chen RH: **Lipolysis and apoptosis of adipocytes induced by neuropeptide Y-Y5 receptor antisense oligodeoxynucleotides in obese rats**. *Acta pharmacologica Sinica* 2003, **24**(6):569-575.
23. Rosmaninho-Salgado J, Cortez V, Estrada M, Santana MM, Goncalves A, Marques AP, Cavadas C: **Intracellular mechanisms coupled to NPY Y2 and Y5 receptor activation and lipid accumulation in murine adipocytes**. *Neuropeptides* 2012, **46**(6):359-366.
24. Gericke MT, Kosacka J, Koch D, Nowicki M, Schroder T, Ricken AM, Nieber K, Spanel-Borowski K: **Receptors for NPY and PACAP differ in expression and activity during adipogenesis in the murine 3T3-L1 fibroblast cell line**. *British journal of pharmacology* 2009, **157**(4):620-632.

25. Sethi JK, Vidal-Puig AJ: **Thematic review series: adipocyte biology. Adipose tissue function and plasticity orchestrate nutritional adaptation**. *Journal of lipid research* 2007, **48**(6):1253-1262.
26. Kopecky J, Clarke G, Enerback S, Spiegelman B, Kozak LP: **Expression of the mitochondrial uncoupling protein gene from the aP2 gene promoter prevents genetic obesity**. *The Journal of clinical investigation* 1995, **96**(6):2914-2923.
27. Lowell BB, V SS, Hamann A, Lawitts JA, Himms-Hagen J, Boyer BB, Kozak LP, Flier JS: **Development of obesity in transgenic mice after genetic ablation of brown adipose tissue**. *Nature* 1993, **366**(6457):740-742.
28. Nedergaard J, Bengtsson T, Cannon B: **Unexpected evidence for active brown adipose tissue in adult humans**. *American journal of physiology Endocrinology and metabolism* 2007, **293**(2):E444-452.
29. Cypess AM, Lehman S, Williams G, Tal I, Rodman D, Goldfine AB, Kuo FC, Palmer EL, Tseng YH, Doria A *et al*: **Identification and importance of brown adipose tissue in adult humans**. *The New England journal of medicine* 2009, **360**(15):1509-1517.
30. Kirkland JL, Dobson DE: **Preadipocyte function and aging: links between age-related changes in cell dynamics and altered fat tissue function**. *Journal of the American Geriatrics Society* 1997, **45**(8):959-967.
31. Turtzo LC, Marx R, Lane MD: **Cross-talk between sympathetic neurons and adipocytes in coculture**. *Proceedings of the National Academy of Sciences of the United States of America* 2001, **98**(22):12385-12390.
32. Morris JL: **Cotransmission from sympathetic vasoconstrictor neurons to small cutaneous arteries in vivo**. *The American journal of physiology* 1999, **277**(1 Pt 2):H58-64.
33. Lundberg JM, Franco-Cereceda A, Hemsen A, Lacroix JS, Pernow J: **Pharmacology of noradrenaline and neuropeptide tyrosine (NPY)-mediated sympathetic cotransmission**. *Fundamental & clinical pharmacology* 1990, **4**(4):373-391.
34. Bartness TJ, Kay Song C, Shi H, Bowers RR, Foster MT: **Brain-adipose tissue cross talk**. *The Proceedings of the Nutrition Society* 2005, **64**(1):53-64.
35. Rosmaninho-Salgado J, Marques AP, Estrada M, Santana M, Cortez V, Grouzmann E, Cavadas C: **Dipeptidyl-peptidase-IV by cleaving neuropeptide Y induces lipid accumulation and PPAR-gamma expression**. *Peptides* 2012, **37**(1):49-54.
36. Bradley RL, Mansfield JP, Maratos-Flier E: **Neuropeptides, including neuropeptide Y and melanocortins, mediate lipolysis in murine adipocytes**. *Obesity research* 2005, **13**(4):653-661.
37. Kuo LE, Czarnecka M, Kitlinska JB, Tilan JU, Kvetnansky R, Zukowska Z: **Chronic stress, combined with a high-fat/high-sugar diet, shifts sympathetic signaling toward neuropeptide Y and leads to obesity and the metabolic syndrome**. *Annals of the New York Academy of Sciences* 2008, **1148**:232-237.
38. Shi YC, Lin S, Castillo L, Aljanova A, Enriquez RF, Nguyen AD, Baldock PA, Zhang L, Bijker MS, Macia L *et al*: **Peripheral-specific y2 receptor knockdown protects mice from high-fat diet-induced obesity**. *Obesity (Silver Spring)* 2011, **19**(11):2137-2148.

39. Baker SB, Cohen M, Kuo L, Johnson M, Al-Attar A, Zukowska Z: **The role of the neuropeptide Y2 receptor in liporemodeling: neuropeptide Y-mediated adipogenesis and adipose graft maintenance**. *Plastic and reconstructive surgery* 2009, **123**(2):486-492.
40. Nguyen NL, Randall J, Banfield BW, Bartness TJ: **Central Sympathetic Innervations to Visceral and Subcutaneous White Adipose Tissue**. *American journal of physiology Regulatory, integrative and comparative physiology* 2014.
41. Li R, Guan H, Yang K: **Neuropeptide Y potentiates beta-adrenergic stimulation of lipolysis in 3T3-L1 adipocytes**. *Regulatory peptides* 2012, **178**(1-3):16-20.
42. Valet P, Berlan M, Beauville M, Crampes F, Montastruc JL, Lafontan M: **Neuropeptide Y and peptide YY inhibit lipolysis in human and dog fat cells through a pertussis toxin-sensitive G protein**. *The Journal of clinical investigation* 1990, **85**(1):291-295.
43. Castan I, Valet P, Quideau N, Voisin T, Ambid L, Laburthe M, Lafontan M, Carpene C: **Antilipolytic effects of alpha 2-adrenergic agonists, neuropeptide Y, adenosine, and PGE1 in mammal adipocytes**. *The American journal of physiology* 1994, **266**(4 Pt 2):R1141-1147.
44. Hausman DB, DiGirolamo M, Bartness TJ, Hausman GJ, Martin RJ: **The biology of white adipocyte proliferation**. *Obesity reviews : an official journal of the International Association for the Study of Obesity* 2001, **2**(4):239-254.
45. Bray GA: **Obesity--a state of reduced sympathetic activity and normal or high adrenal activity (the autonomic and adrenal hypothesis revisited)**. *International journal of obesity* 1990, **14 Suppl 3**:77-91; discussion 91-72.
46. Foster MT, Bartness TJ: **Sympathetic but not sensory denervation stimulates white adipocyte proliferation**. *American journal of physiology Regulatory, integrative and comparative physiology* 2006, **291**(6):R1630-1637.
47. Geloen A, Collet AJ, Bukowiecki LJ: **Role of sympathetic innervation in brown adipocyte proliferation**. *The American journal of physiology* 1992, **263**(6 Pt 2):R1176-1181.
48. Wright JT, Hausman GJ: **Monoclonal antibodies against cell surface antigens expressed during porcine adipocyte differentiation**. *International journal of obesity* 1990, **14**(5):395-409.
49. Kras KM, Hausman DB, Hausman GJ, Martin RJ: **Adipocyte development is dependent upon stem cell recruitment and proliferation of preadipocytes**. *Obesity research* 1999, **7**(5):491-497.
50. Carpene C, Rebourcet MC, Guichard C, Lafontan M, Lavau M: **Increased alpha 2-adrenergic binding sites and antilipolytic effect in adipocytes from genetically obese rats**. *Journal of lipid research* 1990, **31**(5):811-819.
51. Han R, Kitlinska JB, Munday WR, Gallicano GI, Zukowska Z: **Stress hormone epinephrine enhances adipogenesis in murine embryonic stem cells by up-regulating the neuropeptide Y system**. *PloS one* 2012, **7**(5):e36609.
52. Bartness TJ, Song CK: **Thematic review series: adipocyte biology. Sympathetic and sensory innervation of white adipose tissue**. *Journal of lipid research* 2007, **48**(8):1655-1672.

53. Bartness TJ, Song CK: **Innervation of brown adipose tissue and its role in thermogenesis**. *Canadian Journal of Diabetes* 2005, **29**(4):9.
54. Billington CJ, Briggs JE, Grace M, Levine AS: **Effects of intracerebroventricular injection of neuropeptide Y on energy metabolism**. *The American journal of physiology* 1991, **260**(2 Pt 2):R321-327.
55. Chao PT, Yang L, Aja S, Moran TH, Bi S: **Knockdown of NPY expression in the dorsomedial hypothalamus promotes development of brown adipocytes and prevents diet-induced obesity**. *Cell metabolism* 2011, **13**(5):573-583.
56. Shi YC, Lau J, Lin Z, Zhang H, Zhai L, Sperk G, Heilbronn R, Mietzsch M, Weger S, Huang XF *et al*: **Arcuate NPY controls sympathetic output and BAT function via a relay of tyrosine hydroxylase neurons in the PVN**. *Cell metabolism* 2013, **17**(2):236-248.
57. Egawa M, Yoshimatsu H, Bray GA: **Neuropeptide Y suppresses sympathetic activity to interscapular brown adipose tissue in rats**. *The American journal of physiology* 1991, **260**(2 Pt 2):R328-334.
58. Liu Y: **Neural crosstalk between sympathetic nervous system and sensory circuits to brown adipose tissue**. Georgia State University; 2013.
59. Bartness TJ, Song CK: **Brain-adipose tissue neural crosstalk**. *Physiology & behavior* 2007, **91**(4):343-351.
60. Bartness TJ: **Dual innervation of white adipose tissue: some evidence for parasympathetic nervous system involvement**. *The Journal of clinical investigation* 2002, **110**(9):1235-1237.
61. Song CK, Schwartz GJ, Bartness TJ: **Anterograde transneuronal viral tract tracing reveals central sensory circuits from white adipose tissue**. *American journal of physiology Regulatory, integrative and comparative physiology* 2009, **296**(3):R501-511.
62. Ralevic V, Karoon P, Burnstock G: **Long-term sensory denervation by neonatal capsaicin treatment augments sympathetic neurotransmission in rat mesenteric arteries by increasing levels of norepinephrine and selectively enhancing postjunctional actions**. *The Journal of pharmacology and experimental therapeutics* 1995, **274**(1):64-71.
63. Yi CX, Tschop MH: **Brain-gut-adipose-tissue communication pathways at a glance**. *Disease models & mechanisms* 2012, **5**(5):583-587.
64. Yamada T, Katagiri H, Ishigaki Y, Ogihara T, Imai J, Uno K, Hasegawa Y, Gao J, Ishihara H, Niijima A *et al*: **Signals from intra-abdominal fat modulate insulin and leptin sensitivity through different mechanisms: neuronal involvement in food-intake regulation**. *Cell metabolism* 2006, **3**(3):223-229.
65. Baker DG, Bertram TM, Patel PM, Barkauskas DA, Clopton P, Patel S, Geracioti TD, Jr., Haji U, O'Connor DT, Nievergelt CM *et al*: **Characterization of cerebrospinal fluid (CSF) and plasma NPY levels in normal volunteers over a 24-h timeframe**. *Psychoneuroendocrinology* 2013.
66. Baranowska B, Wolinska-Witort E, Martynska L, Chmielowska M, Mazurczak-Pluta T, Boguradzka A, Baranowska-Bik A: **Sibutramine therapy in obese women--effects on plasma neuropeptide Y (NPY), insulin, leptin and beta-endorphin concentrations**. *Neuro endocrinology letters* 2005, **26**(6):675-679.

67. Kastin AJ, Akerstrom V: **Nonsaturable entry of neuropeptide Y into brain**. *The American journal of physiology* 1999, **276**(3 Pt 1):E479-482.
68. Ahlborg G, Weitzberg E, Sollevi A, Lundberg JM: **Splanchnic and renal vasoconstrictor and metabolic responses to neuropeptide Y in resting and exercising man**. *Acta physiologica Scandinavica* 1992, **145**(2):139-149.
69. Zhang K, Rao F, Miramontes-Gonzalez JP, Hightower CM, Vaught B, Chen Y, Greenwood TA, Schork AJ, Wang L, Mahata M *et al*: **Neuropeptide Y (NPY): genetic variation in the human promoter alters glucocorticoid signaling, yielding increased NPY secretion and stress responses**. *Journal of the American College of Cardiology* 2012, **60**(17):1678-1689.
70. Berrettini WH, Oxenstierna G, Sedvall G, Nurnberger JI, Jr., Gold PW, Rubinow DR, Goldin LR: **Characteristics of cerebrospinal fluid neuropeptides relevant to clinical research**. *Psychiatry research* 1988, **25**(3):349-359.
71. Altarejos JY, Montminy M: **CREB and the CRTC co-activators: sensors for hormonal and metabolic signals**. *Nature reviews Molecular cell biology* 2011, **12**(3):141-151.
72. Jaworski K, Sarkadi-Nagy E, Duncan RE, Ahmadian M, Sul HS: **Regulation of triglyceride metabolism. IV. Hormonal regulation of lipolysis in adipose tissue**. *American journal of physiology Gastrointestinal and liver physiology* 2007, **293**(1):G1-4.
73. Townsend K, Tseng YH: **Brown adipose tissue: Recent insights into development, metabolic function and therapeutic potential**. *Adipocyte* 2012, **1**(1):13-24.
74. Ishihara A, Tanaka T, Kanatani A, Fukami T, Ihara M, Fukuroda T: **A potent neuropeptide Y antagonist, 1229U91, suppressed spontaneous food intake in Zucker fatty rats**. *The American journal of physiology* 1998, **274**(5 Pt 2):R1500-1504.
75. Kanatani A, Ishihara A, Asahi S, Tanaka T, Ozaki S, Ihara M: **Potent neuropeptide Y Y1 receptor antagonist, 1229U91: blockade of neuropeptide Y-induced and physiological food intake**. *Endocrinology* 1996, **137**(8):3177-3182.
76. Mullins D, Kirby D, Hwa J, Guzzi M, Rivier J, Parker E: **Identification of potent and selective neuropeptide Y Y(1) receptor agonists with orexigenic activity in vivo**. *Molecular pharmacology* 2001, **60**(3):534-540.
77. Burcelin R, Brunner H, Seydoux J, Thorensa B, Pedrazzini T: **Increased insulin concentrations and glucose storage in neuropeptide Y Y1 receptor-deficient mice**. *Peptides* 2001, **22**(3):421-427.
78. Kushi A, Sasai H, Koizumi H, Takeda N, Yokoyama M, Nakamura M: **Obesity and mild hyperinsulinemia found in neuropeptide Y-Y1 receptor-deficient mice**. *Proceedings of the National Academy of Sciences of the United States of America* 1998, **95**(26):15659-15664.
79. Balasubramaniam A, Joshi R, Su C, Friend LA, James JH: **Neuropeptide Y (NPY) Y2 receptor-selective agonist inhibits food intake and promotes fat metabolism in mice: combined anorectic effects of Y2 and Y4 receptor-selective agonists**. *Peptides* 2007, **28**(2):235-240.

80. Sainsbury A, Schwarzer C, Couzens M, Fetissov S, Furtinger S, Jenkins A, Cox HM, Sperk G, Hokfelt T, Herzog H: **Important role of hypothalamic Y2 receptors in body weight regulation revealed in conditional knockout mice**. *Proceedings of the National Academy of Sciences of the United States of America* 2002, **99**(13):8938-8943.
81. Sainsbury A, Schwarzer C, Couzens M, Jenkins A, Oakes SR, Ormandy CJ, Herzog H: **Y4 receptor knockout rescues fertility in ob/ob mice**. *Genes & development* 2002, **16**(9):1077-1088.
82. Schaffhauser AO, Stricker-Krongrad A, Brunner L, Cumin F, Gerald C, Whitebread S, Criscione L, Hofbauer KG: **Inhibition of food intake by neuropeptide Y Y5 receptor antisense oligodeoxynucleotides**. *Diabetes* 1997, **46**(11):1792-1798.
83. Tang-Christensen M, Kristensen P, Stidsen CE, Brand CL, Larsen PJ: **Central administration of Y5 receptor antisense decreases spontaneous food intake and attenuates feeding in response to exogenous neuropeptide Y**. *The Journal of endocrinology* 1998, **159**(2):307-312.
84. Marsh DJ, Hollopeter G, Kafer KE, Palmiter RD: **Role of the Y5 neuropeptide Y receptor in feeding and obesity**. *Nature medicine* 1998, **4**(6):718-721.
85. Larsen PJ, Kristensen P: **Central Y4 receptor distribution. Radioactive ribonucleotide probe in situ hybridization with in vitro receptor autoradiography**. *Methods Mol Biol* 2000, **153**:185-198.
86. Lin S, Shi YC, Yulyaningsih E, Aljanova A, Zhang L, Macia L, Nguyen AD, Lin EJ, During MJ, Herzog H *et al*: **Critical role of arcuate Y4 receptors and the melanocortin system in pancreatic polypeptide-induced reduction in food intake in mice**. *PloS one* 2009, **4**(12):e8488.

Table 2.1 Neuropeptide Y family receptors with preferred ligands, receptor distribution and function in food intake and fat deposition.

		Y1	Y2	Y4	Y5
Preferred ligand		NPY Requires a complete N terminus	NPY NPY3-36 Requires intact C-terminal fragments	PP NPY	NPY NPY2-36 NPY3-36
Pre vs. post junctional receptor		Post-junctional	Pre-junctional	Post-junctional	Post-junctional
Distribution	Brain (besides hypothalamus)	Cortex, brainstem, hippocampus, thalamus, amygdala	Cortex, brainstem, hippocampus, amygdala, striatum, nucleus accumbens	Subnucleus gelatinosus of NTS, dorsal motor nucleus of the vagus	Cortex, hippocampus, amygdala
	Hypothalamus	ARC, VMN, PVN, DMN, LH Supraoptic nucleus	ARC, PVN, LH, medial preoptical area, anterior hypothalamic	ARC, PVN	PVN, ARC, VMN, DMN, LH

			nucleus		
	Perip-heral	Thyroid, parathyroid glands, heart, spleen and digestive system, adipose tissue	Adipose tissue	Skeletal muscle, small intestine, pancreas, prostate, uterus, lung, colon	Adipose tissue
Types of manipulation/ Effects on food intake and body weight		Y1 antagonist central injection/Reduced food intake [74, 75]; Y1 agonist central injection/ Increase food intake [76]; Y1KO/ Developed	Y2 agonist IP injection/ inhibit food intake [79]; Hypothalamus-specific Y2 KO/Increased food intake and decreased body weight; Germ-line Y2 KO/Reduced body weight and adiposity,	Y4 KO/ Decreased body weight, less WAT, decreased 24-h food intake in male mice [81]	Central administration of Y5 antisense oligodeoxynucleotides/Reduced body weight and a decrease in food intake [82, 83]; Y5 KO/ Mild late-onset obesity, increased body weight, food

	obesity, increased body fat, slight reduction in food intake [77, 78]	reduced food intake in males and increased food intake in females [80]		intake and adiposity [84]

- KO: knock out; NTS: Nucleus of the solitary tract; WAT: white adipose tissue; ARC: arcuate nucleus; PVN: Paraventricular nucleus; VMN: ventromedial nucleus; DMN: dorsomedial nucleus; LH: Lateral hypothalamic area; IP injection: intraperitoneal injection. Other references used for this table besides the papers cited above [13, 15, 85, 86]. The references are not exhaustive but rather indicate key initial and/or representative studies.

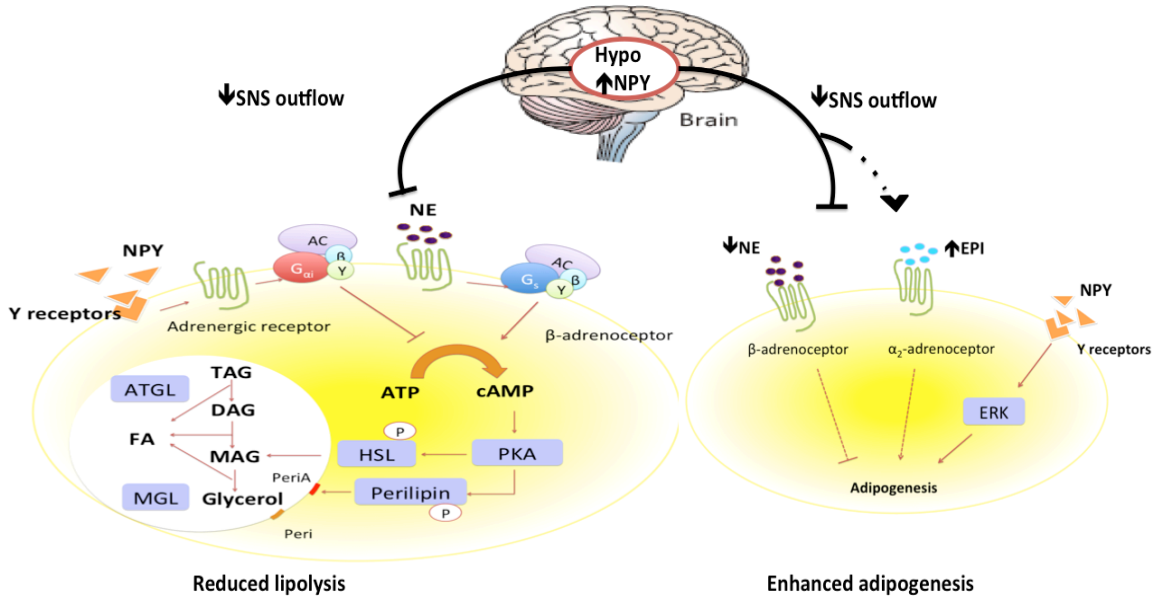

Figure 2.1 Antilipolytic and adipogenic effects of NPY on white adipose tissue. In the peripheral system, NPY binds to receptors 1, 2 and 5 and affects β-adrenergic receptor (β_1-AR, β_2-AR and β_3-AR; mainly through β_2-AR) configuration, the modification thereby leading to improved affinity for Gαi proteins. Subsequently, this activation of inhibitory GTP-binding protein alpha subunit (Gαi) inhibits adenylyl cyclase (AC) and cyclic AMP (cAMP) production. Decreased cellular cAMP levels inhibit protein kinase A (PKA), which phosphorylates and activates hormone-sensitive lipase (HSL). Decreased PKA activity also inhibits phosphorylation of lipid droplet-associated protein perilipin (peri) into PeriA, which controls the magnitude of lipolysis. Lipolysis is catalyzed by 3 lipases. Triacylglycerol is firstly hydrolyzed by adipocyte triglyceride lipase (ATGL) resulting in the formation of diacylglycerol (DAG) and release of a fatty acid (FA). Monoacylglycerol lipase (MGL) catalyzes hydrolysis of MAG, yielding glycerol and a FA. Increased hypothalamic (abbreviated as hypo in the figure) NPY inhibits sympathetic nerve system (SNS) outflow and suppresses catecholamine release, mainly norepinephrine (NE), and thereby their binding to β-adrenergic receptors, which in turn

reduces the cAMP-PKA pathway-associated lipolysis. On the other hand, NPY itself in the peripheral system can stimulate ERK-mediated adipogenesis. Through the hypothalamus-SNS-adipose tissue axis, reduced NE enhances adipogenesis via undefined mechanisms. Reduced SNS outflow is compensated for by adrenal medullary catecholamines, primarily epinephrine (EPI), which was also known to stimulate adipogenesis, possibly through NPY regulation. Parts of the figure are adapted from references [71, 72].

- “  ”: stimulatory effect; “  ”: inhibitory effect ;

  “  ”mechanisms unknown ; “  ” compensatory effect of EPI secretion.

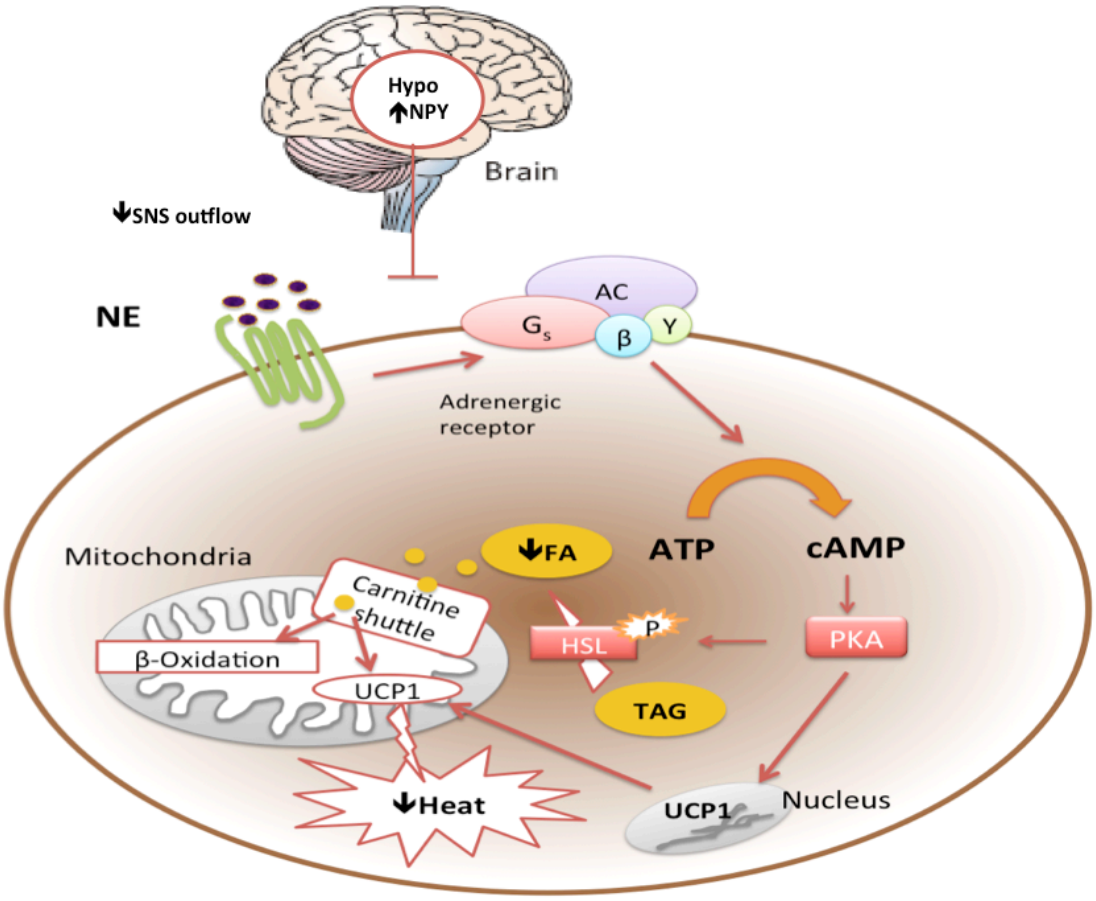

Figure 2.2 NPY inhibits BAT thermogenesis via reduced SNS outflow. Increased release of NPY in the hypothalamus inhibits sympathetic nerve system (SNS) outflow, particularly norepinephrine (NE) release. Consequently, it inhibits the cAMP-PKA signaling pathway via β-adrenergic receptors. Reduced lipolysis decreases the level of fatty acid storage in the brown adipose tissue, together with reduced uncoupling protin 1 (UCP1) expression and secretion, resulting in reduced thermogenic potential. Consequently, with less fatty acids being transported into the mitochondria by the carnitine palmitoyl transferase (carnitine shuttle) and also reduced UCP1 functioning to dissipate the proton-motive force across the mitochondrial membrane, there is less heat production. Part of the picture is summarized from [73].

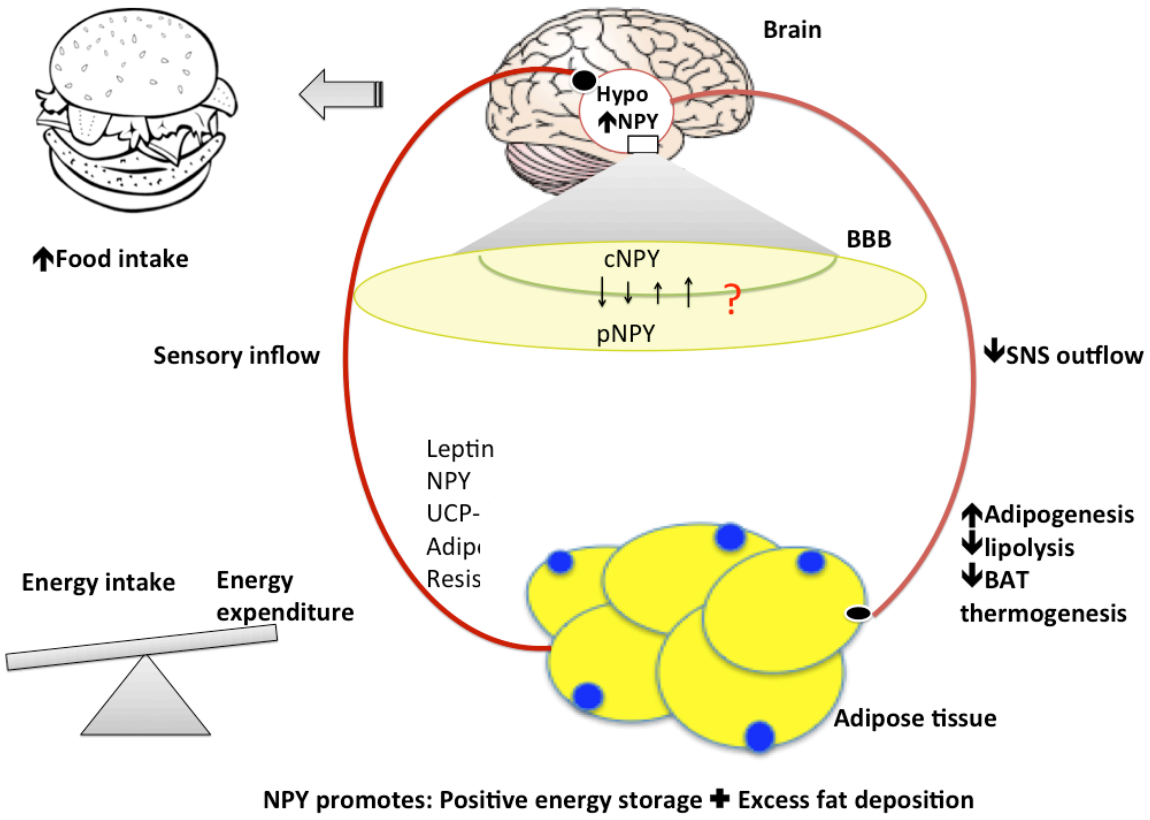

Figure 2.3 Role of NPY in energy intake and expenditure. cNPY: NPY in the central nervous system; pNPY: Peripheral NPY; BBB: Blood brain barrier; Hypo: hypothalamus. The cNPY stimulates food intake mainly via NPYR1 and NPYR5 to increase energy intake. Additionally, through the hypothalamus-SNS-adipose axis, NPY reduces sympathetic nervous system (SNS) outflow, which promotes white adipose tissue (WAT) deposition by enhancing adipogenesis and inhibiting lipolysis, as well as inhibiting brown adipose tissue (BAT) deposition and associated nonshivering thermogenesis. The same effects in WAT were achieved by peripheral NPY via different signaling pathways. This collectively leads to energy storage in adipose tissue. Adipose-hypothalamus crosstalk serves as a feedback loop via sensory inflow that informs the brain of the long-term peripheral energy status so that the brain can make the necessary adjustment. Numerous adipokines, hormones, and appetite regulating factors have been identified that play an

important role in adjusting energy balance through the hypothalamus either by directly affecting food intake or regulating adiposity through SNS outflow, such as leptin, NPY, and UCP1. NPY is more abundant in the central nervous system as compared to the peripheral system. Whether and how it crosses the blood brain barrier is critical for understanding its role in energy regulation.

Chapter 3

Quantity of glucose transporter and appetite-associated factor mRNA in various tissues after insulin injection in chickens selected for low or high body weight

Abstract: Chickens from lines selected for low (LWS) or high (HWS) body weight differ by 10-fold in body weight at 56 days-old with differences in food intake, glucose regulation and body composition. To evaluate if there are differences in appetite-regulatory factor and glucose transporter (*GLUT*) mRNA that are accentuated by hypoglycemia, blood glucose was measured and hypothalamus, liver, *Pectoralis major* and abdominal fat collected at 90 days of age from female HWS and LWS chickens, and reciprocal crosses, HL and LH, at 60 minutes after IP-injection of insulin. Neuropeptide Y (*NPY*) and receptor (*NPYR*) sub-types 1 and 5 mRNA were greater in LWS compared to HWS hypothalamus ($P < 0.05$), but greater in HWS than LWS in fat ($P < 0.05$). Expression of *NPYR2* was greater in LWS than HWS in *Pectoralis major* ($P < 0.05$). There was greater expression in HWS than LWS for *GLUT1* in hypothalamus and liver ($P < 0.05$), *GLUT2* in fat and liver ($P < 0.05$) and *GLUT9* in liver ($P < 0.05$). Insulin was associated with reduced blood glucose in all populations ($P < 0.05$), and reduced mRNA of insulin receptor (*IR*) and *GLUT* 2 and 3 in liver ($P < 0.05$). There was heterosis for mRNA, most notably *NPYR1* (-78%) and *NPYR5* (-81%) in fat and *GLUT2* (-70%) in liver. Results suggest that NPY and GLUTs are associated with differences in energy homeostasis in LWS and HWS. Reduced *GLUT* and *IR* mRNA after insulin injection suggest a compensatory mechanism to arrest the drop in blood glucose concentration.

Introduction

Chickens selected for low (LWS) or high (HWS) juvenile body weight for more than 55 years now display at selection age (56 days) a 10-fold difference in body weight with correlated responses in food intake regulation, body composition, glucose tolerance, and central insulin sensitivity [1-4]. Some of the LWS chickens are anorexic and all are lean with very little adipose tissue accumulation by selection age. The HWS chickens are hyperphagic, with selection for high body weight having favored the accumulation of abdominal fat, with a more than 10-fold difference (as a percentage of body weight) between the lines evident at selection age [3, 5, 6]. The lines display differences in food intake and hypothalamic chemistries in response to central administration of food intake-associated neurotransmitters [7-15]. Our group demonstrated that HWS chickens exhibit impaired glucose tolerance and hyperglycemia [16], and LWS chicks responded to centrally administered insulin with reduced food intake at a much lower threshold as compared to HWS chicks [17]. We also showed differential threshold sensitivity in the effects of insulin on blood glucose concentrations. Results from our group also showed that LWS chicks displayed greater rates of lipolysis and lipogenesis in abdominal fat as compared to HWS, with rates of lipolysis exceeding rates of lipogenesis, providing an explanation for why the LWS are extremely lean and accumulate little adipose tissue with age [18]. While phenotypic differences between the lines have been documented for more than 50 generations, the mechanisms underlying differences in appetite, insulin sensitivity and glucose homeostasis are poorly understood [1, 3].

Birds generally display fasting blood glucose concentrations that are the highest among all vertebrates [19], and chickens are resistant to the hypoglycemic effects of insulin at physiological doses [20]. Insulin signaling is functionally conserved in chickens

and insulin immuno-neutralization caused relative hyperglycemia in fed chicks, and while it did not alter activity of early steps in the insulin signaling cascade, phosphorylation of proteins involved in later steps were all decreased after 1 hour [21]. Other differences in glucose regulation between chickens and mammals include relatively low activity of glucokinase in the liver [22], a key glucose sensor in different tissues, and absence of a glucose transporter 4 (*GLUT4*) orthologue in the chicken genome [23]. In mammals, GLUT4 is the primary insulin-dependent glucose transporter in skeletal muscle and adipose tissue [24]. Relatively low quantities of *GLUT* isoform mRNA were detected in chicken skeletal muscle, liver, and adipose tissue [25] and it is unclear if any of those transporters are insulin-dependent, although insulin injection was associated with an increase in 2-deoxy-D-[^{3}H]-glucose uptake in skeletal muscle and liver tissues at 10 minutes after insulin injection in young broiler chicks, demonstrating the presence of insulin-dependent glucose transport in those tissues [26].

In addition to its role in glucose regulation, insulin is also an important regulator of appetite. Insulin receptors are located on orexigenic neuropeptide Y (NPY)/agouti-related peptide (AGRP) neurons and anorexigenic proopiomelanocortin (POMC) neurons in the arcuate nucleus (ARC) of the hypothalamus. The ARC integrates hormonal and nutrient signals from peripheral tissues to regulate food intake and body weight [27], with insulin stimulating and inhibiting NPY/AGRP and POMC neurons, respectively [28]. These ARC neurons containing insulin receptors are considered to be the first order in peripheral insulin's anorexigenic effects. Insulin receptors are detected in the hypothalamus of 5-day old layer chicks [29], and central injection of insulin was associated with changes in expression of hypothalamic *NPY* and *POMC* [30]. Effects on

gene expression after central administration of insulin in mammals similarly involve up-regulation of *POMC* mRNA [31], and down-regulation of *NPY* [32].

Our laboratories recently showed that NPY elicits different effects on food intake in LWS and HWS [33]. Neuropeptide Y is one of the most potent orexigenic (food-intake stimulating) factors identified to date in birds and mammals [34]. Recent studies in rodents show that NPY also plays a role in adipogenesis, lipogenesis and brown fat activation [35-38]. Thus, NPY may play a role in food intake regulation and body composition in chickens genetically selected for low and high body weight and information on expression of NPY and its receptor sub-types in different tissues may provide clues about functions of the NPY system in avian species and different tissues.

Identifying the underlying mechanisms of differences in food intake, glucose regulation and body composition between LWS and HWS chickens may provide insight on their role in appetite and metabolic disorders across species. Hence, the objective of the present study was to determine the effect of exogenous insulin on mRNA abundance of canonical mediators of appetite and glucose transporters in the hypothalamus, abdominal fat, liver and skeletal muscle of chickens from lines LWS and HWS and their reciprocal crosses.

Material and methods

Animals

All animal protocols were approved by the Institutional Animal Care and Use Committee at Virginia Tech. The chickens used in this experiment were progeny of S_{54} generation matings within parental lines selected for high (HWS) or low (LWS) body weight at 56 days of age and reciprocal crosses between them. For the reciprocal line

crosses, sire parent line is denoted first and the dam parental line second (HWS male x LWS female = HL; LWS male x HWS female = LH). Progeny were produced in a single hatch from breeders between 53 and 54 weeks of age.

Chicks were reared in starter and developer battery pens with free access to feed and water under a continuous photoperiod and thermoneutral conditions. The antibiotic-free mash diets fed were those used throughout the selection experiment. They included a coccidiostat (Deccox) and consisted of 20% crude protein (CP) and 2,685 kcal ME/kg to 56 days of age and 16% CP and 2,761 kcal ME/kg thereafter.

Insulin injection and tissue collection

In preliminary tests, 80 µg of insulin per kg BW was shown to cause hypoglycemia in HWS and LWS, with differences in the response curve of the two lines. Individuals were selected such that sire families were represented across treatments within lines. On day 90, HWS, LWS, LH and HL females (n=10/group) were fasted 16 hours with free access to water. Following the food withdrawal, five individuals from each population were randomly assigned to receive an injection of either human insulin (Sigma) at 80 µg/kg BW diluted in phosphate-buffered saline (PBS) or an equal volume of vehicle intraperitoneally using insulin syringes (BD Biosciences). Sixty minutes post-injection, chickens were euthanized and decapitated. Whole blood glucose was measured from the trunk using hand-held glucometers (Kroger). During the trial, blood glucose was not measured in order to prevent unnecessary stress that could lead to hypothalamic changes. The liver, abdominal fat (attached to gizzard), and *Pectoralis major* skeletal muscle were excised, snap-frozen in liquid nitrogen within 30 seconds and stored at -80°C. For the hypothalamus, the brain was excised from the skull, snap-frozen and the

hypothalamus dissected visually based on the following anatomical landmarks: anterior cut made at the corticoseptomesencephalic tract, posterior cut at the third cranial nerves, laterally cut 1.5 mm parallel to the midline on both sides of the brain and finally the dorsal cut from the anterior commissure to 1.0 mm ventral to the posterior commissure [39]. The isolated hypothalamus was then snap-frozen and stored at -80°C. The procedure was completed within less than 45 sec.

Total RNA isolation and real time PCR

Approximately 200 mg of tissue was homogenized with a Tissue Lyser II (Qiagen) and stainless steel beads (Qiagen) and 1 mL isol-RNA lysis reagent (5-PRIME). Samples were phase-separated according to the manufacturer's instructions (5-PRIME) and total RNA purified with spin columns according to the manufacturer's instructions (Promega SV total RNA isolation kit). An on-column RNase-Free DNase I treatment was included in the kit. Total RNA integrity was assessed by agarose-formaldehyde gel electrophoresis and quantity and purity evaluated by spectrophotometry (260/280/230 nm) using a Nanophotometer^{TM} Pearl (IMPLEN), and samples stored at -80°C. The first strand cDNA was synthesized in 20 µL reactions from 200 ng of total RNA using the High Capacity cDNA Reverse Transcription kit (Invitrogen, USA), following the manufacturer's instructions. Primers were designed with Primer Express 3.0 (Applied Biosystems; **Table 3.1**). Real time PCR reactions contained Fast SYBR Green Master Mix (Applied Biosystems), forward and reverse primers (0.125 µM each), and 10-fold diluted cDNA. Real-time PCR reactions were performed in duplicate for all samples on an Applied Biosystems 7500 FAST system, under the following conditions: enzyme activation for 20 sec at 95°C and 40 cycles of 1) melting step for 3 seconds at 95°C and

2) annealing/extension step for 30 sec at 60°C. Melting curve analyses were performed after all PCR reactions to ensure amplicon specificity.

Data analyses

Chicken was defined as the experimental unit. Blood glucose data were analyzed by ANOVA using the Glimmix procedure of SAS 9.3 (SAS Institute, Cary, NC). The statistical model included the main effects of genetic population (HWS, LWS, HL and LH), treatment (insulin versus vehicle) and the interaction between them.

Model for blood glucose concentrations:

$y= \mu+ \alpha_i +\beta_j + (\alpha\beta)_{ij}+ \xi_{ijk}$

μ: grand mean response, αi: effect of treatment (insulin versus vehicle), βj: effect of population (HWS, LWS, HL and LH), $(\alpha\beta)_{ij}$: interaction effect between treatment and population, ξ_{ijk}: random errors---normal $(0,\delta_\xi)$

Real time PCR data were analyzed using the $\Delta\Delta C_T$ method, where $\Delta C_T = C_{T\ target\ gene} - C_{T\ Actin}$, and $\Delta\Delta C_T = \Delta C_{T\ target\ sample} - \Delta C_{T\ calibrator}$ [40]. The LWS vehicle group was used as the calibrator sample for hypothalamus gene expression and the LWS vehicle hypothalamus group was used as the calibrator for the overall tissue expression analysis. Data normality was evaluated using the Univariate procedure of SAS, and Levene's test was used for evaluating heterogeneity of variances. The $2^{-\Delta\Delta ct}$ values were subjected to ANOVA using the Glimmix procedure of SAS. In the first set of analyses, mRNA abundance was evaluated in only HWS and LWS samples. As described below, for those genes showing significant differences between HWS and LWS, expression was also evaluated in HL and LH for investigating the heterosis for those traits. For genes (*POMC*, *AGRP*, *IAPP*, *TH* and *PC2*) that were evaluated only in the hypothalamus, the statistical

model included the main effects of treatment (insulin or vehicle), line (HWS or LWS), and the interaction between them. For expression of all other genes, which were measured in all tissues, the model included the main effects of insulin treatment, line and tissue, and the interactions between them. Tissue was included in the model as a repeated measure, with Type=csh and ddfm=bw selected based on variance and correlation among different tissues. Post-hoc pairwise comparisons were carried out using Tukey's test. All data are presented as least squares means ± SEM. Differences were considered significant at $P < 0.05$. The statistical models are as follows.

Model for hypothalamic gene expression:

$y= \mu+ \alpha_i +\beta_j + (\alpha\beta)_{ij}+ \xi_{ijk}$

μ: grand mean response, αi: effect of treatment, βj: effect of line, $(\alpha\beta)_{ij}$: interaction effect between treatment and line, ξ_{ijk}: random errors---normal $(0,\delta_\xi)$

Model for gene expression in all tissues:

$y= \mu+ \alpha i +\beta j + (\alpha\beta)_{ij} + \gamma(\alpha\beta)_{k(ij)} + \lambda_l +(\lambda\alpha)_{li} + (\lambda\beta)_{lj} + (\lambda\alpha\beta)_{lij}+ \xi_{ijklm}$

μ: grand mean response, αi: effect of treatment, βj: effect of population, $(\alpha\beta)_{ij}$: interaction effect between treatment and population, $\gamma(\alpha\beta)_{k(ij)}$: birds nested within the cross of treatment and line, λ_l: repeated measure (various tissues), $(\lambda\alpha)_{li}$: interaction effect between tissue and treatment, $(\lambda\beta)_{lj}$: interaction effect between tissue and population, $(\lambda\alpha\beta)_{lij}$: three-way interaction between tissues, population and treatment, ξ_{ijklm}: random error---normal $(0,\delta_\xi)$

Heterosis

For genes that showed significant differences in expression between HWS and LWS lines in various tissues, expression was measured in reciprocal crosses and heterosis was calculated from mRNA abundance data as follows:

% Heterosis = [(crossline average – parental line average) / parental line average] × 100

Significance of heterosis was evaluated using non-orthogonal contrasts between the F1 and the average of the parental lines. Comparison of expression between the populations was:

Model for gene expression across all populations:

$y= \mu+ \alpha_i +\beta_j + (\alpha\beta)_{ij}+ \xi_{ijk}$

μ: grand mean response, αi: effect of treatment, βj: effect of population (HWS, HL, LH, and LWS), $(\alpha\beta)_{ij}$: random interaction effect between treatment and population, ξ_{ijk}: random errors---normal $(0,\delta_\xi)$

Results

Body weights and blood glucose concentrations

The mean body weights of HWS, HL, LH and LWS were 2,000, 1,200, 1,190, and 200 g, respectively. There was an interaction of population and insulin treatment on blood glucose concentration (P = 0.01). In vehicle-treated chickens, there were no significant differences in blood glucose among the populations, whereas concentrations were significantly lower in all insulin-injected than their vehicle controls, with LWS insulin-injected chickens having the lowest blood glucose of all groups (**Table 3.2**).

Appetite-associated factor and glucose transporter mRNA abundance in the LWS and HWS lines

Abundance of mRNA was measured first in different tissues of HWS and LWS, the rationale being that for genes that were different between the lines, heterosis would later be explored using the samples obtained from the reciprocal crosses. Hence, data were first summarized for effects in the parental lines, with main effects and *P*-values for the two-way interactions. Three-way interactions were not significant for any gene and hence removed from the model. Significant two-way interactions are displayed graphically. Thereafter, comparisons among LWS and HWS and their reciprocal crosses are discussed. Among the genes evaluated in only the hypothalamus, there was no effect of insulin treatment or line on gene expression (**Table 3.3**).

Abundance of NPY and NPY receptor sub-type mRNA in all tissues

There were no effects of insulin injection on mRNA abundance of *NPY* or its receptor sub-types (**Table 3.4**). Expression of *NPY* was greater ($P < 0.0001$) in the hypothalamus as compared to the other tissues (50-fold greater than in fat or muscle; 500-fold greater than in liver), and abundance of mRNA was greater ($P < 0.05$) in abdominal fat and muscle as compared to liver. There was an interaction of tissue and line on *NPY* mRNA ($P < 0.0001$) where in the hypothalamus, expression was greater in LWS than in HWS ($P < 0.05$) while in abdominal fat, abundance was greater in HWS than in LWS chickens ($P < 0.05$; **Figure 3.1A**). Expression in other tissues was similar between the lines.

Similarly, *NPYR1* mRNA was greater ($P < 0.0001$) in the hypothalamus than in the other tissues (**Table 3.4**), with approximately 45-fold greater ($P < 0.0001$) and 450-fold greater ($P < 0.0001$) expression as compared with fat and liver, respectively. Neuropeptide *YR1* mRNA was not detected in the *Pectoralis major*. There was also an

interaction of tissue and line on *NPYR1* expression, identical to that observed for *NPY*, where in hypothalamus, expression was greater ($P < 0.01$) in LWS than in HWS, whereas in abdominal fat, abundance was greater ($P < 0.01$) in HWS than in LWS (**Figure 3.1B**).

Abundance of *NPYR2* mRNA was also greater ($P < 0.0001$) in hypothalamus than in the other tissues (**Table 3.4**), with 5-fold greater expression as compared to fat ($P < 0.01$) and skeletal muscle ($P < 0.01$), and 50-fold greater expression than in liver ($P < 0.0001$). There was also a line by tissue interaction ($P = 0.003$), where in *Pectoralis major*, mRNA abundance was greater in LWS than in HWS ($P < 0.05$; **Figure 3.1C**).

Quantities of *NPYR5* mRNA were greater in LWS than in HWS chickens ($P = 0.009$; **Table 3.4**). Expression was greater in hypothalamus than in other tissues ($P < 0.0001$), being approximately 30- and 150-fold greater than in fat ($P < 0.001$) and liver ($P < 0.001$), respectively, with no detectable expression in *Pectoralis major*. There was also a line by tissue interaction ($P = 0.001$), similar to *NPY* and *NPYR1*, where expression in hypothalamus was greater in LWS compared to HWS ($P < 0.01$) and expression in fat was greater in HWS than in LWS ($P < 0.01$; **Figure 3.1D**). Similar to *NPY* and the other receptor sub-types, quantities of *NPYR6* mRNA were greater in hypothalamus than in all other tissues ($P < 0.0001$), with expression more than 5-fold greater than in fat ($P < 0.01$), 15-fold greater than in liver ($P < 0.01$) and more than 2-fold greater abundance as compared to *Pectoralis major* ($P < 0.05$).

The mRNA abundance of FOXO1, glucose transporters and IR

Expression of *FOXO1* (**Table 3.4**), glucose transporters 1, 2, 3, 8 and 9, and *IR* (**Table 3.5**) were summarized for different tissues of vehicle- and insulin-injected HWS and LWS chickens. Abundance of *FOXO1* mRNA was greater ($P = 0.02$) in HWS as

compared to LWS chickens. There was also a tissue-specific distribution ($P < 0.0001$), where expression was greater (at least 3-fold) in skeletal muscle as compared with the other tissues ($P < 0.0001$), and greater in liver than in fat ($P < 0.05$) or hypothalamus ($P < 0.05$). There was an interaction of line and tissue on mRNA abundance ($P = 0.002$), where in *Pectoralis major* and liver, expression was greater in HWS compared to LWS ($P < 0.05$; **Figure 3.3A**).

There were interactions of line and tissue on mRNA abundance of *GLUT1* (**Figure 3.2B**), *2* (**Figure 3.2C**) and *9* (**Figure 3.2D**), and interactions of treatment and tissue on gene expression of *GLUT2* (**Figure 3.3A**) and *3* (**Figure 3.3B**; **Table 3.5**). Expression of *GLUT 1*, *2* and *9* was greater ($P < 0.05$) in HWS as compared to LWS chickens. Abundance of *GLUT1* mRNA was greater in hypothalamus than in the other tissues ($P < 0.001$), and abundance was greater in skeletal muscle than in fat and liver ($P < 0.01$; **Table 3.5**). Expression of *GLUT1* was greater in HWS than LWS in hypothalamus and liver ($P < 0.05$), and was similar for both lines in other tissues (**Figure 3.2B**). For *GLUT2*, expression was greater (> 200-fold) in liver than in the other tissues ($P < 0.0001$), and expression was greater in muscle and fat than in the hypothalamus ($P < 0.05$). In the liver and fat, expression of *GLUT2* was greater in HWS than in LWS ($P < 0.05$), while expression was similar for both lines in the other two tissues (**Figure 3.2C**). Insulin treatment was associated with reduced expression of *GLUT2* in the liver (**Figure 3.3A**). Glucose transporter 3 mRNA was not detected in *Pectoralis major*. Expression was 10-fold greater in the hypothalamus than in abdominal fat and liver ($P < 0.0001$). Similar to *GLUT2*, insulin injection was associated with decreased expression of *GLUT3* in the liver as compared to vehicle-injected birds ($P < 0.05$; **Figure 3.3B**). Glucose

transporter 8 mRNA was greatest in the liver and skeletal muscle, intermediate in hypothalamus and lowest in abdominal fat ($P < 0.05$). Expression of *GLUT9* was more than 10-fold greater in liver compared to other tissues ($P < 0.0001$), and was greater in hypothalamus than in fat or muscle ($P < 0.05$). In the liver, *GLUT9* mRNA was 2-fold greater in HWS as compared to LWS ($P < 0.0001$), while expression was similar in both lines in other tissues (**Figure 3.2D**).

Insulin receptor expression was greatest in *Pectoralis major* as compared with the other tissues ($P < 0.001$; *Pectoralis major* > liver > abdominal fat > hypothalamus). There was an interaction of insulin and tissue on mRNA quantities ($P < 0.0001$) where in the liver, insulin injection was associated with decreased abundance as compared to the vehicle-injected counterparts ($P < 0.001$; **Figure 3.3C**).

Heterosis for mRNA abundance

To investigate heterosis for genes that showed significant differences in mRNA abundance between the HWS and LWS parental lines, we evaluated expression of those genes in HL and LH reciprocal crosses and calculated heterosis (**Table 3.6**). There were no differences in response to insulin treatment on gene expression in the reciprocal crosses. In the abdominal fat, heterosis was negative for all cases, and significant for *IR* ($P < 0.0001$), *NPYR1* ($P = 0.0002$), *NPYR2* ($P = 0.01$) and *NPYR5* ($P = 0.02$). In the liver, heterosis was significant for all glucose transporters and was positive for *GLUT1* (34%) and negative for *GLUT2* (-70%) and *GLUT9* (-20%). In the hypothalamus, heterosis was negative for *NPYR1* ($P = 0.001$). Most of the genes showed less expression in the reciprocal crosses than in parental lines except *GLUT1* in the liver and *GLUT1* and *NPY* in the hypothalamus.

Discussion

Abundance of appetite-associated factor mRNA in the hypothalamus

Expression of *POMC* and several other hypothalamic genes were similar between LWS and HWS, results consistent with those reported at 4 days post-hatch [41]. There was greater expression of two major orexigenic factors, *NPY* and *AGRP,* in the hypothalamus of the relatively hypophagic LWS chickens. As AGRP was described as a lipogenic factor in chickens [42], and NPY has a role in adipose tissue metabolism in mammals [37], their expression and function could be related to differential adiposity in LWS and HWS, although mRNA abundance in whole hypothalamus may not be reflective of peptide release from individual nuclei.

In the present study, there were no changes in mRNA abundance of appetite-associated factors after insulin injection. Blood glucose concentrations were reduced and there were differences in blood glucose between LWS and HWS chickens, however there was not an association between reductions in blood glucose at 1 h and mRNA abundance. In the hypothalamus and brainstem of 3- to 4-day old chicks, there was increased *POMC* and reduced *NPY* at 15 and 30 min, respectively, post ICV-injection of insulin [30]. It is possible that because effects of insulin on food intake are most prominent within the first 30 min [9], the transcriptional effects on appetite-associated factors occurred and disappeared within the first hour after injection. One hour was selected in order to capture changes associated with different blood glucose concentrations. Other studies showing effects of insulin on gene expression in the hypothalamus were conducted in ICV-injected animals [30-32], thus it is possible that both route of injection and duration of

study influence effects on gene expression of appetite-associated factors in the hypothalamus.

Neuropeptide Y and receptor sub-type mRNA abundance

Of the genes evaluated in the hypothalamus, *NPY*, *NPYR1* and *NPYR5* mRNA were greater in LWS than in HWS chickens. These results are in contrast with those reported by Ka et al [41], where *NPY* mRNA abundance was lower in 4-day old LWS females than in HWS. Because we measured expression at 90 days, it is possible that accumulation of adipose tissue is associated with changes in the regulation of appetite and energy metabolism. Abundance of *NPY* mRNA in the hypothalamus is enhanced in response to food deprivation and in genetic and diet-induced rodent models of obesity [43], thus in the present study the effect of genetic line could be influenced by adiposity as well as the 16 hour fast that preceded insulin injection.

Given that LWS are hypophagic with anorexics in the population, it is interesting that *NPY*, which encodes one of the more potent orexigenic factors identified to date in mammals, is more highly expressed in these chickens. Although 5 day-old LWS chicks did not respond to exogenous NPY with increased food intake, the HWS chicks responded at the lowest dose tested, and hypothalamic nuclei activation between lines was similar (39). Those findings coupled with our observation that expression of *NPY* and two of its receptor sub-types is greater in the hypothalamus of LWS chickens suggest that the lack of response to NPY is due to an effect downstream of NPY binding to its receptors rather than a deficiency or dysfunction in NPY or receptors per se. Preliminary bioinformatics analyses suggest that there are no polymorphisms or deletions that would alter the amino acid sequence and hence functionality of NPY or its receptors.

The role of chicken NPY receptor sub-types in food intake and other biological functions is unclear, thus in the present study mRNA was measured for multiple sub-types, including the poorly characterized *YR6*. In mammals, sub-types YR1, 2 and 5 are involved in food intake regulation [44]. Differential expression of *NPY* and its receptors between LWS and HWS in abdominal fat may indicate a role for NPY in fat deposition. Treatment of 3T3-L1 cells (murine pre-adipocytes) with NPY induced *PPAR-γ* expression, differentiation into adipocytes and lipid accumulation [37] and inhibited α-MSH-induced lipolysis [45]. The NPY YR2 and YR5 antagonists inhibited the stimulatory effect of NPY on adipocyte differentiation, whereas treatment with receptor agonists enhanced differentiation and lipogenesis, demonstrating that effects of NPY on adipocyte differentiation were mediated through YR2 and YR5. The YR1 is also present in human adipocytes and mediated the anti-lipolytic effect of NPY on human adipocytes [46]. Based on these reports suggesting a role for NPY in regulating energy storage via white adipose tissue, greater expression of *NPY* and receptor sub-types 1, 2 and 5 in HWS abdominal fat could be involved in their enhanced rate of abdominal fat mass deposition. That heterosis was highly negative for both *YR1* and *YR5* mRNA in the abdominal fat suggests that the encoded receptors play a role in fat deposition in LWS and HWS.

FOXO1 expression in different tissues

Expression of *FOXO1*, which encodes a major transcriptional regulator that is highly expressed in insulin-sensitive tissues, was also evaluated [47]. Expression of FOXO1 was measured because it was hypothesized that differential blood glucose concentrations in LWS and HWS may be associated with differences in expression of

genes associated with insulin resistance and glucose intolerance in humans. The FOXO1 regulates expression of genes associated with gluconeogenesis, energy metabolism and oxidative stress [48]. In the present study, *FOXO1* mRNA was greater in the *Pectoralis major* and liver of HWS than of LWS. In insulin resistant individuals, FOXO1 over-expression in skeletal muscle is associated with hyperglycemia and glucose intolerance [49], thus expression of FOXO1 could be related to differences in energy metabolism between LWS and HWS. Greater rates of adipose tissue lipolysis in LWS [18] could be related to differences in oxidative activity, although these data have not been reported for LWS and HWS in adipose tissue and skeletal muscle.

Tissue distribution of glucose transporters

Phylogenetic analysis of human and chicken *GLUT* amino acid sequences revealed that chicken *GLUT* genes align with their respectively numbered gene in humans and there does not appear to be a chicken *GLUT* gene that is similar to human *GLUT4* (**Figure 3.4**). Because mechanisms controlling glucose uptake in insulin-sensitive tissues of chickens are unclear and there are likely differences in nutrient uptake and utilization between HWS and LWS, we evaluated expression of *GLUT* genes in different tissues.

The glucose transporters showed distinct tissue specificities, with *GLUT1* mRNA most abundant in the hypothalamus, *GLUT2* and *9* in the liver, *GLUT3* absent from the skeletal muscle, and *GLUT8* similarly expressed across all tissues. The GLUT9 was reported to mediate the uptake of uric acid and glucose in mammals, with greatest expression in liver [50], however its substrate specificity in chickens is unclear. Expression of *GLUT2* was more than 200-fold greater in the liver than in other tissues

examined. In mammals, GLUT2 is reported to be a low-affinity, high-capacity transporter that mediates uptake of glucose, galactose and fructose across a wide range of physiological concentrations, playing an important role in maintaining glucose flux in liver cells [51]. Both GLUT1 and GLUT3 are described as being high-affinity, low-capacity transporters that are responsible for basal glucose uptake in the central nervous system of mammals [52], and GLUT8 is described as an intracellular glucose transporter that is ubiquitously expressed across most tissues [53], thus tissue distribution patterns of the GLUT transporters in chickens is similar to those reported in mammalian species. The differences between HWS and LWS were also tissue specific, with *GLUT1* greater in HWS than in LWS in the hypothalamus, and *GLUT2* and *9* greater in HWS in the liver. These results suggest that HWS have a greater capacity for glucose uptake in those tissues, consistent with a greater metabolic demand and glucose load in the relatively hyperphagic and obese HWS chickens. These data may appear counterintuitive, as previous research showed that HWS were relatively hyperglycemic and glucose intolerance; however, it remains to be determined the relative contribution of different glucose transporters to overall glucose uptake in peripheral tissues of chickens and the cellular mechanisms underlying hyperglycemia and glucose regulation in HWS.

Effect of insulin on mRNA abundance in the liver

The liver was the only tissue where there was an effect of insulin treatment on mRNA, where *GLUT2*, *GLUT3* and insulin receptor expression all decreased after insulin injection. These results implicate GLUT2 and GLUT3 as potential insulin-dependent glucose transporters in chickens. Insulin treatment was associated with an increase in 2-deoxy-glucose uptake and abundance of GLUT1 mRNA and protein in chicken

embryonic myoblasts [54], providing evidence for the presence of insulin-stimulated glucose transporters in chickens.

The majority of GLUT2 protein is localized to the plasma membrane in the basal (non-insulin stimulated) state [55] and perfusion of rat liver with insulin was associated with decreased plasma membrane-bound GLUT2 [56]. As suggested by the results in the present study, transcriptional down-regulation of GLUT2 may serve a similar function in reducing glucose flux across the hepatocyte plasma membrane during the hypoglycemic response.

Gene expression was measured at one hour post-injection, with blood glucose concentrations reduced in all insulin-injected chickens as compared to the vehicle-injected controls. As GLUT2 mediates bi-directional transport in hepatocytes, down-regulation of *GLUT2* and *3* may serve as mechanisms to reduce glucose uptake from the blood, thus preventing further hypoglycemia, while down-regulation of the *IR* may also serve as a compensatory mechanism to prevent further utilization of glucose during hypoglycemia. As mentioned earlier, the lack of effects on gene expression of glucose transporters in other tissues may indicate relatively less sensitivity in those tissues, or may represent a time-dependent effect. It is possible that the major transcriptional events in skeletal muscle and adipose tissue in response to the insulin occurred before 1 hour, during the initial decline in blood glucose concentrations, and following glucose clearance, the response shifted to the liver to prevent further decreases in blood glucose. It is also possible that transcriptional changes occurred after 1 hour in response to the onset of hypoglycemia.

Heterosis for NPY, NPYRs and GLUTs in different tissues

Transcriptional diversity at specific sets of genes influences heterosis for different traits [57]. According to the heterosis analysis, the expression of most of the genes was biased towards the LWS line. For *NPY* mRNA in the abdominal fat and hypothalamus, the average of the parental lines was similar to the reciprocal crosses, while all of the *NPY* receptors were different, with *NPYR1* and *NPYR5* mRNA exhibiting much greater heterosis than *NPYR2*. Given the role of *NPY* and its receptors in the hypothalamus and abdominal fat in promoting food intake and fat deposition, the reciprocals crosses may have an advantage in dealing with excess energy by having reduced expression of *NPYR1* and *NPYR5*. In the hypothalamus, *NPYR1* but not *NPY* was significantly reduced in the reciprocal lines as compared to the parental lines, indicating that the receptor may play a more important role in regulation of food intake. All glucose transporters had negative heterosis except *GLUT1* in the liver, suggesting that the HWS line is more efficient in utilizing glucose than all other lines, consistent with their superior feed efficiency [3].

Appetite factors were shown to have high heritability in humans [58, 59], however there is no report on the heritability of appetite regulation in these lines. Moreover, methods for estimating heritability may include non-additive and/or additive genetic variation. As single genes can each have a heterozygous effect, there can be an average across them, thus demonstrating why multiple genes effects can be masked at the phenotypic level. The relevance of heterosis for *NPY*, *NPY* receptor and *GLUT* mRNA may have important implications for appetite and metabolic disorders.

Conclusions and implications

In conclusion, results from this study indicate that there are differences in expression of *NPY* and its receptor-subtypes in the hypothalamus and white adipose

tissue of chickens selected for high or low body weight. We also observed differences in glucose transporter expression between the lines in hypothalamus, abdominal fat and liver, suggestive of more efficient glucose assimilation in the high-weight chickens. Insulin injection was associated with a more pronounced effect on blood glucose in LWS chickens after 1 hour, although effects on gene expression were not different between the lines. The liver was the only organ affected by insulin injection, with a down-regulation of glucose transporters and insulin receptor, suggestive of a compensatory mechanism to prevent further utilization of glucose in the liver during insulin-induced hypoglycemia.

Acknowledgements

We thank the Poultry Center Farm Crew, Mike Graham, John Thomas and Bernard Duncan, for their outstanding care of the animals used in this study.

References

1. Rubin CJ, Zody MC, Eriksson J, Meadows JR, Sherwood E, Webster MT, Jiang L, Ingman M, Sharpe T, Ka S *et al*: **Whole-genome resequencing reveals loci under selection during chicken domestication**. *Nature* 2010, **464**(7288):587-591.
2. Marquez GC, Siegel PB, Lewis RM: **Genetic diversity and population structure in lines of chickens divergently selected for high and low 8-week body weight**. *Poultry science* 2010, **89**(12):2580-2588.
3. Dunnington EA, Siegel PB: **Long-term divergent selection for eight-week body weight in white Plymouth rock chickens**. *Poultry science* 1996, **75**(10):1168-1179.
4. Dunnington EA, Honaker CF, McGilliard ML, Siegel PB: **Phenotypic responses of chickens to long-term, bidirectional selection for juvenile body weight--historical perspective**. *Poultry science* 2013, **92**(7):1724-1734.
5. Katanbaf MN, Dunnington EA, Siegel PB: **Allomorphic relationships from hatching to 56 days in parental lines and F1 crosses of chickens selected 27 generations for high or low body weight**. *Growth, development, and aging : GDA* 1988, **52**(1):11-21.
6. Burgener JA, Cherry JA, Siegel PB: **The Association between Sartorial Fat and Fat Deposition in Meat-Type Chickens**. *Poultry Sci* 1981, **60**(1):54-62.
7. Kuo AY, Cline MA, Werner E, Siegel PB, Denbow DM: **Leptin effects on food and water intake in lines of chickens selected for high or low body weight**. *Physiology & behavior* 2005, **84**(3):459-464.

8. Newmyer BA, Siegel PB, Cline MA: **Neuropeptide AF differentially affects anorexia in lines of chickens selected for high or low body weight**. *Journal of neuroendocrinology* 2010, **22**(6):593-598.
9. Smith ML, Prall BC, Siegel PB, Cline MA: **The threshold of insulin-induced hypophagia is lower in chicks selected for low rather than high juvenile body weight**. *Behavioural brain research* 2011, **216**(2):719-722.
10. Cline MA, Kuo AY, Smith ML, Nandar W, Prall BC, Siegel PB, Denbow DM: **Differential feed intake responses to central corticotrophin releasing factor in lines of chickens divergently selected for low or high body weight**. *Comparative biochemistry and physiology Part A, Molecular & integrative physiology* 2009, **152**(1):130-134.
11. Cline MA, Nandar W, Bowden C, Calchary W, Smith ML, Prall B, Newmyer B, Orion Rogers J, Siegel PB: **The threshold of amylin-induced anorexia is lower in chicks selected for low compared to high juvenile body weight**. *Behavioural brain research* 2010, **208**(2):650-654.
12. Cline MA, Nandar W, Bowden C, Hein PP, Denbow DM, Siegel PB: **Differential feeding responses to central alpha-melanocyte stimulating hormone in genetically low and high body weight selected lines of chickens**. *Life sciences* 2008, **83**(5-6):208-213.
13. Cline MA, Prall BC, Smith ML, Calchary WA, Siegel PB: **Differential appetite-related responses to central neuropeptide S in lines of chickens divergently selected for low or high body weight**. *Journal of neuroendocrinology* 2008, **20**(7):904-908.
14. Cline MA, Siders R, Newmyer BA, Smith ML, Siegel PB: **Both calcitonin and calcitonin gene-related peptides' thresholds of hypophagia are considerably lower in chicks selected for high rather than low juvenile body weight**. *Physiology & behavior* 2010, **101**(2):254-259.
15. Newmyer BA, Nandar W, Webster RI, Gilbert E, Siegel PB, Cline MA: **Neuropeptide Y is associated with changes in appetite-associated hypothalamic nuclei but not food intake in a hypophagic avian model**. *Behavioural brain research* 2012.
16. Sinsigalli NA, McMurtry JP, Cherry JA, Siegel PB: **Glucose tolerance, plasma insulin and immunoreactive glucagon in chickens selected for high and low body weight**. *The Journal of nutrition* 1987, **117**(5):941-947.
17. Smith ML, Prall BC, Siegel PB, Cline MA: **The threshold of insulin-induced hypophagia is lower in chicks selected for low rather than high juvenile body weight**. *Behav Brain Res* 2011, **216**(2):719-722.
18. Calabotta DF, Cherry JA, Siegel PB, Jones DE: **Lipogenesis and lipolysis in fed and fasted chicks from high and low body weight lines**. *Poultry science* 1985, **64**(4):700-704.
19. Polakof S, Mommsen TP, Soengas JL: **Glucosensing and glucose homeostasis: from fish to mammals**. *Comp Biochem Physiol B Biochem Mol Biol* 2011, **160**(4):123-149.
20. Dupont J, Metayer-Coustard S, Ji B, Rame C, Gespach C, Voy B, Simon J: **Characterization of major elements of insulin signaling cascade in chicken**

adipose tissue: apparent insulin refractoriness. *Gen Comp Endocrinol* 2012, **176**(1):86-93.
21. Dupont J, Tesseraud S, Derouet M, Collin A, Rideau N, Crochet S, Godet E, Cailleau-Audouin E, Metayer-Coustard S, Duclos MJ *et al*: **Insulin immuno-neutralization in chicken: effects on insulin signaling and gene expression in liver and muscle**. *The Journal of endocrinology* 2008, **197**(3):531-542.
22. Rideau N, Berradi H, Skiba-Cassy S, Panserat S, Cailleau-Audouin E, Dupont J: **Induction of glucokinase in chicken liver by dietary carbohydrates**. *Gen Comp Endocrinol* 2008, **158**(2):173-177.
23. Seki Y, Sato K, Kono T, Abe H, Akiba Y: **Broiler chickens (Ross strain) lack insulin-responsive glucose transporter GLUT4 and have GLUT8 cDNA**. *General and comparative endocrinology* 2003, **133**(1):80-87.
24. Bell GI, Burant CF, Takeda J, Gould GW: **Structure and function of mammalian facilitative sugar transporters**. *J Biol Chem* 1993, **268**(26):19161-19164.
25. Kono T, Nishida M, Nishiki Y, Seki Y, Sato K, Akiba Y: **Characterisation of glucose transporter (GLUT) gene expression in broiler chickens**. *Br Poult Sci* 2005, **46**(4):510-515.
26. Tokushima Y, Takahashi K, Sato K, Akiba Y: **Glucose uptake in vivo in skeletal muscles of insulin-injected chicks**. *Comparative biochemistry and physiology Part B, Biochemistry & molecular biology* 2005, **141**(1):43-48.
27. Hillebrand JJ, de Wied D, Adan RA: **Neuropeptides, food intake and body weight regulation: a hypothalamic focus**. *Peptides* 2002, **23**(12):2283-2306.
28. Baskin DG, Figlewicz DP, Woods SC, Porte D, Jr., Dorsa DM: **Insulin in the brain**. *Annual review of physiology* 1987, **49**:335-347.
29. Shiraishi J, Tanizawa H, Fujita M, Kawakami S, Bungo T: **Localization of hypothalamic insulin receptor in neonatal chicks: evidence for insulinergic system control of feeding behavior**. *Neuroscience letters* 2011, **491**(3):177-180.
30. Shiraishi J, Yanagita K, Fujita M, Bungo T: **Central insulin suppresses feeding behavior via melanocortins in chicks**. *Domestic animal endocrinology* 2008, **34**(3):223-228.
31. Benoit SC, Air EL, Coolen LM, Strauss R, Jackman A, Clegg DJ, Seeley RJ, Woods SC: **The catabolic action of insulin in the brain is mediated by melanocortins**. *The Journal of neuroscience : the official journal of the Society for Neuroscience* 2002, **22**(20):9048-9052.
32. Sato I, Arima H, Ozaki N, Watanabe M, Goto M, Hayashi M, Banno R, Nagasaki H, Oiso Y: **Insulin inhibits neuropeptide Y gene expression in the arcuate nucleus through GABAergic systems**. *The Journal of neuroscience : the official journal of the Society for Neuroscience* 2005, **25**(38):8657-8664.
33. Newmyer BA, Nandar W, Webster RI, Gilbert E, Siegel PB, Cline MA: **Neuropeptide Y is associated with changes in appetite-associated hypothalamic nuclei but not food intake in a hypophagic avian model**. *Behavioural brain research* 2013, **236**(1):327-331.
34. Tatemoto K, Carlquist M, Mutt V: **Neuropeptide Y--a novel brain peptide with structural similarities to peptide YY and pancreatic polypeptide**. *Nature* 1982, **296**(5858):659-660.

35. Yang K, Guan H, Arany E, Hill DJ, Cao X: **Neuropeptide Y is produced in visceral adipose tissue and promotes proliferation of adipocyte precursor cells via the Y1 receptor**. *Faseb J* 2008, **22**(7):2452-2464.
36. Kos K, Harte AL, James S, Snead DR, O'Hare JP, McTernan PG, Kumar S: **Secretion of neuropeptide Y in human adipose tissue and its role in maintenance of adipose tissue mass**. *American journal of physiology Endocrinology and metabolism* 2007, **293**(5):E1335-1340.
37. Rosmaninho-Salgado J, Cortez V, Estrada M, Santana MM, Goncalves A, Marques AP, Cavadas C: **Intracellular mechanisms coupled to NPY Y2 and Y5 receptor activation and lipid accumulation in murine adipocytes**. *Neuropeptides* 2012, **46**(6):359-366.
38. Chao PT, Yang L, Aja S, Moran TH, Bi S: **Knockdown of NPY expression in the dorsomedial hypothalamus promotes development of brown adipocytes and prevents diet-induced obesity**. *Cell metabolism* 2011, **13**(5):573-583.
39. Puelles L, Martinez-de-la-Torre, M., Paxinos, G., Watson, C., Martinez, S., : **The Chick Brain in Stereotaxic Coordinates: An Atlas Featuring Neurometric Subdivisions and Mammalian Homologies**, First edn: Academic Press.
40. Schmittgen TD, Livak KJ: **Analyzing real-time PCR data by the comparative CT method**. *Nat Proto* 2008, **3**(6):1101-1108.
41. Ka S, Albert FW, Denbow DM, Paabo S, Siegel PB, Andersson L, Hallbook F: **Differentially expressed genes in hypothalamus in relation to genomic regions under selection in two chicken lines resulting from divergent selection for high or low body weight**. *Neurogenetics* 2011, **12**(3):211-221.
42. Yabuuchi M, Bando K, Hiramatsu M, Takahashi S, Takeuchi S: **Local Agouti Signaling Protein/Melanocortin Signaling System that Possibly Regulates Lipid Metabolism in Adipose Tissue of Chickens**. *The Journal of Poultry Science* 2010, **47**(2):176-182.
43. Sousa-Ferreira L, Garrido M, Nascimento-Ferreira I, Nobrega C, Santos-Carvalho A, Alvaro AR, Rosmaninho-Salgado J, Kaster M, Kugler S, de Almeida LP *et al*: **Moderate long-term modulation of neuropeptide Y in hypothalamic arcuate nucleus induces energy balance alterations in adult rats**. *PloS one* 2011, **6**(7):e22333.
44. Chamorro S, Della-Zuana O, Fauchere JL, Feletou M, Galizzi JP, Levens N: **Appetite suppression based on selective inhibition of NPY receptors**. *International journal of obesity and related metabolic disorders : journal of the International Association for the Study of Obesity* 2002, **26**(3):281-298.
45. Bradley RL, Mansfield JP, Maratos-Flier E: **Neuropeptides, including neuropeptide Y and melanocortins, mediate lipolysis in murine adipocytes**. *Obesity research* 2005, **13**(4):653-661.
46. Serradeil-Le Gal C, Lafontan M, Raufaste D, Marchand J, Pouzet B, Casellas P, Pascal M, Maffrand JP, Le Fur G: **Characterization of NPY receptors controlling lipolysis and leptin secretion in human adipocytes**. *FEBS letters* 2000, **475**(2):150-156.
47. Kousteni S: **FoxO1, the transcriptional chief of staff of energy metabolism**. *Bone* 2012, **50**(2):437-443.

48. Gross DN, Van den Heuval APJ, Birnbaum MJ: **The role of FoxO in the regulation of metabolism**. *Oncogene* 2008, **27**:2320-2336.
49. Gross DN, Wan M, Birnbaum MJ: **The role of FOXO in the regulation of metabolism**. *Current diabetes reports* 2009, **9**(3):208-214.
50. Doblado M, Moley KH: **Facilitative glucose transporter 9, a unique hexose and urate transporter**. *American journal of physiology Endocrinology and metabolism* 2009, **297**(4):E831-835.
51. Leturque A, Brot-Laroche E, Le Gall M: **GLUT2 mutations, translocation, and receptor function in diet sugar managing**. *American journal of physiology Endocrinology and metabolism* 2009, **296**(5):E985-992.
52. Scheepers A, Joost HG, Schurmann A: **The glucose transporter families SGLT and GLUT: molecular basis of normal and aberrant function**. *JPEN Journal of parenteral and enteral nutrition* 2004, **28**(5):364-371.
53. Schmidt S, Joost HG, Schurmann A: **GLUT8, the enigmatic intracellular hexose transporter**. *American journal of physiology Endocrinology and metabolism* 2009, **296**(4):E614-618.
54. Zhao JP, Bao J, Wang XJ, Jiao HC, Song ZG, Lin H: **Altered gene and protein expression of glucose transporter1 underlies dexamethasone inhibition of insulin-stimulated glucose uptake in chicken muscles**. *Journal of animal science* 2012, **90**(12):4337-4345.
55. Ciaraldi TP, Horuk R, Matthaei S: **Biochemical and functional characterization of the rat liver glucose-transport system. Comparisons with the adipocyte glucose-transport system**. *The Biochemical journal* 1986, **240**(1):115-123.
56. Andersen DK, Ruiz CL, Burant CF: **Insulin regulation of hepatic glucose transporter protein is impaired in chronic pancreatitis**. *Annals of surgery* 1994, **219**(6):679-686; discussion 686-677.
57. Stupar RM, Gardiner JM, Oldre AG, Haun WJ, Chandler VL, Springer NM: **Gene expression analyses in maize inbreds and hybrids with varying levels of heterosis**. *BMC Plant Biol* 2008, **8**:33.
58. Llewellyn CH, van Jaarsveld CH, Johnson L, Carnell S, Wardle J: **Nature and nurture in infant appetite: analysis of the Gemini twin birth cohort**. *The American journal of clinical nutrition* 2010, **91**(5):1172-1179.
59. Fisher JO, Cai G, Jaramillo SJ, Cole SA, Comuzzie AG, Butte NF: **Heritability of hyperphagic eating behavior and appetite-related hormones among Hispanic children**. *Obesity (Silver Spring)* 2007, **15**(6):1484-1495.

Table 3.1 Primers used for real time PCR[1]

Gene	Accession No.	Sequences (forward/reverse)
Actin	NM_205518.1	GTCCACCGCAAATGCTTCTAA/
		TGCGCATTTATGGGTTTTGTT
NPY	M87294.1	CATGCAGGGCACCATGAG/
		CAGCGACAAGGCGAAAGTC
NPYR1	NM_001031535.1	TAGCCATGTCCACCATGCA/
		GGGCTTGCCTGCTTTAGAGA
NPYR2	NM_001031128.1	TGCCTACACCCGCATATGG/
		GTTCCCTGCCCCAGGACTA
NPYR5	NM_001031130.1	GGCTGGCTTTGTGGGAAA/
		TTGTCTTCTGCTTGCGTTTTGT
NPYR6	NM_001044687.1	TGTGACCTTTGCAGCTTGCT/
		CGTGGTTCCAGTCAAAAACAAC
POMC	AB019555.1	GCCAGACCCCGCTGATG/
		CTTGTAGGCGCTTTTGACGAT
AGRP	AB029443.1	GGTTCTTCAACGCCTTCTGCTA/
		TTCTTGCCACATGGGAAGGT
IAPP	NM_205397.1	GCTAGGTGCAAGCGTGGAA/
		GCACGCCTGCGTTAGTGA
TH	NM_204805.1	CAGGACATTGGGCTTGCAT/
		TGTTGCCAGTTTCTCAATTTCTTC
PC2	XM_419332.3	TGGGAAGGCAAGGCAATG/

		CCTGACTGTTTGCAATGCACTT
FOXO1	NM_204328.1	GCCTCCTTTTCGAGGGTGTT/
		GCGGTATGTACATGCCAATCTC
IR	XM_001233398.2	CGGAACTGCATGGTTGCA/
		TCTCTGGTCATGCCGAAGTCT
GLUT1	NM_205209.1	TCCTGATCAACCGCAATGAG/
		TGCCCCGGAGCTTCTTG
GLUT2	NM_207178.1	GAAGGTGGAGGAGGCCAAA/
		TTTCATCGGGTCACAGTTTCC
GLUT3	NM_205511.1	TTGGGCGCTTCATTATTGG/
		TTGGGCGCTTCATTATTGG
GLUT8	NM_204375.1	GCTGCCTCAGCGTGACTTTT/
		GCTGCCTCAGCGTGACTTTT
GLUT9	XM_420789.3	TTTCTTCTGGCTTAGTTATTGAAC
		GA/ CCAAAGCCCCCGATGAG
PGC-1α	NM_001006457.1	GAGGATGGATTGCCTTCATTTG/
		GCGTCATGTTCATTGGTCACA
UCP3	NM_204107.1	TGGCAGCGAAGCGTCAT/
		TGGGATGCTGCGTCCTATG

[1]Primers were designed with Primer Express 3.0 (Applied Biosystems) for β-actin (*Actin*), neuropeptide Y (*NPY*), *NPY* receptor subtypes 1, 2, 5 and 6 (*NPYR1*, *2*, *5*, and *6*, respectively), pro-opiomelanocortin (*POMC*), agouti-related peptide (*AGRP*), islet amyloid polypeptide (*IAPP*), tyrosine hydroxylase (*TH*), prohormone convertase 2 (*PC2*),

forkhead box protein 01 (*FOXO1*), insulin receptor (*IR*), glucose transporters 1, 2, 3, 8 and 9 (*GLUT1*, *2*, *3*, *8* and *9*, respectively), peroxisome proliferator-activated receptor gamma, coactivator 1 alpha (*PGC-1α*) and uncoupling protein 3 (*UCP3*)**.**

Table 3.2 Blood glucose concentrations at 90-days of age in parental lines (LWS and HWS) and their reciprocal crosses (HL and LH) at 60 minutes following vehicle or insulin injection

Line[1]	Vehicle treatment[2]	Insulin treatment
HWS	198.6±19.5[a]	139±24.5[b]
LH	212.8±13.7[a]	126.4±5.7[b]
HL	213.1±12.7[a]	101.8±6.8[b]
LWS	181.2±12.6[a]	86.6±5.7[c]

[1]The reciprocal cross of a high weight sire and low weight dam, and low weight sire and high weight dam were used to generate HL and LH offspring, respectively.

[2]Data are expressed as least squares means ± SEM (n=5). There was a two-way interaction of genetic line x treatment on blood glucose concentrations (P = 0.01). Different letters across line and treatment indicate a significant difference, $P < 0.05$ (Tukey's pairwise comparisons).

Table 3.3 Expression of appetite-associated factor mRNA in the hypothalamus at 90-days in parental line LWS and HWS chickens[1]

Effect[2]	Gene[3]				
Treatment	*POMC*	*AGRP*	*IAPP*	*TH*	*PC2*
Insulin	2.26	1.83	1.39	1.24	1.24
Vehicle	1.15	1.50	1.06	0.83	1.08
SEM	0.63	0.85	0.18	0.22	0.11
P-value	0.24	0.79	0.21	0.20	0.37
Line	----------				
HWS	1.73	0.50	1.19	0.86	1.27
LWS	1.68	2.82	1.25	1.21	1.05
SEM	0.63	0.84	0.18	0.22	0.11
P-value	0.96	0.07	0.81	0.28	0.20
	----------*P*-values----------				
Tmt x line[4]	0.42	0.86	0.57	0.24	0.71

[1]The high-weight and low-weight chickens, denoted as HWS and LWS, respectively.

[2]Values represent least squares means ± SEM (n=5) and associated *P*-values for main effects, and *P*-values for the 2-way interaction

[3]*POMC* = pro-opiomelanocortin; *AGRP* = agouti-related peptide; *IAPP* = islet amyloid polypeptide; *TH* = tyrosine hydroxylase; *PC2* = prohormone convertase 2

[4]Two-way interaction of treatment by genetic line

Table 3.4 Expression of *NPY, NPY* receptor sub-type and *FOXO1* mRNA in different tissues of chickens selected for high (HWS) or low (LWS) body weight[1]

Effect	Gene[2]					
Treatment	*NPY*	*NPYR1*	*NPYR2*	*NPYR5*	*NPYR6*	*FOXO1*
Insulin	0.27	0.28	0.33	0.29	0.49	5.68
Vehicle	0.24	0.32	0.33	0.28	0.43	4.43
SEM	0.02	0.03	0.02	0.03	0.05	0.73
P-value	0.40	0.25	1.00	0.78	0.35	0.25
Line	----------					
HWS	0.22	0.27	0.35	0.22	0.47	6.39
LWS	0.29	0.34	0.32	0.35	0.45	3.72
SEM	0.02	0.03	0.02	0.03	0.05	0.73
P-value	0.06	0.05	0.21	0.009	0.81	0.02
Tissue	----------					
Hypothalamus	0.98^{a}±0.06	0.89^{a}±0.05	0.9^{a}±0.04	0.82^{a}±0.06	1.09^{a}±0.09	1.0^{c}±0.06
Fat	0.02^{b}±0.001	0.02^{b}±0.002	0.2^{b}±0.04	0.03^{b}±0.003	0.2^{c} ±0.05	1.19^{c}±0.07
Liver	0.002^{c}±0.001	0.003^{c}±0.002	0.02^{c}±0.01	0.005^{c}±0.003	0.07^{c} ±0.01	4.16^{b}±0.2
Muscle	0.02^{b}±0.001	ND[3]	0.15^{b}±0.01	ND	0.47^{b}±0.07	13.9^{a}±2.2
P-Value	<0.0001	<0.0001	<0.0001	<0.0001	<0.0001	<0.0001
Interactions[4]	----------*P*-values----------					
Tmt x tissue	0.82	0.52	0.97	0.91	0.25	0.69
Line x tissue	<0.0001	0.01	0.003	0.001	0.17	0.002
Tmt x line	0.48	0.33	0.38	0.89	0.85	0.64

[1]Different letters within a column for the main effect of tissue indicate a difference at $P < 0.05$ (Tukey's pairwise comparisons). Data are expressed as least squares means ± SEM (n=5)

[2]*NPY* = neuropeptide Y; *NPYR1*, *2*, *5* and *6* = *NPY* receptor sub-types 1, 2, 5 and 6, respectively; *FOXO1* = forkhead box protein 01

[3]ND: The mRNA was not detected

[4] Interactions = two-way interactions on mRNA abundance. Tmt = treatment (insulin or vehicle).

Table 3.5 Abundance of glucose transporter and *IR* mRNA in different tissues of chickens selected for high (HWS) or low (LWS) body weight[1]

Effects	Gene[2]					
Treatment	*GLUT1*	*GLUT2*	*GLUT3*	*GLUT8*	*GLUT9*	*IR*
Insulin	0.40	221.33	0.42	1.00	3.46	0.75
Vehicle	0.40	344.40	0.41	1.09	3.40	0.89
SEM	0.02	25.24	0.02	0.04	0.33	0.07
P-value	0.98	0.003	0.69	0.14	0.91	0.20
Line	----------					
HWS	0.44	330.11	0.42	1.09	4.41	0.91
LWS	0.35	235.63	0.40	1.00	2.44	0.73
SEM	0.02	25.24	0.02	0.04	0.33	0.07
P-value	0.001	0.02	0.59	0.18	0.0007	0.10
Tissue	----------					
Hypothalamus	0.96^{a}±0.04	1.20^{c}±0.17	1.06^{a}±0.05	1.0^{b}±0.02	0.9^{b}±0.09	0.2^{d}±0.03
Fat	0.13^{c}±0.008	4.46^{bc}±1.60	0.1^{b}±0.005	0.33^{c}±0.02	0.44^{c}±0.22	0.54^{c}±0.03
Liver	0.11^{c}±0.01	1121^{a}±71	0.1^{b}±0.005	1.3^{a}±0.08	12.2^{a}±0.97	0.93^{b}±0.03
Muscle	0.39^{b}±0.05	4.3^{b}±0.8	ND[3]	1.6^{a}±0.1	0.2^{c}±0.03	1.60^{a}±0.20
P-value	<0.0001	<0.0001	<0.0001	<0.0001	<0.0001	<0.0001
Interactions[4]	----------*P*-values----------					
Tmt x tissue	0.96	0.01	0.005	0.15	0.64	<0.0001
Line x tissue	0.0004	0.02	0.71	0.32	0.0008	0.31
Tmt x line	0.38	0.40	0.26	0.84	0.07	0.54

[1]Different letters within a column for the main effect of tissue indicate a difference at $P < 0.05$ (Tukey's pairwise comparisons). Data are expressed as least squares means ± SEM (n=5)

[2]*GLUT1*, *2*, *3*, *8* and *9* = glucose transporters 1, 2, 3, 8 and 9, respectively; *IR* = insulin receptor

[3]ND: The mRNA was not detected

[4] Interactions = two-way interactions on mRNA abundance. Tmt = treatment (insulin or vehicle).

Table 3.6 Heterosis for expression of genes that showed significant difference in mRNA abundance among genetic lines[1]

	----------Abdominal fat----------				
Line[2]	*IR*	*NPY*	*NPYR1*	*NPYR2*	*NPYR5*
HWS	0.53^{a}±0.04	8.88^{a}±1.30	5.59^{a}±1.18	2.79^{a}±0.27	7.19^{a}±1.67
HL	0.32^{c}±0.04	6.23^{a}±1.30	0.49^{b}±1.26	1.27^{b}±0.23	0.20^{b}±1.67
LH	0.35^{bc}±0.04	5.07^{a}±1.37	0.30^{b}±1.26	1.26^{b}±0.24	1.71^{ab}±1.67
LWS	0.51^{ab}±0.04	3.01^{b}±1.50	2.21^{ab}±1.37	1.10^{b}±0.27	2.91^{ab}±1.93
Heterosis	-35.58%	-4.96%	-78.21%	-34.96%	-81.09%
P-value[3]	<0.0001	0.82	0.0002	0.01	0.02
	----------Liver----------				
Line	*GLUT1*	*GLUT2*	*GLUT9*	*NPYR2*	
HWS	2.09^{a}±0.21	1.36^{a}±0.14	1.99^{a}±0.14	2.46^{a}±0.28	
HL	2.26^{a}±0.19	0.40^{b}±0.14	1.17^{b}±0.14	1.79^{ab}±0.25	
LH	1.82^{a}±0.19	0.31^{b}±0.14	1.23^{b}±0.14	1.05^{b}±0.24	
LWS	0.96^{b}±0.20	1.15^{a}±0.14	0.99^{b}±0.14	1.13^{b}±0.26	
Heterosis	33.77%	-71.71%	-19.46%	-20.89%	
P-value	0.01	<0.0001	0.04	0.16	
	----------Hypothalamus----------				
Line	*GLUT1*	*NPY*	*NPYR1*		
HWS	1.25^{a}±0.06	0.85±0.11	0.95^{ab}±0.10		
HL	1.16^{ab}±0.06	1.16±0.11	0.76^{ab}±0.09		

LH	1.10^{ab}±0.06	1.17±0.11	0.68^{b}±0.10
LWS	0.97^{b}±0.06	1.12±0.11	1.02^{a}±0.09
Heterosis	1.80%	18.27%	-26.90%
P-value	0.69	0.11	0.001

[1]*IR* = insulin receptor; *NPY* = neuropeptide Y; *NPYR1, 2* and *5* = *NPY* receptors 1, 2 and 5, respectively; *GLUT1*, *2* and *9* = glucose transporter 1, 2 and 9, respectively. Different letters within a column represent significant differences, $P < 0.05$ (Tukey's pairwise comparisons). Values are least squares means ± SEM (n=10).

[2]The reciprocal cross of a high weight sire and low weight dam, and low weight sire and high weight dam were used to generate HL and LH offspring, respectively.

[3]Significance of heterosis.

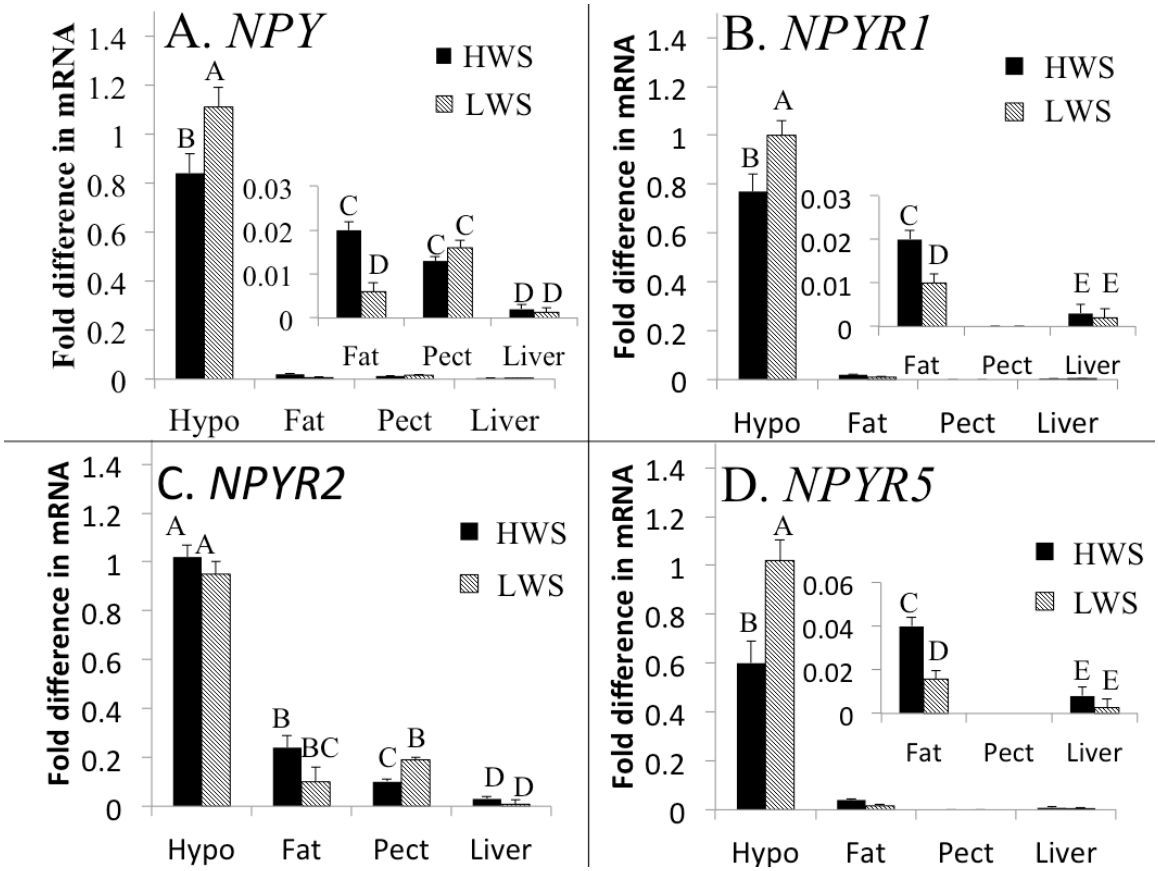

Figure 3.1 Expression of neuropeptide Y (*NPY)* (A), *NPY* receptor 1 (*NPYR1)* (B), *NPYR2* (C) and *NPYR5* (D) mRNA in the hypothalamus (Hypo), abdominal fat (Fat), *Pectoralis major* (Pect) and liver of 90-day old chickens selected for high (HWS) or low (LWS) body weight. Two-way interactions of tissue and genetic line on mRNA abundance ($P < 0.05$). Values represent least squares means ± SEM (n = 10). Differing letters above bars indicate significant difference at $P < 0.05$ (Tukey's pairwise comparisons).

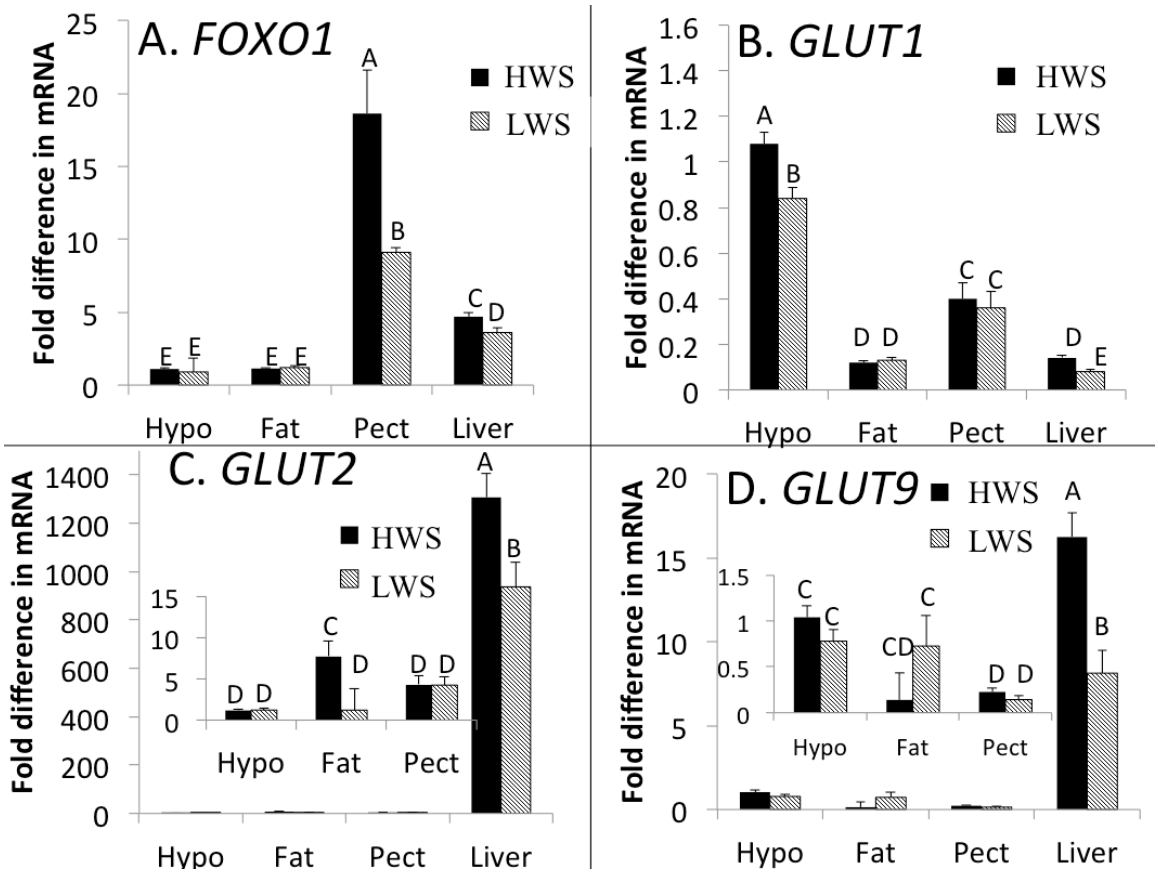

Figure 3.2 Fold differences in forkhead box protein 01 (*FOXO1)* (A), glucose transporter 1 (*GLUT1)* (B), *GLUT2* (C) and *GLUT9* (D) mRNA in the hypothalamus (Hypo), abdominal fat (Fat), *Pectoralis major* (Pect) and liver of 90-day old chickens selected for high (HWS) or low (LWS) body weight. Two-way interactions of tissue and genetic line on mRNA abundance ($P < 0.05$). Values represent least squares means ± SEM (n = 10). Differing letters above bars indicate significant difference at $P < 0.05$ (Tukey's pairwise comparisons).

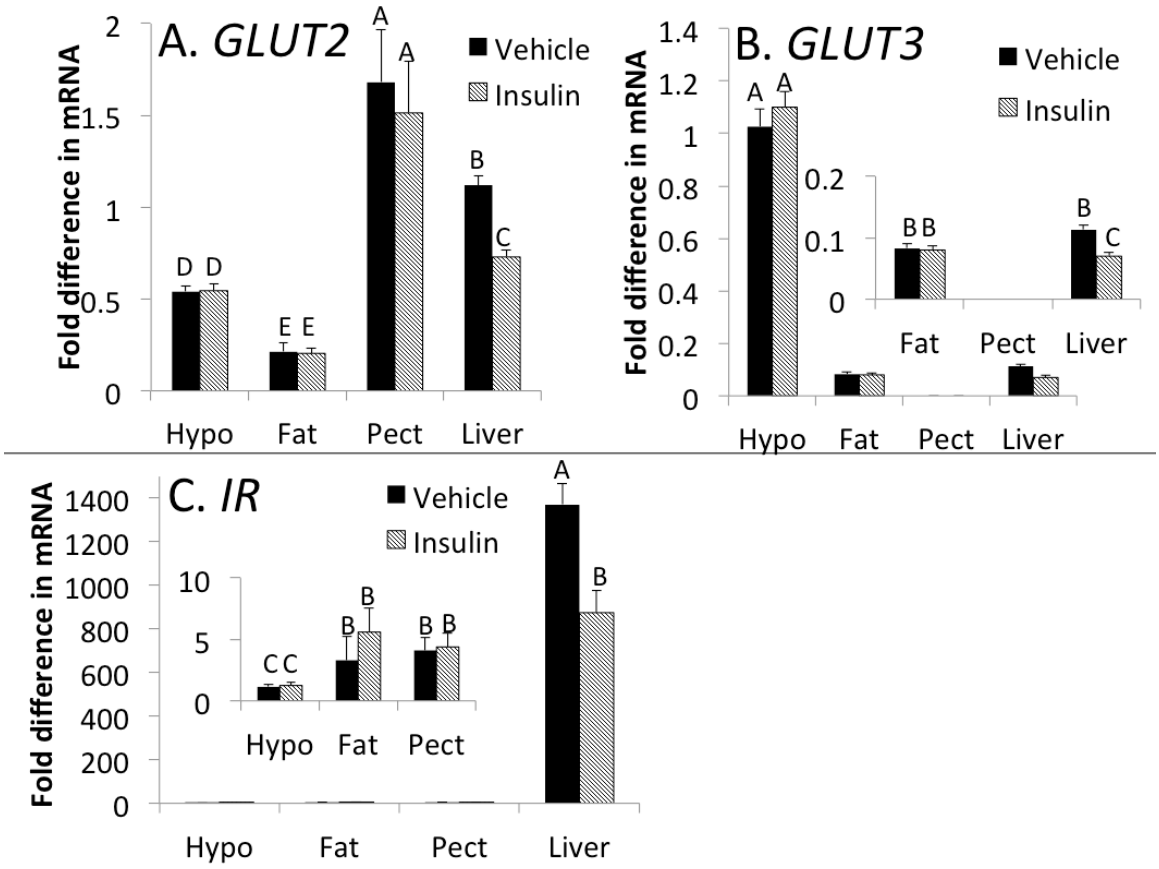

Figure 3.3 Quantities of glucose transporter 2 (*GLUT2)* (A), *GLUT3* (B) and insulin receptor (*IR)* (C) mRNA in the hypothalamus (Hypo), abdominal fat (Fat), *Pectoralis major* (Pect) and liver of vehicle- or insulin-injected 90-day old chickens selected for high (HWS) and low (LWS) body weight. Two-way interactions of tissue and treatment on mRNA abundance ($P < 0.05$). Values represent least squares means ± SEM (n = 10). Differing letters above bars indicate significant difference at $P < 0.05$ (Tukey's pairwise comparisons).

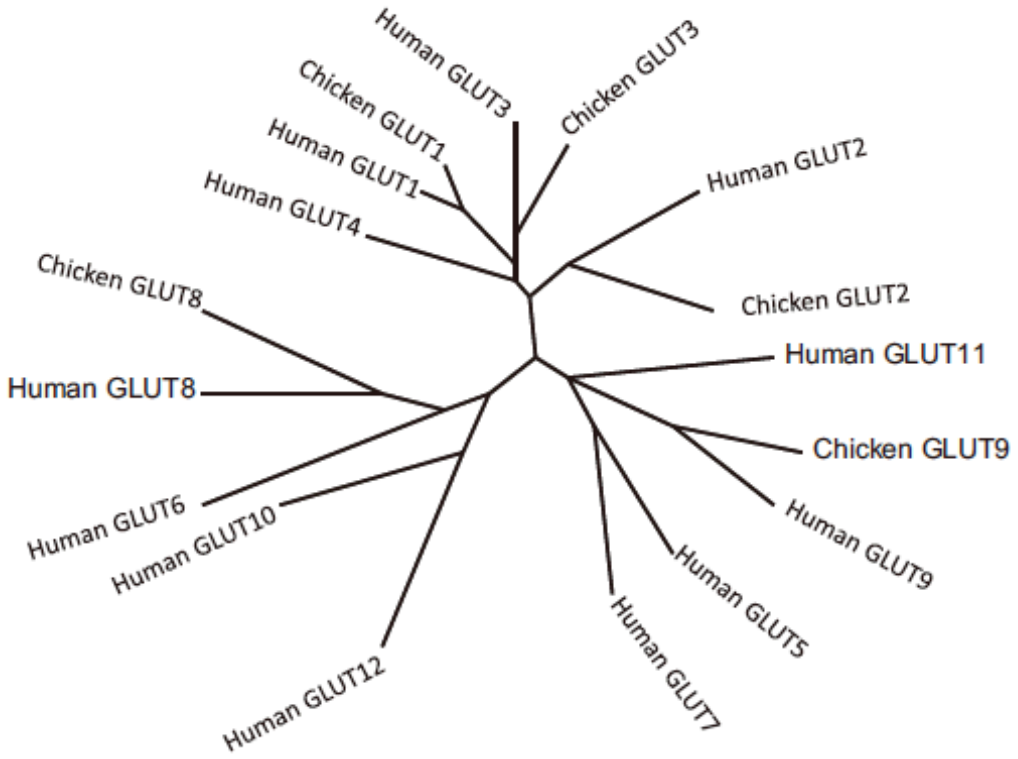

Figure 3.4 Phylogenetic tree showing predicted evolutionary relationship between chicken and human glucose transporter (GLUT) gene family members based on amino acid sequence alignment. Alignments performed using Biology Workbench (workbench.sdsc.edu) and Accession IDs: Human (h) GLUT1, NP_006507.2; h GLUT2; NP_000331.1; h GLUT3, NP_008862.1; h GLUT4, NP_001033.1; h GLUT5, NP_003030.1; h GLUT6, NP_060055.2; h GLUT7, NP_997303.2; h GLUT8, NP_055395.2; h GLUT9, NP_064425.2; h GLUT10, NP_110404.1; h GLUT11, NP_001020109.1; h GLUT12, NP_660159.1; Chicken (c) GLUT1, NP_990540.1; c GLUT2, NP_997061.1; c GLUT3, NP_990842.1; c GLUT8, NP_989706.1; c GLUT9, XP_420789.3

Chapter 4

Neuropeptide Y promotes adipogenesis in chicken adipose cells in vitro

Abstract: Neuropeptide Y is an evolutionarily conserved neurotransmitter that stimulates food intake in various species and also plays a role stimulating adipogenesis in mammalian adipose cells. The objective of this study was to determine the effects of NPY on adipogenesis in an avian species, using chickens as a model. The stromal-vascular fraction of cells was isolated from the abdominal fat of 14 day-old broiler chicks and effects of exogenous NPY on proliferation and differentiation determined. Based on a thymidine analog incorporation assay and gene expression analysis, there was no effect of NPY on proliferation during the first 12 hours post-treatment. However, there were effects of NPY treatment on adipogenesis during the first 6 days post-induction of differentiation. Neuropeptide Y supplementation during induction of differentiation (100 nM) stimulated adipogenesis by enhancing G3PDH activity, which was also associated with greater staining for neutral lipids indicative of increased lipid accumulation. This was accompanied by increased proliferation during differentiation, which was characterized by up-regulation of *Ki67, TOP2A*, and *TPX2* mRNA abundance, and a greater number of proliferating cells in groups that were treated with NPY. Additionally, NPY treatment was associated with increased expression of *FABP4* mRNA on both day 2 and day 6 post-differentiation, and *LPL* expression on day 6 post-differentiation. Transcription factors such as *C/EBPα*, *PPARγ*, and *SREBP* were also differentially regulated during differentiation and in response to NPY treatment, and these results may shed some light on their role in chicken adipogenesis. In conclusion, these results suggest that NPY plays a similar role in promoting adipogenesis in chickens as in mammals and

that the mechanisms involve an increase in the synthesis of new fat cells and heightened rates of lipid synthesis and accumulation.

Introduction

Neuropeptide Y (NPY) is an evolutionarily conserved 36 amino acid peptide important in whole body energy regulation. It was first isolated from pig brain in 1982 [1] and was subsequently identified as a potent orexigenic factor in mammals [2-4] and chickens [5]. More recently, the role of hypothalamic NPY in adipose tissue function has been revealed through knockdown studies. For example, knockdown of *NPY* expression in the dorsomedial hypothalamus using adeno-associated virus-mediated RNA interference promotes brown adipocyte development and prevents diet-induced obesity [6]. The arcuate nucleus-derived NPY also controls brown adipocyte development and brown adipose tissue thermogenesis through the sympathetic nervous system [6]. Apart from the effects of central nervous system-derived NPY on adiposity and energy regulation, NPY and its receptor sub-types are also produced by various peripheral tissues such as thyroid, heart, spleen and various cells in adipose tissue, and NPY was shown to be involved in adipogenesis in various in vivo and in vitro mammalian models as we recently reviewed [7]. Yang et al. reported expression of NPY in visceral adipose tissue, and that supplementation of NPY stimulated the proliferation of primary rat preadipocytes and 3T3-L1 mouse preadipocytes [8]. Studies with 3T3-L1 preadipocyte and sympathetic neuron-derived tumor cell co-cultures revealed that NPY promoted adipocyte proliferation and differentiation through NPY2R [9]. These studies all suggested that NPY system can promote energy storage in adipose tissue and inhibit brown fat activation through both central and peripheral pathways.

In chickens, central injection of NPY stimulates food intake [10, 11]. To the best of our knowledge, there has been no report of the effects of NPY on chicken adipose tissue function. We reported that chickens selected for divergent juvenile body weight showed differences in their food intake response to NPY [11] and adipose tissue gene expression of NPY and its receptors [12]. These two lines have been bi-directionally selected for body weight for 56 generations from a common founder population and now display a 10-fold body weight difference at 56 days of age, with the high weight line chickens being hyperphagic and obese relative to the low weight selected individuals [13]. We showed that *NPY* and its receptor sub-types *NPY1R* and *NPY5R* were more highly expressed in the abdominal fat of the high weight line chickens than the low weight line individuals [12]. Thus, it was hypothesized that the NPY system plays a role in fat accumulation in the adipose tissue of chickens. The objective of this study was to investigate the role of NPY in chicken adipogenesis using a fast growing broiler line as the model.

Materials and methods

Animals

All animal protocols were approved by the Institutional Animal Care and Use Committee at Virginia Tech. Day of hatch Hubbard x Cobb-500 broiler chicks were obtained from a local hatchery. Chicks were group caged at 30 ± 2 °C and 50 ± 5% relative humidity with free access to water and commercial starter diet (23% crude protein, 3,000 kcal metabolizable energy/kg). For all experiments, there were triplicate wells of each treatment, and experiments were repeated at least three times.

Primary adipose cell culture

Reagents were purchased from Sigma Aldrich (MO, USA) unless otherwise stated. Approximately two grams of abdominal fat was collected from 14 day-old chicks by sterile dissection and submerged in DMEM/F12 Glutamax (Gibco, NY, USA) media containing 1% penicillin/streptomycin (HyClone, MA, USA) warmed to 37 °C. Under the biological safety cabinet, adipose tissue was minced into fine sections with scalpel blades and incubated in 10 mL of 4-(2-Hydroxyethyl)piperazine-1-ethanesulfonic acid, N-(2-Hydroxyethyl) piperazine-N′-(2-ethanesulfonic acid) **(**HEPES) solution (0.1 M HEPES, 5 mM D-glucose, 1.5 % bovine serum albumin; BSA) containing 500 units/mL Collagenase, Type I (Worthington Biochemical Corporation, NJ, USA) for 1 hour at 37 °C in a shaking water bath. After the incubation, the contents were filtered through 240 µm filters (Pierce, IL, USA). The filtrate was then centrifuged at 200 x g for 10 min to separate floating adipocytes from the other cell types. The supernatant was discarded, and cell pellets were resuspended in 10 mL of red blood cell lysis buffer (155 mM NH_4Cl, 10 mM $KHCO_3$, 0.1 mM EDTA) to remove the red blood cells. The contents were then filtered through a 20 µm mesh (Celltrics, NJ, USA) to filter out the endothelial clumps. The filtrate was then centrifuged at 200 x g for 5 min to obtain the stromal vascular fraction (SVF) of cells. The SVF was resuspended in plating media (DMEM/F12 containing 10% defined fetal bovine serum; HyClone, and 1% penicillin/streptomycin) at a density of 3×10^4 cells per mL. Cells were then seeded directly into either 12-well plates or petri dishes (Falcon, MA, USA) and incubated at 37°C in a 5 % CO_2 humidified

atmosphere for at least 48 hours (to minimize pro-inflammatory cytokine secretion) before beginning experiments.

NPY treatment and cellular proliferation

Cells were seeded in 12-well plates and cultured in plating media until 50% confluence. Cells were then cultured in serum-free media for 24 h for cell cycle synchronization. In order to minimize the confounding effects of serum-derived NPY, cells were cultured in basic media (DMEM/F12 with1% penicillin/streptomycin) containing 1.5% FBS and 0, 1, 10, or 100 nM chicken NPY (custom synthesized by AnaSpec). In preliminary studies, 1.5 % was the minimum concentration of serum needed to induce proliferation in control cells (data not shown).

The effect of NPY on cellular proliferation was evaluated using the Click-iT® EdU Alexa Fluor® 488 Imaging Kit (Invitrogen). The EdU contains a nucleoside analog of thymidine and alkyne, which allows the thymidine analog to be incorporated into DNA during active DNA synthesis and be detected by the Alexa Fluor dye that contains the azide. Briefly, 1 μL of EdU was added into each well after the addition of the treatment media and cultured for 12 h. Culture media was removed, and cells were fixed with 3.7% methanol-free formaldehyde in phosphate-buffered saline (PBS) for 15 min. Buffer containing 0.5% Triton X-100 in PBS was then added to each well and cells were incubated for 20 min, followed by addition of 0.5 mL of Click-iT reaction cocktail and incubation for 30 min. Cells were then stained with Hoechst 33342 solution for determining total cell number. Digital images of stained cells were captured and analyzed using image overlay functions of NIS-Elements Advanced Research Software (Nikon, NY, USA). Briefly, five images were captured from different fields in each well for both

of the fluorophores and image overlays performed. The new proliferating cells were counted for statistical analysis.

At 4 h post-NPY treatment, cells were harvested for total RNA isolation and gene expression analysis of proliferation markers as described in the methods below.

NPY treatment and adipocyte differentiation

The adipocyte differentiation protocol was similar to a method that has been described [14]. Briefly, cells were cultured in plating media and allowed to reach complete confluence. Plating media (DMEM/F12 basic media with 10% FBS) was replaced with induction media (DMEM/F12 basic media containing 200 nM insulin, 1 μM dexamethasone, 10 U/mL heparin, and 2.5% chicken serum; CS) containing 0, 1, 10, or 100 nM chicken NPY. At 48 h post-induction, media was replaced with insulin-containing media (DMEM/F12 basic media containing 2.5% CS and 200 nM insulin) and the respective NPY treatment. At 48 h later, cells were cultured in maintenance media (DMEM/F12 basic media with 2.5% CS) and the respective NPY treatment for another 48 h. The respective NPY treatment was supplemented daily until the day of the experiment. Analysis of Oil Red O staining, glycerol-3-phosphate dehydrogenase (G3PDH) specific activity, and mRNA abundance of adipose-associated genes as markers for adipocyte differentiation were evaluated at 2, 4 and 6 days post-induction of differentiation as described below.

Oil Red O staining

Cells were fixed with 10% neutral-buffered formalin for 30 min at room temperature and Oil Red O staining was performed according to the manufacturer's instructions (Oil Red O Stain Kit; American Master Tech). Propylene glycol was added

to each well and incubated for 5 minutes, replaced with pre-heated Oil Red O working solution and incubated for another 5 minutes at room temperature, and rinsed with distilled water. Absorbance was measured at 490 nm to estimate lipid accumulation. Cells were then counterstained with Modified Mayer's Hematoxylin (supplied in kit) and imaged to estimate the differentiation ability.

G3PDH specific activity

The method for assaying G3PDH specific activity was adapted from two other studies [15, 16]. Briefly, cells were cultured in 12-well plates and treated as described above. On the day of the experiment, cells were washed with PBS, and 200 μL of lysis buffer (50 mM Tris-Cl, 1 mM EDTA, and 1 mM β-mercaptoethanol, pH 7.5) was added to each well, and cells detached from the plate using cell scrapers. Lysates were transferred to microcentrifuge tubes and sonicated at 4°C using a Bioruptor 300 (Diagenode) with 2 cycles of 30 sec on and 30 sec off at high frequency. Lysates were then centrifuged at 12,000 x g at 4°C for 30 min, and the supernatant used for measuring G3PDH activity and for determining total protein concentration. The G3PDH activity was measured for each sample in duplicate in assay buffer (100 mM Triethanolamine-HCl, 2.5 mM EDTA, 0.12 mM NADH, 0.2 mM Dihydroxyacetone phosphate (DHAP), 0.1 mM β-mercaptoethanol, pH 7.5) in a total reaction volume of 200 μL in UV transparent plates (Corning, MA, USA) using a μQuant plate reader and KC Junior software (Bio-Tek, VT, USA). Absorbance was measured at 340 nm for 20 cycles at 25°C and the maximum slope calculated from the absorbance data. Protein concentration was quantified with Bradford reagent (Sigma-Aldrich, MO, USA) using an Infinite M200Pro multi-mode plate reader and Magellan software (Tecan, CA, USA). The

maximum slope was normalized to the protein concentration to calculate specific activity, which is reported as μmol · min · mg.

Total RNA isolation and gene expression analysis

Cells in 12-well plates were washed with PBS and lysed with a 21 gauge needle in 350 μL RLT buffer (Qiagen, CA, USA). The total RNA was extracted with the RNeasy Mini kit (Qiagen, CA, USA) according to the manufacturer's instructions. An on-column RNase-Free DNase I (Qiagen, CA, USA) treatment was incorporated to eliminate genomic DNA carry-over in the RNA preparations. The eluted total RNA samples were quantified and assessed for purity by spectrophotometry at 260/280/230 nm using a Nanophotometer™ Pearl (IMPLEN, CA, USA), and their integrity evaluated by agarose gel electrophoresis. The first strand cDNA was synthesized from 200 ng total RNA using the High Capacity cDNA Reverse Transcription kit (Applied Biosystems, NY, USA). Primers were designed in Primer Express 3.0 (Applied Biosystems, NY, USA; **Table 4.1**). All primers were evaluated for amplification efficiency before use. Efficiency of target genes was within 5% of the endogenous control (actin). A total volume of 10 μL in each reaction contained 5 μL fast SYBR Green Master Mix (Applied Biosystems, NY, USA), 0.25 μL each of 5 μM forward and reverse primers, and 3 μL of 10-fold diluted cDNA. Real-time PCR reactions were performed in duplicate for all samples on an Applied Biosystems 7500 FAST system, under the following conditions: enzyme activation for 20 sec at 95°C and 40 cycles of 1) melting step for 3 seconds at 95°C and 2) annealing/extension step for 30 seconds at 60°C. A melting curve analysis was performed after all reactions to ensure amplification specificity.

Statistical analysis

The real time PCR data were analyzed using the ΔΔCT method, where ΔCT = CT target gene – CT actin, and ΔΔCT = ΔCT target sample – ΔCT calibrator [17]. The average of the control group within a time point was used as the calibrator sample. The relative quantity ($2^{-\Delta\Delta CT}$) values were subjected to ANOVA using the Glimmix procedure of SAS (SAS Ins., Cary, NC). The statistical model included the main effect of treatment. A similar model was used for the proliferation experiment data and for G3PDH specific activity data. To evaluate the effects of time post-differentiation on gene expression in control cells, CT values from control cell samples were calibrated to the average of day-2 post differentiation and the statistical model included the main effect of time point. Tukey's test was used for pairwise comparisons between treatments. Results were considered significant at $P < 0.05$.

Results

Cellular proliferation

Treatment of cells from the stromal-vascular fraction of chicken adipose with NPY did not affect cellular proliferation at 12 hours post-treatment (**Figure 4.1**). At 4 hours post-treatment, there was also no difference in the mRNA abundance of GATA binding protein 2 (*GATA2*), krüppel-like factor 1 *(KLF1*), krüppel-like factor 7 (*KLF7*), or *Ki67* at any of the NPY doses tested. However, with 100 nM NPY supplementation, topoisomerase II alpha (*TOP2A*) and thioredoxin-dependent peroxidase 2 (*TPX2*) mRNA abundance decreased at 4 hours post-treatment compared with expression in control cells, while expression of *NPY* increased in response to 100 nM NPY treatment (**Figure 4.2**). Treatment with 10 nM NPY was associated with an increase in *NPY2R* (neuropeptide Y

receptor 2) mRNA abundance at 4 hours post-treatment in comparison to non-treated cells (**Figure 4.2**).

Adipocyte differentiation

Treatment of cells with NPY during induction of adipocyte differentiation increased G3PDH activity on day 6 post-differentiation, with greater activity in cells treated with 100 nM NPY as compared to control cells (**Figure 4.3**). This effect was also reflected in the Oil Red O staining, where on day 4 post-differentiation, cells started to display distinct multilocular lipid accumulation (**Figure A.1**). The lipid accumulation continued to increase and by day 6, the NPY treated cells showed greater lipid accumulation than the cells from the control groups, with the most accentuated increase in lipid accumulation observed in cells treated with 100 nM NPY (**Figure 4.4**). After induction of differentiation, there was also an increase in cell density in the NPY-treated cells (**Figure 4.4**).

Treatment with NPY during induction of adipocyte differentiation reduced CCAAT/enhancer binding protein α (*C/EBPα*) expression on day 4 (100 nM NPY; **Figure 4.5A**), peroxisome proliferator-activated receptor γ *(PPARγ*) expression on both day 4 and day 6 (all NPY concentrations; **Figure 4.5B**), and Sterol Regulatory Element-Binding Protein (*SREBP*) on day 4 (10 nM and 100 nM NPY supplementation; **Figure 4.5C**), as compared with non-treated cells. Abundance of CCAAT/enhancer binding protein β (*C/EBPβ*) mRNA was not affected by any dose of NPY on any day post-differentiation (**Figure 4.5D**). Treatment with NPY increased fatty acid binding protein 4 (*FABP4*) mRNA on both day 2 (100 nM NPY) and day 6 (10 and 100 nM NPY) post-differentiation in comparison with control cells (**Figure 4.5E**). Expression of *LPL*

(lipoprotein lipase) was also greater on day 6 post-differentiation in NPY-treated cells (10 and 100 nM NPY) than control cells (**Figure 4.5F**).

Expression of all proliferation markers increased in response to NPY treatment during differentiation, with *TOP2A* mRNA having a more robust response (**Figure 4.6**). Abundance of *Ki67* mRNA was greater in NPY-treated cells than control cells at day 4 (all doses of NPY) and day 6 (10 and 100 nM NPY) post-differentiation (**Figure 4.6A**). Quantities of *TOP2A* mRNA were greater in NPY-treated cells than non-treated cells at day 2 (100 nM NPY), day 4 (all doses of NPY) and day 6 (10 and 100 nM NPY) post-differentiation (**Figure 4.6B**). Treatment with NPY increased abundance of *TPX2* mRNA at day 4 (10 nM NPY) and day 6 (100 nM NPY) post-differentiation as compared with control cells (**Figure 4.6C**).

Treatment of adipose cells with NPY during differentiation also influenced expression of *NPY* at 2 and 6 days post-differentiation, with greater expression in cells treated with 100 nM NPY as compared to non-treated cells (**Figure 4.6D**). Abundance of *NPY2R* mRNA was not influenced by NPY treatment at any of the doses or time points measured (**Figure 4.6E**). Consistent with the expression analysis, treatment with 100 nM NPY increased adipocyte proliferation, as reflected by increases in the number of proliferating cells at day 5 post-differentiation (**Figure 4.7** and **Figure 4.8**).

Abundance of adipose-associated factor mRNA was also regulated by stage of differentiation (**Figure 4.9A**). Expression of *C/EBPα* and *PPARγ* mRNA decreased at days 4 and 6 post-induction of differentiation relative to day 2 (**Figure 4.9A**). Expression of *FABP4* was lower at day 4 than day 2 or 6 post-differentiation, while *LPL* mRNA abundance was reduced at day 6 post-differentiation relative to day 2. Proliferation

marker and *NPY* mRNA also changed during differentiation (**Figure 4.9B**). Expression of *Ki67* was lowest in proliferating cells compared to differentiating cells, and following induction of differentiation, *Ki67* mRNA was decreased at day 6 post-induction of differentiation. Expression of *TOP2A* and *TPX2* were similar between proliferating cells and cells at day 2 post-induction of differentiation, and expression then decreased at day 6 post-differentiation (**Figure 4.9B**). Abundance of *NPY* and *NPY2R* was also similar between proliferating and early differentiating cells, with a striking decrease in expression at days 4 and 6 post-induction of differentiation.

Discussion

To understand the potential role of neuropeptide Y in adipogenesis in chickens, we designed the present study to evaluate the effects of different doses of chicken NPY on chicken primary adipose cell proliferation and differentiation. To our knowledge, this study is the first to report the role of NPY in adipose cell function in an avian species and this study has shown, for the first time, the potential importance of NPY in promoting chicken adipogenesis. The broiler chicken is an important agricultural species and biomedical model. As the intense selection for body weight and feed efficiency has continued, how to control body fat accumulation has become a major concern in the chicken and egg industry, but has also made the chicken an attractive model for understanding the pathogenesis of obesity in humans.

Neuropeptide Y supplementation is not associated with changes in proliferation during the first 12 hours post-treatment

Neuropeptide is secreted in various tissues and also circulates in the serum [18]. To eliminate the confounding effects of serum-derived NPY on cells supplemented with

chicken NPY, I performed dose titration studies to find the minimal concentration of FBS that could be used to support cellular proliferation without introducing an additional source of NPY. I then compared the effects of supplementing 1, 10, and 100 nM NPY on adipogenesis, with doses of NPY based on studies that were conducted with rodent models [9, 19]. However, there was no effect of NPY supplementation on proliferation markers, including staining for incorporation of EdU, a thymidine analog that is incorporated into DNA during DNA replication. This was consistent with the gene expression results showing no effect of NPY treatment on preadipocyte markers during stimulation of proliferation. Krüppel-like factor 7 (KLF7) [20] and GATA-binding protein 2 (GATA2) [21] are factors that were described as being enriched in chicken preadipocytes, associated with preadipocyte proliferation and negligibly expressed in terminally differentiated adipocytes.

The Ki67, TOP2A and TPX2 proteins were described as being excellent proliferation biomarkers for real time PCR analysis [22-24]. With 100 nM NPY supplementation, NPY2R expression was reduced. There was also reduced expression of TOP2A and TPX2. It is possible that the higher concentration of NPY may be associated with secondary effects in the cells, although expression was measured at only 4 hours post-treatment with NPY. It is also possible that 4 and 12 hours were not sufficient time for NPY to exert maximal effects on gene expression regulation and changes in DNA synthesis, respectively. However, at the time points measured in this study, there did not appear to be a direct effect of NPY treatment on markers of cell proliferation.

Chicken adipocyte differentiation

In the present study, I compared different differentiation methods before settling on the method that was used and reported for all experiments. Chicken adipocytes display much greater differentiation efficiency and capacity when cultured in CS rather than FBS. Again, serum concentrations were titrated to minimize the confounding effects of NPY, and 2.5% was the lowest concentration that I found acceptable for the evaluation of effects of NPY on chicken adipogenesis. I also titrated the concentration of insulin in the induction media in order to separate the function of NPY from insulin in promoting adipogenesis, as a previous report indicated that NPY may mimic the role of insulin in promoting adipocyte differentiation [9].

NPY treatment is associated with enhanced rates of chicken adipogenesis

In general, treatment with the higher concentration of NPY was associated with enhanced lipid accumulation and changes in gene expression of adipogenesis-associated factors, with most effects observed after 2 days post-induction of differentiation. Glycerol-3-phosphate dehydrogenase (G3PDH) catalyzes the reversible conversion of dihydroxyacetone phosphate into glycerol-3-phosphate (G3P), which serves as the backbone for fatty acid esterification during triacylglycerol (TAG) synthesis. Because glycerol kinase activity is low in adipose tissue and generation of G3P through G3PDH is the major source for TAG synthesis, activity of G3PDH is highly correlated with differentiation of precursor cells into terminally differentiated adipocytes and is a gold standard for serving as an indirect marker of adipogenesis [25, 26]. Here, I measured the effect of various doses of NPY on G3PDH activity at days 2, 4 and 6 post-induction of differentiation. There was a clear dose-dependent effect of NPY on increasing G3PDH activity, with maximal activity observed in cells that were treated with 100 nM NPY at

day 6 post-differentiation. Enhanced activity of G3PDH was reflected by greater lipid accumulation, with the Oil Red O staining revealing a greater deposition of lipid in NPY-treated cells, especially at day 6 post-differentiation.

To understand the molecular mechanisms underlying NPY's effects on adipogenesis, I measured mRNA abundance of adipose cell differentiation (*PPARα, C/EBPα, C/EBPβ, SREBP, FABP4, LPL*) and proliferation (*Ki67, TOP2A, TPX2*) markers. Expression of *NPY* and *NPY* receptor-subtypes was also measured to determine if NPY treatment has a feedback effect on its own expression and receptor expression in chicken adipose cells. Research on chicken adipogenesis is quite limited. Thus, the involved genes and hypothesized sequential transcriptional events mediating chicken adipogenesis in this study were based on reviews of studies on rodents [27] or the 3T3-L1 mouse preadipocyte cell line [28]. The PPARγ is the master transcriptional regulator of adipogenesis and is involved in the growth arrest that is required for differentiation in mammals. In our study, *PPARγ* expression tended to be increased by NPY treatment at 2 days post-differentiation, but decreased by treatment with all doses of NPY on both day 2 and day 4 post-differentiation.

There was also an effect of NPY treatment on *SREBP* and *C/EBPα* expression on both day 2 and day 4 post-differentiation. In mammals, The C/EBP α and β activate expression of PPARγ and are required for preadipocyte differentiation, while SREBP-1 accelerates differentiation in mammals [27] and chickens [29]. Supplementation of differentiation media with 100 nM NPY was associated with less expression of *SREBP* and *C/EBPα* mRNA than in control cells, on day 4. The expression of *C/EBPβ* was not affected by NPY treatment at any of the doses tested or days analyzed.

Because less is known about factors regulating adipogenesis in chickens as compared to mammals, it is unclear if those gene expression effects reflect the role of those transcription factors as early, intermediate or late regulators of adipocyte differentiation. In order to assess their relative changes during differentiation independent of NPY treatment, real time PCR data for control cells at the different time points were re-analyzed and normalized to the same calibrator sample. Both *C/EBPα* and *PPARγ* had highest expression on day 2 and decreased on day 4 and day 6 post-induction of differentiation. The abundance of *C/EBPβ* mRNA increased with time although its expression was not significantly different between any of the time points. The *SREBP* was most highly expressed on day 4 relative to the other time points. These expression patterns suggest that *C/EBPα* and *PPARγ* might be the early transcriptional factors in chicken adipogenesis following by *SREBP* and *C/EBPβ*. Different from 3T3-L1 cell line, during chicken adipogenesis, *PPARγ* mRNA increased at 9 hours post-induction of differentiation, while *C/EBPα* expression gradually increased until 24 h post-differentiation [28, 30]. Expression of *C/EBPβ* slightly increased during chicken adipogenesis [30], consistent with our observations. Based on these findings, I may have missed the time points that would have captured differences in regulation of *PPARγ* expression during chicken adipocyte differentiation.

Fatty acid-binding protein 4 (*FABP4*; adipocyte FABP) plays an important role in lipid accumulation during adipogenesis [31-33]. Fatty acid binding protein 4 is an intracellular carrier of fatty acids that is considered to be important during adipose development because of its role in sequestering fatty acids for TAG synthesis and as a signaling molecule that regulates activity of enzymes such as hormone sensitive lipase in

the adipocyte [31, 34]. It is a marker for adipocyte differentiation as its expression was shown to increase up to 50-fold during adipocyte differentiation in mammals [35] and chickens [33]. I found that NPY supplementation increased *FABP4* expression, with approximately 2-fold greater expression in cells treated with 10 or 100 nM NPY compared with non-treated cells, by day 6 post-differentiation. Knockdown of *PPARγ* expression in chicken primary adipose cells inhibited adipocyte differentiation and was associated with reduced *FABP4* mRNA abundance [36]. However, high expression of *FABP4* was shown to trigger the ubiquitination and subsequent proteasomal degradation of *PPARγ* in mammals [37]. These findings suggest that *PPARγ* might be an early adipogenic regulator for initiating the downstream transcriptional and signaling cascades and might also explain why NPY supplementation was associated with reduced *PPARγ* expression on day 4 and day 6 post-induction of differentiation in our study and support the observation that *PPARγ* expression decreased with progression of differentiation in control cells. The expression of *FABP4* was elevated in the adipose tissue of obese individuals, and *FABP4* expression was greater and *PPARγ* expression reduced in visceral as compared to the subcutaneous fat [37]. Together, our results indicate that NPY promoted lipid accumulation in chicken adipogenesis, and that this process is associated with transcriptional regulation of key transcription factors.

As an additional marker for lipid accumulation in the adipocyte, I also measured expression of lipoprotein lipase (*LPL*), a rate-limiting enzyme for the hydrolysis of TAG-derived fatty acids [33]. It is critical for lipid utilization in muscle and fat deposition in adipose tissue [38]. In vitro studies using 3T3-L1 cells showed that the adipocyte is capable of up-regulating *LPL* and other regulatory factor expression for more efficient

intracellular lipid storage during adipogenesis [39]. Thus, *LPL* is an indicator for adipogenesis in mammalian cells [40, 41]. In penguin chicks, *LPL* mRNA increased age-dependently with greater body adiposity [42]. Greater *LPL* expression in 10 nM and 100 nM NPY-treated cells on day 6 post-differentiation also supports a role for NPY in promoting adipogenesis and is consistent with the greater rates of G3PDH activity and *FABP4* expression, as a mechanism to enhance rates of TAG synthesis in the adipocyte.

NPY supplementation also increased the expression of *NPY* on both days 2 and 6 post-differentiation, suggesting a positive feedback effect on its own expression in adipose cells. To better understand the regulation of the NPY system during adipogenesis, I also measured expression of the best-characterized NPY receptors: *NPY1R, NPY2R*, and *NPY5R*. The expression of *NPY1R* and *NPY5R* were barely detectable (data not shown), implying that *NPY2R* plays the dominant role in adipogenesis and liporemodeling as has been demonstrated in rodents and humans [9, 43]. Expression of *NPY2R*, while not affected by NPY treatment, showed decreased expression from 2 to 6 days post-differentiation in control cells, similar to *NPY*, suggesting that these factors are involved in adipocyte dynamics and are regulated during different stages of the adipose cell life cycle.

Interested in how cell proliferation was affected during differentiation, I also measured the expression of the major proliferation makers that were assessed during the proliferation experiment. The *Ki67, TOP2A*, and *TPX2* mRNA quantities were greater on day 2 post-differentiation and decreased as the differentiation continued. Increased proliferation on day 2 post-differentiation versus 12 hours post-treatment in proliferating cells is probably due to the difference in the media composition, where proliferation

media contains 1.5% FBS and differentiation media contains 2.5 % CS. Intrigued by the potential role of NPY in proliferation during differentiation I also assessed EdU incorporation on day 5 post-differentiation and found a striking increase in DNA synthesis in NPY-treated cells during differentiation. 3T3-L1 cells that are induced to differentiate show a post-confluent round of mitosis followed by growth arrest that is usually complete by day 2, and over the next few days an increase in expression of lipogenic markers with differentiation usually complete by 7 days [28, 44], thus it is possible that the NPY treatment is associated with a clonal expansion that leads to terminal differentiation of the adipocyte, although these mechanisms have not been reported for chickens.

Independent of NPY treatment, there was a decrease in proliferation and gene expression of proliferation markers on day 4 and day 6 post-differentiation, possibly due to the growth arrest and terminal differentiation that occurs during adipogenesis, as well as space limitation as differentiation is induced after confluency. These results suggest that proliferation and differentiation are not mutually exclusive events, but how these two processes interact with each other during chicken adipogenesis remains to be elucidated. An additional explanation for why NPY-mediated proliferation was greater during differentiation than during the specific proliferation experiment, may be that the cells require regulatory factors for proliferation that are secreted by differentiation or are present in the CS. Fetal bovine serum was used for the proliferation experiments, because in our preliminary experiments CS inclusion was associated with spontaneous differentiation into adipocytes that confounded effects on proliferation (data not shown).

Moreover, the physiological relevance of the concentrations of NPY used in these studies is unclear. In vivo, NPY may affect the adipocyte through neuroendocrine, endocrine, paracrine and autocrine routes and typical concentrations of NPY exposed to the chicken adipocyte are unknown. Finally, it is worth noting that the stromal-vascular fractions were able to be passaged for 7 generations and still maintain suitable proliferation and differentiation capacity.

In summary, we found that NPY may play a similar role in promoting adipogenesis in chickens as in mammals although the underlying mechanisms might be slightly different due to species differences in physiology. While there was not an apparent effect on proliferation during the first 12 hours post-treatment, there were clearly effects of NPY treatment on adipocyte differentiation during the first 6 days post-induction of differentiation. Specifically, activity of G3PDH, a marker for adipogenesis was increased in NPY-treated cells at 6 days post-differentiation, and this was also accompanied by greater gene expression of *LPL* and *FABP4*, which both play an important role in providing fatty acids for TAG synthesis in the adipocyte. These results would suggest a greater availability of glycerol-3-phosphate and fatty acids for TAG synthesis, respectively, which was also reflected in the neutral lipid staining, where NPY treatment was associated with greater lipid accumulation in differentiating cells. There were also distinct changes in gene expression of key adipogenic transcription factors, such as *C/EBPα*, *PPARγ*, and *SREBP*. These adipogenic effects are most likely mediated by NPY2R as its expression was greater than the other tested receptors in the adipose cell cultures. The present study provides a model to study the role of neurotransmitters and other factors in chicken adipogenesis, which may be beneficial for the understanding of

brain adipose tissue crosstalk and sheds light on the physiology of adipogenesis, a relatively unstudied phenomenon in avian species.

Acknowledgements

Special thanks to Guoqing Wang and Betty McConn for help in taking care of the chicks. This research was supported by a National Science Foundation EAGER grant (IOS 1420285).

References

1. Tatemoto K, Carlquist M, Mutt V: **Neuropeptide Y--a novel brain peptide with structural similarities to peptide YY and pancreatic polypeptide**. *Nature* 1982, **296**(5858):659-660.
2. Clark JT, Kalra PS, Crowley WR, Kalra SP: **Neuropeptide Y and human pancreatic polypeptide stimulate feeding behavior in rats**. *Endocrinology* 1984, **115**(1):427-429.
3. Levine AS, Morley JE: **Neuropeptide Y: a potent inducer of consummatory behavior in rats**. *Peptides* 1984, **5**(6):1025-1029.
4. Pau MY, Pau KY, Spies HG: **Characterization of central actions of neuropeptide Y on food and water intake in rabbits**. *Physiology & behavior* 1988, **44**(6):797-802.
5. Kuenzel WJ, Douglass LW, Davison BA: **Robust feeding following central administration of neuropeptide Y or peptide YY in chicks, Gallus domesticus**. *Peptides* 1987, **8**(5):823-828.
6. Chao PT, Yang L, Aja S, Moran TH, Bi S: **Knockdown of NPY expression in the dorsomedial hypothalamus promotes development of brown adipocytes and prevents diet-induced obesity**. *Cell metabolism* 2011, **13**(5):573-583.
7. Zhang W, Cline MA, Gilbert ER: **Hypothalamus-Adipose Tissue Crosstalk: Neuropeptide Y and the Regulation of Energy Metabolism**. *Nutrition and Metabolism* 2014, **In press**.
8. Yang K, Guan H, Arany E, Hill DJ, Cao X: **Neuropeptide Y is produced in visceral adipose tissue and promotes proliferation of adipocyte precursor cells via the Y1 receptor**. *The FASEB J* 2008, **22**:2452-2464.
9. Kuo LE, Kitlinska JB, Tilan JU, Li L, Baker SB, Johnson MD, Lee EW, Burnett MS, Fricke ST, Kvetnansky R *et al*: **Neuropeptide Y acts directly in the periphery on fat tissue and mediates stress-induced obesity and metabolic syndrome**. *Nature medicine* 2007, **13**(7):803-811.
10. Bungo T, Ando R, Kawakami S, Ohgushi A, Shimojo M, Masuda Y, Furuse M: **Central bombesin inhibits food intake and the orexigenic effect of neuropeptide Y in the neonatal chick**. *Physiology & behavior* 2000, **70**(5):573-576.

11. Newmyer BA, Nandar W, Webster RI, Gilbert E, Siegel PB, Cline MA: **Neuropeptide Y is associated with changes in appetite-associated hypothalamic nuclei but not food intake in a hypophagic avian model**. *Behavioural brain research* 2013, **236**(1):327-331.
12. Zhang W, Sumners LH, Siegel PB, Cline MA, Gilbert ER: **Quantity of glucose transporter and appetite-associated factor mRNA in various tissues after insulin injection in chickens selected for low or high body weight**. *Physiological genomics* 2013, **45**(22):1084-1094.
13. Dunnington EA, Honaker CF, McGilliard ML, Siegel PB: **Phenotypic responses of chickens to long-term, bidirectional selection for juvenile body weight--historical perspective**. *Poultry science* 2013, **92**(7):1724-1734.
14. Ramsay TG, Rosebrough RW: **Hormonal regulation of postnatal chicken preadipocyte differentiation in vitro**. *Comparative biochemistry and physiology Part B, Biochemistry & molecular biology* 2003, **136**(2):245-253.
15. Wise LS, Green H: **Participation of one isozyme of cytosolic glycerophosphate dehydrogenase in the adipose conversion of 3T3 cells**. *The Journal of biological chemistry* 1979, **254**(2):273-275.
16. Lengi AJ, Corl BA: **Factors influencing the differentiation of bovine preadipocytes in vitro**. *Journal of animal science* 2010, **88**(6):1999-2008.
17. Schmittgen TD, Livak KJ: **Analyzing real-time PCR data by the comparative C(T) method**. *Nature protocols* 2008, **3**(6):1101-1108.
18. Baker DG, Bertram TM, Patel PM, Barkauskas DA, Clopton P, Patel S, Geracioti TD, Jr., Haji U, O'Connor DT, Nievergelt CM *et al*: **Characterization of cerebrospinal fluid (CSF) and plasma NPY levels in normal volunteers over a 24-h timeframe**. *Psychoneuroendocrinology* 2013, **38**(10):2378-2382.
19. Yang K, Guan H, Arany E, Hill DJ, Cao X: **Neuropeptide Y is produced in visceral adipose tissue and promotes proliferation of adipocyte precursor cells via the Y1 receptor**. *FASEB J* 2008, **22**:2452-2464.
20. Zhang Z, Wang H, Sun Y, Li H, Wang N: **Klf7 modulates the differentiation and proliferation of chicken preadipocyte**. *Acta biochimica et biophysica Sinica* 2013, **45**(4):280-288.
21. Shang Z, Guo L, Wang N, Shi H, Wang Y, Li H: **Oleate promotes differentiation of chicken primary preadipocytes in vitro**. *Bioscience reports* 2014.
22. Brizova H, Kalinova M, Krskova L, Mrhalova M, Kodet R: **A novel quantitative PCR of proliferation markers (Ki-67, topoisomerase IIalpha, and TPX2): an immunohistochemical correlation, testing, and optimizing for mantle cell lymphoma**. *Virchows Archiv : an international journal of pathology* 2010, **456**(6):671-679.
23. Milde-Langosch K, Karn T, Muller V, Witzel I, Rody A, Schmidt M, Wirtz RM: **Validity of the proliferation markers Ki67, TOP2A, and RacGAP1 in molecular subgroups of breast cancer**. *Breast cancer research and treatment* 2013, **137**(1):57-67.
24. Struikmans H, Rutgers DH, Hordijk GJ, Slootweg PJ, van der Tweel I, Battermann JJ: **Prognostic significance of cell proliferation markers and DNA-**

ploidy in head and neck tumors. *International journal of radiation oncology, biology, physics* 1998, **40**(1):27-34.
25. Sledzinski T, Korczynska J, Goyke E, Stefaniak T, Proczko-Markuszewska M, Kaska L, Swierczynski J: **Association between cytosolic glycerol 3-phosphate dehydrogenase gene expression in human subcutaneous adipose tissue and BMI**. *Cellular physiology and biochemistry : international journal of experimental cellular physiology, biochemistry, and pharmacology* 2013, **32**(2):300-309.
26. Swierczynski J, Zabrocka L, Goyke E, Raczynska S, Adamonis W, Sledzinski Z: **Enhanced glycerol 3-phosphate dehydrogenase activity in adipose tissue of obese humans**. *Molecular and cellular biochemistry* 2003, **254**(1-2):55-59.
27. Symonds ME: **Adipose tissue biology**; 2011.
28. Ntambi JM, Young-Cheul K: **Adipocyte differentiation and gene expression**. *The Journal of nutrition* 2000, **130**(12):3122S-3126S.
29. Liu S, Wang Y, Wang L, Wang N, Li Y, Li H: **Transdifferentiation of fibroblasts into adipocyte-like cells by chicken adipogenic transcription factors**. *Comparative biochemistry and physiology Part A, Molecular & integrative physiology* 2010, **156**(4):502-508.
30. Matsubara Y, Sato K, Ishii H, Akiba Y: **Changes in mRNA expression of regulatory factors involved in adipocyte differentiation during fatty acid induced adipogenesis in chicken**. *Comparative biochemistry and physiology Part A, Molecular & integrative physiology* 2005, **141**(1):108-115.
31. Smathers RL, Petersen DR: **The human fatty acid-binding protein family: evolutionary divergences and functions**. *Human genomics* 2011, **5**(3):170-191.
32. Samulin J, Berget I, Lien S, Sundvold H: **Differential gene expression of fatty acid binding proteins during porcine adipogenesis**. *Comparative biochemistry and physiology Part B, Biochemistry & molecular biology* 2008, **151**(2):147-152.
33. Regassa A, Kim WK: **Effects of oleic acid and chicken serum on the expression of adipogenic transcription factors and adipogenic differentiation in hen preadipocytes**. *Cell biology international* 2013, **37**(9):961-971.
34. Veerkamp JH, Maatman RG: **Cytoplasmic fatty acid-binding proteins: their structure and genes**. *Progress in lipid research* 1995, **34**(1):17-52.
35. Reese-Wagoner A, Thompson J, Banaszak L: **Structural properties of the adipocyte lipid binding protein**. *Biochimica et biophysica acta* 1999, **1441**(2-3):106-116.
36. Wang Y, Mu Y, Li H, Ding N, Wang Q, Wang Y, Wang S, Wang N: **Peroxisome proliferator-activated receptor-gamma gene: a key regulator of adipocyte differentiation in chickens**. *Poultry science* 2008, **87**(2):226-232.
37. Garin-Shkolnik T, Rudich A, Hotamisligil GS, Rubinstein M: **FABP4 attenuates PPARgamma and adipogenesis and is inversely correlated with PPARgamma in adipose tissues**. *Diabetes* 2014, **63**(3):900-911.
38. Weinstock PH, Levak-Frank S, Hudgins LC, Radner H, Friedman JM, Zechner R, Breslow JL: **Lipoprotein lipase controls fatty acid entry into adipose tissue, but fat mass is preserved by endogenous synthesis in mice deficient in adipose tissue lipoprotein lipase**. *Proceedings of the National Academy of Sciences of the United States of America* 1997, **94**(19):10261-10266.

39. Gonzales AM, Orlando RA: **Role of adipocyte-derived lipoprotein lipase in adipocyte hypertrophy**. *Nutrition & metabolism* 2007, **4**:22.
40. MacDougald OA, Lane MD: **Transcriptional regulation of gene expression during adipocyte differentiation**. *Annual review of biochemistry* 1995, **64**:345-373.
41. Gregoire FM, Johnson PR, Greenwood MR: **Comparison of the adipoconversion of preadipocytes derived from lean and obese Zucker rats in serum-free cultures**. *International journal of obesity and related metabolic disorders : journal of the International Association for the Study of Obesity* 1995, **19**(9):664-670.
42. Raccurt M, Baudimont F, Tirard J, Rey B, Moureaux E, Geloen A, Duchamp C: **Growing in Antarctica, a challenge for white adipose tissue development in Adelie penguin chicks (Pygoscelis adeliae)**. *American journal of physiology Regulatory, integrative and comparative physiology* 2008, **295**(5):R1671-1679.
43. Baker SB, Cohen M, Kuo L, Johnson M, Al-Attar A, Zukowska Z: **The role of the neuropeptide Y2 receptor in liporemodeling: neuropeptide Y-mediated adipogenesis and adipose graft maintenance**. *Plastic and reconstructive surgery* 2009, **123**(2):486-492.
44. Bernlohr DA, Bolanowski MA, Kelly TJ, Jr., Lane MD: **Evidence for an increase in transcription of specific mRNAs during differentiation of 3T3-L1 preadipocytes**. *The Journal of biological chemistry* 1985, **260**(9):5563-5567.

Table 4.1 Primers used for real time PCR

Gene[1]	Accession No.	Sequences 5' to 3' (forward/reverse)
KLF1	XM_422416.4	GGCTGATTCTGGCCAAGCT/
		GAGCGGAACCCAGAGTTGTG
KLF7	XM_004942643.1	GATGCTGGTTTTCCTCACAGTTT/
		CCTCCTGTCCCAAAAGTGTTCA
GATA2	NM_001003797.1	CCACGAAGCAAGGCCAGAT/
		GGTAGCGGTTGCTCCACAGT
Ki67	XM_004942360.1	AAAAACCTGATTCCTGAACAATCTG/
		GACCTAGAGCTATCAGGCTGTGAAG
TOP2A	NM_204791.1	GCACAGCTGGCGGAAGTAAT/
		TGCAGTGACCCGAGGAACA
TPX2	NM_204437.1	TGGAGGGTGGGCCAATC/
		TTGGCTGTGTGAGTTCCTTCAC
PPARγ	NM_001001460.1	CACTGCAGGAACAGAACAAAGAA/
		TCCACAGAGCGAAACTGACATC
C/EBPα	NM_001031459.1	CGCGGCAAATCCAAAAAG/
		GGCGCACGCGGTACTC
C/EBPβ	NM_205253.2	GCCGCCCGCCTTTAAA/
		CCAAACAGTCCGCCTCGTAA
SREBP	NM_204126.1	CATCCATCAACGACAAGATCGT/
		CTCAGGATCGCCGACTTGTT
FABP4	NM_204290.1	CAGAAGTGGGATGGCAAAGAG/

		CCAGCAGGTTCCCATCCA
LPL	NM_205282.1	GACAGCTTGGCACAGTGCAA/
		CACCCATGGATCACCACAAA
NPY	NM_205473.1	CATGCAGGGCACCATGAG/
		CAGCGACAAGGCGAAAGTC
NPY2R	NM_001031128.1	TGCCTACACCCGCATATGG/
		GTTCCCTGCCCCAGGACTA

[1]*KLF1*: krüppel-like factor 1; *KLF7*: krüppel-like factor 7; *GATA2*: GATA binding protein 2; *TOP2A*: topoisomerase II alpha; *TPX2*: Thioredoxin-dependent peroxidase 2; *PPARγ* : peroxisome proliferator-activated receptor gamma; *C/EBPα*: CCAAT/enhancer binding protein alpha; *C/EBPβ* : CCAAT/enhancer binding protein beta; *SREBP*: Sterol regulatory element-binding protein; *FABP4*: Fatty acid binding protein 4; *LPL*: lipoprotein lipase; *NPY*: neuropeptide Y; *NPY2R*: neuropeptide Y receptor 2.

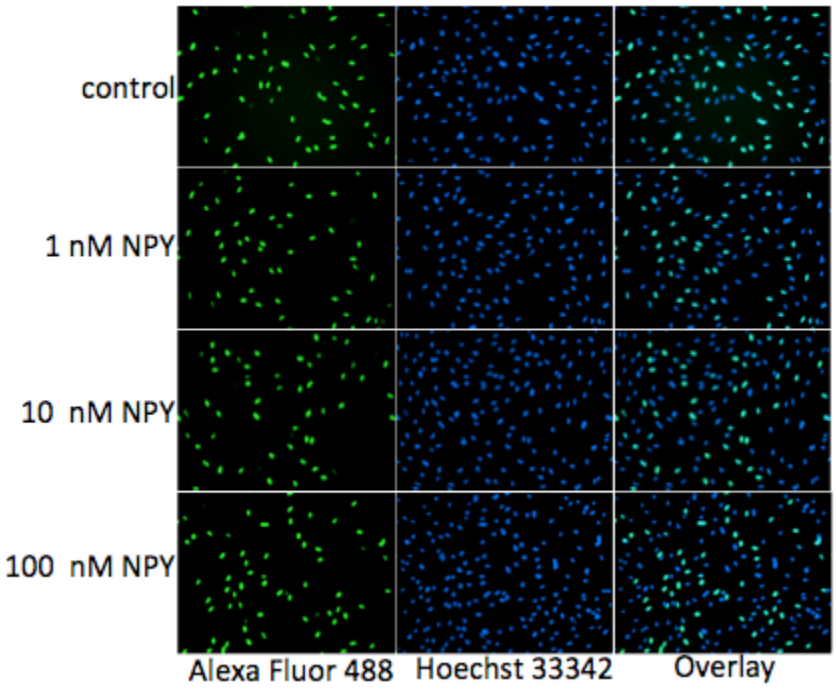

Figure 4.1 Effects of neuropeptide Y (NPY) treatment on chicken adipose cell proliferation. The stromal-vascular fraction of cells was isolated from abdominal fat of 14 day-old broilers and incubated in serum-depleted media overnight. Cells were then treated with 0, 1, 10 or 100 nM NPY in media containing 5-ethynyl-2′-deoxyuridine (EdU) and cells were then stained at 12 hours post-treatment. The Alexa Fluor 488 represents staining for the EdU (DNA synthesis indicative of proliferating cells) and Hoechst 33342 represents nuclear staining as an estimator of total cell number. Numbers of EdU-positive cells were analyzed by ANOVA with no significant differences detected among treatment groups. Images are representative of n=3 experiments.

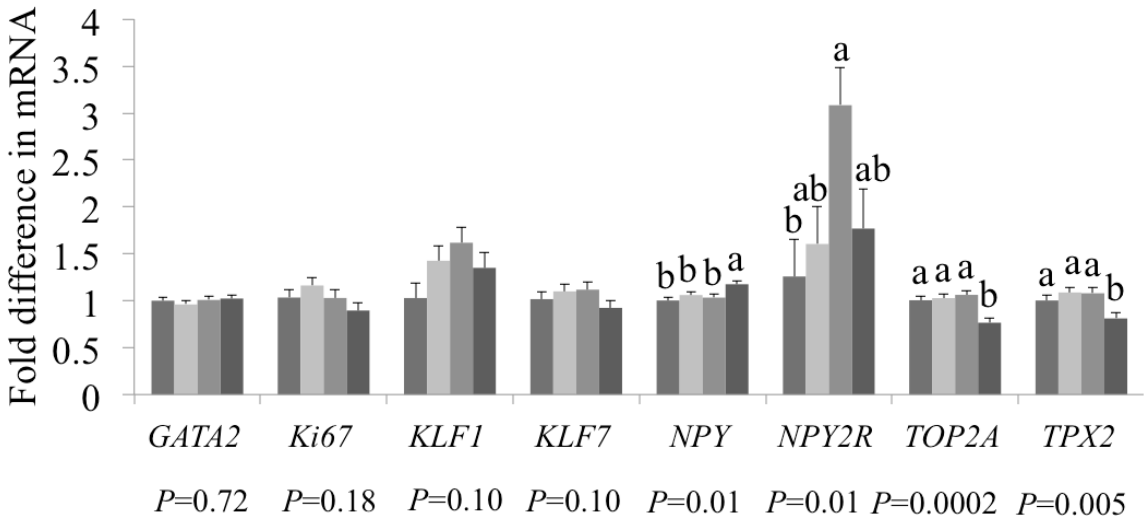

Figure 4.2 Effects of neuropeptide Y (NPY) treatment on gene expression of proliferation markers in chicken adipose cells. The stromal-vascular fraction of cells was isolated from abdominal fat of 14 day-old broilers and incubated in serum-depleted media overnight. Cells were then treated with 0, 1, 10 or 100 nM NPY in complete media and cells were harvested at 4 hours post-treatment for total RNA isolation. *GATA2*: GATA-binding protein 2; *Ki67*: *Ki67*; *KLF1*: Krüppel-like factor 1; *KLF7*: Krüppel-like factor 7; *NPY*: neuropeptide Y; *NPY2R*: *NPY* receptor sub-type 2; *TOP2A*: topoisomerase II alpha; *TPX2*: thioredoxin-dependent peroxidase 2. Values represent least squares means ± SEM (n=3). Different letters within a gene indicate a significant difference ($P < 0.05$; Tukey's test). The *P*-value under each gene indicates significance for the main effect of treatment.

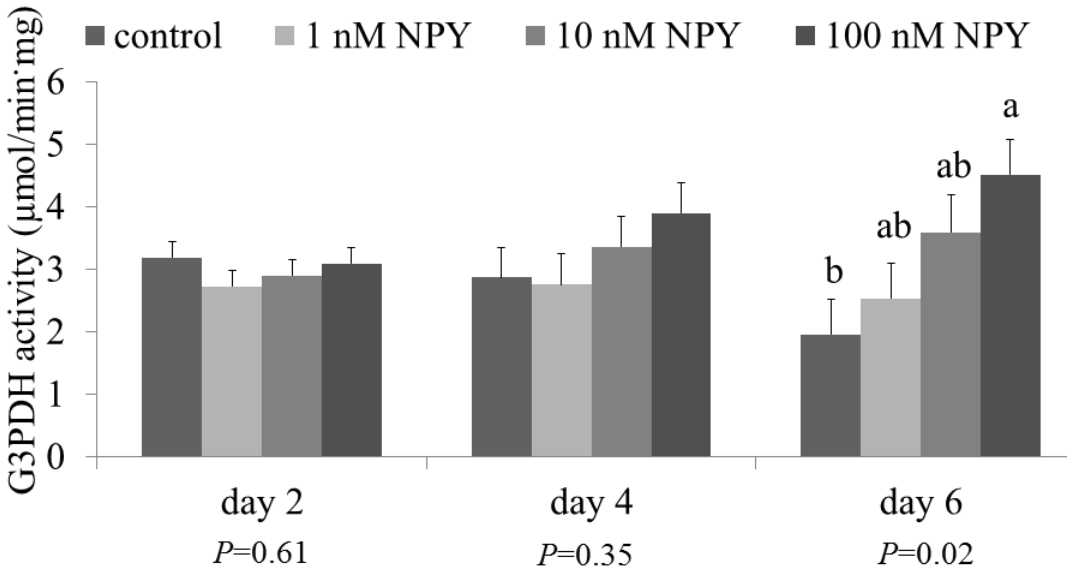

Figure 4.3 Specific activity of glycerol-3-phosphate dehydrogenase (G3PDH) at days 2, 4 and 6 post-differentiation in chicken abdominal adipose cells treated with different concentrations of neuropeptide Y (NPY). Values represent least squares means ± SEM (n=3). Different letters indicate a significant difference ($P < 0.05$). The *P*-value under each time point indicates significance for the main effect of treatment.

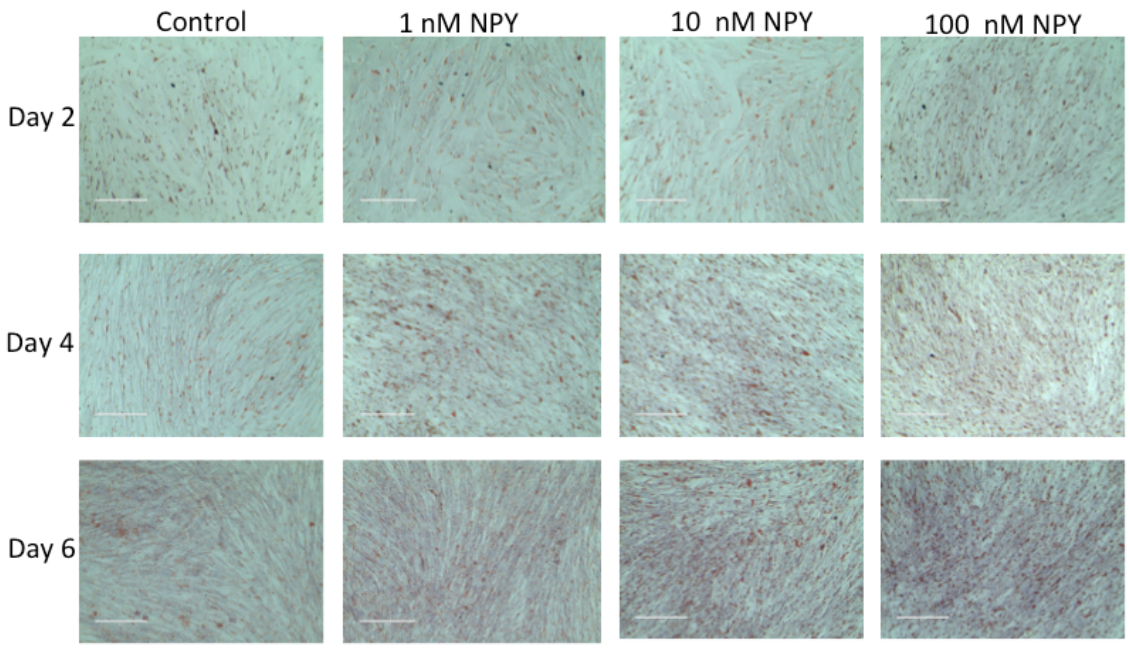

Figure 4.4 Oil Red O staining of chicken adipose cells treated with neuropeptide Y (NPY) during adipocyte differentiation. The stromal-vascular fraction of cells were isolated from abdominal fat of 14 day-old broilers and upon confluence were induced to differentiate in the presence of 0, 1, 10 or 100 nM chicken NPY. At 2, 4 and 6 days post-induction of differentiation cells were stained with Oil Red O and counter-stained with Modified Mayer's Hematoxylin and images captured. The red color indicates the staining of neutral lipids. The scale bar on each image represents a distance of 200 μm.

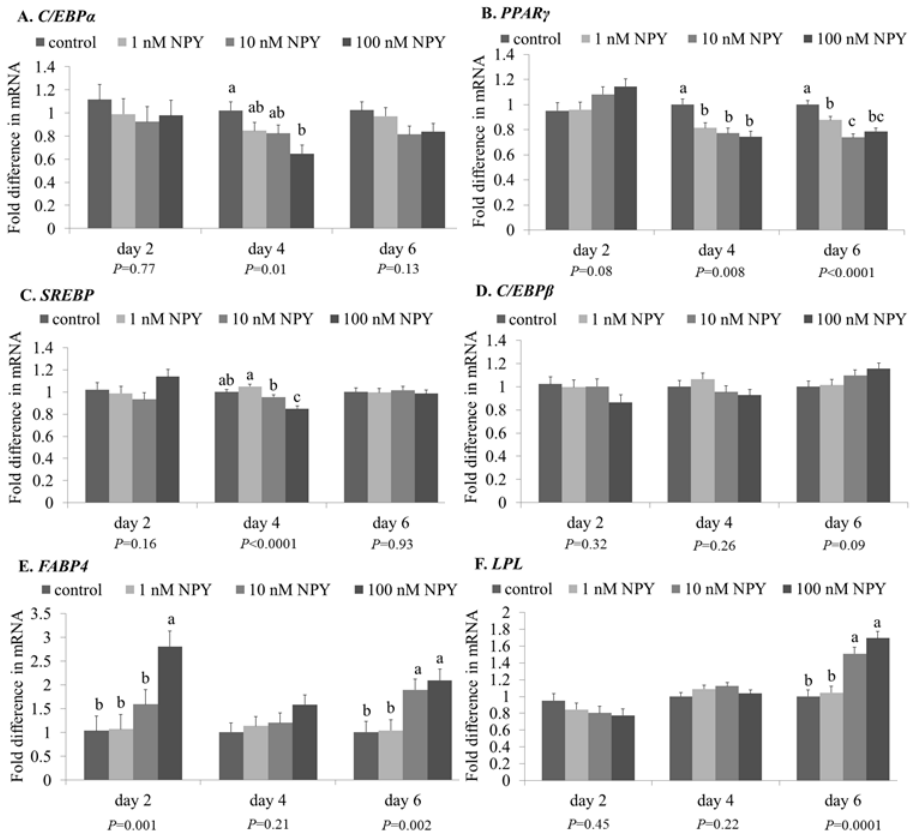

Figure 4.5 The mRNA abundance of A) CCAAT/Enhancer Binding Protein *α* (*C/EBPα)*, B) peroxisome proliferator activated receptor *γ* (*PPARγ)*, C) Sterol Regulatory Element-Binding Protein (*SREBP)*, D) *C/EBPβ*, E) fatty acid binding protein 4 (*FABP4)* and F) lipoprotein lipase (*LPL)* at days 2, 4 and 6 post-induction of differentiation in chicken adipose cells treated with 0, 1, 10 or 100 nM chicken NPY. Values represent least squares means ± SEM (n=3). The *P*-value under each time point represents the significance for main effect of treatment within a gene. Bars with different letters within a time point represent a significant difference, $P < 0.05$ (Tukey's test).

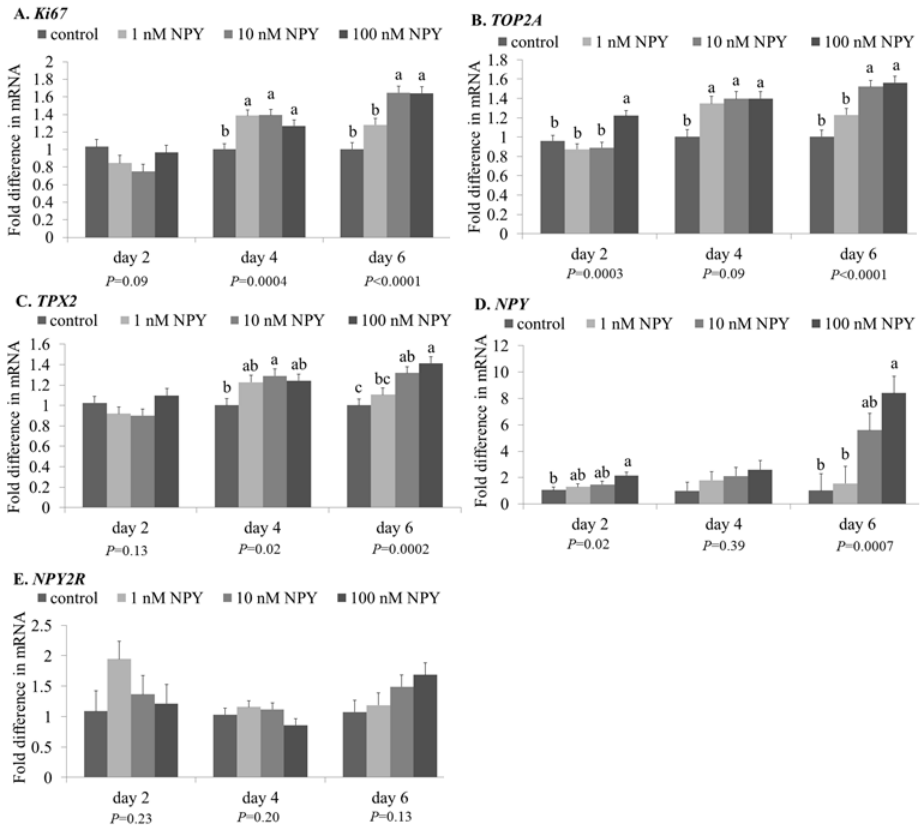

Figure 4.6 The mRNA abundance of A) *Ki67*, B) *TOP2A*, C) *TPX2*, D) neuropeptide Y (*NPY)*, and E) NPY receptor sub-type 2 (*NPY2R)* at days 2, 4 and 6 post-induction of differentiation in chicken adipose cells treated with 0, 1, 10 or 100 nM chicken NPY. Values represent least squares means ± SEM (n=3). The *P*-value under each time point represents the significance for main effect of treatment within a gene. Bars with different letters within a time point represent a significant difference, $P < 0.05$ (Tukey's test).

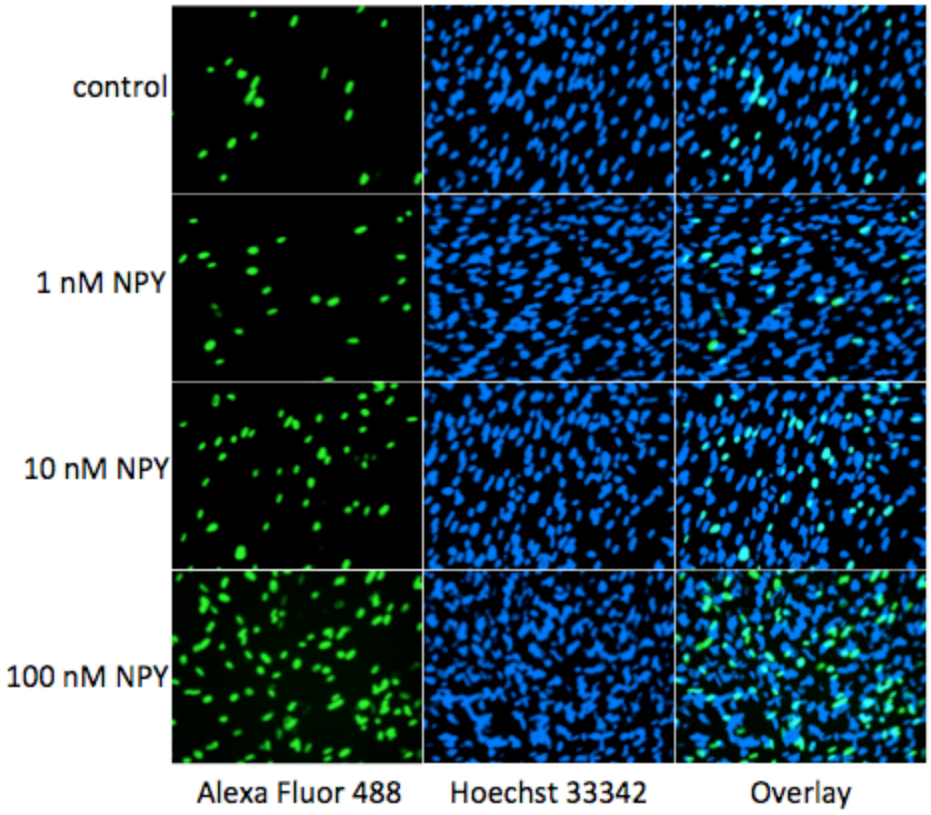

Figure 4.7 Effects of neuropeptide Y (NPY) treatment on cellular proliferation in chicken adipose cells at day 5 post-differentiation. The stromal-vascular fraction of cells were isolated from abdominal fat of 14 day-old broilers and upon confluence were induced to differentiate in the presence of 0, 1, 10 or 100 nM chicken NPY. At day 5 post-differentiation, cells were incubated in media containing 5-ethynyl-2′-deoxyuridine (EdU) and stained at 12 hours post-treatment. The Alexa Fluor 488 represents staining for the EdU (DNA synthesis indicative of proliferating cells) and Hoechst 33342 represents nuclear staining as an estimator of total cell number. Images are representative of n=3 experiments.

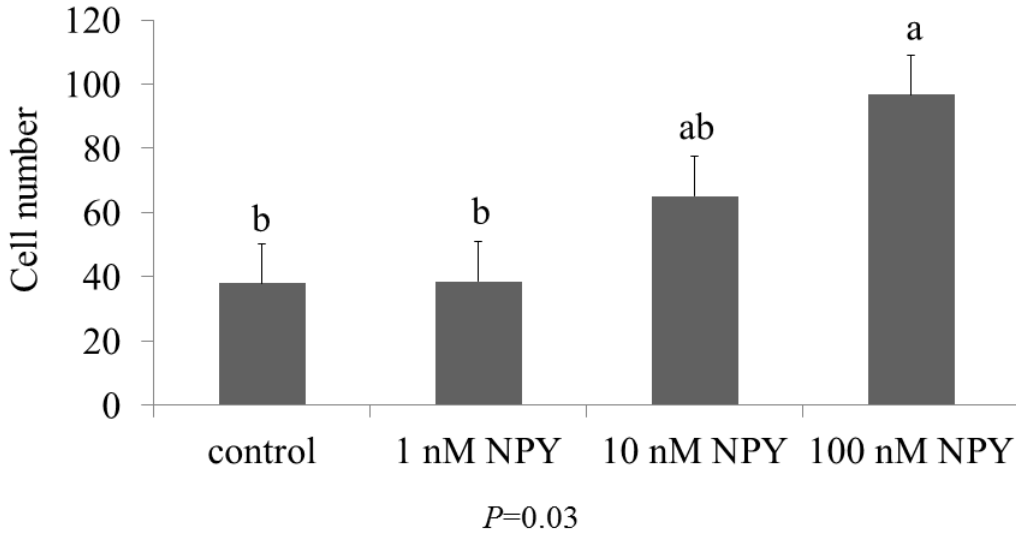

Figure 4.8 Effects of neuropeptide Y (NPY) treatment on proliferating cell number at day 5 post-differentiation of chicken adipose cells. The stromal-vascular fraction of cells was isolated from abdominal fat of 14 day-old broilers and upon confluence were induced to differentiate in the presence of 0, 1, 10 or 100 nM chicken NPY. At day 5 post-differentiation, cells were incubated in media containing 5-ethynyl-2′-deoxyuridine (EdU) and stained at 12 hours post-treatment. Cells were counted and the numbers of EdU-positive cells were analyzed by ANOVA which revealed a main effect of treatment ($P = 0.03$). Values represent least squares means ± SEM (n=3). Bars with different letters represent a significant difference at $P < 0.05$ (Tukey's test).

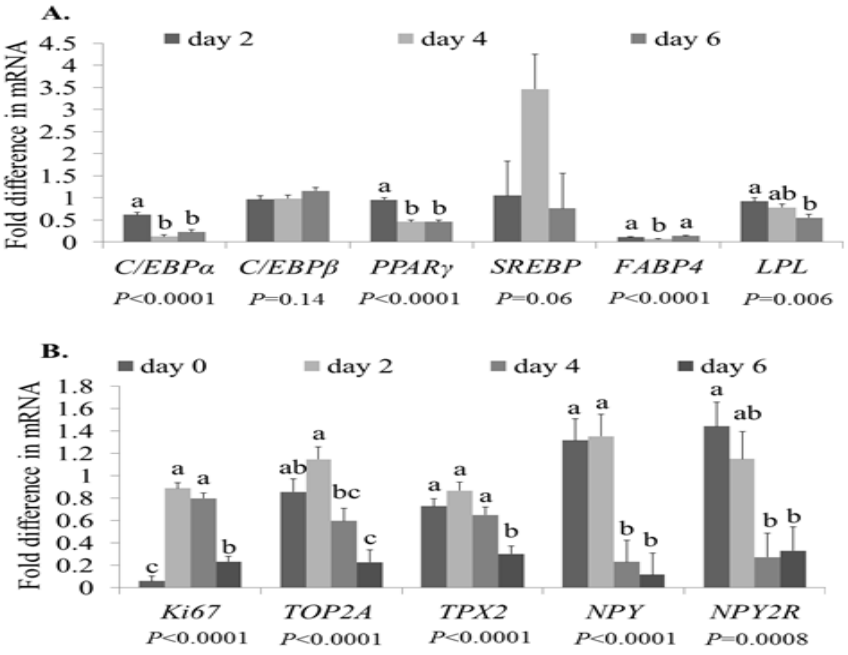

Figure 4.9 Gene expression of A) adipogenesis-associated factors and B) proliferation markers in adipose cells induced to differentiate. The stromal vascular fraction of cells from abdominal fat of 14 day-old broilers was plated and induced to differentiate, and CCAAT/Enhancer Binding Protein *α* (*C/EBPα)*, *C/EBPβ*, peroxisome proliferator activated receptor *γ* (*PPARγ)*, Sterol Regulatory Element-Binding Protein (*SREBP)*, fatty acid binding protein 4 (*FABP4)* and lipoprotein lipase (*LPL)* mRNA measured at 2, 4 and 6 days post-induction of differentiation, and abundance of *Ki67*, topoisomerase II alpha (*TOP2A*), Thioredoxin-dependent peroxidase 2 (*TPX2*), neuropeptide Y (*NPY*), and *NPY* receptor sub-type 2 (*NPY2R*) mRNA measured in proliferating cells (day 0) and at 2, 4 and 6 days post-induction of differentiation. Values represent least squares means ± SEM (n=3). The *P*-values under each gene represent the significance for the main effect of time. Bars with different letters represent a significant difference at $P < 0.05$ (Tukey's test).

Chapter 5

RNA sequencing of the hypothalamus after insulin injection in chickens selected for high and low body weight reveals differences in expression of genes associated with monoamine synthesis and signaling

Abstract: Long-term selection for juvenile body weight resulted in two extremely divergent chicken lines (low-weight: LWS; high-weight: HWS) that display distinct food intake and blood glucose responses to neuropeptides and insulin. The objective of this study was to elucidate putative targets affecting food intake and energy homeostasis by sequencing hypothalamic RNA from LWS and HWS chickens after insulin injection. Ninety day-old female LWS and HWS chickens were injected with either vehicle or insulin, and hypothalamus collected at 1 hour post-injection. Total RNA was extracted and sequenced via the Illumina HiSeq platform. A total of 361 differentially expressed genes (DEGs) were identified. There was greater expression of genes involved in serotonin and dopamine biosynthesis and signaling in HWS than LWS vehicle-injected chickens. In contrast, these genes were more highly expressed in HWS than LWS after insulin injection. We identified 90 SNPs existing only in the HWS and 121 SNPs specific to LWS, and 5,119 SNPs close to fixation (with absolute frequency difference ≥ 0.9). Four were located in genes encoding enzymes associated with serotonergic and dopaminergic pathways, such as L-aromatic amino acid decarboxylase (DDC), tyrosine hydroxylase (TH), and solute carrier family 18 member 2 (vesicular monoamine transporter; SLC18A2). These data implicate differences in biogenic amines such as serotonin and dopamine in hypothalamic physiology between the two chicken lines, and these differences might be associated with polymorphisms during long-term selection. Changes in serotonergic and dopaminergic signaling pathways in response to insulin injection suggest a role in whole body energy homeostasis.

Introduction

Regulation of energy intake and adipose tissue deposition has been the focus of significant attention because of the recent obesity epidemic that is sweeping across the United States and many other countries. Obesity is associated with excess caloric intake, insulin resistance and is a predisposing factor for developing other metabolic disorders such as type 2 diabetes. Thus, animal models of divergent appetite, body composition and glucose regulation may provide valuable insight into the molecular mechanisms underlying the complex relationship between appetite regulation in the brain and peripheral energy storage and metabolism. Two body weight-selected lines of chickens (high weight: HWS; and low weight: LWS) have been developed from a single founder population by divergent selection for body weight at 8 weeks of age. After 55 generations of selection, the two lines display a 10-fold difference in body weight and correlated physiological and behavioral phenotypes, with complete pedigrees that go back to the original founder population [1]. Among the correlated responses, the feeding behavior and food consumption are of the most notable responses that have been selected along this process. The HWS chickens are hyperphagic and obese, whereas the LWS chickens have very low appetite. In addition, some LWS chickens showed severe anorexia, resulting in starving to death during the first two weeks of age or surviving with delayed sexual maturity [2, 3]. These two lines thus provide a valuable model for the study of appetite regulation and energy storage. Recent studies revealed that the lines are equipped with different strategies for regulating energy homeostasis in the central nervous system, particularly the hypothalamus [4, 5]. However, more studies are needed to elucidate the underlying molecular mechanisms.

The hypothalamus plays a central role in regulating energy intake and homeostasis. The importance of the hypothalamus in explaining differences in body weight of the selected lines was first shown through electrolytic lesioning of the ventromedial hypothalamus (VMH), where lesions in the LWS VMH led to obesity, but had no effect on HWS chickens [6]. These results suggested that differences in body weight and appetite in the lines were of hypothalamic origin. In the past decade, our group has focused much effort on understanding differences in food intake between the lines. Notably, various neurotransmitters have been screened for central effects on food intake via intracerebroventricular (ICV) injection. Our results have revealed that the LWS show a lower threshold food intake response to the anorexigenic neuropeptides α-melanocyte stimulating hormone (α-MSH) [7], corticotropin releasing factor (CRF) [8], amylin [9], and neuropeptide AF (NPAF) [10], whereas the HWS are more sensitive to neuropeptide S[11], and calcitonin and calcitonin gene-related peptide (CGRP) [12]. Leptin injection caused a linear decrease in food intake in chickens from the LWS line but no effect in those from the HWS line [13]. Also, it was shown that the LWS line has a lower threshold of central insulin-induced decreased food and water intake and blood glucose concentrations than the HWS line [14]. We recently demonstrated that the two lines also have different threshold sensitivity in the blood glucose response to peripherally-administered insulin, as well as differences in glucose clearance rate during a glucose tolerance test [15]. Disparities in both central and peripheral insulin sensitivity and distinct responses to various neurotransmitters between the two lines may be driving factors for differences in appetite and body weight. Microarray analyses in the hypothalamus of early post-hatch LWS and HWS revealed differences in expression of genes involved in neuronal plasticity, development and apoptosis [4, 5].

Next-generation sequencing technologies have become a popular tool for molecular biology research, through which the presence and level of both known and unknown genes in the whole transcriptome can be obtained [16]. By profiling the transcriptome of the hypothalamus of insulin-injected LWS and HWS, we hope to gain insight into the central mechanisms mediating energy regulation in response to insulin injection. Because of the role of insulin resistance in the pathogenesis of obesity and diabetes, understanding the mechanisms underlying effects of insulin-induced hypoglycemia on hypothalamic gene expression in lines of chickens, may shed light on important pathways involved in hypothalamic signaling in obesity. The aim of this study was to characterize genome-scale pathways and networks involved in hypothalamic appetite regulation of two body-weight lines of chickens in response to exogenous insulin injection using next-generation sequencing technologies.

Materials and methods

Animals

The two body weight chicken lines were bidirectionally selected for body weight at 8-weeks of age from a common population of White Plymouth Rocks with progeny from the S_{54} generation used in the present study. Chickens were reared in batteries with free access to water and a starter diet (20 % crude protein (CP), 2,685 kcal ME/kg) in mash form until 56 days of age. A coccidiostat (Deccox) was supplemented in the starter diet and all diets were free of antibiotics. The chickens were fed the grower diet (16% CP, 2,761 kcal ME/kg) starting at 56 days until the termination of the experiment. These diets have remained constant for the duration of selection (54 years).

Insulin injection and hypothalamus collection

Individuals were selected such that sire families were evenly distributed across treatments within lines. The animal experiment was conducted as previously described [17]. Briefly, female 90-day old HWS and LWS line chickens (n=10/group) were fasted overnight with free access to water. Following the food withdrawal, five chickens from each line were randomly assigned to receive either injection of human insulin (Sigma-Aldrich, MO, USA) diluted in PBS or equal volume of vehicle (PBS) intraperitoneally at 80 µg/kg body weight using insulin syringes (3/10cc 31G × 8 mm, BD Biosciences) [15]. The dose was based on an earlier study showing that a 80 µg/kg body weight injection leads to hypoglycemia in both lines, with differences in the response curve with a striking line difference within the first one hour post-injection [15].

Chickens were euthanized and decapitated at 1 hour (h) post-injection. To harvest the hypothalamus, the brain was excised from the skull, snap-frozen for 12 seconds (sec), and then the hypothalamus was dissected visually based on the following anatomical landmarks: anterior cut made at the corticoseptomesencephalic tract, posterior cut at the third cranial nerves, laterally cut 1.5 mm parallel to the midline on both sides of the brain and finally the dorsal cut from the anterior commissure to 1.0 mm ventral to the posterior commissure [18]. The dissected hypothalamus was then snap-frozen and stored at -80°C. All protocols were approved by the Institutional Animal Care and Use Committee at Virginia Tech.

Total RNA extraction and sequencing

Total RNA was extracted using the combination of chemical and column based methods. Briefly, the hypothalamus was pulverized in liquid nitrogen to a fine powder. Approximately 200 mg of tissue was submerged in 1 mL Isol-RNA Lysis Reagent (5 PRIME), and homogenized with a TissueLyser II (Qiagen) for 2 min at 20 Hz using 5 mm stainless steel beads (Qiagen). Homogenized debris was removed by centrifugation at 12,000 x *g* for 10 min at 4°C, and the

supernatant was mixed with 0.2 mL chloroform. The aqueous phase were separated by centrifugation, collected and mixed with an equal volume of 70% ethanol, followed by transfer onto an SV Total RNA Isolation Column (Promega) to purify total RNA according to the manufacturer's instructions. An on-column RNase-Free DNase I treatment was performed to remove any residual genomic DNA. The concentration of total RNA was measured with a NanoDrop (NanoDrop, DE) and purity assessed by examining the ratio of 260/280 and 260/230. The integrity of the total RNA was evaluated with an Agilent 2100 Bioanalyzer and RNA 600 Nano Kit (Agilent). RNA-Seq libraries were prepared by the poly A-selection method using the Illumina TruSeq™ DNA Library Preparation kit according to the manufacturer's instructions, followed by sequencing on a HiSeq 1000 using 101-cycle single reads at Virginia Bioinformatics Institute (VBI).

Mapping and gene expression analysis

To generate predicted transcripts, RNA-Seq reads were trimmed for adaptor and quality, and then assembled and trimmed reads mapped to the chicken genome, the Gallus_gallus-4.0 (released 2011), using Cufflinks and Tophat, respectively [19, 20]. The assembled reads were counted via HTSeq (**Table B.1**), and fold-change and significance values were determined using DESeq for between lines and treatments. For each experimental condition, loci were called significantly differentially expressed if the adjusted *P*-value was less than 0.05.

Transcriptome Analysis

Single nucleotide polymorphism (SNP) analysis was performed by aligning reads to Gallus_gallus-4.0 (released 2011) using rnaseqmut, which detects variants (or mutations including SNPs and indels) from the transcriptome (by Wei Li from github.com). In this study, the HWS and LWS lines were used as the two groups and we performed the search with each

genotype in each position and combined the unique results to achieve a symmetrical analysis. The identified SNPs were cross analyzed with GO and DEGs.

To predict splice variants in the DEGs, DEGs were analyzed against the Ensembl chicken transcript database through Ensembl BioMart. Genes with multiple transcript IDs were further analyzed virtually at the genomic level. The GO annotations for the DEGs were downloaded from Ensembl (BioMart, Ver. 0.7). The density of each DEG in each chicken was distributed among its annotated GO categories (total DEG density/No. GO categories for the transcript). The GO categories were sorted by the total transcriptome density across lines and treatments, followed by analysis of significance using the R-based GOseq and GOstats packages [21, 22].

To understand the biological systems involved, the identified differentially expressed molecules were mapped and molecular networks generated using Ingenuity Pathways Analysis (IPA) software (Ingenuity® Systems), which constructed predicted protein interactions based on a regularly updated "Ingenuity Pathways Knowledge Database" [23, 24]. Pre-filtered DEG ($P < 0.05$) data were uploaded and the significant pathways were identified using Fisher's exact test with the cutoff P-value of 0.001. The P-value indicates the likelihood of the uploaded gene list in a given pathway or network being found together due to random chance.

Quantitative real-time PCR (qRT-PCR) validation

To validate the results of RNA-Seq, random DEGs were chosen between each group comparison, and primers were designed with Primer Express 3.0 (Applied Biosystems; **Table B.2**). Amplification efficiencies were validated for all primer sets before use, with efficiencies ranging from below or above 5% of the amplification efficiency of beta actin. Linear regressions were calculated using the R program to determine the correlation of results from between the RNA-Seq and qRT-PCR.

Results

Sequencing mapping

The average read number after quality control was 12810201, ranging from 8079508 to 15306333. The average number of reads that mapped to the chicken genome was 12291516, which represents about 96% of the totals. Sequencing depth in this study was around 432 (**Table B.1**).

SNP analysis

With RNA sequencing, we were able to identify polymorphisms associated with long-term selection in the low and high body weight-selected lines of chickens. We identified a total of 39,565 SNPs in the two lines combined. On average, the HWS line had a lower frequency of the reference allele (0.47) as compared to the LWS line (0.55), indicating that the genome of the LWS line is relatively more close to the reference genome than that of the HWS line. A large number of mutations within pyrimidines (CT) and purines (AG) were found, for example, the frequency for A->G=0.17; G->A=0.23; C->T=0.23; and T->C=0.16, and the remainder of the mutations were all below 0.03 (**Figure 5.1**).

The histogram of allele frequency differences between HWS and LWS lines shows a peak at approximately 0.9 (**Figure 5.2)**. Filtering for those SNPs with a differential allele frequency ≥ 0.9 identified 5,119 SNPs close to fixation for alternatives alleles between the lines, potentially as a result of long-term selection. A greater number of SNPs were identified in the first 6 macrochromosomes, which is proportional to the chromosome length, and also in chromosomes 13, 14, 15, 19 and the Z chromosome (**Figure 5.3**). The HWS line had more SNPs on chromosomes 4, 13, and 19 whereas the LWS line had more SNPs on chromosome 6 and 14. These regions were thus more likely to have undergone intensive selection during the selection

for body weight. Further analysis revealed that 3,287 SNPs were within protein coding regions and represented 1,130 distinct genes.

Identification of DEGs and data validation

In this study, a total of 361 DEGs were identified using an adjusted *P*-value of <0.05. Among them, 152 DEGs were identified in the high weight line vehicle versus low weight line vehicle treated comparison (HWSLWSv), 196 DEGs in high weight line insulin treated versus low weight line insulin treated (HWSLWSi), 26 DEGs in the low weight insulin versus low weight vehicle treated (LWSiv), and 132 DEGs in the high weight line insulin treated versus vehicle treated (HWSiv). There were 64 DEGs that overlapped between the HWSLWSv and HWSLWSi comparisons, and 9 that overlapped between LWSvi and HWSvi (**Figure 5.4**). In other words, 64 DEGs were reflective of potential genetic differences between the two selected lines and 9 DEGs were associated with insulin injection independent of genetic line. The DEGs revealed by RNA sequencing were further validated by real time PCR, showing a strong correlation (R^2=0.88 (*P*<0.0001)) (**Figure 5.5**).

Gene ontology (GO) and pathway analysis

The results of the GO analysis show the molecular function, cellular component, and biological process of DEGs in each group (**Table 5.1)**. Many of the DEGs in the HWSLWSv group encode factors that are involved in cellular growth and proliferation, cellular development, and cell-to-cell signaling and interaction. However, for all other comparison groups that involve insulin injection, small molecular biosynthesis and transport genes were highly differentially expressed and predicted to be activated by insulin-induced hypoglycemia. Most of these processes are associated with changes in membrane receptors, various receptor-mediated signaling pathways and transcription factors (**Table 5.1**).

All of the DEGs were subjected to pathway analysis and the top up- and down-regulated genes in each group are listed in **Table 5.2**. The top associated diseases and disorders, molecular and cellular functions, and physiological system development and functions associated with these DEGs and their predicted interactions are shown in **Figures B.1-4** and **Table B.3**.

Through IPA analysis, we identified a list of top canonical pathways for each group (-log (*p*-value) ≥1.5) (**Figure B.1**). The results of IPA analysis revealed that pathways associated with monoamine synthesis and signaling, such as catecholamine biosynthesis (dopamine biosynthesis and receptor signaling), serotonin receptor signaling, and tryptophan degradation were predicted to be different between the LWS and HWS lines in the hypothalamus (**Figure B.1** and **Figure B.2**). Additionally, a pathway related to nucleotide degradation was predicted to differ between the two lines, based on up-regulation of 5'-Nucleotidase, cytosolic 1A (NT5C1A), and down regulation of aldehyde oxidase 1 (AOX1) in the HWS as compared to LWS chickens. Eicosanoid signaling and prostanoid biosynthesis pathways were also predicted to be activated in the HWS compared to LWS chickens.

Pathway analyses indicated that DEGs that were enriched in processes of catecholamine biosynthesis and serotonin receptor-mediated signaling pathways were also affected by insulin injection (**Figure B.3** and **Figure B.4**). The signaling pathways are summarized in **Figure 5.6**, illustrating that serotonin and dopamine biosynthesis were predicted to be greater in the HWS line as compared to the LWS line in vehicle-injected chickens (**Figure 5.6A**), whereas, the opposite was predicted after insulin injection (**Figure 5.6B**). The major molecules involved in these processes include tyrosine hydroxylase (TH), aromatic L-amino acid decarboxylase (DDC), solute carrier family 18, member 2 (SLC18A2), and solute carrier family 6, member 4 (SLC6A4). As compared to the vehicle-treated chickens, the HWS line showed greater

expression of DDC, SLC18A2, and TH after insulin injection. In addition, DEGs were enriched in the process of glutamate receptor signaling in the HWS hypothalamus after insulin injection as compared to the vehicle injected chickens, including genes encoding glutamate receptor (GR1A1), glutamate receptor, Ionotropic, N-methyl D-Aspartate 2B (GRIN2B), glutamate receptor, metabotropic (GRM2), and glutamate receptor, metabotropic 5 (GRM5).

Identification of DEGs that contained SNPs

Through genome mapping, 14 DEGs were identified that contained SNPs (**Table 5.3**). Among these genes, DDC, TH, and SLC18A2 were associated with serotonin and dopamine biogenesis and receptor signaling pathways that were predicted to be different between the two lines based on pathway analysis of DEGs.

Discussion

Long-term selection for body weight in chickens from a common founder population has generated two distinct lines with marked differences in food intake, body composition and both central and peripheral insulin sensitivity. To help elucidate the molecular mechanisms underlying the hypothalamic response to insulin-induced hypoglycemia in the body weight chicken lines, we profiled the hypothalamic transcriptome of the two lines under vehicle- and insulin-treated conditions using next-generation sequencing technologies. This study has greatly expanded our understanding of differences in the genetics of the two lines and also their distinct hypothalamic responses to insulin injection. A goal was to reveal DEGs and associated important canonical pathways and networks involved in appetite and energy regulation in the bidirectional selection for juvenile body weight in chickens, as well as their response to exogenous insulin intraperitoneal injection in order to help explain their differences in the central response to exogenous insulin.

The SNP analysis provides us valuable information about the intrinsic differences in genetic makeup between the two lines that may help explain their distinct body weight. Here, a total of 39,565 SNPs were identified with 5,119 SNPs having an absolute frequency difference ≥0.9. In general, the first 6 macrochromosomes have more SNPs. Distinct differences of unique SNPs in only one line indicates that chromosome 4, 13, and 19 may have some candidate genes for body weight and growth rate. According to the chicken QTL database (http://www.animalgenome.org/cgi-bin/QTLdb/GG/index), chromosomes 4, 13 and 19 have a great number of QTLs associated with body weight. Previous studies indicated recent divergence on chromosome 4 between the two lines over the course of selection [25]. In female chickens of a broiler-layer cross, chromosome 4 plays a critical role in controlling growth and body weight and explains a great proportion of the related phenotypic variation [26]. Also, QTLs on chromosome 4 were detected for growth rate across different growth phases and peaks right before sexual maturity [26], indicating that QTLs associated with body weight and growth rate are age specific. This implies that similar patterns may exist for SNP effects. The present study, therefore, represents differences of juvenile SNP effects between the two lines, and their overall effects may thus be different from other ages.

The two body-weight chicken lines provide a versatile model for the study of appetite regulation due to their differences in food intake and growth rate. It is important to emphasize that the current study focused on transcriptomic differences in the hypothalamus, a region of the brain that ultimately controls appetite. There are other brain regions involved in appetite regulation and the hypothalamus is involved in many other physiological processes; thus, DEGs identified in the current study may or may not be related to appetite regulation, although changes in response to insulin injection are more likely directly related to energy balance regulation.

Numerous studies have shown that the two lines respond differently to injection of various neurotransmitters such as neuropeptide Y (NPY), CRH, NPAF, β-endorphin etc. [10, 27-29] and neurochemicals such as methoxamine and serotonin [30, 31]. The pathway analysis results imply that the HWS line has less serotonin and dopamine biosynthesis and receptor-mediated signaling pathways in the hypothalamus than the LWS. These data are consistent with an earlier study on the two lines carried out with 4 day-old chicks using microarrays, showing differences in serotonin and dopamine receptor expression [4]. In rodents, hypothalamic serotonin and dopamine together reduce food intake by decreasing meal size via the activation of the lateral hypothalamus (LH), and reduce meal number through the depolarization of the VMH [32]. In birds, serotonin has been shown to reduce food intake in a dose-dependent manner [33]. However, the underlying mechanism is unclear. Also, dopamine was shown to reduce food intake via the D1 receptor, where D1 receptor antagonism blocked the anorexic effect of dopamine [33]. More interesting, interaction between the dopaminergic and serotonergic systems was shown to be regulated by the 5-HT_{2C} receptor in chickens [34]. Based on these findings, our data suggest an important role of serotonergic and dopaminergic systems in appetite regulation between the two lines. This is especially critical considering that long-term selection has resulted in polymorphisms in DDC, TH, and SLC8A2, which are down-regulated in the HWS line as compared to the LWS. The TH in the central nervous system is an important indicator for sympathetic nervous system (SNS) outflow [35]. The SNS plays an important role in both energy intake and energy expenditure. Reduced sympathetic tone has been shown to be associated with weight gain, which may be a factor in the pathogenesis of obesity [36]. A study in the two lines suggested that the HWS line has lower sympathetic activity than the LWS [37]. On the other hand, some genes encoding important appetite regulatory factors, such as NPY, POMC, and

agouti-related peptide (AgRP), were not significantly different between the two lines in this study. This can be explained several ways. Firstly, the threshold level of significance used to define a DEG can affect the identification of genes as being differentially expressed through transcriptomic profiling versus finding a statistically significant difference using a gene expression detection method such as real time PCR. In our previous study with the same samples, mRNA abundance of NPY and several of its receptor sub-types were more highly expressed in the LWS than HWS in hypothalamus [17], and thus the level of significance used in the present study (in order to prevent a type II error) may have eliminated the more subtle effects identified via real time PCR analysis of target genes. Also, there are many appetite regulatory factors with overlapping functions, each thereby contributing a partial role in appetite regulation. Finally, different mRNA levels may not reflect changes at the neurochemical level, thus transcriptional data should be interpreted with due caution.

Overall, the present findings suggest that various neurochemicals such as serotonin, dopamine, and glutamate are responsible for the differences in energy regulation both between the lines and in response to injection with insulin. Interestingly, exogenous insulin led to around 5-fold higher expression of proopiomelanocortin (POMC) in both LWS and HWS as compared to their vehicle-injected counterparts. This implies that POMC neurons are insulin sensitive and might be a major player in the chicken for regulating energy homeostasis upon insulin stimulation.

Besides predicted changes in signaling pathways that may underlie appetite regulatory differences in the body weigh lines of chickens, it was also predicted that the high weight line chickens have a greater rate of degradation of nucleotides, such as guanosine, adenosine, and purine, which may be an indicator of neuronal apoptosis. The microarray analysis of

hypothalamus from 4 day-old LWS and HWS also identified enrichment of the process "DNA metabolism, repair, induction of apoptosis and metabolism"; however, it was the LWS line that was suspected to suffer from greater neuronal degeneration with increased mortality. The effects observed here are possibly age-specific. At 90 days of age the HWS already display excess fat accumulation and represent an obese state with insulin insensitivity [15, 17, 38]. These metabolic phenotypes may have detrimental effects on the central nervous system and result in neuronal apoptosis in the HWS chickens.

Insulin plays an important role in glucose metabolism and energy homeostasis in various species. As compared to humans, chickens are naturally hyperinsulinemic and hyperglycemic [17]. How chickens respond to insulin and are able to cope with chronically elevated levels of blood glucose that would be lethal in humans remains a mystery. With this question in mind, we aims to elucidate the hypothalamic differences in gene expression between the two lines in response to peripheral insulin challenge. In rats, insulin was shown to cross the blood brain barrier through saturated active transporters [39, 40]. In the hypothalamus, insulin interacts with multiple nuclei such as the ARC, paraventricular nucleus (PVN), and VMH, which together inhibit food intake and reduce blood glucose [41]. We previously demonstrated that central injection of insulin was associated with a lower threshold response in food intake reduction in the LWS as compared to HWS, as well as a similar difference in their blood glucose response [14], and we recently demonstrated a differential sensitivity in the blood glucose response to peripheral insulin in selection-age chickens [15]. It is very interesting that genes associated with serotonin and dopamine biosynthesis and receptor signaling, such as DDC, TH and SLC18A2, were down regulated in the HWS line as compared to the LWS in vehicle-treated chickens. However, after insulin injection, those same genes were up regulated in the HWS. One of the

phenomena we have observed during insulin challenge studies is that after we re-feed the two lines (2 h post insulin injection following an overnight food withdrawal), it is the LWS that show a greater compensatory re-feeding response as well as greater pancreatic expression of preproglucagon [15]. This may help explain some of the underlying mechanisms for how the LWS and HWS chickens differentially respond to insulin-induced hypoglycemia. However, how insulin regulates serotonergic and dopaminergic systems remains to be elucidated. Emerging evidence has indicated crosstalk between serotonin and insulin signaling pathways through the POMC neurons in the hypothalamic arcuate (ARC) in rodents [42, 43]. Insulin and serotonin injection increase each other's concentrations reciprocally, and this interaction was suggested to occur in the VMH- PVN area [44]. Our results also showed that both lines had 5-fold up-regulation of POMC mRNA after insulin injection, suggesting the importance of POMC neurons in response to insulin and in contributing to serotonin signaling pathways in energy homeostasis.

According to the pathway analysis of the DEGs, insulin injection was also predicted to have decreased glutamate receptor signaling in the HWS compared to LWS. Glutamate is known as an excitatory neurotransmitter and inhibition of glutamate receptor signaling is closely associated with synaptic long-term potentiation, depression, nNOS signaling-mediated neuronal excitotoxicity, and CREB signaling-mediated transcription factors, which together suppress the excitability of the hypothalamus. Enrichment of synaptic long-term depression and long-term potentiation in the HWSiv group pathways was closely associated with glutamate signaling. In rodents, insulin has been shown to retain its role as a growth factor that plays an important role in synaptogenesis, nerve growth, and neuronal plasticity in the central nervous system [45-47]. In our study, we observed changes in genes associated with neuron morphology (**Figure B.5)**. However, exploring the neuronal plasticity is beyond the scope of our study, and it is risky to

describe differences in neuronal plasticity with data from only a single time point in development and single time point after insulin injection. In the LWS line, insulin injection increased the expression of ALDH1A1, which is a major regulator of many activated pathways from this study, such as histamine, serotonin and dopamine degradation. The ALDH1A1 functions mainly in acetaldehyde neurotransmitter metabolism and is also known as a rate-limiting enzyme for the conversion of retinaldehyde to retinoic acid [48, 49]. Here high expression of ALDH1A1 is possibly associated with neurotransmitter degradation.

Together, our data suggest the importance of serotonergic and dopaminergic systems in energy homeostasis in the two lines, as well as their response to insulin-induced hypoglycemia. These findings provide insight for understanding differences in the hypothalamus of chickens after long-term selection for divergent juvenile body weight and also differential responses in hypothalamic signaling to exogenous insulin.

Acknowledgements

This research was supported by a Virginia Bioinformatics Institute / Fralin Life Sciences Institute Small Genome Research Grant (VBI/Fralin-GRL-01) awarded to ERG and MAC.

References

1. Dunnington EA, Honaker CF, McGilliard ML, Siegel PB: **Phenotypic responses of chickens to long-term, bidirectional selection for juvenile body weight--historical perspective**. *Poultry science* 2013, **92**(7):1724-1734.
2. Dunnington EA, Siegel PB: **Long-term divergent selection for eight-week body weight in white Plymouth rock chickens**. *Poult Sci* 1996, **75**(10):1168-1179.
3. Zelenka DJ, Dunnington EA, Cherry JA, Siegel PB: **Anorexia and sexual maturity in female white rock chickens. I. Increasing the feed intake**. *Behav Genet* 1988, **18**(3):383-387.
4. Ka S, Albert FW, Denbow DM, Paabo S, Siegel PB, Andersson L, Hallbook F: **Differentially expressed genes in hypothalamus in relation to genomic regions under selection in two chicken lines resulting from divergent selection for high or low body weight**. *Neurogenetics* 2011, **12**(3):211-221.
5. Ka S, Lindberg J, Stromstedt L, Fitzsimmons C, Lindqvist N, Lundeberg J, Siegel PB, Andersson L, Hallbook F: **Extremely different behaviours in high and low body**

weight lines of chicken are associated with differential expression of genes involved in neuronal plasticity. *J Neuroendocrinol* 2009, **21**(3):208-216.
6. Burkhart CA, Cherry JA, Van Krey HP, Siegel PB: **Genetic selection for growth rate alters hypothalamic satiety mechanisms in chickens**. *Behav Genet* 1983, **13**(3):295-300.
7. Cline MA, Nandar W, Bowden C, Hein PP, Denbow DM, Siegel PB: **Differential feeding responses to central alpha-melanocyte stimulating hormone in genetically low and high body weight selected lines of chickens**. *Life Sci* 2008, **83**(5-6):208-213.
8. Cline MA, Kuo AY, Smith ML, Nandar W, Prall BC, Siegel PB, Denbow DM: **Differential feed intake responses to central corticotrophin releasing factor in lines of chickens divergently selected for low or high body weight**. *Comp Biochem Physiol* 2009, **152**(1):130-134.
9. Cline MA, Nandar W, Bowden C, Calchary W, Smith ML, Prall B, Newmyer B, Orion Rogers J, Siegel PB: **The threshold of amylin-induced anorexia is lower in chicks selected for low compared to high juvenile body weight**. *Behav Brain Res* 2010, **208**(2):650-654.
10. Newmyer BA, Siegel PB, Cline MA: **Neuropeptide AF differentially affects anorexia in lines of chickens selected for high or low body weight**. *J Neuroendocrinol* 2010, **22**(6):593-598.
11. Cline MA, Prall BC, Smith ML, Calchary WA, Siegel PB: **Differential appetite-related responses to central neuropeptide S in lines of chickens divergently selected for low or high body weight**. *J Neuroendocrinol* 2008, **20**(7):904-908.
12. Cline MA, Siders R, Newmyer BA, Smith ML, Siegel PB: **Both calcitonin and calcitonin gene-related peptides' thresholds of hypophagia are considerably lower in chicks selected for high rather than low juvenile body weight**. *Physiol Behav* 2010, **101**(2):254-259.
13. Kuo AY, Cline MA, Werner E, Siegel PB, Denbow DM: **Leptin effects on food and water intake in lines of chickens selected for high or low body weight**. *Physiol Behav* 2005, **84**(3):459-464.
14. Smith ML, Prall BC, Siegel PB, Cline MA: **The threshold of insulin-induced hypophagia is lower in chicks selected for low rather than high juvenile body weight**. *Behav Brain Res* 2011, **216**(2):719-722.
15. Sumners LH, Zhang W, Zhao X, Honaker CF, Zhang S, Cline MA, Siegel PB, Gilbert ER: **Chickens from lines artificially selected for juvenile low and high body weight differ in glucose homeostasis and pancreas physiology**. *Comp Biochem Physiol* 2014, **172**:57-65.
16. Wang Z, Gerstein M, Snyder M: **RNA-Seq: a revolutionary tool for transcriptomics**. *Nat Rev Genet* 2009, **10**(1):57-63.
17. Zhang W, Sumners LH, Siegel PB, Cline MA, Gilbert ER: **Quantity of glucose transporter and appetite-associated factor mRNA in various tissues after insulin injection in chickens selected for low or high body weight**. *Physiological genomics* 2013, **45**(22):1084-1094.
18. Puelles L, Martinez-de-la-Torre, M., Paxinos, G., Watson, C., Martinez, S., : **The Chick Brain in Stereotaxic Coordinates: An Atlas Featuring Neurometric Subdivisions and Mammalian Homologies**, First edn: Academic Press.

19. Potter SC, Clarke L, Curwen V, Keenan S, Mongin E, Searle SM, Stabenau A, Storey R, Clamp M: **The Ensembl analysis pipeline**. *Genome Res* 2004, **14**(5):934-941.
20. Collins JE, White S, Searle SM, Stemple DL: **Incorporating RNA-seq data into the zebrafish Ensembl genebuild**. *Genome Res* 2012, **22**(10):2067-2078.
21. Young MD, Wakefield MJ, Smyth GK, Oshlack A: **Gene ontology analysis for RNA-seq: accounting for selection bias**. *Genome biology* 2010, **11**(2):R14.
22. Falcon S, Gentleman R: **Using GOstats to test gene lists for GO term association**. *Bioinformatics* 2007, **23**(2):257-258.
23. Xu X, Zhang Y, Williams J, Antoniou E, McCombie WR, Wu S, Zhu W, Davidson NO, Denoya P, Li E: **Parallel comparison of Illumina RNA-Seq and Affymetrix microarray platforms on transcriptomic profiles generated from 5-aza-deoxy-cytidine treated HT-29 colon cancer cells and simulated datasets**. *BMC bioinformatics* 2013, **14 Suppl 9**:S1.
24. Janssen SF, van der Spek SJ, Ten Brink JB, Essing AH, Gorgels TG, van der Spek PJ, Jansonius NM, Bergen AA: **Gene expression and functional annotation of the human and mouse choroid plexus epithelium**. *PloS one* 2013, **8**(12):e83345.
25. Johansson AM, Pettersson ME, Siegel PB, Carlborg O: **Genome-wide effects of long-term divergent selection**. *PLoS Genet* 2010, **6**(11):e1001188.
26. Podisi BK, Knott SA, Burt DW, Hocking PM: **Comparative analysis of quantitative trait loci for body weight, growth rate and growth curve parameters from 3 to 72 weeks of age in female chickens of a broiler-layer cross**. *BMC Genet* 2013, **14**:22.
27. Newmyer BA, Nandar W, Webster RI, Gilbert E, Siegel PB, Cline MA: **Neuropeptide Y is associated with changes in appetite-associated hypothalamic nuclei but not food intake in a hypophagic avian model**. *Behav Brain Res* 2013, **236**(1):327-331.
28. Cline MA, Prall BC, Rogers JO, Tachibana T: **Satiety induced by central stresscopin is mediated by corticotrophin-releasing factor receptors and hypothalamic changes in chicks**. *Pharmacol Biochem Behav* 2009, **92**(4):663-669.
29. McCormack JF, Denbow DM: **Feeding, drinking and temperature responses to intracerebroventricular beta-endorphin in the domestic fowl**. *Peptides* 1988, **9**(4):709-715.
30. Denbow DM, Van Krey HP, Siegel PB: **Selection for growth alters the feeding response to injections of biogenic amines**. *Pharmacol Biochem Behav* 1986, **24**(1):39-42.
31. Richards MP: **Genetic regulation of feed intake and energy balance in poultry**. *Poult Sci* 2003, **82**(6):907-916.
32. Meguid MM, Fetissov SO, Varma M, Sato T, Zhang L, Laviano A, Rossi-Fanelli F: **Hypothalamic dopamine and serotonin in the regulation of food intake**. *Nutrition* 2000, **16**(10):843-857.
33. Zendehdel M, Hamidi F, Babapour V, Mokhtarpouriani K, Fard RM: **The effect of melanocortin (Mc3 and Mc4) antagonists on serotonin-induced food and water intake of broiler cockerels**. *J Vet Sci* 2012, **13**(3):229-234.
34. Zendehdel M, Hasani K, Babapour V, Mortezaei SS, Khoshbakht Y, Hassanpour S: **Dopamine-induced hypophagia is mediated by D1 and 5HT-2c receptors in chicken**. *Vet Res Comm* 2014, **38**(1):11-19.
35. Burgi K, Cavalleri MT, Alves AS, Britto LR, Antunes VR, Michelini LC: **Tyrosine hydroxylase immunoreactivity as indicator of sympathetic activity: simultaneous**

evaluation in different tissues of hypertensive rats. *Am J Physiol Regul Integr Comp Physiol* 2011, **300**(2):R264-271.
36. Snitker S, Macdonald I, Ravussin E, Astrup A: **The sympathetic nervous system and obesity: role in aetiology and treatment**. *Obes Rev* 2000, **1**(1):5-15.
37. Alice Yi-Wen K: **Altered autonomic nervous system function in chickens divergenetly selected for body weight**. Virginia Tech; 2000.
38. Zhang S, McMillan RP, Hulver MW, Siegel PB, Sumners LH, Zhang W, Cline MA, Gilbert ER: **Chickens from lines selected for high and low body weight show differences in fatty acid oxidation efficiency and metabolic flexibility in skeletal muscle and white adipose tissue**. *Int J Obes (Lond)* 2014.
39. Banks WA, Owen JB, Erickson MA: **Insulin in the brain: there and back again**. *Pharmacol Ther* 2012, **136**(1):82-93.
40. Bingham EM, Hopkins D, Smith D, Pernet A, Hallett W, Reed L, Marsden PK, Amiel SA: **The role of insulin in human brain glucose metabolism: an 18fluoro-deoxyglucose positron emission tomography study**. *Diabetes* 2002, **51**(12):3384-3390.
41. Vogt MC, Bruning JC: **CNS insulin signaling in the control of energy homeostasis and glucose metabolism - from embryo to old age**. *Trends Endocrinol Metab* 2013, **24**(2):76-84.
42. Papazoglou I, Berthou F, Vicaire N, Rouch C, Markaki EM, Bailbe D, Portha B, Taouis M, Gerozissis K: **Hypothalamic serotonin-insulin signaling cross-talk and alterations in a type 2 diabetic model**. *Mol Cell Endocrinol* 2012, **350**(1):136-144.
43. Xu Y, Berglund ED, Sohn JW, Holland WL, Chuang JC, Fukuda M, Rossi J, Williams KW, Jones JE, Zigman JM *et al*: **5-HT2CRs expressed by pro-opiomelanocortin neurons regulate insulin sensitivity in liver**. *Nat Neurosci* 2010, **13**(12):1457-1459.
44. Orosco M, Rouch C, Gerozissis K: **Activation of hypothalamic insulin by serotonin is the primary event of the insulin-serotonin interaction involved in the control of feeding**. *Brain Res* 2000, **872**(1-2):64-70.
45. Nelson TJ, Sun MK, Hongpaisan J, Alkon DL: **Insulin, PKC signaling pathways and synaptic remodeling during memory storage and neuronal repair**. *Eur J Pharmacol* 2008, **585**(1):76-87.
46. Hoyer S: **Glucose metabolism and insulin receptor signal transduction in Alzheimer disease**. *Eur J Pharmacol* 2004, **490**(1-3):115-125.
47. Chiu SL, Chen CM, Cline HT: **Insulin receptor signaling regulates synapse number, dendritic plasticity, and circuit function in vivo**. *Neuron* 2008, **58**(5):708-719.
48. Wu J, Cohen P, Spiegelman BM: **Adaptive thermogenesis in adipocytes: is beige the new brown?** *Genes Dev* 2013, **27**(3):234-250.
49. Moore SM, Liang T, Graves TJ, McCall KM, Carr LG, Ehlers CL: **Identification of a novel cytosolic aldehyde dehydrogenase allele, ALDH1A1*4**. *Hum Genom* 2009, **3**(4):304-307.

Table 5.1 Pathways predicted by gene ontology (GO) function analysis to be altered in each group comparison*.

5.1.1 HWSLWSv

Molecular Function	%
Protein Binding	17.29
DNA/Nucleotide Binding	11.68
Protein Kinase/Signal Transducer	11.37
Cellular Component	
(Integral to) Membrane	20.00
Cytoplasm	10.44
Nucleus	6.44
Biological Process	
Cellular Growth and Proliferation	5.56
Cellular Development	5.05
Cell-to-Cell Signaling and Interaction	4.55

5.1.2 HWSLWSi

Molecular Function	%
Protein Binding	16.08
Protein Kinase/Signal Transducer	14.15
DNA/Nucleotide Binding	10.40
Cellular Component	
(Integral to) Membrane	23.39
Cytoplasm	10.31
Nucleus	10.13
Biological Process	
Small Molecule Biochemistry	8.91
Molecular Transport	8.53
Cell Morphology	8.14

5.1.3 HWSiv

Molecular Function	%
Protein Binding	13.95
DNA/Nucleotide Binding	13.64
Kinase Activity	13.17
Cellular Component	
(Integral to) Membrane	26.97
Nucleus	10.39

Cytoplasm	7.02
Biological Process	
Cell-to-Cell Signaling and Interaction	12.59
Molecular Transport	11.95
Small Molecule Biochemistry	11.95

5.1.4 LWSiv

Molecular Function	**%**
Protein Binding	13.24
Hormone Activity	7.35
Transporter Activity	5.88
Cellular Component	
Extracellular Region	22.22
Cytoplasm	9.26
Nucleus	7.41
Biological Process	
Small Molecule Biochemistry	39.29
Molecular Transport	35.71
Lipid Metabolism	32.14

*%: percent of genes involved in that function, position, and process; LWS: low-weight selected line; HWS: high-weight selected line; i: insulin-injected; v: vehicle-injected.

Table 5.2 Top differentially expressed genes in each group

5.2.1 High weight vehicle versus low weight vehicle-injected (HWSLWSv)

Up-regulated			Down-regulated		
Gene	Accession No.	Fold change	Gene	Accession No.	Fold change
DYNLRB2	XM_414162	4.3	*POU4F3*	NM_204759	-12.1
HPGDS	NM_205011	2.8	*AKR1D1*	XM_416341	-7.7
NPVF	NM_204363	2.2	*PAX7*	NM_205065	-7.4
HLA-A	NM_001031338	2.1	*ALDH1A1*	NM_204577	-5.8
NT5C1A	XM_417822	2.1	*OXT*	XM_001231491	-3.9
TAGLN	NM_205494	2.1	*GATA3*	NM_001008444	-3.8
S100B	XM_001233034	2.0	*MGP*	NM_205044	-3.7
HEYL	XM_001234405	2.0	*CGA*	XM_429886	-3.1
APOD	NM_001011692	2.0	*HSPB1*	NM_205290	-2.5
HCRT	NM_204185	2.0	*CRIP2*	XM_422218	-2.5

* *DYNLRB2*: dynein, light chain, roadblock-type 2; *HPGDS*: hematopoietic prostaglandin D synthase; neuropeptide VF precursor; *HLA-A*: major histocompatibility complex, class I, A; *NT5C1A*: 5'-nucleotidase, cytosolic IA; *TAGLN*: transgelin; *S100B*: S100 calcium binding protein B; *HEYL*: hes-related family bHLH transcription factor with YRPW motif-like; *APOD*: apolipoprotein D; *HCRT*: hypocretin (orexin) neuropeptide precursor; *POU4F3*: POU class 4 homeobox 3; *AKR1D1*: aldo-keto reductase family 1, member D1; *PAX7*: paired box 7; *ALDH1A1*: aldehyde dehydrogenase 1 family, member A1; *OXT*: oxytocin; *GATA3*: GATA binding protein 3; *MGP*: matrix Gla protein; *CGA*: glycoprotein hormones, alpha polypeptide; *HSPB1*: heat shock 27kDa protein 1; *CRIP2*: cysteine-rich protein; LWS: low-weight selected line; HWS: high-weight selected line; v: vehicle-injected.

5.2.2 High weight insulin versus low weight insulin-injected (HWSLWi)

Up-regulated			Down-regulated		
Gene	Accession No.	Fold change	Gene	Accession No.	Fold change

SLC6A4	NM_213572	30.2	*CGA*	XM_429886	-30.3
TFAP2B	NM_204895	11.9	*ALDH1A1*	NM_204577	-22.8
FEV	XM_003641646	7.4	*SLCO1C1*	NM_001039097	-21.5
CHAT	NM_204610	5.1	*FABP4*	NM_204290	-9.2
DYNLRB2	XM_414162	5.1	*AKR1D1*	XM_416341	-8.6
EN2	XM_003640676	4.9	*FAM107A*	XM_425164	-5.0
MPO	XM_415716	4.0	*PDK4*	NM_001199909	-3.7
SPARCL1	XM_420545	2.7	*SLCO2A1*	NM_001198927	-3.6
PTGER3	NM_001040468	2.6	*OXT*	XM_001231491	-3.5
SLC18A2	XM_421782	2.5	*NMU*	XM_420701	-3.4

**SLC6A4*: solute carrier family 6 (neurotransmitter transporter), member 4; *TFAP2B*: transcription factor AP-2 beta (activating enhancer binding protein 2 beta); *FEV*: FEV (ETS oncogene family); *CHAT*: choline O-acetyltransferase; *DYNLRB2*: dynein, light chain, roadblock-type 2; *EN2*: engrailed homeobox 2; *MPO*: myeloperoxidase; *SPARCL1*: SPARC-like 1 (hevin); *PTGER3*: prostaglandin E receptor 3 (subtype EP3); *SLC18A2*: solute carrier family 18 (vesicular monoamine transporter), member 2; *CGA*: glycoprotein hormones, alpha polypeptide; *ALDH1A1*: aldehyde dehydrogenase 1 family, member A1; *SLCO1C1*: solute carrier organic anion transporter family, member 1C1; *FABP4*: fatty acid binding protein 4; *AKR1D1*: aldo-keto reductase family 1, member D1; *FAM107A*: family with sequence similarity 107, member A; *PDK4*: pyruvate dehydrogenase kinase, isozyme 4; *SLCO2A1*: solute carrier organic anion transporter family, member 2A1; *OXT*: oxytocin/neurophysin I prepropeptide; *NMU*: neuromedin U; LWS: low-weight selected line; HWS: high-weight selected line; i: insulin-injected.

5.2.3 High weight insulin versus high weight vehicle-injected (HWSiv)

Up-regulated			Down-regulated		
Gene	Accession No.	Fold change	Gene	Accession No.	Fold change
EN2	XM_003640676	66.2	*TTR*	NM_205335	-26.6
SLC6A4	NM_213572	19.9	*FAM107A*	XM_425164	-12.0
PAX7	NM_205065	11.0	*FOXG1*	NM_205193	-6.8
FEV	XM_003641646	9.6	*GRM2*	XM_425148	-3.8

POMC	NM_001031098	5.9	*DUSP5*	XM_421754	-3.0
GATA3	NM_001008444	5.0	*KCNJ4*	XM_416263	-3.0
TFAP2B	NM_204895	4.9	*CPNE7*	XM_414211	-2.7
MPO	XM_415716	4.4	*LHCGR*	NM_204936	-2.6
SLC18A2	XM_421782	4.2	*ITPKA*	NM_204881	2.5
CHAT	NM_204610	3.6	*CAMK2A*	NM_204295	2.5

**EN2*: engrailed homeobox 2; *SLC6A4*: solute carrier family 6 (neurotransmitter transporter), member 4; *PAX7*: paired box 7; *FEV*: FEV (ETS oncogene family); *POMC*: proopiomelanocortin; *GATA3*: GATA binding protein 3; *TFAP2B*: transcription factor AP-2 beta (activating enhancer binding protein 2 beta); *MPO*: myeloperoxidase; *SLC18A2*: solute carrier family 18 (vesicular monoamine transporter), member 2; *CHAT*: choline O-acetyltransferase; *TTR*: transthyretin; *FAM107A*: family with sequence similarity 107, member A; *FOXG1*: forkhead box G1; *GRM2*: glutamate receptor, metabotropic 2; *DUSP5*: dual specificity phosphatase 5; *KCNJ4*: potassium inwardly-rectifying channel, subfamily J, member 4; *CPNE7*: copine VII; *LHCGR*: luteinizing hormone/choriogonadotropin receptor; *ITPKA*: inositol-trisphosphate 3-kinase A; *CAMK2A*: calcium/calmodulin-dependent protein kinase II alpha; HWS: high-weight selected line; i: insulin-injected; v: vehicle-injected.

5.2.4 Low weight insulin versus low weight vehicle-injected (LWSiv)

Up-regulated			Down-regulated		
Gene	Accession No.	Fold change	Gene	Accession No.	Fold change
FABP4	NM_204290	12.3	*TTR*	NM_205335	-17.9
SLCO1C1	NM_001039097	6.8	*CPNE7*	XM_414211	-2.7
CGA	XM_429886	5.7	*OXT*	XM_001231491	-2.4
POMC	NM_001031098	5.2			
ALDH1A1	NM_204577	2.2			

PDK4	NM_001199909	2.2
AQP1	NM_001039453	2.0
TIPARP	XM_422828	2.0
GADD45B	XM_003643820	1.8
PDYN	XM_003642463	1.7

*_FABP4_: fatty acid binding protein 4, adipocyte; _SLCO1C1_: solute carrier organic anion transporter family, member 1C1; _CGA_: glycoprotein hormones, alpha polypeptide; _POMC_: proopiomelanocortin; _ALDH1A1_: aldehyde dehydrogenase 1 family, member A1; _PDK4_: pyruvate dehydrogenase kinase, isozyme 4; _AQP1_: aquaporin 1 (Colton blood group); _TIPARP_: TCDD-inducible poly(ADP-ribose) polymerase; _GADD45B_: growth arrest and DNA-damage-inducible, beta; _PDYN_: prodynorphin; _TTR_: transthyretin; _CPNE7_: copine VII; _OXT_: oxytocin; LWS: low-weight selected line; i: insulin-injected; v: vehicle-injected.

Table 5.3 Differentially expressed genes with SNPs in their transcriptional regulatory and exon regions

Gene Name	RefSeq	Fold Change	Adjust *P* value	SNP No.
TIE1	XM_422400	3.345	9.5E-16	1
GABRG4	NM_205245	2.087	3.5E-08	1
DYNLRB2	XM_414162	4.328	2.3E-05	2
NT5C1A	XM_417822	2.107	4.3E-05	3
DDC	XM_419032	0.536	2.9E-04	1
GLRA4	XM_00123299	0.582	1.1E-03	2
TH	NM_204805	0.475	1.1E-03	2
HSPB1	NM_205290	0.400	1.3E-03	3
SLC18A2	XM_421782	0.524	1.6E-03	1
TMEM63A	XM_419384	1.689	1.9E-03	1
TCTEX1D1	XM_422530	2.083	2.2E-03	1
RNF219	XM_416999	1.656	6.4E-03	1
PIH1D3	XM_420180	1.911	1.4E-02	2
C15orf27	XM_00123362	0.597	1.8E-02	3

* *TIE1*: tyrosine kinase with immunoglobulin-like and EGF-like domains 1; *GABRG4*: gamma-aminobutyric acid receptor subunit gamma-4; *DYNLRB2*: Dynein, light chain, roadblock-type 2; NT5C1A: 5'-nucleotidase, cytosolic1A; *DDC*: dopa decarboxylase (aromatic L-aminoacid decarboxylase); *GLRA4*: glycine receptor, alpha 4; *TH*: tyrosine hydroxylase; *HSPB1*: heat shock 27kDa protein 1; *SLC18A2*: solute carrier family 18, member 2; *TMEM63A*: transmembrane protein 63A; *TCTEX1D*: tctex1 domain containing 1. *RNF219*: ring finger protein 219; *PIH1D3*: PIH1 domain containing 3; *C15orf 27*: chromosome 15 open reading frame 27.

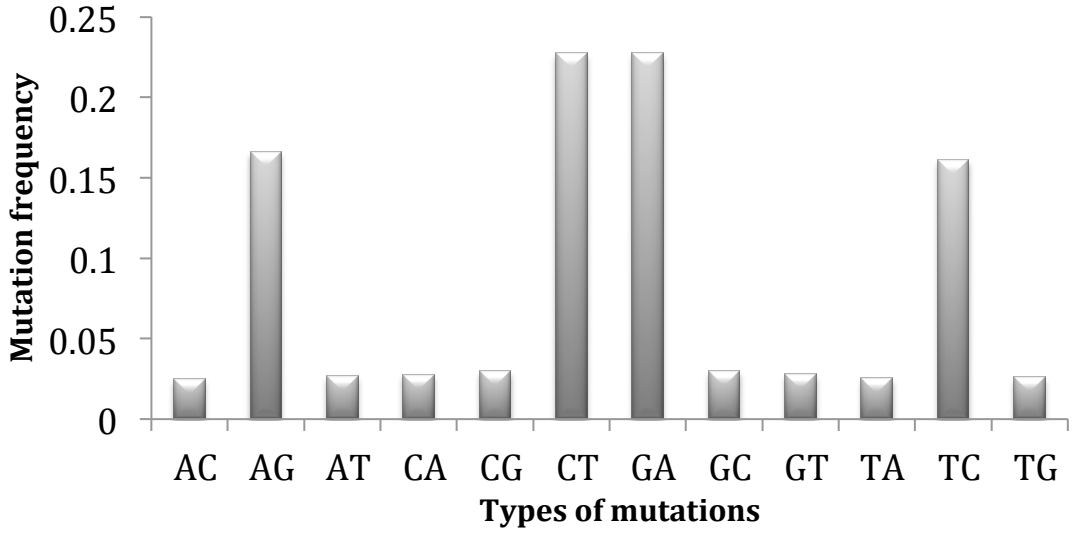

Figure 5.1 Mutation frequency of different types of SNPs identified in the hypothalamus of chickens selected for low (LWS) or high (HWS) body weight. Samples are RNA (Illumina HiSeq platform) from hypothalamus of 90 day-old female LWS and HWS chickens.

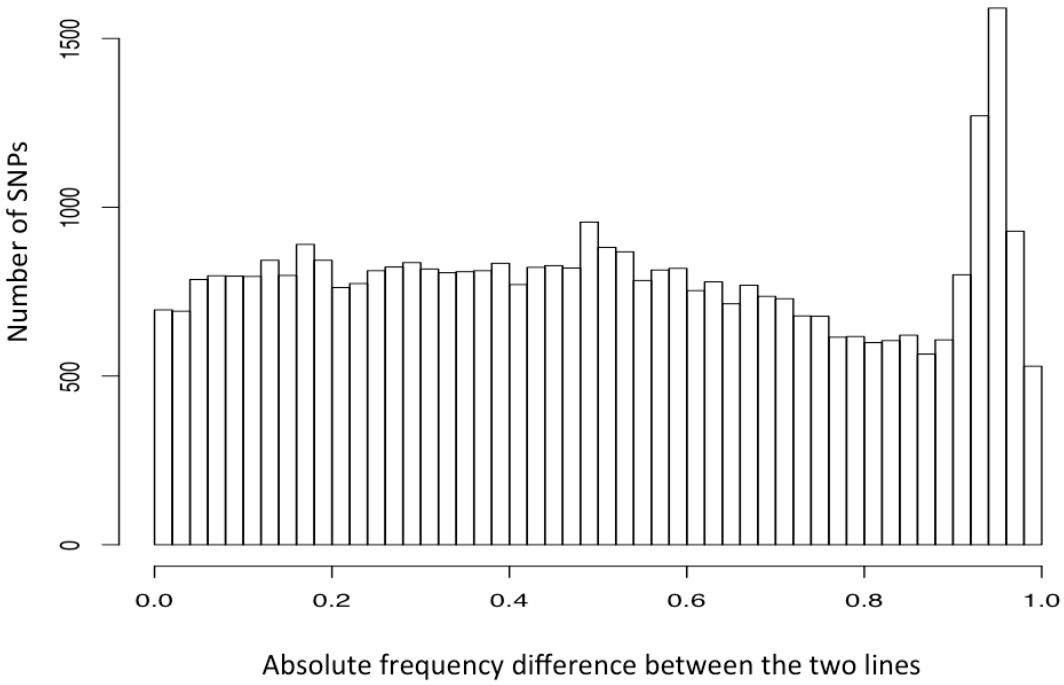

Figure 5.2 Absolute value of frequency differences in SNPs between chickens selected for low or high body weight.

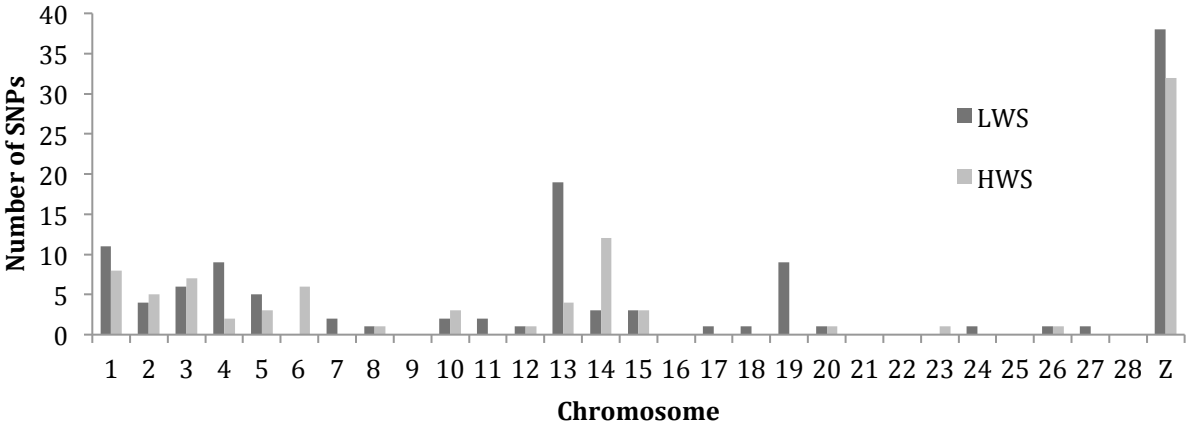

Figure 5.3 The distribution of polymorphisms existing only in the low-weight selected (LWS) or high-weight selected (HWS) line (absolute allele frequency difference=100%).

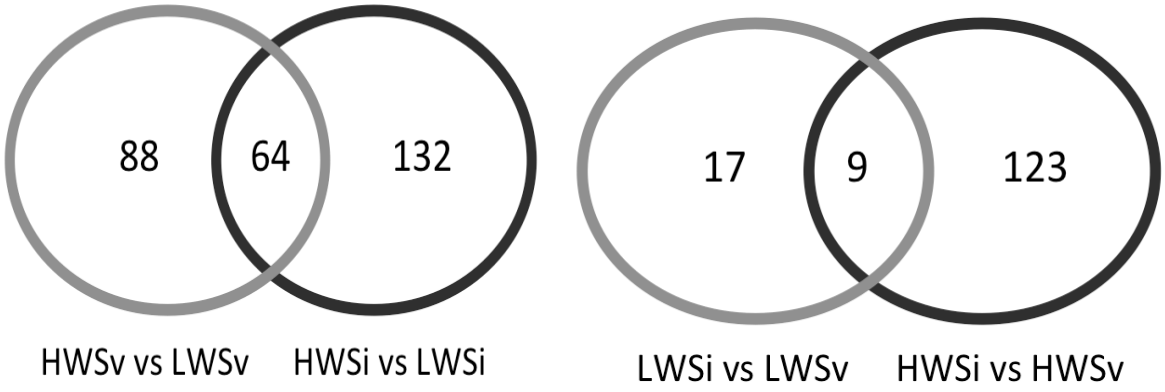

Figure 5.4 Venn diagrams for DEGs in each group and their overlapping DEGs. LWS: low-weight selected line; HWS: high-weight selected line; i: insulin-injected; v: vehicle-injected. Numbers represent number of differentially expressed genes (DEGs) in each group.

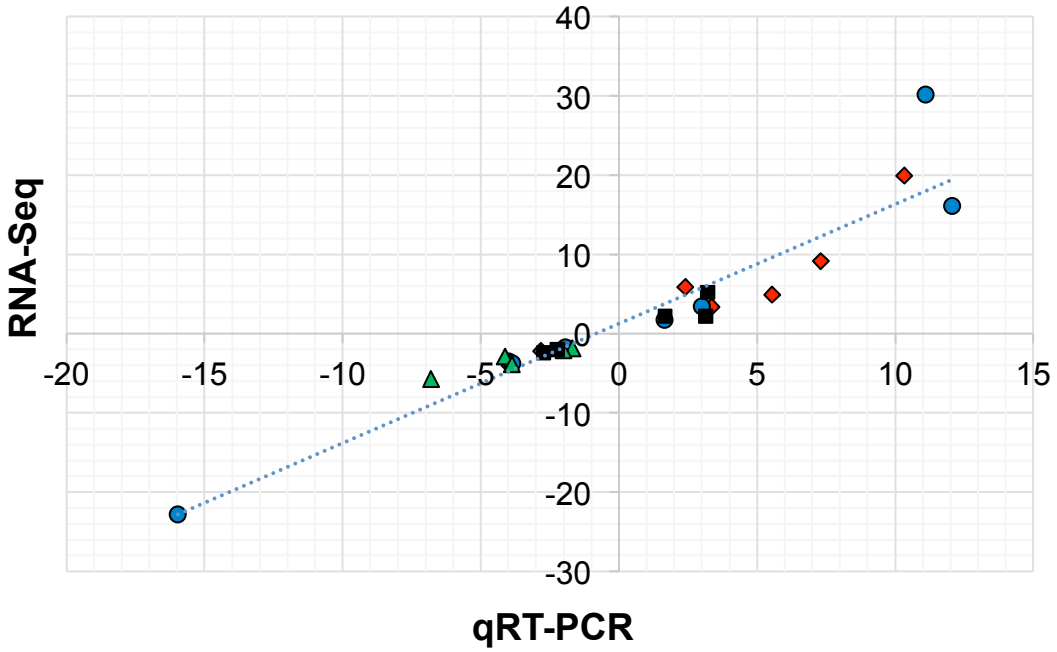

Figure 5.5 Linear regression for real time PCR and RNA sequencing data. Green triangles: HWSLWSv; Red diamond: HWSiv; Blue circles: HWSLWSi; Black squares: LWSiv. Adjusted coefficient of determination: R^2=0.88 with *P*-value<0.0001.

7.2

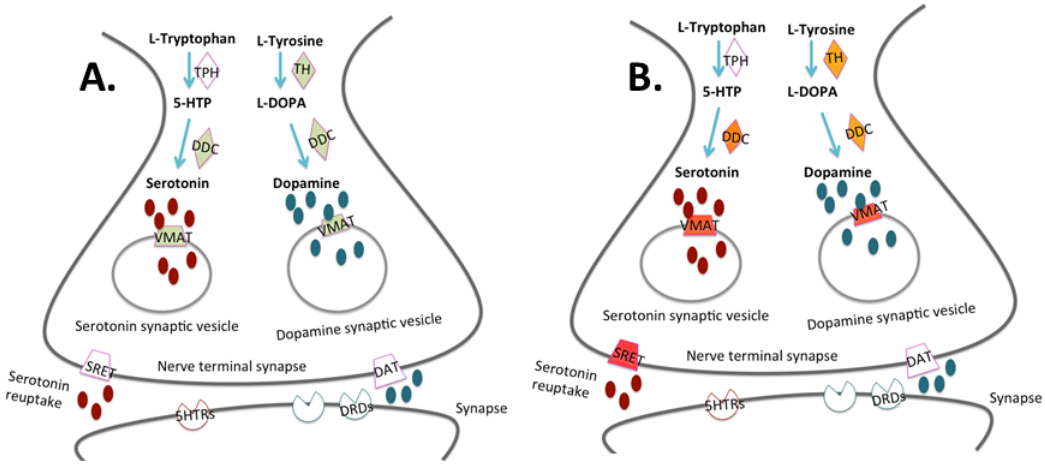

Figure 5.6 Serotonin and dopamine signaling pathways in the hypothalamus of HWS as compared to LWS chickens in vehicle (A) and insulin injected (B) groups. The pathways are based on IPA analysis of differentially-expressed genes identified after RNA sequencing of RNA collected from hypothalamus of 90 day-old female LWS and HWS from vehicle- and insulin-injected groups. The green color represents down-regulation and orange to red colors indicate up-regulation of the respective gene in HWS compared to LWS chickens. Darker coloration indicates a greater magnitude of difference in expression for those genes. Tryptophan is converted to 5-hydroxytryptamine through tryptophan hydroxylase (TPH), and then rapidly decarboxylated by aromatic amino acid decarboxylase (DDC) to produce cytosolic serotonin. Serotonin is transported via vesicular monoamine transporter (VMAT) to be stored in the serotonin synaptic vesicle. Upon activation, serotonin can be released from the presynaptic vehicle and bind to its receptors (5HTRs) in the postsynaptic vehicle. Extra serotonin in the synaptic cleft can also be taken back up by presynaptic neurons through serotonin transporters (SERT) re-uptake. Dopamine is generated from L-tyrosine, which is dehydrated by tyrosine

hydroxylase and then decarboxylated by aromatic-L-amino-acid decarboxylase (DDC). Similar to serotonin, dopamine is also stored in the vesicle upon synthesis via VMAT. In response to action potential, dopamine can be released and either binds to dopamine receptors (DRDs) or is taken back up through the dopamine active receptor (DAT, also known as SLC6A3). In summary, in this study, genes encoding factors involved in serotonin and dopamine biosynthesis and receptor-mediated signaling were down-regulated in HWS vs. LWS (6A). After insulin injection, these down-regulated genes were more highly expressed in HWS than LWS (6B).

Chapter 6

Anorexigenic effect of serotonin is associated with changes of hypothalamic nuclei activity in an avian model

Abstract: The anorexigenic effect of serotonin (5HT) has been documented for decades; however, its central mechanism has not been fully elucidated, especially so in non-mammalian vertebrates. Therefore, we centrally injected 5HT to chicks and measured several appetite-associated parameters. Chicks that received central 5HT dose- and time-dependently decreased food intake while water intake was not affected. To determine which hypothalamic nuclei were associated with this effect c-Fos immunoreactivity was measured in appetite-associated nuclei. Only the ventromedial hypothalamus and arcuate nucleus were activated. Whole blood glucose was measured after 5HT injection but was not affected. From the hypothalamus, several appetite-associated mRNAs were measured by real-time PCR after 5HT injection but not oneof these showed any difference in expression level. Lastly, a comprehensive behavior analysis demonstrated that 5HT caused reducing pecking and increased deep rest. Together we interpret these results as exogenous 5HT injection causes short-term satiety that is likely a secondary effect to an increase in the amount of time spent in deep rest.

Introduction

The biogenic amine 5HT, also known as 5-Hydroxytryptamine (5-HT), was first isolated and characterized in 1948 [1, 2]. It is one of the most abundant neurotransmitters distributed throughout the brain, and is also found in several peripheral organs [3]. The central serotonergic system is evolutionarily conserved across a range of species and is a component of numerous physiological processes [4], including the regulation of food intake [5]. However, despite that the anorexigenic effects of 5HT have long been documented, the precise mechanism of action is largely not understood. Research with rodent models has demonstrated that the hypothalamus plays an important role in 5HT-mediated regulation of food intake [6-8]. The potential pathway involves activation of pro-opiomelanocortin (POMC) neurons through the 5HT 2C receptor by transient receptor potential channels [9]. In turn POMC neurons secrete α-melanocyte stimulating hormone (α-MSH), which causes melanocortin-induced satiety via MC4R [8, 10, 11]. Both the 2C receptor (5-HT_{2C}R) and the 1B receptor (5-HT_{1B}R) have been shown to be critical in this process [11]. It has also been demonstrated that the anorexic effects of 5HT in

mice are partly due to the generation of reactive oxygen species (ROS) in the hypothalamus via an NADPH oxidase-dependent pathway [12]. In addition to food intake, 5HT also affects blood glucose concentrations in mammals. A 5-HT_{2C}R agonist improves insulin sensitivity and glucose tolerance in diet-induced obese mice [6].

As knowledge advances in 5HT-mediated regulation of food intake in rodents, it is important to understand its function in other vertebrate species. As birds are the closest out group to mammals, here we have evaluated the effects of exogenous 5HT injection in chicks and started to elucidate the central mechanism of action. Chicks are an excellent alternative vertebrate model to study neurochemistry due to their unique brain developmental processes and anatomy. For example, the chicken brain is neurologically mature at hatch despite having an incomplete blood-brain barrier [13]. Here, we measured behavior, hypothalamic c-Fos immunoreactivity and mRNA expression after exogenous 5HT injection in 4 day post-hatch chicks.

Materials and methods

Animals

Hubbard x Cobb-500 chicks from a 42 week of age breeder flock were obtained on the morning of hatch from a commercial hatchery and were individually caged in a room at a 30 ± 2 °C with 50 ± 5% humidity. Chicks were provided ad libitum access to food (22% crude protein, 3,000 kcal/kg metabolizable energy) and tap water. All experiments were conducted with chicks that were 4 days post-hatch between 06:00 and 10:00. All experimental procedures were performed according to the National Research Council publication, Guide for Care and Use of Laboratory Animals and were approved by the Virginia Tech Institutional Animal Care and Use Committee. Experiments were conducted sequentially as described and in each experiment chicks were from different hatches.

Intracerebroventricular (ICV) 5HT injection

Chicks were injected using an adapted freehand injection method [14] that does not appear to induce physiological stress [15]. The head of the chick was briefly inserted into a restraining device that left the cranium exposed and allowed for a free-hand injection to be performed. Injection coordinates were 3 mm anterior to the coronal suture, 1 mm lateral from the sagittal suture, and 2 mm deep targeting the left lateral ventricle. Anatomical landmarks were determined visually and by palpation. Injection depth was controlled by placing a plastic tubing

sheath over the needle. The needle remained at injection depth in the un-anaesthetized chick for 5 s to reduce backflow. Chicks were assigned to treatments at random. 5HT hydrochloride (molecular weight 212.68) was purchased from VWR (VWR, USA) and diluted in chicken artificial cerebrospinal fluid [16] that served as the vehicle for a total injection volume of 5 uL with 0.06% Evans blue dye. After data collection, each chick was decapitated and its head sectioned coronally to determine site of injection. Any chick without dye present in the lateral ventricle system was eliminated from further use. Sex was determined visually by dissection.

Experiment 1: Effects on food and water intake

Chicks, fasted 3 h prior to injection, were randomly assigned to receive 0, 12, 24, or 48 nmol 5HT based on a previous study (Denbow et al., 1982). After injection, chicks were returned to their individual cages and given ad libitum access to both food and water, with individual food and water containers weighed every 30 min for 180 min post-injection. Data were analyzed using analysis of variance (ANOVA) at each time point using the GLM procedure of SAS (SAS Inst., Inc., Cary, NC). The model included 5HT dose, sex and the interaction of sex with 5HT dose. Sex and the interaction of sex and 5HT dose were not significant and were eliminated from the model (and the effect of sex was not tested in subsequent experiments). If significant treatment effects were found, Tukey's method of multiple comparisons was used to separate the means at each time period. For this and all proceeding experiments, statistical significance was set at $P < 0.05$.

Experiment 2: c-Fos immunohistochemistry for the evaluation of neuronal activation

Chicks, fasted for 3 h, were randomly assigned to receive either vehicle or 48 nmol 5HT by ICV injection. Following injection, food was withheld to prevent effects associated with food consumption. One h post-injection, indicated as the time of most robust c-Fos expression [17], chicks were deeply anesthetized with an intraperitoneal (IP) injection of sodium pentobarbital (30 mg/kg body weight) via cardiopuncture, decapitated and then perfused via the carotid artery with saline followed by 4% paraformaldehyde in 0.1M phosphate buffer (PB) containing 0.2% picric acid at pH 7.4. Brains were removed from skulls and post-fixed for 1 h in the same solution, after which they were blocked and placed through a series of graded sucrose incubations, consisting of 20% and 30% sucrose in 0.1 M PB, until they sank. Using a cryostat at -15 °C, several 60 mm coronal sections corresponding to interaural 2.08 mm and interaural 1.12 mm that contained hypothalamic appetite-related nuclei based on anatomies described by Puelles

et al. [18] were collected in 0.02 M phosphate buffered saline (PBS) containing 0.1% sodium azide. The paraventricular nucleus including its parvocellular (PAPC) and magnocellular (PAMC) divisions, and dorsomedial hypothalamus (DMN), were collected at interaural 2.08, and the arcuate nucleus (ARC) at interaural 1.12 mm, while both the ventromedial hypothalamus (VMH) and lateral hypothalamic area (LH) were collected at both interaural 1.12 mm (caudal) and 2.08 (rostral). Procedures for c-Fos immunohistochemistry were performed as described previously [19]. Bright field images were captured at a magnification of 4X and complete hypothalamus section image stitched together. Overlays containing the respective nuclei boundaries were digitally merged with micrographs and the number of c-Fos immunoreactive cells within each respective nucleus were counted by a technician blind to treatment. Data were analyzed by Student t test procedure of SAS.

Experiment 3: Blood glucose measurement

Chicks received the same treatments as described in Experiment 2. At 1 h post-injection chicks were decapitated and whole blood glucose concentration was measured using a handheld glucometer (Agamatrix, Inc.) with a sensitivity range from 20 to 600 mg/dL. Blood glucose data were analyzed by the Student's t-test procedure of SAS.

Experiment 4: Total RNA isolation and real time PCR

Chicks were fasted 3 h prior to injection and received either vehicle or 48 nmol 5HT by ICV injection with ad libitum access to water after injection. Sixty min following injection, chicks were deeply anesthetized with sodium pentobarbital via cardiopuncture, decapitated, and brains removed. The whole upside-down brain was lowered into liquid nitrogen to the point where the most ventral aspect of the optic lobe was level with the surface of the liquid nitrogen. The brain was left in this position for 11 seconds. This procedure resulted in brain regions around the hypothalamus freezing and providing firmness necessary to make precise cuts for hypothalamus extraction. Perpendicular to the midline suture a cut was made at the septopallio-mesencephalic tract and at the third cranial nerves. 2.0 mm parallel to the midline two cuts were made. Lastly, a cut from the anterior commissure to 1.0 mm ventral to the posterior commissure was made. The hypothalamus blocks were collected and preserved in RNA later. The whole hypothalamus was homogenized with a Tissue Lyser II (Qiagen) twice at 20 Hz for 2 min using 5 mm stainless steel beads (Qiagen) and 1 mL isol-RNA Lysis Reagent (5-PRIME). Samples were then centrifuged at 12,000 x g for 10 min at 4°C, supernatant transferred and mixed with

0.2 mL chloroform, and centrifuged again under the same conditions. The supernatant was removed and mixed with an equal volume of 70% ethanol and loaded onto a spin column and total RNA purified using the RNeasy Mini Kit (Qiagen, USA). An on-column RNase-Free DNase I treatment was performed. Total RNA integrity was assessed by agarose-formaldehyde gel electrophoresis and quantity and purity evaluated by spectrophotometry (260/280/230 nm) using a NanophotometerTM Pearl (IMPLEN), and samples stored at -80°C. The first strand cDNA was synthesized in 20 µL reactions from 200 ng of total RNA using the High Capacity cDNA Reverse Transcription kit (Invitrogen, USA), following the manufacturer's instructions. Primers were designed with Primer Express 3.0 (Applied Biosystems; (**Table 6.1**) and amplification efficiency was validated for all primer pairs before use (95-100% efficiency). Real time PCR reactions contained Fast SYBR Green Master Mix (Applied Biosystems), forward and reverse primers (0.125 µM each), and 10-fold diluted cDNA. Real-time PCR reactions were performed in duplicate for all samples on an Applied Biosystems 7500 FAST system, under the following conditions: enzyme activation for 20 sec at 95°C and 40 cycles of 1) melting step for 3 seconds at 95°C and 2) annealing/extension step for 30 seconds at 60°C. Melting curve analyses were performed after all PCR reactions to ensure amplicon specificity. Chicken was defined as the experimental unit. The real time PCR data were analyzed using the ΔΔCT method, where ΔCT = CT (target gene) – CT (β-actin), and ΔΔCT = ΔCT target sample – ΔCT calibrator [20]. β-actin was the endogenous control and the average of the chicks that received vehicle injection served as the calibrator sample [21]. The $2^{-\Delta\Delta ct}$ values were used for statistical analysis. Data normality was evaluated by the Univariate procedure of SAS 9.3 (SAS Institute, Cary, NC). A Student's t-test was used to compare treatment and vehicle groups.

Experiment 5: Behavioral analysis

Chicks, fasted for 3 h, were randomly assigned to receive either vehicle or 48 nmol 5HT by ICV injection. Chicks were immediately placed in a 290 × 290 mm acrylic recording arena with food and water containers in diagonal corners. Chicks were simultaneously and automatically recorded from three angles for 30 min post-injection on DVD and data were analyzed in 5 min intervals using ANY-maze behavioral analysis software (Stoelting, Wood Dale, IL). The amount of time spent standing, sitting, preening, or in deep rest, and the number of jumps, steps, feed and exploratory pecks, drinks, defecations, and chirps were quantified. Deep rest was defined as the eyes closed for greater than 3 s starting 3 s after eye closure.

Preening was defined as trimming or dressing of down with the beak. Food pecks were defined as pecks within the feed container, whereas any other pecks were counted as exploratory pecks. Drinks were defined as the chick dipping its beak in water, then raising and extending its head to swallow. Data were analyzed by the Mann–Whitney U test (due to non-heterogeneous variance).

Results

Food intake

Exogenous administration of 5HT caused reduced food intake (**Figure 6. 1**). Chicks that received 24 and 48 nmol 5HT reduced food intake from 30 to 90 min following injection. At no observation time was 12 nmol 5HT efficacious at reducing food intake. Not one of the doses of 5HT caused a reduction in water intake (data not shown).

c-Fos immunoreactivity

Chicks that were injected with 5HT had more than double the amount of c-Fos immunoreactive neurons (**Figure 6.2** and **Figure 6.3**). The number of c-Fos immunoreactive neurons in the caudal VMH and ARC was increased by 5HT injection. However, the rostral LH and rostral VMH, caudal LH, PaPC, PaMC and DMN were not affected by 5HT injection.

Whole blood glucose concentration

No effect on whole blood glucose concentration was detected at 1 h post injection. Whole blood glucose concentrations were 203.7 ± 7.9 mg/dL and 197.8 ± 7.6 mg/dL for the vehicle and 5HT injected groups, respectively.

Gene expression analysis for the hypothalamus

There was no significant difference for any of the genes evaluated between the 5HT injection group and the vehicle-treated group at 1 h post-injection (**Figure 6.4**).

Behavior analysis

5HT treatment was associated with changes in timed-type behaviors (**Table 6.2**). 5HT-treated chicks spent more time in deep rest at 1200 through 1800 s following injection. However, other timed behaviors including sitting, standing and preening were not affected. Count-type behaviors were also affected (**Table 6.3**). Chicks that received 5HT reduced feeding pecks at 900 through 1800 s, decreased steps from 600 to 1800 s, decreased defecations at 1800 s and decreased chirps at all observation times. Exploratory pecks, jumps, and drinks were not affected.

Discussion

We interpret the results as exogenous 5HT injection induces short-term satiety in chicks at 4 days post-hatch. The highest magnitude of food intake suppression occurred during the first 30 min following injection where 48 nmol 5HT-treated chicks consumed around 10% the mass of food that vehicle-treated chicks ingested (**Figure 6.1**); however food intake on a cumulative basis was suppressed for up to 150 min following injection but at a much lower magnitude (around 60% of vehicle-treated chicks) than at the other observation times. Additionally, compensatory food intake was not observed during the observation period. With respect to other neurotransmitters that have been evaluated for effects on ingestive behavior in chicks, relatively high doses of 5HT were required to affect food intake. This may be due to the location of first-order neurons that initiate 5HT-induced anorexia. Alternatively, the relatively high doses suggest that 5HT is not involved in natural regulation of food intake in chicks, and that the effects we are observing are pharmacological. However, that water intake was not affected implies that the reduction in food intake we observed was not due to malaise.

The suppression of food intake in chickens after central 5HT injection was first reported in the early 1980's with Leghorn chicks at 4 and 7 weeks of age [22, 23], and the dose response and duration of effect is similar to the result of Experiment 1. Our effect on food intake is also consistent with reports of central injections in broiler chicks at 2 weeks of age [24] and intraperitoneal broilers from 3 to 25 days of age [25]. However, with respect to water intake, reports of 5HT's effect are conflicting. In Leghorns that are fed ad libitum, ICV 5HT causes increased water intake, whereas fasted 5HT-injected chickens decrease water intake. However, in broiler chicks that were fasted for 24 h, 5HT stimulated water intake [24]. Our water intake result differs as 5HT did not affect water intake. The reason for these different dipsogenic effects may be stock, age or duration of fasting period-dependent, which warrants further study. However, as our primary interest is food intake we have not further investigated this effect.

To our knowledge the precise hypothalamic nuclei that mediate 5HT-induced anorexia are unreported in the avian class. Thus, we measured hypothalamic neuronal activation by quantifying c-Fos immunoactivity, the product of an early intermediate gene [26]. Among the nuclei evaluated, only the ARC and caudal VMH were affected. Although we are using the most detailed chick stereotaxic atlas available [18], it has much less detail than is available for rats. For example, the rat stereotaxic atlas has at least 4 subdivisions of the VMH defined in coronal section [27]. As **Figure 6.3** shows, the number of c-Fos reactive cells in the most lateral aspect

of the VMH is responsible for the increase in this nucleus. Although not defined by the chick stereotaxic atlas in coronal section, this region may correspond to the shell of the VMH. In rats, food restriction for 2 wk causes ectopic expression of 5HT-positive neurons in the ARC and VMH, thus this may imply thqt the c-Fos positive neurons in our study are serotonergic. That the VMH is a classical satiety-related nucleus [28, 29] implies that this may be the hypothalamic region causing the chick to reduce food intake following 5HT injection. Because the ARC is a circumventricular organ that receives and integrates signals from the periphery and then communicates with the other hypothalamic nuclei [30], results suggest that ICV 5HT is causing peripheral effects which are then secondarily signaling the hypothalamus. This is especially relevant as the blood-brain barrier is incomplete in 4 day post-hatch chicks.

5HT mediates food intake via its receptors 5HT1A, 5HT1B, and 5HT2C in mammals [11] and its mechanism of action involves stimulation of POMC neurons in the ARC, which further modulate the expression of the endogenous MC4 receptor antagonist agouti-related peptide (AgRP) and its agonist α-MSH [10]. In chicks it has also been shown that downstream melanocortin signaling is involved in 5HT-induced satiety via the MC4 receptor [11, 24]. Therefore, we conducted Experiment 4 in an attempt to further explore this mechanism in chicks. That mRNA for MC3 and MC4 receptors were not affected is not surprising as transcriptional changes are not necessary for existing receptors to bind ligand and cause cellular cascades. However, we did expect to detect a difference in POMC or AgRP if the 5HT mechanism was conserved during divergent evolution of birds and mammals. That these were not affected may imply that some other non-POMC derived ligand of MC4 mediates 5HT-satiety in chicks, or the effect is secondary to some other 5HT-induced behavior that is competitive with food intake. Additionally, Aromatic L-amino acid decarboxylase (DDC) is one of the major enzymes for both serotonin and dopamine biosynthesis, and both have been reported to have anorexigenic effects in chickens [31], and thus we assayed its expression to gauge effects associated with dopamine. Based on the results, no significant difference was found for DDC, as well as aldehyde dehydrogenase 1A1 (ALDH1A1), an enzyme that is associated with dopamine metabolism in mammals [32, 33].

Activation of the VMH after 5HT injection is associated with reduced meal number in rodents [34], and the VMH contains neurons that dynamically respond to blood glucose level in response to feeding [35, 36]. Thus, we determined whether blood glucose concentration was

affected by 5HT during the period of reduced food intake. Our result did not support that 5HT-induced satiety was associated with blood glucose availability in chicks.

Because our real-time PCR results do not support a direct effect on feeding circuitry known to mediate 5HT satiety as demonstrated in rodents, and that we propose the effect in chicks may be a secondary response, we designed Experiment 5 to measure other behaviors. Feeding pecks were reduced by 5HT injection, and although chicks are not meal eaters, in rodents 5HT reduced food intake by affecting meal number [34]. 5HT has been reported to induce sleep-like behavior in chickens [37, 38], where its administration induced eyelid closure, immobility, and lowered responsiveness to stimulation. 5HT was demonstrated as a neuromodulator of sleep in rodents [39] and is selectively involved in the regulation of the different sleep states depending on the activated area in the brain and receptors [40]. It has dense innervation to orexin neurons, known for their role in the coordination of arousal with food-seeking behavior [41, 42]. However, there is no reported evidence that orexins stimulate food intake in chicks [15]. Perhaps the reduced food intake that we observed after 5HT injection is a secondary effect to deep rest, which may be MC4-related. This is a thesis that warrants further exploration.

In sum, we have demonstrated that central injection of 5HT to chicks causes reduced food intake without an effect on water intake. This coincides with activation of the VMH and ARC, although POMC and AgRP do not appear to be associated with this response. Our results demonstrate that satiety after 5HT injection in chicks may be secondary to induced deep rest. This may indicate that 5HT is not a major regulator of food intake in chicks.

Reference

1. Rapport MM, Green AA, Page IH: **Serum vasoconstrictor, serotonin; isolation and characterization**. *The Journal of biological chemistry* 1948, **176**(3):1243-1251.
2. Rapport MM, Green AA, Page IH: **Crystalline Serotonin**. *Science* 1948, **108**(2804):329-330.
3. Mohammad-Zadeh LF, Moses L, Gwaltney-Brant SM: **Serotonin: a review**. *Journal of veterinary pharmacology and therapeutics* 2008, **31**(3):187-199.
4. Nichols DE, Nichols CD: **Serotonin receptors**. *Chemical reviews* 2008, **108**(5):1614-1641.
5. Blundell JE: **Serotonin and the biology of feeding**. *The American journal of clinical nutrition* 1992, **55**(1 Suppl):155S-159S.
6. Xu Y, Berglund ED, Sohn JW, Holland WL, Chuang JC, Fukuda M, Rossi J, Williams KW, Jones JE, Zigman JM *et al*: **5-HT2CRs expressed by pro-opiomelanocortin neurons regulate insulin sensitivity in liver**. *Nature neuroscience* 2010, **13**(12):1457-1459.

7. Xu Y, Jones JE, Kohno D, Williams KW, Lee CE, Choi MJ, Anderson JG, Heisler LK, Zigman JM, Lowell BB *et al*: **5-HT2CRs expressed by pro-opiomelanocortin neurons regulate energy homeostasis**. *Neuron* 2008, **60**(4):582-589.
8. Xu Y, Jones JE, Lauzon DA, Anderson JG, Balthasar N, Heisler LK, Zinn AR, Lowell BB, Elmquist JK: **A serotonin and melanocortin circuit mediates D-fenfluramine anorexia**. *The Journal of neuroscience : the official journal of the Society for Neuroscience* 2010, **30**(44):14630-14634.
9. Sohn JW, Xu Y, Jones JE, Wickman K, Williams KW, Elmquist JK: **Serotonin 2C receptor activates a distinct population of arcuate pro-opiomelanocortin neurons via TRPC channels**. *Neuron* 2011, **71**(3):488-497.
10. Heisler LK, Jobst EE, Sutton GM, Zhou L, Borok E, Thornton-Jones Z, Liu HY, Zigman JM, Balthasar N, Kishi T *et al*: **Serotonin reciprocally regulates melanocortin neurons to modulate food intake**. *Neuron* 2006, **51**(2):239-249.
11. Lam DD, Garfield AS, Marston OJ, Shaw J, Heisler LK: **Brain serotonin system in the coordination of food intake and body weight**. *Pharmacology, biochemistry, and behavior* 2010, **97**(1):84-91.
12. Fang XL, Shu G, Yu JJ, Wang LN, Yang J, Zeng QJ, Cheng X, Zhang ZQ, Wang SB, Gao P *et al*: **The anorexigenic effect of serotonin is mediated by the generation of NADPH oxidase-dependent ROS**. *PloS one* 2013, **8**(1):e53142.
13. Lajtha A: **The development of the bloodbrain barrier**. *Journal of neurochemistry* 1957, **1**(3):216-227.
14. Davis JL, Masuoka DT, Gerbrandt LK, Cherkin A: **Autoradiographic distribution of L-proline in chicks after intracerebral injection**. *Physiology & behavior* 1979, **22**(4):693-695.
15. Furuse M, Ando R, Bungo T, Ao R, Shimojo M, Masuda Y: **Intracerebroventricular injection of orexins does not stimulate food intake in neonatal chicks**. *British poultry science* 1999, **40**(5):698-700.
16. Anderson DK, Heisley SR: **Clearance of molecules from cerebrospinal fluid in chickens**. *The American journal of physiology* 1972, **222**(3):645-648.
17. Muller R, Bravo R, Burckhardt J, Curran T: **Induction of c-fos gene and protein by growth factors precedes activation of c-myc**. *Nature* 1984, **312**(5996):716-720.
18. Puelles L, Martinez-de-la-Torre M, Paxinos G, Watson C, Martinez S: **The Chick Brain in Stereotaxic Coordinates: An Atlas featuring Neuromeric Subdivisions and Mammalian Homologies**. Burlington: Academic Press; 2007.
19. Newmyer BA, Nandar W, Webster RI, Gilbert E, Siegel PB, Cline MA: **Neuropeptide Y is associated with changes in appetite-associated hypothalamic nuclei but not food intake in a hypophagic avian model**. *Behavioural brain research* 2013, **236**(1):327-331.
20. Schmittgen TD, Livak KJ: **Analyzing real-time PCR data by the comparative CT method**. *Nat Proto* 2008, **3**(6):1101-1108.
21. Piorkowska K, Oczkowicz M, Rozycki M, Ropka-Molik K, Piestrzynska-Kajtoch A: **Novel porcine housekeeping genes for real-time RT-PCR experiments normalization in adipose tissue: assessment of leptin mRNA quantity in different pig breeds**. *Meat science* 2011, **87**(3):191-195.

22. Denbow DM, Van Krey HP, Cherry JA: **Feeding and drinking response of young chicks to injections of serotonin into the lateral ventricle of the brain**. *Poultry science* 1982, **61**(1):150-155.
23. Denbow DM, Van Krey HP, Lacy MP, Dietrick TJ: **Feeding, drinking and body temperature of Leghorn chicks: effects of ICV injections of biogenic amines**. *Physiology & behavior* 1983, **31**(1):85-90.
24. Zendehdel M, Hamidi F, Babapour V, Mokhtarpouriani K, Fard RM: **The effect of melanocortin (Mc3 and Mc4) antagonists on serotonin-induced food and water intake of broiler cockerels**. *Journal of veterinary science* 2012, **13**(3):229-234.
25. Baranyiova E: **Effects of serotonin on the food intake in chickens in the post-hatching period**. *Acta Veterinaria Brno* 1990, **59**:23-33.
26. Morgan JI, Curran T: **Stimulus-transcription coupling in the nervous system: involvement of the inducible proto-oncogenes fos and jun**. *Annual review of neuroscience* 1991, **14**:421-451.
27. Paxinos G, Watson C: **The rat brain in stereotaxic coordinates**, 6th edn. Amsterdam ; Boston ;: Academic Press/Elsevier; 2007.
28. Brobeck JR: **Mechanism of the development of obesity in animals with hypothalamic lesions**. *Physiological reviews* 1946, **26**(4):541-559.
29. Kalra SP, Dube MG, Pu S, Xu B, Horvath TL, Kalra PS: **Interacting appetite-regulating pathways in the hypothalamic regulation of body weight**. *Endocrine reviews* 1999, **20**(1):68-100.
30. Arora S, Anubhuti: **Role of neuropeptides in appetite regulation and obesity--a review**. *Neuropeptides* 2006, **40**(6):375-401.
31. Richards MP: **Genetic regulation of feed intake and energy balance in poultry**. *Poultry science* 2003, **82**(6):907-916.
32. Bai X, Fermandez E, Gould G, Strong R: **Homozygous Deletion of Glutathione Peroxidase 1 and Aldehyde Dehydrogenase 1a1 Genes Is Not Associated with Schizophrenia-Like Behavior in Mice**. *Journal of biochemical and pharmacological research* 2013, **1**(4):228-235.
33. Anderson DW, Schray RC, Duester G, Schneider JS: **Functional significance of aldehyde dehydrogenase ALDH1A1 to the nigrostriatal dopamine system**. *Brain research* 2011, **1408**:81-87.
34. Meguid MM, Fetissov SO, Varma M, Sato T, Zhang L, Laviano A, Rossi-Fanelli F: **Hypothalamic dopamine and serotonin in the regulation of food intake**. *Nutrition* 2000, **16**(10):843-857.
35. King BM: **The rise, fall, and resurrection of the ventromedial hypothalamus in the regulation of feeding behavior and body weight**. *Physiology & behavior* 2006, **87**(2):221-244.
36. Oomura Y: **Chemical and neuronal control of feeding motivation**. *Physiology & behavior* 1988, **44**(4-5):555-560.
37. Furuse M, Cline MA, Bungo T, Sugahara K: **Neuroendocrine regulation of sedation and excitation in neonatal chicks**. New York: Nova Science Publishers, INC.; 2013.
38. Sabelli HC, Giardina WJ: **Tryptaldehydes (indoleacetaldehydes) in serotonergic sleep of newly hatched chicks**. *Arzneimittel-Forschung* 1970, **20**(1):74-80.

39. Jouvet M: **Sleep and serotonin: an unfinished story**. *Neuropsychopharmacology : official publication of the American College of Neuropsychopharmacology* 1999, **21**(2 Suppl):24S-27S.
40. Dugovic C: **Role of serotonin in sleep mechanisms**. *Revue neurologique* 2001, **157**(11 Pt 2):S16-19.
41. Muraki Y, Yamanaka A, Tsujino N, Kilduff TS, Goto K, Sakurai T: **Serotonergic regulation of the orexin/hypocretin neurons through the 5-HT1A receptor**. *The Journal of neuroscience : the official journal of the Society for Neuroscience* 2004, **24**(32):7159-7166.
42. Sakurai T: **Roles of orexin/hypocretin in regulation of sleep/wakefulness and energy homeostasis**. *Sleep medicine reviews* 2005, **9**(4):231-241.

Table 6.1 Real time PCR primers

Gene[1]	Accession No.	Sequences (forward/reverse)
POMC	NM_001031098.1	GCCAGACCCCGCTGATG/ CTTGTAGGCGCTTTTGACGAT
NPY	NM_205473.1	CATGCAGGGCACCATGAG/ CAGCGACAAGGCGAAAGTC
CRF	NM_001123031.1	TCAGCACCAGAGCCCATCACA/ GCTCTATAAAAATAAAGAGGTGACATCAGA
AgRP	XM_004950992.1	GGTTCTTCAACGCCTTCTGCTA/ TTCTTGCCACATGGGAAGGT
MC4R	NM_001031514.1	CCTCGGGAGGCTGCTATGA/ GATGCCCAGAGTCACAAACACTT
DDC	XM_004935144.1	TGGAATCCACCCACGTCAA/ TCGGTCGCCAGCTGTGA
ALDH1A1	NM_214399.1	CAGTGTTGTATAGCAGGATCCAGAA/ TCCGGCGAACAAACTCATC
MC3R	XM_004947236.1	GCCTCCCTTTACGTTCACATGT/ GCTGCGATGCGCTTCAC

**POMC*: proopiomelanocortin; *NPY*: neuropeptide Y; *CRF*: corticotropin-releasing factor; *AgRP*: agouti-related peptide; *MC4R*: melanocortin 4 receptor; *DDC*: aromatic L-amino acid decarboxylase; *ALDH1A1*: aldehyde dehydrogenase 1A1; *MC3R*: melanocortin 3 receptor

Table 6.2 Time type behavior after 5HT central injection

Behavior	Treatment	Time post injection (s)					
		300	600	900	1200	1500	1800
Deep rest	Vehicle	0	20.2±13.1	7.3±8.5	9.5±39.4	10.7±58.7	16.2±79.1
	Serotonin	0	21.7±13.6	23.1±8.9	164.8±39.4*	305±58.7*	438±79.1*
Sit	Vehicle	31.9±28.0	63.7±52.9	88.6±73.3	119.3±87.5	163.1±102.1	240.9±87.3
	Serotonin	68.2±29.3	165.3±55.3	273.5±76.6	344.7±91.4	403.4±106.6	342.3±95.5
Stand	Vehicle	242.1±28.7	454.6±58.9	653.9±85.5	836.4±110.9	1006.5±133.3	1151.6±156.8
	Serotonin	205.3±30.0	377.1±61.6	523.8±89.3	629.9±115.8	704.9±139.2	795.2±163.8
Preen	Vehicle	0	0	0	0.2±0.2	0.2±0.2	0.4±0.2
	Serotonin	0	0	0	0.5±0.2	0.6±0.2	0.7±0.2

Values represent least squares means ± SE. * indicates difference from vehicle within a time point for a behavior. Number of chicks are n=12 per treatment

Table 6.3 Count type behaviors after 5HT central injection

Behavior	Treatment	Time post injection (s)					
		300	600	900	1200	1500	1800
Feeding pecks	Vehicle	0.8±0.4	2.3±1.1	4.3±1.2	5.5±1.4	6.8±1.7	7.9±2.0
	Serotonin	0.8±0.6	1.4±1.1	1.9±1.6*	1.9±1.6*	2.3±1.7*	2.6±2.0*
Exploratory pecks	Vehicle	0.1±0.1	0.1±0.1	0.3±0.3	0.6±0.4	0.7±0.4	0.8±0.4
	Serotonin	0.1±0.1	0.2±0.2	0.4±0.4	0.5±0.4	0.6±0.4	0.7±0.4
Jumps	Vehicle	1.8±1.2	2.7±1.5	5.8±2.7	7.2±3.0	8.8±3.2	10.9±3.7
	Serotonin	0.2±0.2	0.8±0.4	1.2±0.7	1.2±0.8	1.3±0.8	1.5±0.8
Drinks	Vehicle	0	0	0.1±0.1	0.1±0.1	0.1±0.1	0.1±0.1
	Serotonin	0.1±0.1	0.1±0.1	0.1±0.1	0.1±0.1	0.3±0.3	0.4±0.4
Steps	Vehicle	26.1±9.9	75.0±25.3	120.3±36.1	157.8±42.7	188.5±49.1	222.5±59.8
	Serotonin	7.1±3.6	15.6±7.5*	25.1±14.4*	37.5±21.9*	45.0±24.7*	58.0±27.6*
Defecates	Vehicle	0.2±0.1	0.4±0.2	0.5±0.3	0.5±0.3	0.7±0.3	0.8±0.3
	Serotonin	0	0	0.1±0.1	0.1±0.1	0.2±0.1	0.2±0.1*
Chirps	Vehicle	97.0±27.7	199.6±51.7	275.6±58.9	365.2±75.2	451.8±90.4	527.6±106.4
	Serotonin	0.6±0.3*	17.0±15.9*	27.8±26.3*	41.4±39.2*	53.1±50.3*	75.0±62.4*

Values represent least squares means ± SEM. * indicates difference from vehicle within a time point for a behavior. Number of chicks are n=12 per treatment.

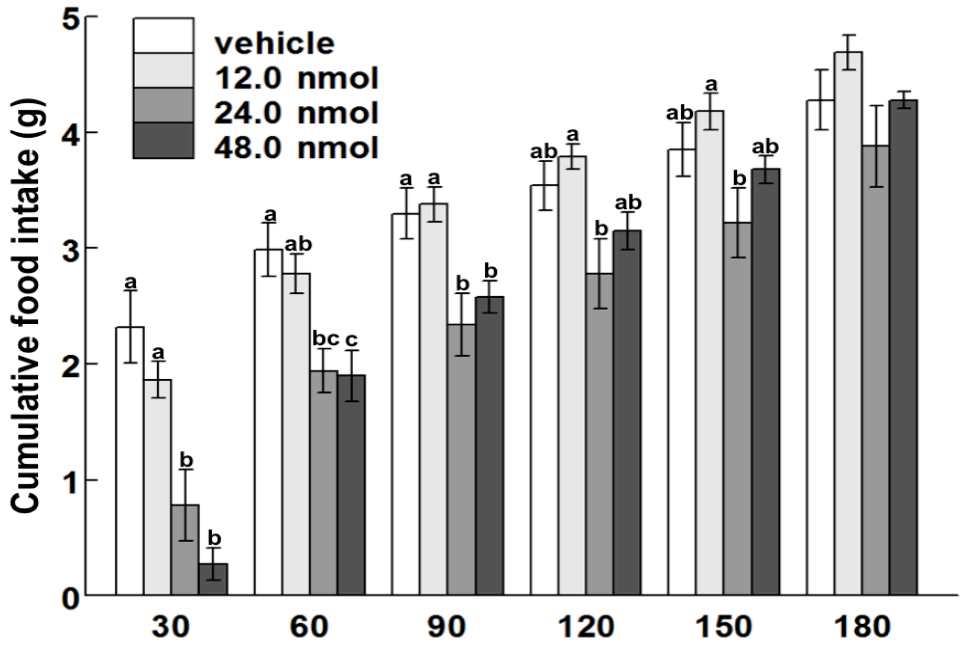

Figure 6.1 Cumulative food intake during 180 min post injection. Data are expressed as means ± standard errors. Bars with different letters are different from each other within a time point (P<0.05). Number of birds are n=10 per treatment.

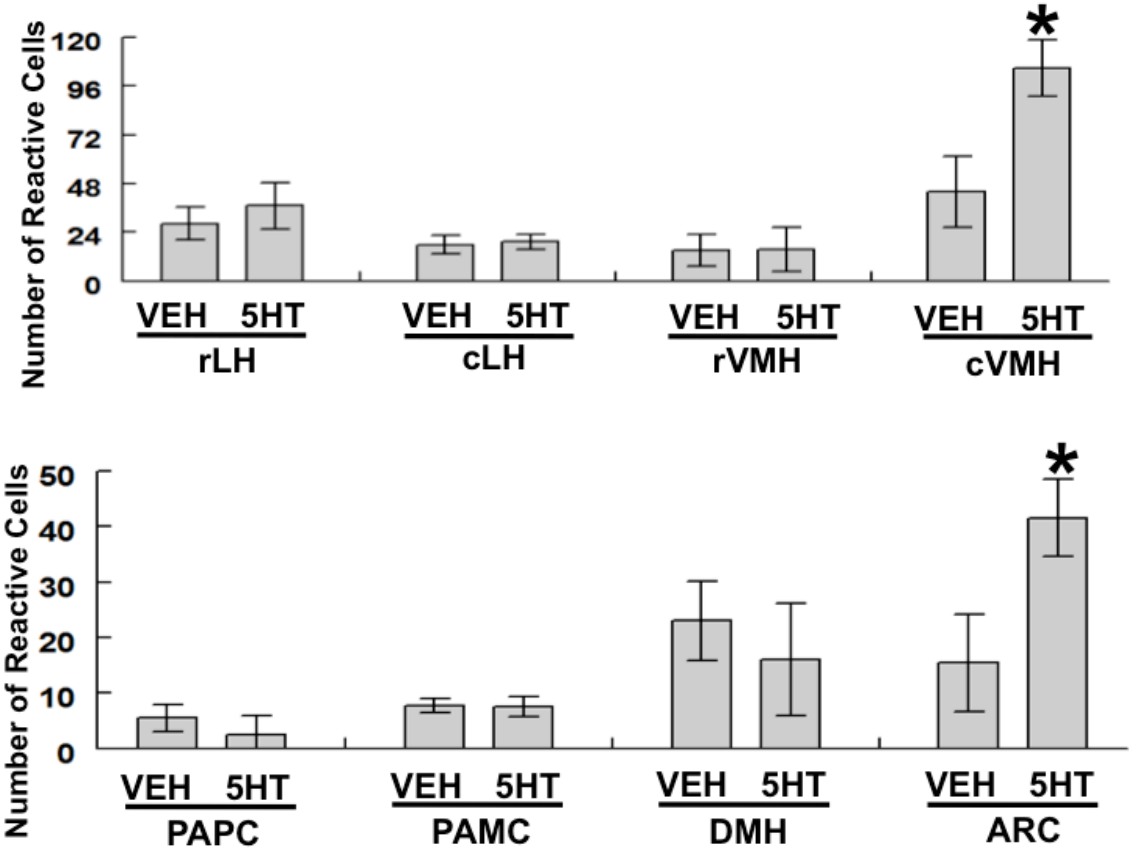

Figure 6.2 c-fos immunohistochemistry in the hypothalamus of 5 day-old chicks. rLH: rostral lateral hypothalamus; cLH: caudal lateral hypothalamus; rVMH: rostral ventromedial nucleus; cVMH: caudal ventromedial nucleus; PAPC and PAMC: paraventricular hypothalamic nucleus; DMH: dorsomedial hypothalamic nucleus; ARC: arcuate nucleus. Values represent means and standard errors (n=10). *Different from vehicle within a nucleus, $P < 0.05$. VEH: vehicle-injected chicks; 5HT: 48 nmol 5HT-injected chicks.

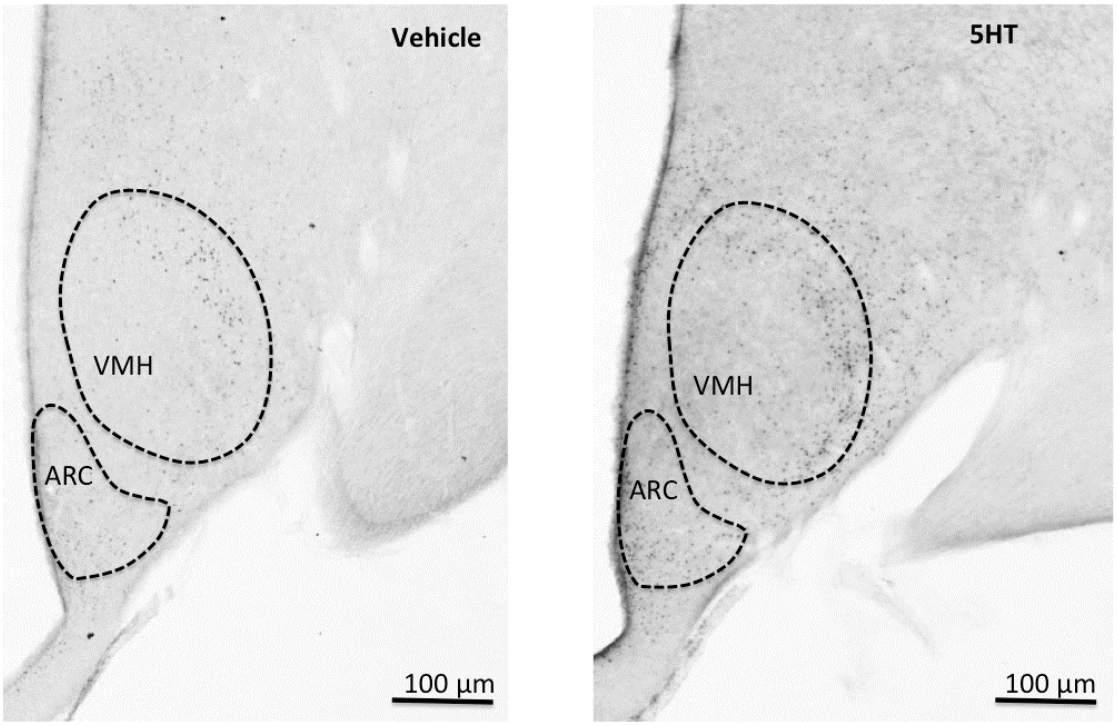

Figure 6.3 c-Fos immunoactivity of ventromedial hypothalamus (VMH) and arcuate (ARC) at interaural 1.12 mm.

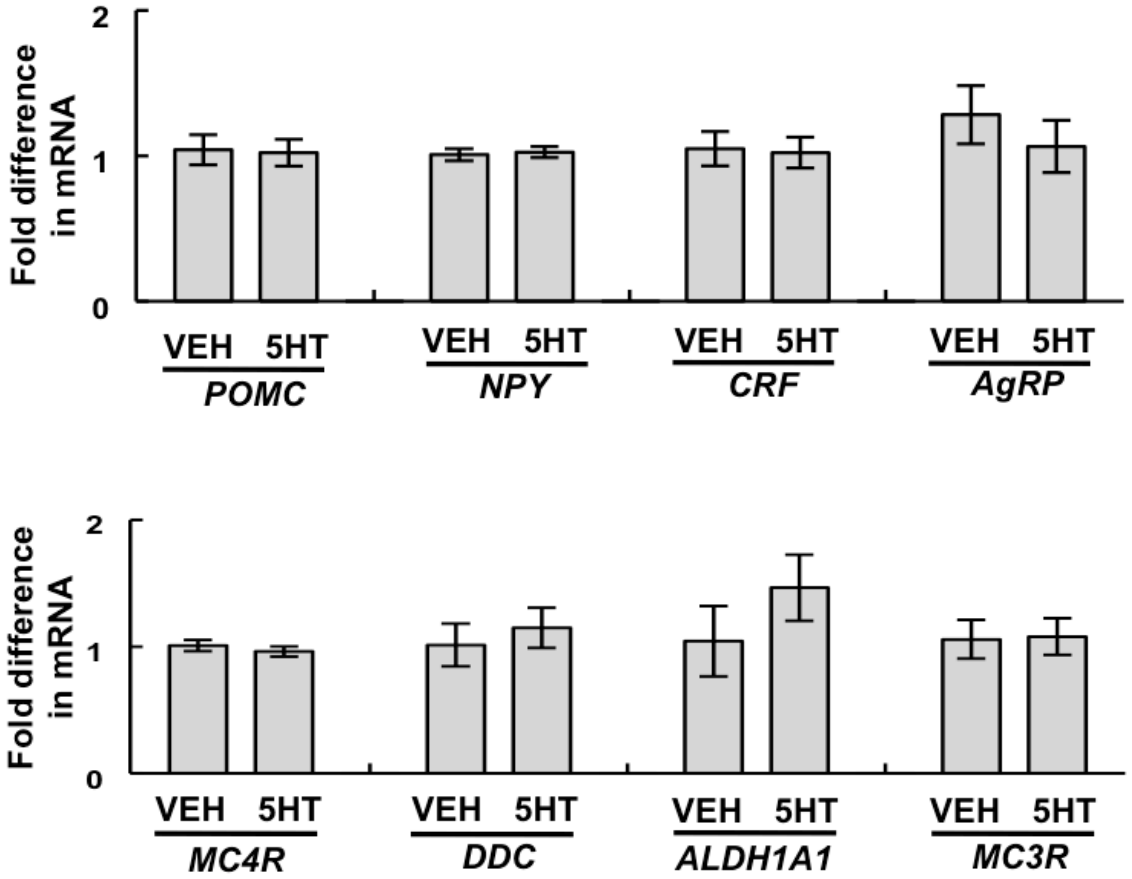

Figure 6.4 Relative mRNA expression of appetite regulatory factors in the hypothalamus. *POMC*: proopiomelanocortin; *NPY*: neuropeptide Y; *CRF*: corticotropin-releasing factor; *AgRP*: agouti-related peptide; *MC4R*: melanocortin 4 receptor; *DDC*: aromatic L-amino acid decarboxylase; *ALDH1A1*: aldehyde dehydrogenase 1A1; *MC3R*: melanocortin 3 receptor Values represent means and standard errors (n=10). VEH: vehicle-injected chicks; 5HT: 48 nmol 5HT-injected chicks.

Chapter 7

Knockdown of *ZBED6* is not associated with changes in murine preadipocyte proliferation or differentiation

Abstract: ZBED6 was identified as a transcription factor that affects muscle mass and fat deposition in pigs. Mechanisms mediating effects on fat mass are unclear. The objective was to determine the effect of *ZBED6* mRNA knockdown on 3T3-L1 preadipocyte differentiation and gene expression. Differentiation was associated with increased mRNA abundance of *CEBP/α* ($P < 0.05$), *CEBP/β* ($P < 0.05$), *CEBP/δ* ($P < 0.05$), *FASN* ($P < 0.05$), *PPARγ* ($P < 0.05$) and *SREBP-1* ($P < 0.05$), and decreased abundance of *PREF-1* ($P < 0.05$). Knockdown of *ZBED6* was not associated with changes in mRNA abundance of selected genes, lipid accumulation, lipid droplet size or cell number. These results suggest that ZBED6 does not play a major role in preadipocyte differentiation.

Introduction

Modern commercial pigs selected for lean meat production have increased skeletal muscle mass and reduced backfat thickness compared with their ancestor, the European wild boar. Gene mapping studies revealed a single nucleotide transition from G to A in intron 3 of the insulin-like growth factor 2 (*IGF2)* gene as being responsible for much of the difference in body composition between lean pigs and wild boars[1]. This mutation is located in a CpG site surrounded by a 16 bp evolutionarily conserved region [1]. It is associated with threefold greater postnatal expression of *IGF2* mRNA in skeletal muscle and heart and accounted for 3-4% increased skeletal muscle mass and reduced backfat thickness in pigs that carry the mutation on the paternal allele [2]. The mechanism underlying the effect of the *IGF2* mutation is partly understood, as it disrupts

binding with a recently identified transcription factor, ZBED6, a domesticated DNA transposon, unique to placental mammals, located in intron 1 of a "host" gene called *Zc3h11a* [3]. Chromatin immunoprecipitation experiments indicated that ZBED6 has thousands of potential target sites associated with growth, cell differentiation, transcriptional regulation, development and neurogenesis in C2C12 mouse myoblast cells. The role of ZBED6 in other tissues is unclear. Because the *IGF2* mutation is associated with reduced backfat accumulation in pigs, we hypothesized that ZBED6 might play a role in adipogenesis.

Adipocytes are derived from mesenchymal stem cells that differentiate into preadipocytes, when then terminally differentiate into adipocytes [4]. In vitro, following induction with differentiation media containing a cocktail of insulin, dexamethasone and isobutylmethylxanthine (a non-selective phosphodiesterase inhibitor), preadipocytes will undergo growth arrest and one round of clonal expansion, followed by terminal differentiation. Adipose tissue accumulation involves extensive cellular remodeling and is dependent on the coordinated interplay between adipocyte hypertrophy and hyperplasia. There is no evidence that ZBED6 and IGF2 are directly associated with fat deposition or that ZBED6 regulates *IGF2* transcription in adipocytes. In this study we investigated the effect of *ZBED6* knockdown on adipocyte differentiation and *IGF2* expression with the goal to provide novel insight on the function of ZBED6 as well as molecular mechanisms underlying adipocyte differentiation and fat deposition.

Materials and Methods

Animals

All procedures were approved by the Institutional Animal Care and Use Committee at Virginia Tech. Six month-old male C57B6/N mice were obtained from the National Cancer Institute of NIH and housed individually in standard sized cages (29 x 14 x 13 cm) arranged in a double-faced 140-cage ventilation rack in a temperature and humidity controlled, pathogen-free room on a 12 h light cycle (6 am to 6 pm) with free access to a standard rodent chow (Research Diet, Inc, New Brunswick, New Jersey). Eight animals were euthanized by CO_2 asphyxiation after an overnight fast and gonadal fat pads and gastrocnemius skeletal muscle removed and submerged in RNAlater (Qiagen, CA, USA).

Cell culture

The 3T3-L1 cells (Eton Bioscience Inc.) were cultured in preadipocyte growth media (DMEM high-glucose, 10% fetal bovine serum, penicillin/streptomycin; Hyclone, Thermo Fisher Scientific) at 37°C in a humidified atmosphere of 5% CO_2, according to the supplier's instructions. Culture medium was changed every other day. At 70-80% confluence, cells were trypsin-digested for further sub-culturing or seeded into 12-well plates (Falcon, MA, USA) for siRNA transfection and induction of differentiation. Passages less than 4 were used for these experiments.

RNA interference

Three *ZBED6* specific siRNA oligonucleotides were designed to target three different regions of mouse *ZBED6* mRNA (Ambion) [2]. Scrambled siRNA (silencer select No. 2; Ambion) was used as a negative control [2]. The RNA interference was performed as previously described [2]. Briefly, suspensions containing 100,000 cells/mL were reverse transfected in triplicate with siRNA using lipofectamine 2000 (Invitrogen,

CA, USA) and Optimem-I reduced serum media (Invitrogen, CA, USA) with the 3 siRNAs pooled at equal amounts to a final concentration of 50 n*M*. Triplicate wells of non-transfected cells were also included. To evaluate the effects of *ZBED6* knockdown on cell growth and morphology, cells were imaged daily with a digital inverted microscope (EVOS). The average of the triplicates within an assay was considered the experimental unit and the experiment was repeated at least 3 times on independent passages of cells.

Adipocyte differentiation

Preadipocytes were induced to differentiate into adipocytes based on the following induction protocol for 2 weeks: At 48 h post-siRNA transfection, media was changed to complete adipogenic induction media (growth media containing 5 µg/ml insulin (Sigma-Aldrich, MO, USA), 1µ*M* dexamethasone (Sigma-Aldrich, MO, USA), and 0.5 m*M* isobutylmethylxanthine; Sigma) and incubated for 3 d, then changed to maintenance media (growth media containing 5 µg/ml insulin, 1 µ*M* dexamethasone). Maintenance media was changed every two days.

Cell viability assay

Cell viability was evaluated at day 0 (48 hours post-siRNA transfection), and days 1 and 8 post-induction of differentiation with Alamar blue reagent (Invitrogen, CA, USA). Alamar blue reagent was added to each well of 12-well plates and incubated for 1 to 4 hours. Absorbance was measured at 570 nm (reduced) and 600 nm (oxidized) using a multi-mode plate reader (M200 Pro; Tecan Instruments). Cell viability was calculated as the ratio of reduced/oxidized relative to the negative control group.

Oil Red O staining

Cells were fixed with 10% formalin for 30 min at room temperature and Oil Red O staining performed according to the manufacturer's instructions (American Master Tech). Propylene glycol was added to each well and incubated for 5 minutes, replaced with Oil Red O working solution and incubated for another 5 minutes at room temperature, and rinsed with water. Absorbance was measured at 490 nm to estimate lipid accumulation. Cells were then counterstained with hematoxylin and imaged to estimate the number of adipocytes and size of lipid droplets.

Total RNA isolation and real time PCR

At 48, 144 and 216 hours post-siRNA transfection (Day 0, 4 and 7 relative to induction of adipocyte differentiation), cells were washed with phosphate-buffered saline and lysed with a 21 gauge needle in 350 µL RLT buffer (Qiagen Science, USA). The total RNA was extracted with the RNeasy Mini kit (Qiagen Sciences, USA) according to the manufacturer's instructions. An on-column RNase-Free DNase I (Qiagen Science, USA) treatment was incorporated to eliminate genomic DNA carry-over in the RNA preparations. The eluted total RNA samples were quantified and assessed for purity by spectrophotometry at 260/280/230 nm using a Nanophotometer^{TM} Pearl (IMPLEN), and integrity evaluated by agarose gel electrophoresis. The first strand cDNA was synthesized from total RNA using the High Capacity cDNA Reverse Transcription kit (Applied Biosystems). Primers were designed in Primer Express 3.0 (Applied Biosystems; **Table 7.3**). All primers were evaluated for amplification efficiency before use. Efficiency of target genes was within 5% of the house keeping gene (*18S* rRNA). A total volume of 10 µL in each reaction contained 5 µL fast SYBR Green Master Mix (Applied Biosystems), 0.25 µL each of 5 µM forward and reverse primers, and 1 µL of cDNA. Real-time PCR

reactions were performed in duplicate for all samples on an Applied Biosystems 7500 FAST system, under the following conditions: enzyme activation for 20 sec at 95°C and 40 cycles of 1) melting step for 3 seconds at 95°C and 2) annealing/extension step for 30 seconds at 60°C. Melting curve analysis was performed after all reactions to ensure amplification specificity.

For tissue samples collected in RNAlater, approximately 200 mg was homogenized with a Tissue Lyser II (Qiagen, USA) twice at 20 Hz for 2 minutes using 5 mm stainless steel beads (Qiagen, USA) and 1 mL isol-RNA lysis reagent (5-PRIME). Samples were then centrifuged at 12,000 x g for 10 min at 4°C, supernatant transferred and mixed with 0.2 mL chloroform, and centrifuged again under the same conditions. The supernatant was removed and mixed with an equal volume of 70% ethanol and loaded onto a spin column and total RNA purified according to the manufacturer's instructions (Qiagen RNeasy Mini). An on-column RNase-Free DNase I (Qiagen, USA) treatment step was included. Reverse transcription and real time PCR were performed as described above.

Statistical Analysis

The real time PCR data for cells were analyzed using the $\Delta\Delta C_T$ method, where $\Delta C_T = C_{T\ \text{target gene}} - C_{T\ 18S}$, and $\Delta\Delta C_T = \Delta C_{T\ \text{target sample}} - \Delta C_{T\ \text{calibrator}}$ [11]. To evaluate the effect of *ZBED6* knockdown on gene expression, the negative control was used within a time point as the calibrator sample. In non-transfected cells, the day 0 values were used as the calibrator to evaluate changes in gene expression during differentiation. The relative quantity ($2^{-\Delta\Delta Ct}$) values were subjected to ANOVA using the Proc Glimmix procedure of SAS. The statistical model included the main effect of treatment for

ZBED6-knockdown cells and main effect of time for non-transfected cells. A similar model was used for cell viability (normalized absorbance), lipid accumulation (Oil Red O normalized absorbance) and cell morphology data. Tukey's test was used for pairwise comparisons across time points. For tissue real time PCR data, the skeletal muscle was used as the calibrator, and differences between muscle and fat tested using Student's t-test. Results were considered significant at $P < 0.05$.

Results and Discussion

Because the *IGF2* mutation discovered in pigs is associated with enhanced muscle mass and reduced backfat, with the mechanism involving the release of postnatal ZBED6-mediated transcriptional repression of *IGF2* in skeletal muscle, we hypothesized that ZBED6 may also play a role in regulating adipose tissue expansion. In this study we evaluated the effects of knocking down *ZBED6* mRNA on 3T3-L1 mouse preadipocyte proliferation and differentiation. There was 81% knockdown efficiency at 48 h post-*ZBED6* siRNA transfection. Knockdown efficiency was reduced from 81 % at 48 h to 40 % at 96 h post-transfection. It is possible that ZBED6 exerts effects at later stages of differentiation, however with the transient nature of siRNA transfections is difficult to assess the role of ZBED6 at later stages of differentiation without a stable knockdown approach. Cell viability was evaluated to investigate how *ZBED6* knockdown affects preadipocyte proliferation, as knockdown in C2C12 mouse myoblasts was associated with increased proliferation at 3 days post-silencing [2]. There were no significant differences at 48 or 216 hours post-siRNA transfection (day 0 and 7 relative to initiation of differentiation, respectively) in cell viability (normalized relative absorbance) between *ZBED6* siRNA-transfected cells and scrambled siRNA cells (overall treatment means:

1.04±0.016 vs. 1.05±0.016, respectively; $P = 0.6$). Similarly, there were no changes in lipid accumulation between the *ZBED6* siRNA group (0.081 ±0.002) and scrambled siRNA cells (.084±0.002) at 7 days post-differentiation ($P = 0.5$), as measured by absorbance following Oil Red O staining (**Figure 7.1**). The area and numbers of adipocytes were also not different among treatment groups.

The mRNA abundance results for non-transfected cells showed that several genes were up- or down-regulated during 3T3L1 cell differentiation (**Table 7.2**). Differentiation was associated with an increase in *CEBP/α* (> 15-fold; $P < 0.05$), *CEBP/β* (2-fold; $P < 0.05$), *CEBP/δ* (>20-fold; $P < 0.05$), *FASN* (1.5-fold; $P < 0.05$), *PPARγ* (> 15-fold; $P < 0.05$) and *SREBP-1* (5-fold; $P < 0.05$) mRNA at days 4 and 7 relative to day 0, and decrease in *PREF-1* (2-fold; $P < 0.05$) at 4-days post-induction of differentiation compared to day 0 (**Table 7.2**). These results are consistent with other reports of transcriptional events mediated during adipocyte differentiation [5].

Adipocyte differentiation was not associated with a change in *ZBED6* or *IGF2* mRNA abundance, although it should be noted that both preadipocytes and adipocytes expressed very low levels of *IGF2* as estimated from raw C_T data, which may also explain the high variability among the biological replicates. Knockdown of *ZBED6* was not associated with any differences in expression of adipogenesis-associated factors or *IGF2* (**Table 7.3**). These results are in contrast to effects in myoblasts, where knockdown of *ZBED6* was associated with enhanced differentiation into myotubes at 6 days post-induction of differentiation [2]. Insulin-like growth factor 2 plays a role in tumor progression, and there was a report that increased expression of *IGF2* was associated with reduced adipocyte differentiation in human hemangioma cells [6]. In the present study,

mRNA abundance of *ZBED6* and *IGF2* was measured in skeletal muscle and white adipose tissue of adult mice, with approximately twofold greater expression of both genes in skeletal muscle (**Figure 7.2**), consistent with the idea that ZBED6 plays a more prominent role in skeletal muscle as compared to fat.

In summary, we did not find any evidence that ZBED6 plays a role in mouse preadipocyte proliferation or differentiation, or that *IGF2* expression in these cells was dependent on the presence of ZBED6. It is possible that *IGF2* does not play a critical role in the maintenance and differentiation of 3T3L1 cells, as expression was almost undetectable and was not affected by induction of differentiation. These results are consistent with the current theory that the effect of the *IGF2* mutation in pigs is to partition energy towards muscle mass accretion at the expense of white adipose tissue accumulation (i.e., dependent on *IGF2* expression in skeletal muscle rather than adipose tissue) [2, 3]. One caveat to the present study though, is that 3T3-L1 cells are a clonal mouse-derived cell live with an unstable karyotype and may not be representative of in-vivo adipogenesis between fat depots of different species. Expression and secretion of IGF2 was reported in white adipose tissue of humans [7] and neonatal pigs [8], and in pigs it was demonstrated that *IGF2* was expressed in the stromal-vascular fraction of white adipose tissue with expression decreasing after induction of adipocyte differentiation [9]. Our real time PCR results are consistent with a report showing by northern blot, a far less sensitive method for detecting mRNA, that *IGF2* was not expressed in 3T3-L1 cells [10]. With respect to transcriptional regulation of *IGF2* in 3T3-L1 cells, it is possible that ZBED6 doesn't repress *IGF2* in these cells or that other co-factors also contribute to suppressing *IGF2* expression in 3T3-L1 cells. Moreover,

ZBED6 may play a different role in fatness, through effects on adipocyte hypertrophy, which was not addressed in this study because of the multilocular nature of differentiated 3T3-L1 cells.

References

1. Van Laere AS, Nguyen M, Braunschweig M, Nezer C, Collette C, Moreau L, Archibald AL, Haley CS, Buys N, Tally M *et al*: **A regulatory mutation in IGF2 causes a major QTL effect on muscle growth in the pig**. *Nature* 2003, **425**(6960):832-836.
2. Markljung E, Jiang L, Jaffe JD, Mikkelsen TS, Wallerman O, Larhammar M, Zhang X, Wang L, Saenz-Vash V, Gnirke A *et al*: **ZBED6, a novel transcription factor derived from a domesticated DNA transposon regulates IGF2 expression and muscle growth**. *PLoS Biol* 2009, **7**(12):e1000256.
3. Andersson L, Andersson G, Hjalm G, Jiang L, Lindblad-Toh K, Lindroth AM, Markljung E, Nystrom AM, Rubin CJ, Sundstrom E: **ZBED6: The birth of a new transcription factor in the common ancestor of placental mammals**. *Transcription* 2010, **1**(3):144-148.
4. Poulos SP, Dodson MV, Hausman GJ: **Cell line models for differentiation: preadipocytes and adipocytes**. *Exp Biol Med (Maywood)* 2010, **235**(10):1185-1193.
5. Ntambi JM, Young-Cheul K: **Adipocyte differentiation and gene expression**. *The Journal of nutrition* 2000, **130**(12):3122S-3126S.
6. Kleiman A, Keats EC, Chan NG, Khan ZA: **Elevated IGF2 prevents leptin induction and terminal adipocyte differentiation in hemangioma stem cells**. *Experimental and molecular pathology* 2013, **94**(1):126-136.
7. Gude MF, Frystyk J, Flyvbjerg A, Bruun JM, Richelsen B, Pedersen SB: **The production and regulation of IGF and IGFBPs in human adipose tissue cultures**. *Growth hormone & IGF research : official journal of the Growth Hormone Research Society and the International IGF Research Society* 2012, **22**(6):200-205.
8. Hausman GJ, Poulos SP, Richardson RL, Barb CR, Andacht T, Kirk HC, Mynatt RL: **Secreted proteins and genes in fetal and neonatal pig adipose tissue and stromal-vascular cells**. *Journal of animal science* 2006, **84**(7):1666-1681.
9. Gardan D, Mourot J, Louveau I: **Decreased expression of the IGF-II gene during porcine adipose cell differentiation**. *Molecular and cellular endocrinology* 2008, **292**(1-2):63-68.
10. Boney CM, Moats-Staats BM, Stiles AD, D'Ercole AJ: **Expression of insulin-like growth factor-I (IGF-I) and IGF-binding proteins during adipogenesis**. *Endocrinology* 1994, **135**(5):1863-1868.
11. Schmittgen TD, Livak KJ: **Analyzing real-time PCR data by the comparative CT method**. *Nat Proto* 2008, **3**(6):1101-1108.
12. Symonds ME: **Adipose tissue biology**; 2011.

Table 7.1 Primers used for real time PCR

Gene[1]	Accession No.	Sequences (forward/reverse)
PREF-1	NM_001190705.1	CCAACGTGACCAAAGATCAAGA/
		GGATGCCGTGGAATTTTGAC
C/EBPα	NM_007678.3	CAGTTGGGCACTGGGTGGGC/
		CCGCGGCTCCACCTCGTAGAAG
C/EBPβ	NM_009883.3	CGCAACACACGTGTAACTGTCA/
		AACAACCCCGCAGGAACAT
C/EBPδ	NM_007679.4	TCCAACCCCTTCCCTGATC/
		CCCTGGAGGGTTTGTGTTTTC
SREBP-1	NM_011480.3	GCCTAGTCCGAAGCCGGGTG/
		GGAGCATGTCTTCGATGTCGTTCA
PPARγ	NM_001127330.1	GCCTGCGGAAGCCCTTTGGT/
		AAGCCTGGGCGGTCTCCACT
FASN	NM_001146708.1	TGCCAACCTGAAAACTAGGCTGAG/
		TACCCACCCCACCCCCTTCTC
GPDH	NM_001145820.1	AGAGCTGCAGGCCGAGTCCC/
		GCTCAGCCTGATCACCCGTCGC
ZBED6	NM_001166552.1	CAAGACATCTGCAGTTTGGAATTT/
		TGTCGTTGAAGTGTTGAAGTTCCTA
IGF2	NM_001122737.1	CGTGGCATCGTGGAAGAGT/
		ACACGTCCCTCTCGGACTTG
18S	NR_003278.3	ACCTGGTTGATCCTGCCAGTAG/

	TTAATGAGCCATTCGCAGTTTC

[1]Primers were designed for a variety of genes associated with adipogenesis, as reviewed by [12]. Preadipocyte Factor 1 (*PREF-1*) encodes a preadipocyte secreted factor that serves as a marker for preadipocytes. The CCAAT/enhancer Binding Protein (CEBP) α and β activate expression of PPARγ and are required for preadipocyte differentiation, while CEBP/δ and Sterol Regulatory Element-Binding Protein-1 (SREBP-1) accelerate but are not required for differentiation. Peroxisome Proliferator-Activated Receptor γ (PPARγ) is the master transcriptional regulator of adipogenesis and is involved in the growth arrest that is required for differentiation. Also investigated in this study was expression of fatty acid synthase (*FASN*), a key enzyme in de novo lipogenesis that catalyzes the synthesis of saturated fatty acids, and glycerol-3-phosphate-dehydrogenase (*GPDH*), an enzyme that catalyzes the reversible conversion of dihydroxyacetone phosphate to sn-glycerol-3-phosphate. Expression of zinc finger, BED-type containing 6 (*ZBED6*) and insulin-like growth factor 2 (*IGF2*) was also evaluated. The 18S ribosomal subunit served as the endogenous control

Table 7.2 Gene expression in non-transfected 3T3-L1 cells at 0, 4 and 7 days post-induction of adipocyte differentiation[1]

day	*Cebp/α*	*Cebp/β*	*Cebp/δ*	*FASN*	*GPDH*	*IGF2*	*PPARϒ*	*PREF-1*	*SREBP-1*	*ZBED6*
0	1.0±5.7^{b}	1.0±0.1^{b}	1.1±2.7^{b}	1.0±0.1^{b}	1.08±0.4^{a}	1.7±16^{a}	1.02±2.8^{b}	1.00±0.1^{a}	1.00±0.3^{c}	1.04±0.2^{a}
4	17.8±5.7^{a}	2.1±0.1^{a}	21.9±2.7^{a}	1.6±0.1^{a}	1.04±0.4^{a}	28.8±16^{a}	15.84±2.8^{a}	0.59±0.1^{b}	5.22±0.3^{a}	2.04±0.2^{a}
7	16.1±7.0^{a}	1.7±0.1^{a}	16.9±3.3^{a}	1.3±0.1^{a}	1.4±0.5^{a}	13±19^{a}	11.54±3.5^{a}	1.01±0.1^{a}	2.5±0.3^{b}	1.75±0.3^{a}

[1]LSmeans ± pooled SEM; mRNA abundance calibrated to day 0 within a gene. Different letter within a column indicates $P<0.05$, Tukey's test, n=3 experiments

Table 7.3 Effects of *ZBED6* mRNA knockdown on gene expression at day 0, day 4 and day 7 post-differentiation[1]

Treatment	Day	*C/EBPα*	*C/EBPβ*	*C/EBPδ*	*FASN*	*GPDH*	*PPARγ*	*PREF-1*	*SREBP-1*	*IGF2*	*ZBED6*
Scrambled	0	1.0±0.7	1.0±0.1	1.1±0.2	1.0±0.1	1.0±0.3	1.0±0.3	1.0±0.1	1.0±0.1	1.2±5.4	1.07±0.2[a]
siZBED6	0	0.7±0.7	0.7±0.1	0.6±0.2	0.9±0.1	0.6±0.3	0.8±0.3	0.9±0.1	1.1±0.1	1.7±5.4	0.2±0.2[b]
Scrambled	4	1.3±0.7	1.0±0.1	1.0±0.2	1.0±0.1	1.1±0.3	1.1±0.3	1.0±0.1	1.0±0.1	4.4±5.4	1.1±0.2[a]
siZBED6	4	1.9±0.7	1.0±0.1	0.8±0.2	0.8±0.1	0.9±0.3	1.3±0.3	1.0±0.1	1.1±0.1	7.6±5.4	0.4±0.2[b]
Scrambled	7	1.4±0.8	1.0±0.1	1.2±0.3	1.0±0.1	1.3±0.4	1.3±0.4	1.0±0.1	1.0±0.1	1.1±6.6	1.09±0.2
siZBED6	7	1.8±0.8	1.0±0.1	0.9±0.3	0.9±0.1	1.2±0.4	1.2±0.4	0.9±0.1	1.0±0.1	0.6±6.6	0.8±0.2

[1]LSmeans ± pooled SEM; mRNA abundance calibrated to the scrambled siRNA group within a time point. Different letter within a column and day indicates $P<0.05$, Tukey's test, n=3 experiments

A. *ZBED6* siRNA

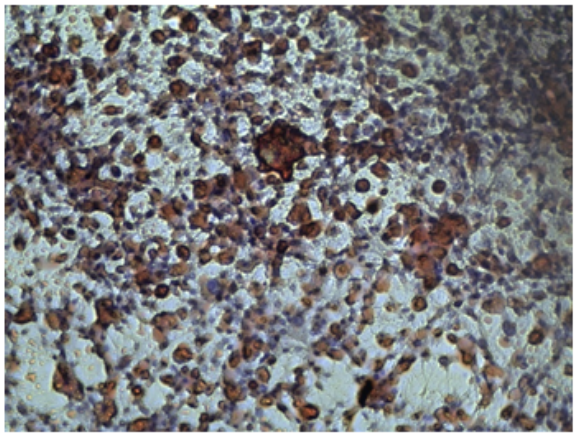

B. Scrambled siRNA

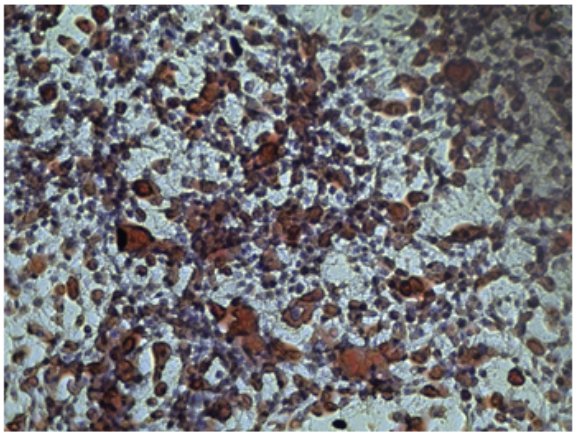

C. Non-transfected

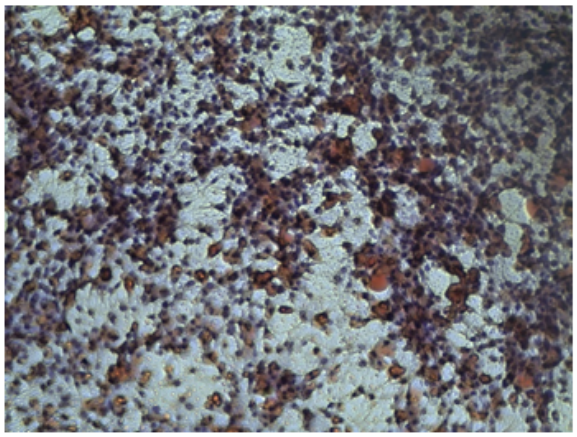

Figure 7.1 Oil Red O staining at day 7 post-induction of differentiation in zinc finger, BED-type containing 6 (*ZBED6)* siRNA-transfected (A), scrambled siRNA (B) and non-transfected 3T3-L1 cells (C). Differentiation was induced at 48 hours post-transfection (n = 3).

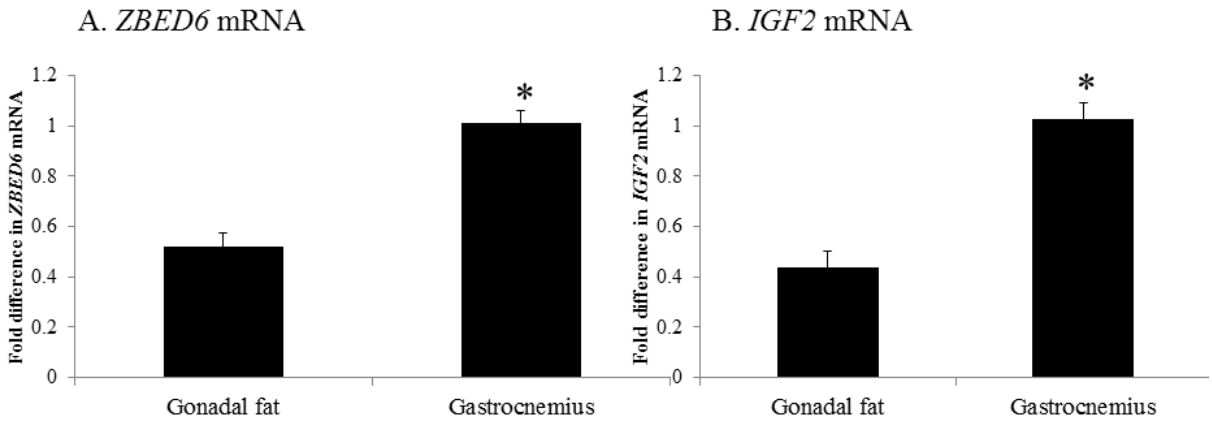

Figure 7.2 Relative abundance of zinc finger, BED-type containing 6 (*ZBED6)* (A) and insulin-like growth factor 2 (*IGF2)* (B) mRNA in gonadal fat and gastrocnemius skeletal muscle of 6 month-old male C57B6/N mice. Values represent LSmeans ± pooled SEM (n=8). *$P < 0.0001$.

Chapter 8

Porcine prepubertal obesity is associated with altered adipokine gene expression in both visceral and subcutaneous adipose tissue

Abstract: Obesity is associated with mild inflammation that originates in white adipose tissue, with metabolic differences between different fat depots. The objective of this study was to determine body composition and expression of adipokines and pro-inflammatory cytokines in adipose tissue of porcine with prepubertal obesity induced by high fat and high energy diet. Pigs were randomly divided into 4 dietary treatment groups (n=6), including 1) control or high-fat (HF) diets that contained 2) complex carbohydrates (CC) or refined sugars (SC) in the form of 3) glucose or 4) fructose. After 56 day, pigs were weighed and euthanized. Subcutaneous, mesenteric, and perirenal fat were harvested for expression analysis. Weight gain was similar among treatments ($P = 0.81$) whereas body fat composition significantly increased in high fat pigs as compare to the control. Dietary treatment (glucose > control; $P<0.05$) and fat depot (perirenal fat > subcutaneous; $P<0.05$) affected adiponectin expression. Pigs consumed the CC diet has greater pro-inflammatory factors, such as MCP1 and TNFα ($P < 0.05$), than the control diet. HIF1 expression was significantly higher in perirenal fat than subcutaneous and mesenteric fat. The TNFα mRNA was more abundant in perirenal fat as compared with mesenteric fat ($P<0.05$). Visfatin expression was significantly higher in perirenal fat and mesenteric fat than subcutaneous fat. In summary, these data demonstrate that high-fat diets are associated with increased adipokine gene expression, and independent of diet effects, adipokines display site-specific differences in gene expression that may help explain regional differences in adipose tissue inflammation.

Introduction

The prevalence of obesity has increased dramatically in recent years, with more than 30% of US adults now classified as being overweight or obese [1]. Obesity is a predisposing risk factor for other health complications such as arthritis, diabetes, hypertension, cardiovascular disease and certain types of cancer. Because of the lack of effective preventative and therapeutic strategies for combatting obesity, insulin resistance, and type 2 diabetes, there is an imperative need for animal models that more closely mimic the human condition. Obesity in humans is associated with chronic mild inflammation in white adipose tissue and insulin resistance, predisposing an individual to diabetes. Mechanisms underlying the cause of inflammation and site-specific differences in inflammation throughout the body are unclear.

Adipose tissue is the largest endocrine organ in most humans [2, 3], secreting a wide range of hormones and cytokines (adipokines) such as leptin, adiponectin, resistin, visfatin, tumor necrosis factor α (TNFα), Interleukin-6 (IL6), monocyte chemo attractant protein-1 (MCP1), plasminogen activator inhibitor-1 (PAI1) and hypoxia-inducible factor-1 (HIF1), which play various roles in food intake regulation, insulin resistance, lipid metabolism, inflammation, macrophage recruitment and fibrinolysis [4, 5].

White adipose tissue can be categorized into different depots based on regional accumulation and metabolic characteristics. Visceral fat that surrounds the organs is associated with insulin resistance and inflammation, while subcutaneous fat is considered to be 'benign'. Perirenal fat was indicated as one of the significant predictors of carcinoma development [6, 7], and para and perirenal fat thickness is an independent predictor of kidney dysfunction in type-2 diabetes [8]. Mesenteric fat accumulation was shown to be regulated by hormone such as neuropeptide Y [9], and mesenteric fat thickness was an independent risk factor associated with fatty liver and a predictor for diabetes [10]. In general, visceral fat is directly associated with

liver inflammation and fibrosis independent of insulin resistance and hepatic steatosis [11]. Subcutaneous fat, such as back fat, is considered to be benign, less metabolically active and not associated with negative health outcomes. Thiazolidinediones (TZD), a drug class approved for treatment of type 2 diabetes, are synthetic agonists of the peroxisome proliferator activated receptor (PPARγ) [12] that also activate AMPK [13]. Treatment with TZDs leads to increased adipogenesis in subcutaneous fat and weight gain [14]. Hence, TZDs enhance insulin sensitivity by promoting glucose uptake and utilization in subcutaneous white adipose tissue, leading to reduced free fatty acid concentrations [15].

The objective of this study was to determine the effect of high-fat and high- carbohydrate diets on body composition, mRNA abundance of adipokines and inflammatory factors in different sources of adipose tissue, and pancreatic islet mass in prepubertal pigs. We hypothesized that porcine prepubertal obesity is associated with chronic inflammation that is characterized by up-regulation of pro-inflammatory cytokines in adipose tissue with differences between subcutaneous (backfat) and visceral (perirenal and mesenteric) depots.

Materials and methods

Animals

Female 28-d-old Premium Genetics 1020 pigs were randomly divided into 4 dietary treatment groups (n=6), including 1) Control or high-fat (HF) diets that contained 2) complex carbohydrates (CC) or refined sugars (SC) in the form of 3) glucose or 4) fructose. Details of animal husbandry, diet composition and feeding were reported elsewhere [24]. Control pigs were pair-fed to HF pigs based on lysine levels to normalize body weight gain, as previously described [24]. After 56 d, pigs were weighed and euthanized. Weight gain and final body weights did not differ across treatments ($P = 0.81$), whereas body fat composition increased ($P < 0.001$) from

18.4±1.3% in control pigs to 28.0±1.1% in HF pigs, regardless of carbohydrate type. Metabolizable energy (ME) intakes were the same for all of the 4 dietary treatment groups [27]. The pancreas was removed from the animal and separated lengthwise into four equal pieces. A cubic centimeter of tissue was excised from the center of each piece and submerged in 10% neutral-buffered formalin. Samples were incubated overnight at 4°C, washed in PBS and transferred to 70% ethanol. Subcutaneous, mesenteric, and perirenal fat were harvested from all pigs and submerged in RNA Later (Life Technologies). Samples were stored at 4°C overnight and then transferred to -80°C. The Virginia Tech Institutional Animal Care and Use Committee approved all experimental procedures; this study was conducted in accordance with the Federation of Animal Science Societies' Guide for the Care and Use of Agricultural Animals in Research and Teaching.

Total RNA isolation and gene expression analysis

Approximately 0.3 g of white adipose tissue from each depot of each pig was weighed and homogenized twice at 20 Hz for 2 minutes using 5mm stainless steel beads (Qiagen, USA) and 1mL RNA lysis reagent (5-Prime) using a Tissue Lyser II (Qiagen, USA). Samples were then centrifuged, fat layer removed, supernatant transferred to a clean tube and mixed with chloroform, and centrifuged again. The supernatant was mixed with ethanol and loaded onto a spin column and total RNA purified according to the manufacturer's instructions (Promega SV total RNA isolation kit). An on-column Rnase-Free Dnase I treatment step was included in the kit. The purified total RNA samples were evaluated for integrity by agarose-formaldehyde gels and quantified by spectrophotometry (260/280nm) using a Nanophotometer™ Pearl (IMPLEN, USA). The first stand cDNA was synthesized from total RNA using the High Capacity cDNA Reverse Transcription kit (Applied Biosystems, USA). Primers were designed with Primer

Express 3.0 (Applied Biosystems; **Table 8.1**). All primers were validated for similar amplification efficiency before use. Quantitative real-time (RT) PCR was performed using an Applied Biosystems 7500 Fast PCR machine and Fast SYBR green (Applied Biosystems, USA). Samples were run in duplicate in 96-well plates. Melting curve analyses were performed to ensure amplicon specificity.

Islet mass

Pancreas samples in 70% ethanol were shipped to HSRL Laboratories (Woodstock, VA), paraffin-embedded, sectioned at 5 μm, and mounted and stained with hematoxylin and eosin. Brightfield images were captured using a Nikon Eclipse 80i microscope and DS-Ri1 camera at a magnification of 4x (**Figure C.2**) and complete pancreas section image tiles compiled using the large image stitching method of the NIS-Elements Advanced Research Software (Nikon, USA). The relative islet mass was determined as the fraction of pancreas tissue occupied by islets. The islet to pancreas ratio was calculated for each slide, and the average of all 5 slides per animal was used for statistical analysis.

Statistical analysis

Pig was defined as the experimental unit. The real time PCR data were analyzed using the $\Delta\Delta C_T$ method, where $\Delta C_T = C_{T\ \text{target gene}} - C_{T\ OAZ1}$, and $\Delta\Delta C_T = \Delta C_{T\ \text{target sample}} - \Delta C_{T\ \text{calibrator}}$ [28]. Ornithine decarboxylase antizyme 1 (OAZ1) was the housekeeping gene and backfat from control diet pigs served as the calibrator sample [29]. The $2^{-\Delta\Delta ct}$ values were used for statistical analysis. Data normality was evaluated by the Univariate procedure of SAS 9.3 (SAS Institute, Cary, NC). The Glimmix procedure of SAS was used for mixed models ANOVA with treatment as a fixed effect and pig as random effect nested within treatment. Fat depot was included in the model as a repeated measure, with random Type=vc and ddfm=bw selected based on variance

and correlation among different fat depots. Thus, the model included the main effects of dietary treatment and fat depot and the interaction between them. Tukey's test was used for pairwise comparisons. All the data are presented as least squares means ± SEM. Differences were considered significant at $P < 0.05$.

For the islet data, the average relative islet mass (expressed as a ratio of islets to total pancreas area) were subjected to ANOVA using the Proc Glimmix procedure of SAS. Pig was considered the experimental diet and the statistical model included the main effect of diet, with Tukey's test as a post-hoc test for pairwise comparisons among diets.

Results

We evaluated gene expression of adipokines with known roles in mediating changes in adipocyte hypertrophy, insulin sensitivity, and inflammation during obesity in three fat depots of pigs that consumed one of four different diets. There was no dietary treatment by fat depot interaction for any of the genes evaluated (**Tables 8.2** and **Table 8.3**). Leptin, resistin and PAI1 (**Table 8.2**) and IL6 (**Table 8.3**) mRNA were not influenced by diet or fat depot. Dietary treatment affected adiponectin mRNA abundance, where there was greater ($P = 0.039$) expression in pigs that consumed the glucose diet than those that consumed the control diet (**Table 8.2**). Expression of adiponectin was greater ($P = 0.042$) in perirenal than subcutaneous fat. While visfatin mRNA was not affected by diet, its expression differed among adipose tissue depots, with greater ($P < 0.01$) expression in subcutaneous and perirenal fat as compared to mesenteric fat. HIF1 was not affected by diet, and its expression was greater in perirenal fat as compared to subcutaneous ($P = 0.0001$) and mesenteric fat ($P = 0.031$).

Abundance of MCP1 mRNA was greater ($P = 0.03$) in pigs that were fed the CC diet as compared to those on the control diet (**Table 8.3**). Expression of MCP1 was greater ($P < 0.04$) in

perirenal fat than mesenteric and subcutaneous fat. Tumor necrosis factor α mRNA abundance was greater ($P = 0.03$) in CC-fed pigs than control pigs, similar to MCP1. Quantities of MCP1 mRNA were greater ($P = 0.02$) in perirenal than subcutaneous fat.

Relative islet mass in the pancreas was not influenced by diet, with similar ratios (%) in pigs that consumed the fructose (0.33±0.007), glucose (0.34±0.007), control (0.25±0.008) and CC (0.33±0.007) diets ($P = 0.85$) (**Table C.1**).

Discussion

In the present study we measured mRNA abundance of a variety of adipose-derived factors that are associated with obesity, insulin resistance and inflammation. Back fat (subcutaneous fat), mesenteric fat and perirenal fat were used to evaluate how adipokine gene expression varies in different fat depots of pigs that consume different diets. While mesenteric and perirenal fat are both visceral fat depots, a key difference is that mesenteric fat drains into the portal circulation. One theory for why visceral fat is associated with liver dysfunction is that secreted factors drain directly into the portal vein. In our study, most of the genes evaluated showed distinct differences in regional distribution across fat depots and several showed dietary differences. It is important to point out though, that while inflammation-associated genes showed differences in our study, measurements were made at a single time point. Inflammation is a transient and dynamic event and it is possible that changes would be greater with longer exposure to the diets or that differences were more accentuated earlier in the trial and dampened as the pigs became more acclimated to the diets. Based on our data though, it is clear that the pigs consuming the high fat diets were obese and displayed differences in gene expression suggestive of an inflammatory state.

Both TNFα and IL6 are inflammatory mediators that can be secreted from white adipose tissue and showed increased expression in fat from pigs that ate the HF diets as compared to the controls. Only TNFα showed a significant difference between the CC and control group in this study. TNFα, a pro-inflammatory cytokine produced by adipose tissue and lymphoid cells, plays a pivotal role in macrophage infiltration that leads to amplification of the inflammatory state in white fat tissue. It exerts a range of actions such as the induction of adipocyte apoptosis and the stimulation of lipolysis [16, 17], and inhibits feeding and increases metabolic rate. Wong et al. reported that MCP-1 expression was up-regulated by TNFα in vitro [18].

Adiponectin secreted from adipose tissue plays an important role as an insulin sensitizer, both at the level of the skeletal muscle and the liver. A study showed that adiponectin improves insulin sensitivity and increases insulin-mediated glucose uptake by the skeletal muscle and suppresses hepatic glucose production [19, 20]. In this study, we found that adiponectin expression was affected by both diet and fat depot. Among the dietary groups, we found that all pigs that ate HF diets showed much higher adiponectin expression compared to the controls with greater expression in pigs that consumed glucose than those that consumed the control diet. Comparing adiponectin expression in different fat depots, there was greater expression in perirenal fat than backfat. Earlier studies in 3T3L1 cells indicated that both glucose and fructose medium enhanced the expression of adiponectin expression [21]. Also, there is evidence that glucose stimulated adiponectin gene expression by increasing the expression of the CCAT/enhancer binding protein and nuclear factor-Y genes [22].

Both MCP1 and TNFα were expressed the greatest in fat from pigs that consumed the CC diet in our study. It was indicated that the concentration of MCP1 in fat cells and blood plasma was increased both in genetically obese diabetic mice as well as healthy mice in which obesity

had been induced by feeding a high-fat diet. However, these effects were not observed in mice lacking MCP1, even when fed the high-fat diet [23]. These results indicated that MCP1 links obesity and insulin resistance though the induction of an inflammatory response in fatty tissue. This finding was consistent with other results generated from this experiment, where pigs fed with HF diets (including fructose, glucose, and CC treatments) had the most significant ultrasound back fat depth, as well as increased fasting blood glucose levels but lowered insulin, with no significant difference between SC diets [24]. These findings implied that the HF diet possibly leads to insulin resistance and pancreatic β cell dysfunction in the long-term.

To evaluate whether differences in body composition and insulin sensitivity were associated with changes in β-cell mass, relative islet mass was measured in the pancreas. There were no significant differences ($P = 0.85$) in islet mass among dietary groups (**Table C.1**). Diabetes, which is associated with a reduction in islet mass due to β-cell apoptosis, is preceded by hyperinsulinemia, a state where there is hyper-secretion of insulin to compensate for insulin resistance. In the present study, although pigs were hyperglycemic and there were indirect indicators of insulin resistance (insert Reaves citation), the islet mass data suggest that pigs had not progressed to an advanced state of insulin resistance or diabetes.

Most of the adipokines measured in this study, including adiponectin, HIF1, and Visfatin had the lowest expression in subcutaneous fat and highest expression in perirenal fat. IL6 and Leptin had similar expression levels among different fat depots. Among the genes that showed significant differences among fat regions, HIF1 is a transcription factor induced by adipose tissue hypoxia. There are many factors in obesity that can stimulate the secretion of HIF1 such as adipogenesis, insulin and hypoxia [25]. In general, HIF1 is constitutively expressed at the mRNA level, with most of its regulation occurring by post-translational events. Thus, it would be

unexpected for HIF1 mRNA to be influenced by diet. Visfatin is predominantly secreted from visceral adipose tissue and has insulin-mimetic action by binding to the insulin receptor [26]. Greater expression of these genes in perirenal fat may indicate enhanced metabolic activity in that fat depot, which may make it more susceptible to oxidative stress and inflammation.

In conclusion, pigs fed the HF diets had greater body fat composition and increased gene expression of several adipokines. In general, there was greater inflammatory adipokine gene expression in mesenteric and perirenal fat compared to subcutaneous fat, which may be associated with more metabolic activity in those regions.

References

1. Hammond RA, Levine R: **The economic impact of obesity in the United States**. *Diabetes, metabolic syndrome and obesity : targets and therapy* 2010, **3**:285-295.
2. DiGirolamo M, Fine JB, Tagra K, Rossmanith R: **Qualitative regional differences in adipose tissue growth and cellularity in male Wistar rats fed ad libitum**. *The American journal of physiology* 1998, **274**(5 Pt 2):R1460-1467.
3. Trayhurn P: **Endocrine and signalling role of adipose tissue: new perspectives on fat**. *Acta physiologica Scandinavica* 2005, **184**(4):285-293.
4. Ahima RS: **Central actions of adipocyte hormones**. *Trends in endocrinology and metabolism: TEM* 2005, **16**(7):307-313.
5. Hajer GR, van Haeften TW, Visseren FL: **Adipose tissue dysfunction in obesity, diabetes, and vascular diseases**. *European heart journal* 2008, **29**(24):2959-2971.
6. Noguchi G, Makiyama K, Sano F, Nakaigawa N, Yao M, Kubota Y: **[A renal cell carcinoma metastasis to the contralateral perirenal fat : a case report]**. *Hinyokika kiyo Acta urologica Japonica* 2011, **57**(7):391-394.
7. Okhunov Z, Mues AC, Kline M, Haramis G, Xu B, Mirabile G, Vira M, Landman J: **Evaluation of perirenal fat as a predictor of cT 1a renal cortical neoplasm histopathology and surgical outcomes**. *Journal of endourology / Endourological Society* 2012, **26**(7):911-916.
8. Lamacchia O, Nicastro V, Camarchio D, Valente U, Grisorio R, Gesualdo L, Cignarelli M: **Para- and perirenal fat thickness is an independent predictor of chronic kidney disease, increased renal resistance index and hyperuricaemia in type-2 diabetic patients**. *Nephrology, dialysis, transplantation : official publication of the European Dialysis and Transplant Association - European Renal Association* 2011, **26**(3):892-898.
9. Kos K, Harte AL, James S, Snead DR, O'Hare JP, McTernan PG, Kumar S: **Secretion of neuropeptide Y in human adipose tissue and its role in maintenance of adipose tissue mass**. *American journal of physiology Endocrinology and metabolism* 2007, **293**(5):E1335-1340.

10. Karagiannides I, Pothoulakis C: **Neuropeptides, mesenteric fat, and intestinal inflammation**. *Annals of the New York Academy of Sciences* 2008, **1144**:127-135.
11. Van der Poorten D, Milner KL, Hui J, Hodge A, Trenell MI, Kench JG, London R, Peduto T, Chisholm DJ, George J: **Visceral fat: a key mediator of steatohepatitis in metabolic liver disease**. *Hepatology* 2008, **48**(2):449-457.
12. Philippe J, Raccah D: **Treating type 2 diabetes: how safe are current therapeutic agents?** *International journal of clinical practice* 2009, **63**(2):321-332.
13. Hardie DG, Ross FA, Hawley SA: **AMP-activated protein kinase: a target for drugs both ancient and modern**. *Chemistry & biology* 2012, **19**(10):1222-1236.
14. Tontonoz P, Spiegelman BM: **Fat and beyond: the diverse biology of PPARgamma**. *Annual review of biochemistry* 2008, **77**:289-312.
15. Akkati S, Sam KG, Tungha G: **Emergence of promising therapies in diabetes mellitus**. *Journal of clinical pharmacology* 2011, **51**(6):796-804.
16. Prins JB, Niesler CU, Winterford CM, Bright NA, Siddle K, O'Rahilly S, Walker NI, Cameron DP: **Tumor necrosis factor-alpha induces apoptosis of human adipose cells**. *Diabetes* 1997, **46**(12):1939-1944.
17. Ryden M, Arvidsson E, Blomqvist L, Perbeck L, Dicker A, Arner P: **Targets for TNF-alpha-induced lipolysis in human adipocytes**. *Biochemical and biophysical research communications* 2004, **318**(1):168-175.
18. Wang B, Jenkins JR, Trayhurn P: **Expression and secretion of inflammation-related adipokines by human adipocytes differentiated in culture: integrated response to TNF-alpha**. *American journal of physiology Endocrinology and metabolism* 2005, **288**(4):E731-740.
19. Berg AH, Combs TP, Du X, Brownlee M, Scherer PE: **The adipocyte-secreted protein Acrp30 enhances hepatic insulin action**. *Nature medicine* 2001, **7**(8):947-953.
20. Yamauchi T, Kamon J, Waki H, Terauchi Y, Kubota N, Hara K, Mori Y, Ide T, Murakami K, Tsuboyama-Kasaoka N *et al*: **The fat-derived hormone adiponectin reverses insulin resistance associated with both lipoatrophy and obesity**. *Nature medicine* 2001, **7**(8):941-946.
21. Carvalho CR, Bueno AA, Mattos AM, Biz C, de Oliveira C, Pisani LP, Ribeiro EB, do Nascimento CM, Oyama LM: **Fructose alters adiponectin, haptoglobin and angiotensinogen gene expression in 3T3-L1 adipocytes**. *Nutr Res* 2010, **30**(9):644-649.
22. Park SK, Oh SY, Lee MY, Yoon S, Kim KS, Kim JW: **CCAAT/enhancer binding protein and nuclear factor-Y regulate adiponectin gene expression in adipose tissue**. *Diabetes* 2004, **53**(11):2757-2766.
23. Kanda H, Tateya S, Tamori Y, Kotani K, Hiasa K, Kitazawa R, Kitazawa S, Miyachi H, Maeda S, Egashira K *et al*: **MCP-1 contributes to macrophage infiltration into adipose tissue, insulin resistance, and hepatic steatosis in obesity**. *The Journal of clinical investigation* 2006, **116**(6):1494-1505.
24. Reeves HF, Van Eyk GR, Seelenbinder KM, Price KL, Scheffler TL, Gerrard DE, Scheffler JM, Escobar J: **Increased fat and simple carbohydrate consumption results in obese prepubertal pigs without an increase in body weight**. *The FASEB Journal* 2012, **26**(113):1.
25. He Q, Gao Z, Yin J, Zhang J, Yun Z, Ye J: **Regulation of HIF-1{alpha} activity in adipose tissue by obesity-associated factors: adipogenesis, insulin, and hypoxia**. *American journal of physiology Endocrinology and metabolism* 2011, **300**(5):E877-885.

26. Davutoglu M, Ozkaya M, Guler E, Garipardic M, Gursoy H, Karabiber H, Kilinc M: **Plasma visfatin concentrations in childhood obesity: relationships with insulin resistance and anthropometric indices**. *Swiss medical weekly* 2009, **139**(1-2):22-27.
27. Van Eyk GR: **Dietary Fat and Sugar Induce Obesity and Impair Glucose Tolerance in Prepubertal Pigs**. Virginia Tech; 2012.
28. Schmittgen TD, Livak KJ: **Analyzing real-time PCR data by the comparative CT method**. *Nat Proto* 2008, **3**(6):1101-1108.
29. Piorkowska K, Oczkowicz M, Rozycki M, Ropka-Molik K, Piestrzynska-Kajtoch A: **Novel porcine housekeeping genes for real-time RT-PCR experiments normalization in adipose tissue: assessment of leptin mRNA quantity in different pig breeds**. *Meat science* 2011, **87**(3):191-195.

Table 8.1 Primers used for real time PCR

Gene1	Accession No.	Sequence (forward/reverse)
TNFα	NM_214022.1	CTTGGGTTTGGATTCCTGGAT/ CTTCCCTGGCAGCCACAT
Visfatin	NM_001031793.2	TCCAAGAAGCCAAAGAGGTGTAC/ TGTAGTTCCATCCCTTTTCATTAAAGA
Adiponectin	NM_214370.1	GCTGTTGTTGGGAGCTGTTCT/ TGGTTTCCTGGCCGAGACT
HIF1	NM_001123124.1	CCATGCCCCAGATTCAAGAT/ GGTGAACTCTGTCTAGTGCTTCCA
IL6	NM_214399.1	GCGCAGCCTTGAGGATTTC/ CCCAGCTACATTATCCGAATGG
Leptin	NM_213840.1	CGGCGGTTCACCCTTTT/ GGATGTTCTCTGCTCTCAAGTAGCT
MCP1	NM_214214.1	TCCCACACCGAAGCTTGAAT/ CACAGGAGGGCTGCAGAGA
PAI1	NM_213910.1	CACCCAGCAGCAGATCCAA/ CCATGCCCTTCTCCTCAATC
Resistin	AY528644.1	TGAGCCCACAGAGAGGGTAAG/ CCAGCTTTGCCCCCAAA
OAZ1	NM_001122994.1	TGCAGCGGATCCTCAACA/ TGGGTTTATCCCCCTCCTTCT

[1]*TNFα*: tumor necrosis factor α; *HIF1*: hypoxia-inducible factor 1; *IL6*: interleukin 6; *MCP1*: monocyte chemoattractant protein 1; *PAI1*; plasminogen activator inhibitor 1; *OAZ1*: ornithine decarboxylase antizyme 1

Table 8.2 Effects of diet and adipose tissue location on mRNA abundance of adipokines[1]

Diet	*Adiponectin*	*Visfatin*	*Leptin*	*Resistin*	*HIF1*[2]	*PAI1*
Fructose	2.74±0.44[ab]	1.81±0.24	1.28±0.32	8.97±2.62	2.15±0.27	7.02±1.78
Glucose	3.29±0.44[a]	1.57±0.24	1.15±0.32	2.79±2.54	1.86±0.27	2.30±1.78
Control	1.16±0.57[b]	1.32±0.30	1.18±0.42	3.34±3.27	1.26±0.34	1.34±2.30
CC[3]	3.45±0.46[ab]	2.29±0.24	2.36±0.33	4.00±2.62	2.42±0.28	2.75±1.84
P-value	0.03	0.09	0.06	0.35	0.09	0.18
Fat Depot						
Subcutaneo	2.34±0.43[ab]	1.93±0.23[a]	1.35±0.31	5.78±2.45	1.83±0.26[b]	2.03±1.73
Mesenteric	2.09±0.42[b]	0.94±0.22[b]	1.28±0.30	6.68±2.43	1.15±0.25[b]	2.95±1.67
Perirenal	3.55±0.41[a]	2.36±0.22[a]	1.86±0.30	1.87±2.33	2.78±0.25[a]	5.07±1.64
P-value	0.04	0.0002	0.34	0.32	0.0002	0.43
Diet x Fat[4]	0.48	0.08	0.41	0.79	0.13	0.88

[1]Values represent LS means ± SEM, n = 6. Letters that differ within a column and main effect, P < 0.05 (Tukey's pairwise comparisons).

[2]HIF1: hypoxia-inducible factor 1; PAI1: plasminogen activator inhibitor 1

[3]CC: complex carbohydrate diet

[4]Two-way interaction of diet and fat depot on mRNA abundance

Table 8.3 Effect of diet and adipose tissue location on mRNA abundance[1]

Diet	*MCP1*[2]	*IL6*	*TNFα*
Fructose	3.25±0.60[ab]	3.51±0.68	5.64±1.41[ab]
Glucose	3.47±0.60[ab]	3.09±0.68	6.55±1.41[ab]
Control	1.09±0.77[b]	1.16±0.88	1.37±1.81[b]
CC[3]	4.14±0.62[a]	3.39±0.70	8.21±1.45[a]
P-value	0.043	0.19	0.06
Fat Depot	----------	----------	----------
Subcutaneou	1.76±0.58	2.24±0.66	2.86±1.36[b]
Mesenteric	3.54±0.56	2.86±0.64	4.75±1.32[ab]
Perirenal	3.66±0.55	3.26±0.62	8.72±1.29[a]
P-value	0.043	0.53	0.01
	----------	----------	----------
Diet x Fat[4]	0.76	0.41	0.70

[1]Values represent LS means ± SEM, n = 6. Letters that differ within a column represent significant differences, $P < 0.05$ (Tukey's pairwise comparisons);

[2]MCP1: monocyte chemoattractant protein 1; IL6: interleukin 6; TNFα: tumor necrosis factor α;

[3]CC: complex carbohydrate diet;

[4]Two-way interaction of diet and fat depot on mRNA abundance

Chapter 9

Conclusions and future directions

Chickens are naturally hyperglycemic and hyperinsulinemic compared to mammals. Unlike humans, chickens do not have the insulin-dependent glucose transporter 4 (GLUT4) and their normal fasting blood glucose levels equate to a diabetic condition in humans. Because chickens lack GLUT4 in their genome and insulin-dependent glucose transporters have not been identified in chickens, mechanisms for glucose clearance during insulin sensitivity tests in avian species are unclear. Understanding the physiological mechanisms that allow chickens to cope with chronic hyperglycemia and identifying pathways for glucose uptake in chicken adipose tissue and skeletal muscle may provide some insight for the treatment of obesity and diabetes. Using the high and low body weight-selected lines of chickens, we found that the low weight line more promptly reduces their blood glucose in response to insulin injection than the high weight line. However, the low weight line appears to be less efficient in utilizing blood glucose based on previously published studies. To shed some light on mechanisms responsible for insulin-dependent glucose uptake in chickens in insulin-dependent tissues, we measured in different tissues the gene expression of all glucose transporter (GLUT) isoforms for which sequences are available in the chicken genome. The glucose transporters in chicken are clearly tissue specific, where *GLUT1* is highly expressed in the hypothalamus and *GLUT2* and *GLUT9* are highly expressed in the liver. Insulin injection decreased *GLUT2* and *GLUT3* expression at 1-hour post injection in the liver, suggesting that they may play an important role in blood glucose homeostasis.

NPY was identified as a strong orexigenic factor in chickens [1, 2]. Studies from our group also showed that central injection or NPY can promote food intake in high weight but not

the low weight line, after immediate post-hatch stressor exposure [3]. Counterintuitively, we found that the high weight line had lower expression of *NPY*, *NPY1R* and *NPY5R* mRNA than low weight line in the hypothalamus. But given that high weight chickens at 90-days of age are already obese and that expression was measured at a single time point post-insulin injection, it is difficult to conclude whether the lower *NPY* expression is a cause or a result of appetite regulation. Also, there is a chance that the expression at the protein level for the NPY system in high weight line chickens is greater than in low weights. One of the more interesting findings was that *NPY* and its receptors *NPY1R* and *NPY2R* all had higher expression in the abdominal fat in chickens from the low weight than high weight line.

Through in vitro studies, we have provided evidence to support that NPY promotes adipogenesis in chickens. This effect is similar to what has been found in humans. However, the adipogenesis process in chickens is different from the 3T3-L1 mouse preadipocyte cell line, where differentiation takes the place of proliferation to support the lipid accumulation in the cells. In our chicken primary adipose cell culture model, proliferation and differentiation occur simultaneously. Supplementation of cells with 100 nM NPY was able to stimulate expression of proliferation markers such as *Ki67*, *TOP2A*, *TPX2*, and therefore promote stimulation of proliferation. Both the G3PDH activity assay results and the Oil Red O staining showed that NPY supplementation increased lipid accumulation after the induction of differentiation. The adipogenic effect of NPY was supported by increased expression of *FABP4* and *LPL*, and also changes in *PPARγ, C/EBPα, C/EBPβ,* and *SREBP* expression. These findings indicate the importance of NPY in energy regulation in chickens. Most importantly, our findings have generated a foundation for further study in hypothalamus-adipose tissue cross talk using chickens as a model.

In the study of the two body weight lines, we also analyzed heterosis of reciprocal crosses between the high and low body weight lines at the gene level. Both *GLUT2* mRNA in the liver and *NPY1R* and *NPY2R* in the abdominal fat had a greater level of heterosis with expression levels much lower in the reciprocal crosses than in either parental lines, indicating superior phenotypes in dealing with excess energy, and also implicating the importance of the NPY system from a genetic point of view.

Whole hypothalamic transcriptome profiling in the body weight line chickens revealed differentially expressed genes that were enriched in "serotonin and dopamine biogenesis and receptor-signaling pathways". High weight line chickens had much lower expression of aromatic-L-amino-acid decarboxylase, tyrosine hydroxylase, and monoamine transporters than those from the low weight line. This phenomenon was reversed after insulin injection. Serotonin has been shown to reduce food intake in human and rodents and has been a pharmacological target for the treatment of obesity since the 1970s. Findings from this dissertation suggest serotonin as an important candidate for the study of appetite regulation in chickens. In vivo studies in 4-day-old chicks demonstrated that central injection of serotonin reduced food intake in a dose and time dependent manner. This process was coupled with the activation of the ventromedial hypothalamus and arcuate nucleus. Gene expression analysis in the whole hypothalamus showed that oxytocin and ALDH1L1 might be involved in the anorexigenic effects of serotonin. Due to the heterogeneous characteristics of the hypothalamus, further studies should evaluate the expression of target genes in specific nuclei that are activated in response to serotonin injection.

Direction for future study includes developing an understanding of out the molecular mechanisms of NPY-mediated effects on appetite regulation and fat deposition in chickens. For

example, knockdown of the expression of NPY in specific hypothalamic nuclei can be used to understand the role of hypothalamic NPY in whole body energy homeostasis. Our understanding of the role of NPY in adipogenesis in chickens is still in its infancy, especially given that chicken adipogenesis is different from rodents. To better understand NPY's role in adipogenesis in chicken adipocytes, NPY and/or its receptor expression can be knocked down or their function blocked in adipocytes in an experiment to eliminate other confounding factors. Key signaling pathways such as MAPK, PKA, PCK, PI3KI, and ERK can also be further explored because they have been implicated in the adipogenic response to NPY in mammals [4]. The present study tested effects of NPY in Cobb-500 broilers. It would be interesting to evaluate how the two body weight lines and their reciprocal crosses respond to NPY in terms of adipogenesis. This is especially critical given that NPY may be able to alter adipogenesis via an autocrine mechanism. One other potential avenue is to compare adipogenic effects of NPY on different fat depots considering that functions, metabolic characteristics and adipocyte turnover are distinct among different fat depots. Basic on these in vitro studies, the role of NPY in energy balance can also be evaluated in vivo studies though both central and peripheral injections.

This research has broader implications for the study of hypothalamus-adipose tissue crosstalk given that NPY is expressed in these two systems, thereby contributing to energy storage in both. It may provide us with an opportunity for the treatment of obesity through modulating regional fat deposition.

References

1. Jonaidi H, Noori Z: **Neuropeptide Y-induced feeding is dependent on GABAA receptors in neonatal chicks**. *Journal of comparative physiology A, Neuroethology, sensory, neural, and behavioral physiology* 2012, **198**(11):827-832.
2. Ando R, Kawakami SI, Bungo T, Ohgushi A, Takagi T, Denbow DM, Furuse M: **Feeding responses to several neuropeptide Y receptor agonists in the neonatal chick**. *European journal of pharmacology* 2001, **427**(1):53-59.

3. Newmyer BA, Nandar W, Webster RI, Gilbert E, Siegel PB, Cline MA: **Neuropeptide Y is associated with changes in appetite-associated hypothalamic nuclei but not food intake in a hypophagic avian model**. *Behavioural brain research* 2013, **236**(1):327-331.
4. Rosmaninho-Salgado J, Cortez V, Estrada M, Santana MM, Goncalves A, Marques AP, Cavadas C: **Intracellular mechanisms coupled to NPY Y2 and Y5 receptor activation and lipid accumulation in murine adipocytes**. *Neuropeptides* 2012, **46**(6):359-366.

Appendix A

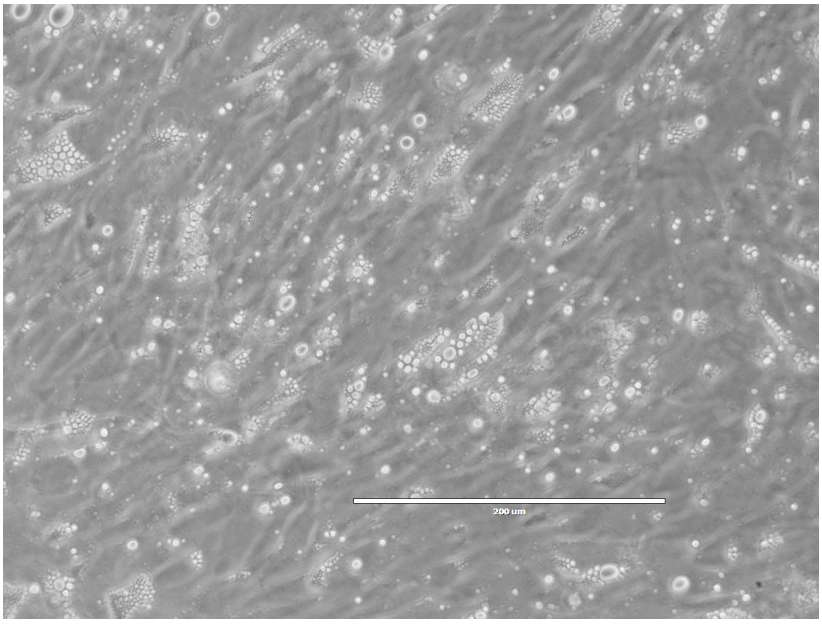

Figure A.1 Multilocular lipid accumulation in chicken adipocytes during the early stage of differentiation (day 4 post differentiation

Appendix B

Table B.1 Alignment statistics for genomic reads of each individual bird from low-weight vehicle (LWSv), low-weight insulin (LWSi), high-weight vehicle (HWSv), and high-weight insulin (HWSi) groups*

B.1.1 Total sequence read counts post QC

Genotype	Vehicle		Insulin	
	Bird ID	Reads	Bird ID	Reads
	5490	14625581	5421	8079508
LWS	5492	13824319	5422	12279542
	5503	15306333	5424	9565802
	5390	13689282	5365	14113431
HWS	5458	14530018	5366	11910649
	5467	14759088	5367	11038856

B.1.2 Total reads mapped to genome

Genotype	Vehicle		Insulin	
	Bird ID	Reads	Bird ID	Reads
	5490	13890762	5421	7650713
LWS	5492	13084340	5422	12163232
	5503	14606067	5424	9211150
	5390	12888712	5365	13735080
HWS	5458	13705803	5366	11287147

	5467	14521145	5367	10754048

B.1.3 Total reads mapped uniquely to known exome

Genotype	Vehicle		Insulin	
	Bird ID	Reads	Bird ID	Reads
	5490	8431977	5421	4691847
LWS	5492	7871856	5422	7154700
	5503	8948164	5424	5568535
	5390	7804165	5365	8335205
HWS	5458	8226903	5366	6865568
	5467	8424271	5367	6378578

B.1.4 Average exome sequence depth

Genotype	Vehicle		Insulin	
	Bird ID	Depth	Bird ID	Depth
	5490	493	5421	274
LWS	5492	460	5422	418
	5503	523	5424	325
	5390	456	5365	487
HWS	5458	481	5366	401
	5467	492	5367	373

*Reads are averaged for individuals in each group.

Table B.2 Primers used for qPCR validation

Gene[1]	Accession No.	Sequence (forward/reverse; 5' to 3')
NPY	NM_205473.1	CATGCAGGGCACCATGAG/CAGCGACAAGGCGAAAGTC
POMC	NM_001031098.1	GCCAGACCCCGCTGATG/CTTGTAGGCGCTTTTGACGAT
TPH2	NM_001001301.1	ACGATTGAATTTGGTCTTTGCA/CAGAAGTCCTGCCCCATAAGC
FOXO1	NM_204328.1	GCCTCCTTTTCGAGGGTGTT/ GCGGTATGTACATGCCAATCTC
ALDH1A1	NM_214399.1	CAGTGTTGTATAGCAGGATCCAGAA/TCCGGCGAACAAACTCATC
PDK4	NM_001199909.1	GCTGGACTTCGGCTCGACTA/TCGCAGGAACGCAAAGG
GRP	NM_001277900.1	AAACAAGATCCCATTGTCAGCAT/TCCCGCTGCAGGTAGTCATC
OXT	XM_001231491.3	TGGCTCTCTCCTCAGCTTGTTAT/GGCACGGCACGCTTACC
SLC6A4	NM_213572.1	CTGGGATACATGGCCGAGAT/TCCCATGTCTTTGGCAACCT
TH	NM_204805.1	CAGGACATTGGGCTTGCAT/TGTTGCCAGTTTCTCAATTTCTTC

[1]*NPY*: neuropeptide Y; *POMC*: proopiomelanocortin; *TPH2*: tryptophan hydroxylase 2; *FOXO1*: forkhead box O1; *ALDH1A1*: aldehyde dehydrogenase 1 family, member A1; *PDK4*: pyruvate dehydrogenase kinase, lysozyme 4; *GRP*: gastrin-releasing peptide; *OXT*: oxytocin; *SLC6A4*: solute carrier family 6, member 4; *TH*: tyrosine hydroxylase.

Table B.3

B.3.1 Top diseases and Bio Functions in HWS line compared to LWS vehicle-injected chickens based on prediction analysis of differentially-expressed genes.

Disease and disorders	*P*-value	Molecules
Cardiovascular disease	1.95E-04-321E-02	5
Organismal injury and abnormalities	1.95E-04-4.78E-02	10
Metabolic disease	3.64E-04-3.64E-04	7
Neurological disease	3.64E-04-4.78E-02	25
Psychological disease	3.64E-04-3.22E-02	16
Molecular and cellular functions	*P*-value	Molecules
Molecular transport	1.28E-05-4.00E-02	10
Small molecule biochemistry	1.28E-05-4.00E-02	12
Cell-to-cell signaling and interaction	5.52E-05-4.78E-02	17
Cellular development	5.96E-05-4.94E-02	11
Lipid metabolism	6.52E-05-4.00E-02	3
Physiological system development and function	*P*-value	Molecules
Nervous system development and function	5.96E-05-4.94E-02	28
Tissue morphology	2.81E-03-4.78E-02	13
Hematological system development and function	6.39E-03-1.62E-02	2
Organismal functions	6.39E-03-3.21E-02	3
Auditory and vestibular system development and function	8.12E-03-3.21E-02	1

B.3.2 Top disease and bio functions in HWS compared to LWS after insulin injection

Disease and disorders	*P*-value	Molecules
Hereditary disorder	4.14E-04-8.63E-03	17
Neurological disease	4.14E-04-4.68E-02	35
Psychological disorders	4.14E-04-4.61E-02	25
Cancer	3.13E-03-4.68E-02	3
Development disorder	3.76E-03-2.37E-02	2
Molecular and cellular functions	*P*-value	Molecules
Cell-to-cell signaling and interaction	2.44E-05-4.68E-02	30
Cell death and survival	5.10E-05-4.78E-02	24
Cell morphology	5.57E-05-4.68E-02	27
Cellular assembly and organization	6.69E-05-4.68E-02	22
Molecular transport	4.32E-04-4.68E-02	18
Physiological system development and function	*P*-value	Molecules
Nervous system development and function	2.41E-05-4.68E-02	50
Tissue morphology	2.41E-05-4.68E-02	23
Behavior	5.05E-05-4.68E-02	9
Endocrine system development and function	8.31E-04-4.68E-02	9
Digestive system development and function	9.92E-04-4.68E-02	4

B.3.3 Top disease and bio functions in insulin-injected as compared to the vehicle-treated HWS.

Disease and disorders	*P*-value	Molecules
Hereditary disorder	3.11E-07-1.62E-02	23
Neurological disease	3.11E-07-4.20E-02	33
Psychological disorders	3.11E-07-4.20E-02	31
Skeletal and muscular disorders	7.09E-05-1.62E-02	12
Organismal injury and abnormalities	1.95E-04-4.78E-02	4
Molecular and cellular functions	*P*-value	Molecules
Cell-to-cell signaling and interaction	1.94E-09-4.78E-02	28
Molecular transport	1.94E-09-4.00E-02	19
Small molecule biochemistry	1.94E-09-4.00E-02	21
Drug metabolism	1.82E-07-4.00E-02	12
Cell morphology	3.22E-07-4.78E-02	33
Physiological system development and function	*P*-value	Molecules
Nervous system development and function	4.15E-08-4.78E-02	48
Tissue morphology	4.15E-08-4.78E-02	23
Tissue Development	5.18E-07-4.78E-02	27
Embryonic development	2.06E-06-4.00E-02	18
Behavior	8.92E-06-4.78E-02	8

B.3.4 Top disease and bio functions in vehicle-injected compared to insulin-injected LWS.

Disease and disorders	*P*-value	Molecules
Developmental disorder	1.29E-03-2.58E-03	1
Endocrine system disorder	1.29E-03-7.73E-03	2
Neurological disease	1.29E-07-2.93E-02	5
Hereditary disorder	2.58E-03-2.93E-02	2
Psychological disorder	2.58E-03-1.84E-02	4
Molecular and cellular functions	*P*-value	Molecules
Cell-to-cell signaling and interaction	9.00E-04-3.68E-02	2
Cell cycle	1.29E-03-1.29E-03	1
Carbohydrate metabolism	2.58E-03-5.16E-03	1
Cellular function and maintenance	2.58E-03-3.68E-02	2
Lipid metabolism	2.58E-03-6.45E-03	2
Physiological system development and function	*P*-value	Molecules
Behavior	6.15E-06-2.18-02	3
Endocrine system Development and function	5.34E-04-1.54E-02	3
Nervous system development and function	5.34E-04-3.68E-02	5
Tissue morphology	5.34E-04-1.54E-02	2
Organismal function	1.29E-03-1.29E-03	1

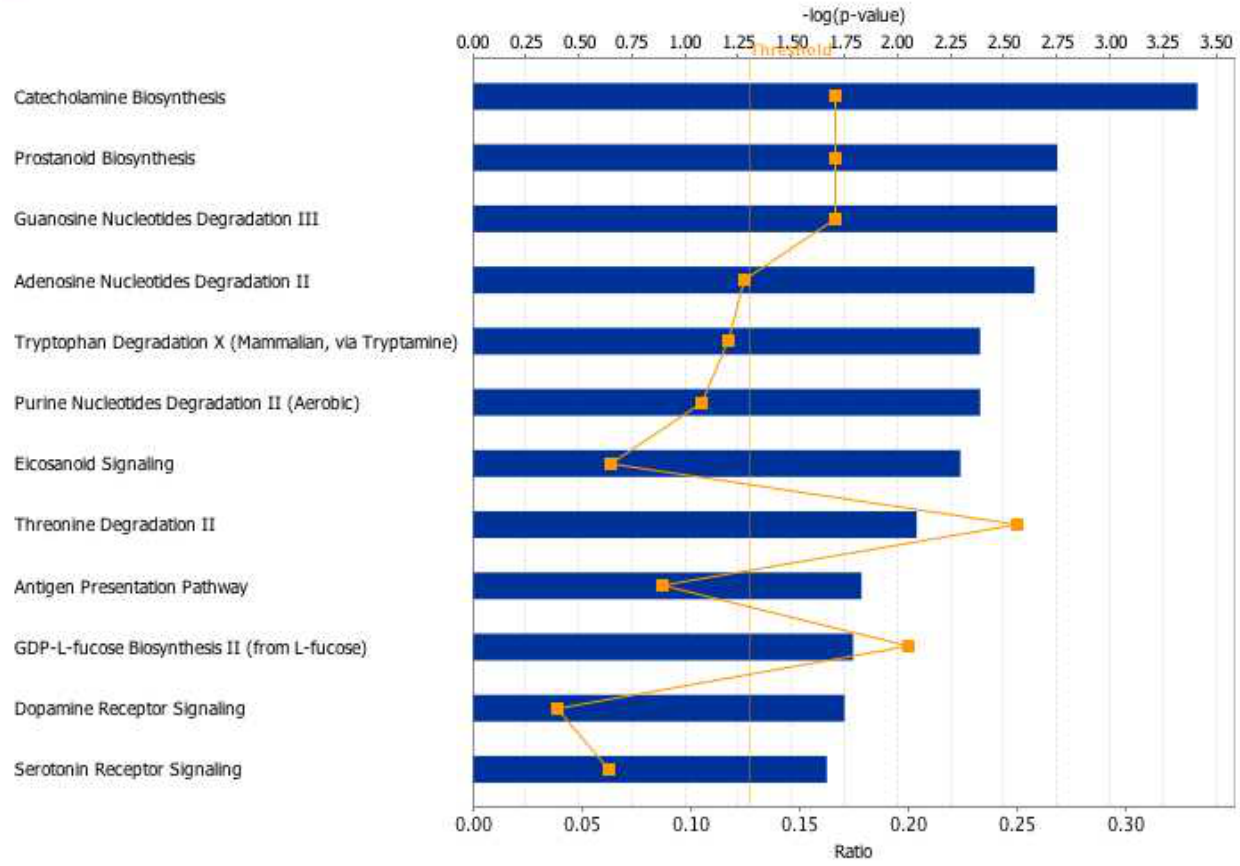

Figure B.1 Bar chart for top canonical pathways (-log (*p*-value) ≥1.5 as the threshold). Pathways involved in HWSLWSv (HWS as compared to LWS in vehicle treatment). The length of the bar indicates the significance level of the pathway. The orange square line indicates the ratio of number of genes that meet the cutoff criteria / the total number of genes that make up that pathway.

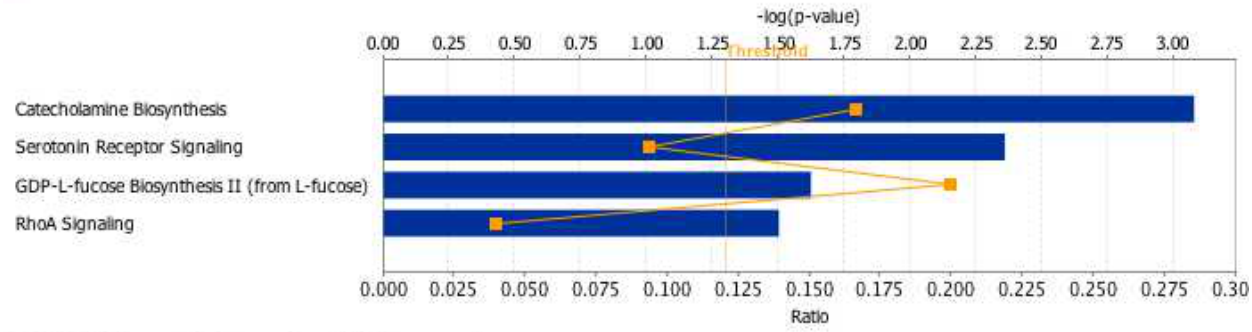

Figure B.2 Bar chart for top canonical pathways (-log (*p*-value) ≥1.5 as the threshold) involved in HWSLWSi (HWS as compared to LWS in insulin treated chickens. The length of the bar indicates the significance level of the pathway. The orange square line indicates the ratio of number of genes that meet the cutoff criteria / the total number of genes that make up that pathway.

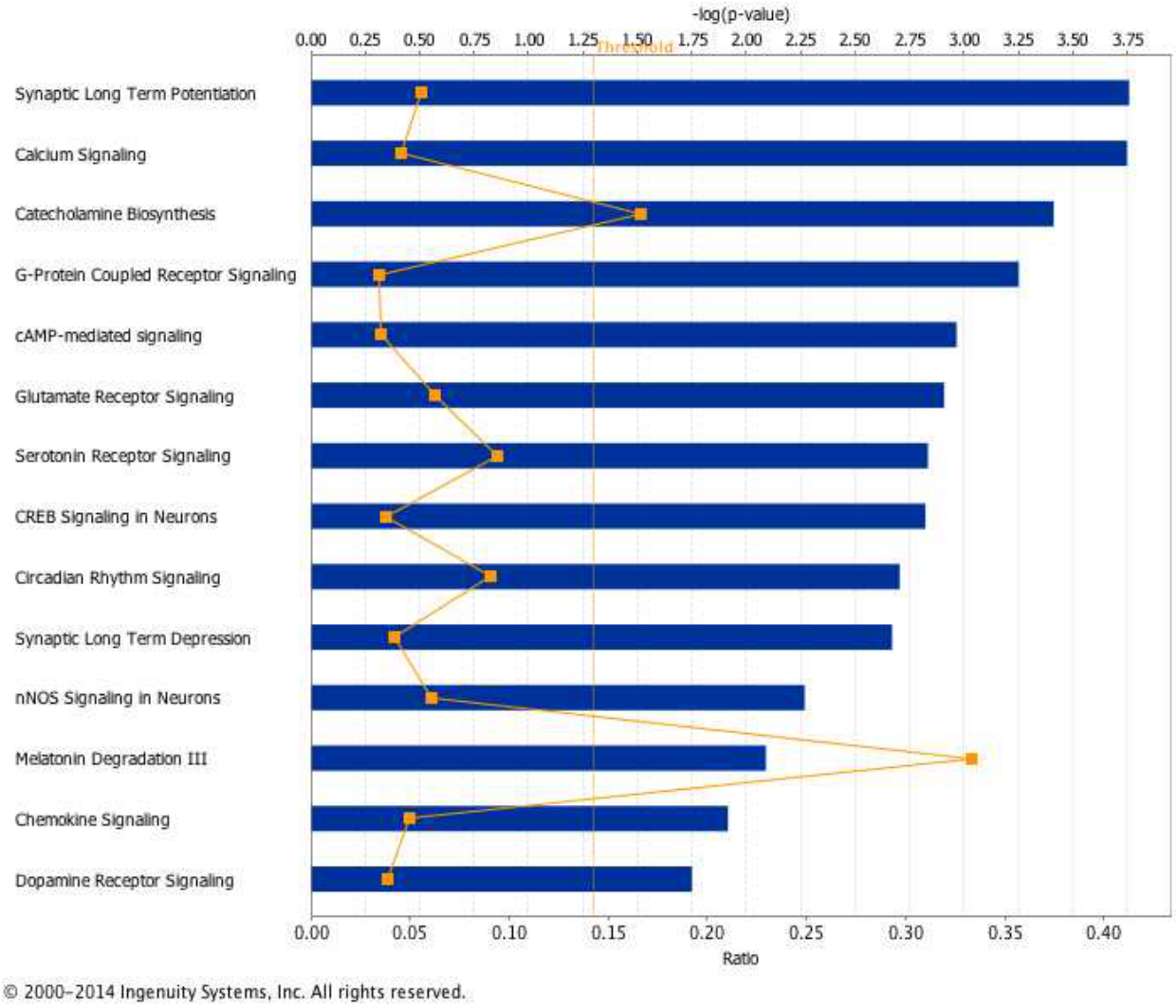

Figure B.3 Bar chart for top canonical pathways (-log (*p*-value) ≥1.5 as the threshold) involved in HWSiv (insulin treatment as compared to the vehicle treatment in high weight line chickens). The length of the bar indicates the significance level of the pathway. The orange square line indicates the ratio of number of genes that meet the cutoff criteria / the total number of genes that make up that pathway.

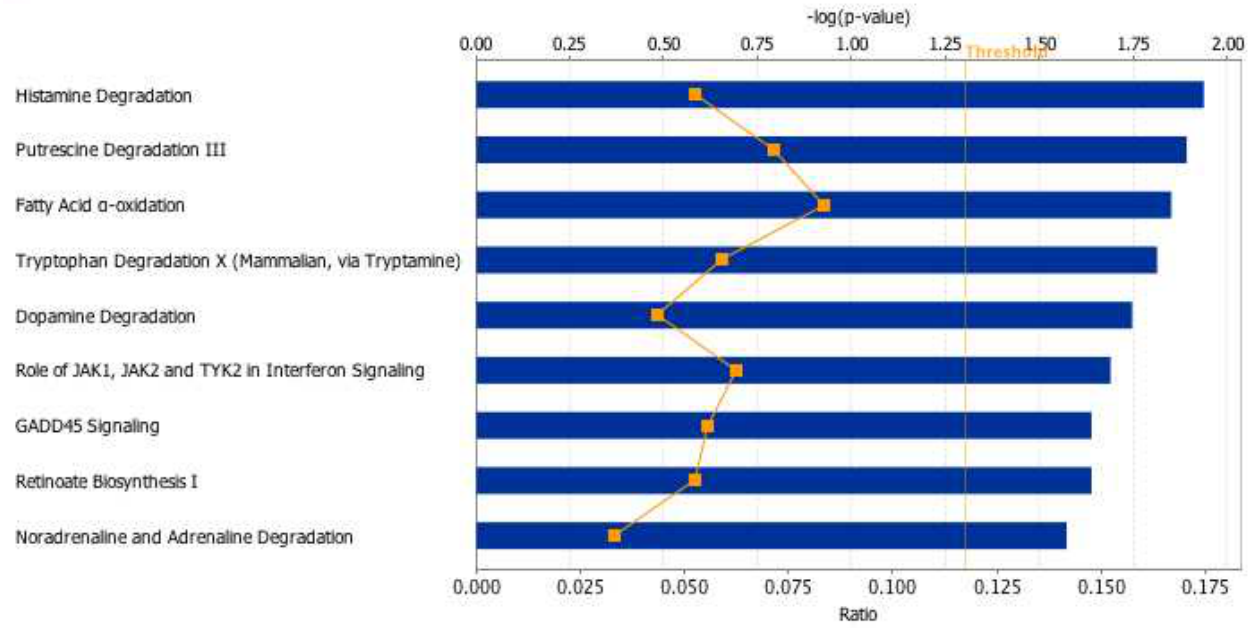

Figure B.4 Bar chart for top canonical pathways in each group (-log (*p*-value) ≥1.5 as the threshold) involved in LWSiv (insulin treatment as compared to the vehicle in the low weight line). The length of the bar indicates the significance level of the pathway. The orange square line indicates the ratio of number of genes that meet the cutoff criteria / the total number of genes that make up that pathway.

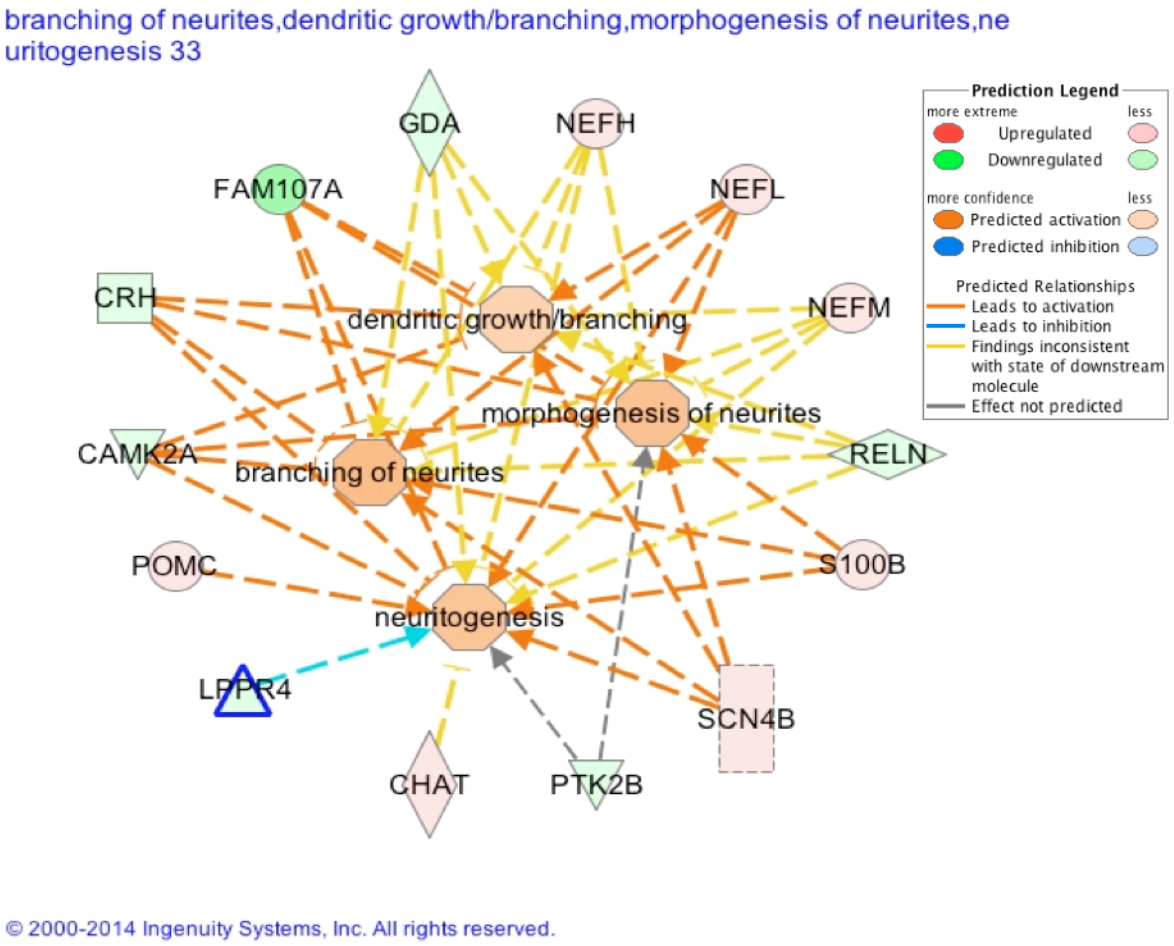

Figure B.5 Predicted changes in cell morphology in the high weight line after insulin injection, based on pathway analysis of differentially expressed genes

Appendix C

Table C.1 Pancreas islets to mass ratio for each pig

Animal No.	Treatment	Islets mass ratio				
714	Control	0.000677	0.000818	0.000963	0.000826	0.000821
718	Control	0.000194	0.000261	0.000133	0.000170	0.000190
722	Control	0.005891	0.003292	0.005860	0.007654	0.005674
725	Control	0.003341	0.003134	0.003859	0.002158	0.003123
701	CC[1]	0.006065	0.003430	0.003488	0.006703	0.004922
703	CC	0.003398	0.001617	0.003369	0.003510	0.002974
707	CC	0.002801	0.002706	0.003497	0.002962	0.002992
712	CC	0.002995	0.004092	0.002324	0.003043	0.003114
721	CC	0.002220	0.002745	0.002260	0.000940	0.002041
723	CC	0.002813	0.004663	0.004204	0.002381	0.003515
702	Fructose	0.000983	0.001942	0.001473	0.001531	0.001482
709	Fructose	0.004032	0.007556	0.003615	0.005729	0.005233
713	Fructose	0.003147	0.002100	0.001628	0.001385	0.002065
715	Fructose	0.004996	0.003527	0.004434	0.003687	0.004161
717	Fructose	0.002882	0.002254	0.003177	0.003080	0.002848
724	Fructose	0.003042	0.002679	0.004235	0.004992	0.003737
704	Glucose	0.001864	0.000900	0.001817	0.003301	0.001971
706	Glucose	0.004503	0.004484	0.00444	0.003204	0.004158
708	Glucose	0.000150	0	0	0	0.000038
711	Glucose	0.004190	0.004351	0.004664	0.003223	0.004107
716	Glucose	0.002261	0.003177	0.009700	0.000853	0.003998
720	Glucose	0.006978	0.007003	0.006902	0.002725	0.005902

[1]CC: complex carbohydrate diet

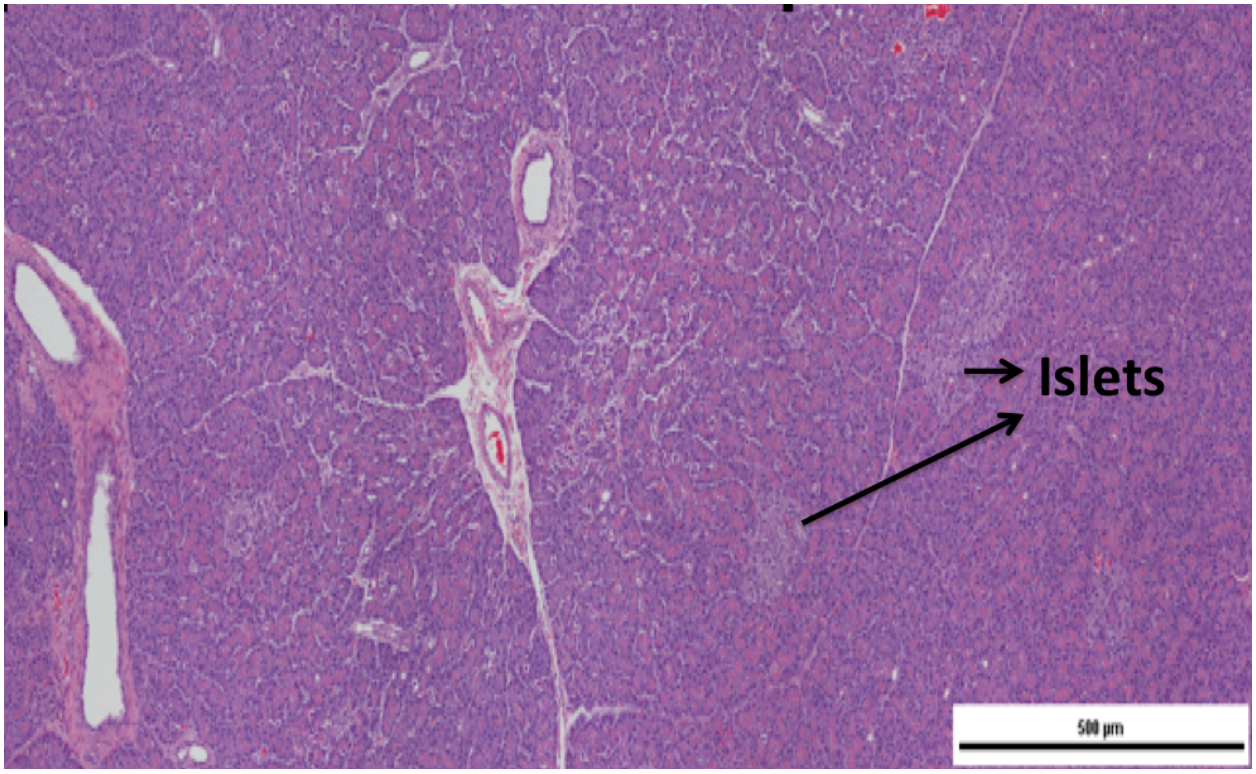

Figure C.2 Representative image of hematoxylin and eosin stained cross-section of pancreas with arrows indicating the location of islets.